



HAL
open science

Cellules Club et susceptibilité respiratoire environnementale

Charlotte Vernisse

► **To cite this version:**

Charlotte Vernisse. Cellules Club et susceptibilité respiratoire environnementale. Médecine humaine et pathologie. Université Montpellier, 2020. Français. NNT : 2020MONTT007 . tel-02899833

HAL Id: tel-02899833

<https://theses.hal.science/tel-02899833v1>

Submitted on 15 Jul 2020

HAL is a multi-disciplinary open access archive for the deposit and dissemination of scientific research documents, whether they are published or not. The documents may come from teaching and research institutions in France or abroad, or from public or private research centers.

L'archive ouverte pluridisciplinaire **HAL**, est destinée au dépôt et à la diffusion de documents scientifiques de niveau recherche, publiés ou non, émanant des établissements d'enseignement et de recherche français ou étrangers, des laboratoires publics ou privés.

THÈSE POUR OBTENIR LE GRADE DE DOCTEUR DE L'UNIVERSITÉ DE MONTPELLIER

En Biologie Santé

École doctorale Sciences Chimiques Biologiques pour la santé

Unité de recherche UMR CNRS 9214 - INSERM U1046

CELLULES CLUB ET SUSCEPTIBILITE RESPIRATOIRE ENVIRONNEMENTALE

Présentée par Charlotte Vernisse
Le 16 Mars 2020

Sous la direction de Arnaud BOURDIN

Devant le jury composé de

Pr. Christian JORGENSEN, DU, PU-PH, Inserm U1183
Pr. Patrick BERGER, PU-PH, Université de Bordeaux
Pr. Pascal BARBRY, DR, IPMC, Université Côte d'Azur
Pr. Pascal CHANEZ, PU-PH, Université d'Aix-Marseille
Dr. Cindy BARNIG, MCU-PH, INSERM, UMR-S U1109
Pr. Arnaud BOURDIN, PU-PH, Université de Montpellier

Président du jury
Rapporteur
Rapporteur
Examineur
Examinatrice
Directeur de these



UNIVERSITÉ
DE MONTPELLIER

Remerciements

Tout d'abord, je tiens à remercier les membres de mon jury d'avoir accepté d'évaluer mon travail de thèse. Je suis honorée d'avoir un jury de thèse aussi prestigieux. Je tiens à remercier tout particulièrement Pr Pascal Barbry et Pr Patrick Berger d'avoir accepté d'être mes rapporteurs de thèse. Je remercie également Dr Cindy Barnig, Pr Pascal Chanez d'avoir accepté d'être examinateurs de mon travail de thèse. Je tiens également à remercier Pr Christian Jorgensen d'avoir accepté d'être le président de mon jury de thèse.

Je souhaite remercier Pr John De vos, et Dr Edouard Tuaille, pour m'avoir suivi et aidé tout au long de ma thèse. Merci d'avoir fait preuve de bienveillance, mais aussi d'avoir su me pousser quand il le fallait.

Au Pr Arnaud Bourdin, trois années de thèse qui auront été intenses... Cette thèse aura été une aventure pleine de rebondissement et ça jusqu'au bout... Je crois que l'on peut résumer ces trois années par des problèmes de fixations, d'extractions et d'intégrité de l'ARN... Merci de m'avoir accueilli et fait découvrir le monde de la Pneumologie. Merci d'avoir été présent au moment où il le fallait mais aussi de m'avoir poussé dans mes retranchements. Je ressors de cette thèse grandie et plus autonome. Par contre, l'ASM restera toujours la meilleure équipe du Top 14, il va falloir vous y faire...

Au Dr Isabelle Vachier, merci de m'avoir accueilli au sein du laboratoire. Merci pour tes conseils et ton aide scientifique. Merci pour les relectures de ma thèse ainsi que pour les moments de partages sur les traditions du Sud. Je pars de la région mais je garderais des bons souvenirs au sein du laboratoire.

Au Dr Aurélie Petit, merci de m'avoir transmis tes connaissances sur l'épithélium bronchique. Merci de m'avoir aidé durant ce projet et de m'avoir soutenu quand peu de choses fonctionnaient. J'espère que tu pourras continuer ce projet après mon départ et que ces petites cellules Club révéleront leurs secrets.

A Anne Sophie B, merci pour ta gentillesse. Merci de ton aide pour les analyses de cytométrie en flux.

A l'U1046, merci de m'avoir accueilli au sein de votre laboratoire. Un merci tout particulier à Pierre Edouard pour son aide et son soutien.

Merci aux généticiennes pour votre aide sur mes problèmes d'extractions.

Merci à la recherche clinique, à l'IRMB, aux Marseillais, aux Bordelais, aux statisticiens, aux stagiaires, à mes co-thésards pour leur aide et leur soutien durant ces longues années de thèse.

A mes ami(e)s Anaïs, Elodie, Emilie, Florian, Merci d'avoir été à mes côtés durant cette thèse, pour tous les moments de fous rires et d'aventures en dehors de cette thèse.

Aux Saint priestois pour leur soutien et leur écoute

A ma famille pour le cocon qu'ils m'ont offert pour réaliser mes études et leur soutien durant ces années de thèse.

A Baptiste, merci pour tout, merci pour ce soutien et avoir vécu cette thèse à mes côtés.

SOMMAIRE

<u>ABBREVIATIONS</u>	i
<u>LISTE DES FIGURES</u>	iv
<u>LISTE DES TABLEAUX</u>	vi
<u>RECAPTULATIF DES ARTICLES</u>	vii
A- INTRODUCTION	1
I- La BPCO, une maladie épithéliale.....	3
I-1. Définition.....	3
I-2. Les facteurs de risque	5
a- Origine Génétique	6
b- Origine Pédiatrique.....	6
c- Les réponses inflammatoires	7
I-3. Les traitements actuels.....	8
II- Phénotype et plasticité de l'épithélium.....	9
II-1. Des voies aériennes proximales à distales.....	9
II-2. L'épithélium respiratoire	9
II-3. Les différents types cellulaires composant l'épithélium des voies aériennes.....	10
a- Les cellules basales.....	10
b- Les cellules ciliées.....	11
c- Les cellules caliciformes	11
d- Les cellules neuroendocrines.....	12
e- Les cellules Club	12
II-4. L'épithélium des voies aériennes dans la BPCO.....	13
II-5. La modulation du phénotype épithélial dans les voies aériennes	15
a- Voie Notch	15
b- Voie ROCK	17
c- Voie BMP.....	17
III- Les cellules Club.....	19
III-1. L'origine des cellules Club	19
III-2. Déficit des cellules Club dans l'épithélium bronchique des patients BPCO.....	20

III-3. Fonctions des cellules Club.....	21
a- Fonction de prolifération/différenciation.....	21
b- Fonction de métabolisme des xénobiotiques.....	22
c- Fonction de sécrétion.....	22
III-4. La protéine CCSP.....	23
III-5. Modèles d'études des cellules Club et de sa protéine	24
III-6. Potentiel thérapeutique.....	25
IV- Pattern inflammatoires dans les voies aériennes.....	26
IV-1. Endotypes T1/T2 dans la BPCO	27
a- Endotype T1	27
b- Endotype T2	28
c- Autres endotypes	28
IV-2. Alarmines	29
a- IL33-ST2	29
b- TSLP.....	34
c- IL25	35
IV-3. Futures thérapies	35
B- OBJECTIFS	37
C- RESULTATS	43
I- Les modèles d'étude des maladies chroniques des voies aériennes	45
Résumé	45
<i>Les organoïdes pulmonaires.....</i>	47
Conclusion.....	63
II- La plasticité des cellules Club dans l'épithélium bronchique humain	65
II-1. Protocole pour obtenir la carte d'identité des cellules Club à partir de cultures primaires de cellules épithéliales bronchiques humaines en modèle ALI.....	65
Résumé	65
<i>Microarray protocol for intracellular-target-sorted, formalin-fixed human bronchial epithelial cells</i>	67
Discussion	93
Conclusion.....	94

II-2. Identité des cellules Club dans l'épithélium des voies aériennes	95
Résumé	95
<i>Different Club cells in human bronchial epithelium</i>	97
Discussion	111
Conclusion.....	112
III- Superviser la différenciation pour adapter le phénotype des cellules épithéliales bronchiques humaines en culture ALI	113
Résumé	113
<i>Supervising differentiation for tailoring the airway epithelial cell phenotype</i>	115
Discussion	149
Conclusion.....	150
IV-Le rôle des alarmines dans les maladies chroniques des voies aériennes	151
IV-1. La place des cytokines dans les maladies chroniques des voies aériennes	151
Résumé	151
<i>What is the rationale for targeting alarmins to treat chronic obstructive pulmonary disease? ..</i>	153
Discussion	171
Conclusion.....	171
IV-2. Les cytokines sécrétées par les cellules de l'épithélium bronchique dans les maladies chroniques des voies aériennes reconstituées en ALI	173
Résumé	173
<i>Alarmins secretions by human bronchial epithelial cells in air liquid interface model correlate with blood eosinophils in chronic airways diseases</i>	175
Discussion	189
Conclusion.....	189
D- CONCLUSIONS/PERSPECTIVES	191
ANNEXES	197
REFERENCES	199

ABBREVIATIONS

ALI : Air Liquid Interface

BODE : B pour « Body-Mass Index » ou BMI, O pour le degré d'obstruction des voies respiratoires, D pour la dyspnée et E pour la capacité d'exercice

BPCO : BronchoPneumopathie Chronique Obstructive

BMP : Bone Morphogenetic Protein ou protéines morphogénétiques oseuses

CC : Club Cell

CD : Cluster Differentiation

CEBH : Cellules Epithéliales Bronchiques Humaines

CF : Cystic Fibrosis

CGRP : Calcitonine Gene-Related Peptide

CCSP : Club Cell Secretory Protein

CSP : Cellules Souches Pluripotentes

COPD : Chronic Obstructive Pulmonary Disease

CVF : Capacité Vitale Forcée

CXCL : C-X-C motif Ligand

CYP : Cytochrome

FFPE : Formaldehyde-Fixed Paraffin-Embedded

GHS : Gluthation

GOLD : Global initiative for chronic Obstructive Lung Disease

GRP : Gastrine

HBEC : Human Bronchial Epithelial Cells

IL : Interleukine

IL1RAcP : IL-1 Receptor Accessory Protein

IPS : Induced Pluripotent Stem cells ou cellules souches pluripotentes induites humaines

LBA : Lavage BronchoAlvéolaire

MMP-12 : Metalloproteinase 12

MUC : Mucine

NEB : Neuro-Epithelial Bodies ou corpuscules neuro-épithéliaux

NF-HEV : Nuclear Factor from High Endothelial Venules

PCB : PolyChloroBiphényles

PDMS : PolyDiMethylSiloxane

PG : ProstaGlandine

PLG : Poly(Lactide-co-Glycolide)

PM : Particulate Matter

PNI : Pneumocytes de type I

PNII : Pneumocytes de type II

RV : RhinoVirus

SCGB : Secretoglobin

SERPIN : Serpin peptidase inhibitor

SLPI : Secretory Leukocyte Peptidase Inhibitor

ST2 : Suppression of Tumorigenicity 2

TNF : Tumor Necrosis Factor

VEMS : Volume Expiratoire Maximal par Seconde

LISTE DES FIGURES

<i>Figure 1 : Modifications physiopathologiques retrouvées dans la BPCO</i>	4
<i>Figure 2 : Trajectoires fonctionnelles respiratoires susceptibles d'aboutir au développement d'une BPCO</i>	7
<i>Figure 3 : Composition cellulaire des différentes divisions de l'arbre bronchique chez l'homme et la souris</i>	10
<i>Figure 4 : Modifications physiopathologiques retrouvées dans la BPCO</i>	13
<i>Figure 5 : Accumulation de mucus dans les bronchioles des patients BPCO</i>	15
<i>Figure 6 : Les étapes de différenciation des cellules épithéliales des voies aériennes</i>	16
<i>Figure 7 : Voie de signalisation Notch</i>	16
<i>Figure 8 : Voie de signalisation TGFβ/BMP</i>	18
<i>Figure 9 : Schéma récapitulatif des cibles des différents inhibiteurs commercialisés</i>	18
<i>Figure 10 : Expression de la protéine CCSP au niveau des petites voies aériennes de sujets témoins et de patients BPCO</i>	20
<i>Figure 11 : Versant T2 dans la BPCO</i>	26

<i>Figure 12 : La séquence de l'IL33</i>	29
<i>Figure 13 : De la forme longue dans le noyau des cellules à la forme active sur les cellules ST2⁺</i>	30
<i>Figure 14 : Rôle des caspases dans l'inactivation de l'IL33</i>	31
<i>Figure 15 : La forme ST2 membranaire</i>	31
<i>Figure 16 : Voie de signalisation ST2/IL33</i>	32
<i>Figure 17 : Les autres formes du récepteur ST2</i>	33
<i>Figure 18 : Action du TSLP sur les différents types cellulaires</i>	34

LISTE DES TABLEAUX

<i>Tableau 1 : Classification des patients BPCO en fonction de la sévérité de l'obstruction ventilatoire</i>	5
--	---

RECAPITULATIF DES ARTICLES

Articles publiés (Annexes)

- Mucus Microrheology Measured on Human Bronchial Epithelium Culture

Myriam Jory, Karim Bellouma, Christophe Blanc, Laura Casanellas, Aurélie Petit, Paul Reynaud, **Charlotte Vernisse**, Isabelle Vachier, Arnaud Bourdin and Gladys Massiera

Frontiers in Physics 7:19 · February 2019, DOI: 10.3389/fphy.2019.00019

- CCSP counterbalances airway epithelial-driven neutrophilic chemotaxis

Knabe L, Petit A, **Vernisse C**, Charriot J, Pugnère M, Henriquet C, Sasorith S, Molinari N, Chanez P, Berthet JP, Suehs C, Vachier I, Ahmed E, Bourdin A.

Eur Respir J. 2019 Jul 11;54(1). pii: 1802408. doi: 10.1183/13993003.02408-2018. Print 2019 Jul.

- Goblet cell hyperplasia as a feature of neutrophilic asthma.

Alagha K, Bourdin A, **Vernisse C**, Garulli C, Tummino C, Charriot J, Vachier I, Suehs C, Chanez P, Gras D.

Clin Exp Allergy. 2019 Jun;49(6):781-788. doi: 10.1111/cea.13359. Epub 2019 Feb 27.

- Vitiligo Skin Is Imprinted with Resident Memory CD8 T Cells Expressing CXCR3

Boniface K, Jacquemin C, Darrigade AS, Dessarthe B, Martins C, Boukhedouni N, **Vernisse C**, Grasseau A, Thiolat D, Rambert J, Lucchese F, Bertolotti A, Ezzedine K, Taieb A, Seneschal J.

J Invest Dermatol. 2018 Feb;138(2):355-364. doi: 10.1016/j.jid.2017.08.038. Epub 2017 Sep 18.

Articles soumis (Partie Résultats)

- Les organoïdes pulmonaires

Chloé Bourguignon, **Charlotte Vernisse**, Joffrey Mianné, Mathieu Fieldès, Engi Ahmed, Aurélie Petit, Isabelle Vachier, Thierry Lavabre Bertrand, Said Assou, Arnaud Bourdin, John De Vos

Revue Médecine/Science

- Microarray protocol for intracellular-target-sorted, formalin-fixed human bronchial epithelial cells

Vernisse C, Petit A, Pantesco V, Chanez P, Gras D, Duperray C, Vachier I, Bourdin A

Scientific report

Articles en cours d'écriture (Partie Résultats)

- Supervising differentiation for tailoring the airway epithelial cell phenotype

Charlotte Vernisse and Noémie Drappier, Aurélie Petit, Lucie Knabe, John de Vos, Said Assou, Mathieu Fieldès, Chloé Bourguignon, Joffrey Mianne, Jérémy Charriot, Isabelle Vachier, Delphine Gras, Pascal Chanez, Arnaud Bourdin and Engi Ahmed.

- Different Club cells in human bronchial epithelium

Vernisse C, Assou S, Petit A, Fieldès M, De Vos J, Vachier I, Bourdin A

- What is the rationale for targeting alarmins to treat chronic obstructive pulmonary disease?

Vernisse C, Bedin AS, Petit A, Chanez P, Gras D, Vachier I, Charriot J, Ahmed E, Tuailon E, Bourdin A

- Alarmins secretions by human bronchial epithelial cells in air liquid interface model correlate with blood eosinophils in chronic airways diseases

Vernisse C, Petit A, Suesh C, Chanez P, Gras D, Molinari N, Vachier I, Bourdin A

A- INTRODUCTION

I- La BPCO, une maladie épithéliale

La BronchoPneumopathie Chronique Obstructive (BPCO) est une maladie chronique des voies aériennes. En 2012, plus de 3 millions de personnes sont décédées à cause de cette maladie ce qui représente 6 % des décès mondiaux. De plus, cette maladie progresse de manière constante depuis 20 ans avec plus de 44 millions de patients souffrant de BPCO. En 2020, elle devient la troisième cause de décès au niveau mondial ce qui en fait actuellement un problème de santé publique majeur¹.

En France, la prévalence de la BPCO s'élève à plus de 3,5 millions de personnes, soit 6 à 8 % de la population adulte touchée par cette maladie². Elle représente une cause majeure de morbidité et mortalité et le fardeau représenté par cette maladie ne devrait qu'augmenter au cours des prochaines décennies en raison de la poursuite de l'exposition des populations aux facteurs de risque³. Mais malgré cette progression, la connaissance de la maladie ainsi que ses mécanismes physiopathologiques restent largement méconnus, par conséquent, il n'existe pas de traitement curatif.

I-1. Définition

La BPCO est caractérisée par un trouble ventilatoire obstructif (VEMS/CVF <0,7, « Volume Expiratoire Maximal par Seconde / Capacité Vitale Forcée ») persistant et non réversible, et une réponse inflammatoire chronique accrue et exagérée des voies aériennes face à une agression, pouvant conduire à un déclin accéléré de la fonction respiratoire de manière non réversible⁴. Cliniquement, il n'existe pas de symptômes respiratoires spécifiques à la BPCO mais il existe une association à d'autres entités, clinique (bronchite chronique) et anatomique (l'emphysème). Par contre, leurs contributions relatives à la maladie varient d'un individu à l'autre. La bronchite chronique est souvent associée au diagnostic de cette maladie mais celle-ci ne préjuge pas de la présence de la BPCO⁵. Elle est caractérisée par une toux et des expectorations pendant au moins 3 mois durant deux années consécutives. L'emphysème, lui, est une entité anatomique qui peut coexister avec la BPCO. Il correspond à une dilatation permanente avec destruction des espaces aériens distaux, affectant notamment les surfaces des échanges gazeux (Figure 1).

Les modifications physiopathologiques caractéristiques de la BPCO comprennent l'hypersécrétion de mucus, un dysfonctionnement mucociliaire, un excès de dépôt de matrice extracellulaire, une hyper vascularisation, un changement du phénotype du muscle lisse qui passe de contractile à sécrétoire, une diminution du calibre des petites voies aériennes distales, une réponse inflammatoire chronique accrue et exagérée^{6,7} et la formation de follicule tertiaire⁸ (Figure 1). Tout ceci a pour conséquence de limiter les flux aériens et contribuer à l'obstruction des voies aériennes surtout distales.

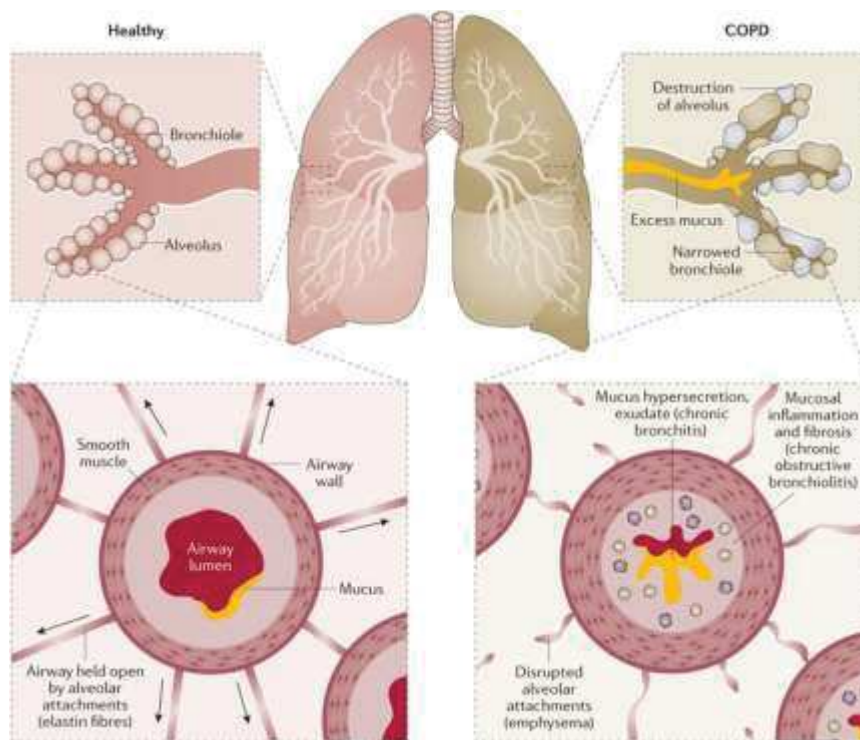


Figure 1 : Modifications physiopathologiques retrouvées dans la BPCO⁹

Mais la BPCO est une maladie complexe et hétérogène tant du point de vue clinique que du point de vue de la réponse inflammatoire des patients (de type T1, T2) face à une « agression environnementale »¹⁰. La différente contribution relative de ces différents éléments d'un patient à un autre pourrait expliquer la variabilité interindividuelle des phénotypes cliniques observée dans la BPCO. Toutefois, des classifications sont utilisées pour tenter de regrouper des phénotypes harmonieux de patients atteints de BPCO, au-delà de la classification GOLD, où la sévérité de la BPCO est basée sur le VEMS (Tableau 1)¹.

GOLD 1:	Mild	$FEV_1 \geq 80\%$ predicted
GOLD 2:	Moderate	$50\% \leq FEV_1 < 80\%$ predicted
GOLD 3:	Severe	$30\% \leq FEV_1 < 50\%$ predicted
GOLD 4:	Very Severe	$FEV_1 < 30\%$ predicted

Tableau 1 : Classification des patients BPCO en fonction de la sévérité de l'obstruction ventilatoire¹

Certains patients atteints de la BPCO peuvent présenter des manifestations systémiques non directement corrélées à leur trouble ventilatoire obstructif. Il est donc nécessaire d'avoir une approche plus globale tenant compte de l'imagerie, de l'évaluation de la tolérance à l'exercice et de l'indice de masse corporelle. L'indice de BODE prend en compte certaines de ces valeurs comme l'indice de masse corporelle ((B) pour « Body-Mass Index » ou BMI), le degré d'obstruction des voies respiratoires (O), la dyspnée (D) et la capacité d'exercice (E). Cette approche semble prédire la mortalité à un an. Mais ce score pronostic ne permet pas d'obtenir des groupes « homogènes » notamment à la lumière, des nouveaux traitements disponibles ou en cours d'évaluation, ciblant soit des cytokines particulières (T1/T2) soit des modifications anatomiques spécifiques (réduction d'emphysème par voie endoscopique).

I-2. Les facteurs de risque

Au niveau mondial, la pollution atmosphérique est la première cause du développement de la BPCO^{11,12}. Notamment, il a été montré que diminuer le taux de NO₂ ambiant et de PM_{2.5} (Particulate Matter) atténuait le risque d'un développement pulmonaire altéré¹³. Mais, dans les pays développés, le tabagisme actif et/ou passif reste la principale cause de cette pathologie avec 90 % des cas alors que dans les pays à faibles revenus, ce sont plutôt les pollutions domestiques et industrielles (biomasse, silice, charbon) qui sont en cause.

Par contre, seuls 20 à 25 % des fumeurs développent cette maladie, suggérant ainsi l'existence de facteurs de prédispositions génétiques, épigénétiques et l'intervention de facteurs environnementaux^{14,15}. Ceci permet de suspecter une susceptibilité très hétérogène dans cette

maladie et l'existence de facteurs ou mécanismes de protection et/ou de réparation efficaces dans les lésions causées par le tabac chez les fumeurs ne développant pas cette maladie.

a- Origine Génétique

La déficience en alpha 1 anti-trypsine est connue comme constituant un risque majeur de développer la BPCO¹⁶. Cette enzyme sécrétée par le foie protège les poumons de produits toxiques comme la fumée de cigarette. Mais ce déficit est relativement rare, il ne correspondrait qu'à environ 1 % des patients atteints de BPCO. D'autres gènes comme le MMP-12 (metalloprotéinase 12)¹⁷ et le glutathion S-transférase¹⁸ semblent aussi reliés au déclin de la fonction pulmonaire ou au risque de développer une BPCO. D'autres polymorphismes ont aussi été évoqués comme pouvant être la cause de cette maladie, notamment celui affectant un gène codant pour le complexe télomérase¹⁹ ou les gènes codant pour des alarmines²⁰.

b- Origine Pédiatrique

L'origine pédiatrique avec le développement pulmonaire est aussi un déterminant dans cette maladie²¹. L'acquisition d'une fonction respiratoire maximale à l'âge adulte est conditionnée par le développement pulmonaire dans l'enfance. De plus, les processus présents durant la gestation (l'exposition du fœtus au tabac pendant la grossesse affecterait le développement *in utero*), la naissance, les expositions durant l'enfance et l'adolescence, les infections respiratoires de la petite enfance sont autant d'éléments qui affectent le développement pulmonaire^{22,23}. L'étude de Lange et al. permet de mettre en évidence l'importance des racines pédiatriques de la maladie chez les patients développant une BPCO à l'âge adulte avec une fonction respiratoire initiale altérée mais sans déclin accéléré²⁴ (Figure 2). Ceci remet en question le diagramme de Fletcher où le déclin paraissait aussi inéluctable que systématiquement caractéristique de la maladie²⁵.

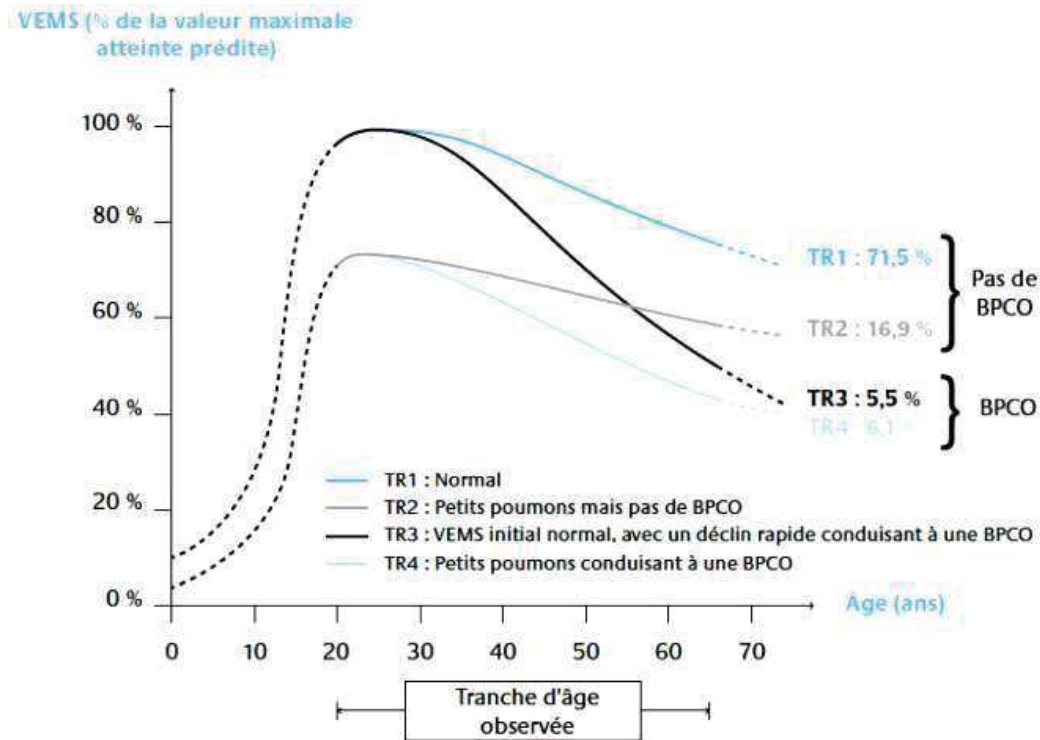


Figure 2 : Trajectoires fonctionnelles respiratoires susceptibles d'aboutir au développement d'une BPCO^{24,14}

c- Les réponses inflammatoires

Les réponses inflammatoires bronchiques exagérées ainsi que leur persistance après l'arrêt du tabac chez les patients atteints de BPCO suggèrent une prédisposition génétique (polymorphisme des alarmines) et une autonomisation de cette dernière qui pourrait s'expliquer par l'acquisition de modifications épigénétiques affectant les alarmines retrouvées augmentées chez les patients atteints de BPCO^{26,27}.

Par conséquent, la cause de cette maladie semble plutôt être une association de plusieurs facteurs ce qui explique l'hétérogénéité des phénotypes cliniques et inflammatoires observés chez les patients BPCO et la difficulté actuelle à trouver un traitement curatif²⁸.

I-3. Les traitements actuels

Cette maladie est très hétérogène aussi bien au niveau des facteurs la déclenchant qu'au niveau de la susceptibilité des patients. Mais, pour tenter de faire face à cette maladie, des mesures de type préventives et symptomatiques ont été mise en place pour essayer de diminuer la fréquence des exacerbations et ralentir le déclin de la fonction respiratoire. Les mesures actuelles passent par un sevrage tabagique, des bronchodilatateurs de courte et de longue durée d'action, et des corticoïdes inhalés, selon le stade de la maladie et le nombre d'exacerbations annuelles. L'oxygénothérapie et la réhabilitation respiratoire peuvent aussi être prescrites dans les cas les plus sévères. Mais, la totalité des traitements disponibles ne permettent pas de guérir la BPCO, car ces traitements ne ciblent pas la cause de la maladie mais les conséquences de celle-ci²⁹.

Par conséquent, ces dernières années, des recherches de nouvelles cibles thérapeutiques via la compréhension des mécanismes physiopathologiques, sont en cours. Notamment, des essais cliniques tentent de cibler la réponse inflammatoire exagérée des patients avec des anti-cytokines ciblant soit le bas (IL5³⁰, IL13³¹) soit le haut (IL33, TSLP)³² de la cascade immunitaire. Ces cytokines augmentées chez les patients atteints de BPCO sont sécrétées soit directement par les cellules épithéliales comme les alarmines (IL33 et TSLP) soit indirectement après l'activation de la cascade immunitaire (IL5 et IL13)³³.

Les cellules épithéliales semblent être le chef d'orchestre de cette cascade inflammatoire et ainsi jouer un rôle important dans cette maladie¹. Pouvoir agir sur les alarmines sécrétées comme sur l'épithélium bronchique semblent de futures pistes thérapeutiques intéressantes dans cette maladie.

II- Phénotype et plasticité de l'épithélium

II-1. Des voies aériennes proximales à distales

L'arbre bronchique est composé de différentes parties : les voies aériennes supérieures et inférieures. Les voies aériennes supérieures sont composées de la cavité nasale, des sinus, du pharynx et du larynx. Elles sont le premier filtre de l'air inspiré grâce au mucus et aux nombreux cils présents dans les cavités. Notamment, ce couple cils-mucus permet de filtrer l'air inspiré en ôtant tout ce qui est néfaste comme les poussières. Cette partie permet également de réchauffer et d'humidifier l'air. Les voies aériennes inférieures, elles, correspondent à l'ensemble qui va de la trachée jusqu'aux bronchioles terminales. Les voies aériennes supérieures comme inférieures ont un rôle commun de conduction de l'air oxygéné de la cavité nasale jusqu'aux sacs alvéolaires (lieu des échanges gazeux) lors de l'inspiration et l'évacuation de l'air riche en dioxyde de carbone lors de l'expiration³⁴.

II-2. L'épithélium respiratoire

L'épithélium respiratoire des voies aériennes est en contact permanent avec de multiples agressions contenues dans l'air inspiré comme les produits toxiques, les agents pathogènes tels que les bactéries ou les virus. Mais cet épithélium est capable d'éliminer l'essentiel de ces différentes agressions grâce à son appareil mucociliaire composé du mucus et des cils présents à la surface de l'épithélium des voies aériennes²².

Pour répondre à ses différents rôles/fonctions, l'épithélium est composé de différents types cellulaires dont leur nombre (et pour certaines leurs fonctions) peut varier en fonction de la localisation de l'épithélium dans l'arbre bronchique. Ces différents types cellulaires sont : les cellules basales, les cellules Club, les cellules ciliées, les cellules neuroendocrines et les cellules caliciformes (Figure 3). En plus de la composition cellulaire, l'épaisseur et le type de cet épithélium varient aussi en fonction de sa localisation dans l'arbre bronchique (Figure 3). Chez l'homme, l'épithélium est de type pseudo-stratifié de la trachée jusqu'aux bronchioles avec toutes les cellules d'ancrées sur la membrane basale. Au niveau bronchiolaire, l'épithélium est d'abord cylindrique pseudo-stratifié puis il va évoluer au niveau des bronchioles terminales en

un épithélium cuboïde monocouche constitué théoriquement seulement de cellules ciliées et de cellules Club. Pour finir, au niveau des alvéoles, l'épithélium est de type pavimenteux simple, constitué de pneumocytes de type I (PNI) et de type II (PNII). Cet épithélium repose sur une membrane basale puis sur un chorion dans lequel sont localisés le muscle lisse, les glandes et le cartilage. Par contre, comme présenté dans la figure 3, cet épithélium va varier en fonction des espèces. On remarque qu'entre la souris et l'homme, le type d'épithélium et sa composition cellulaire ne sont pas les mêmes pour la même localisation dans l'arbre bronchique³⁵.

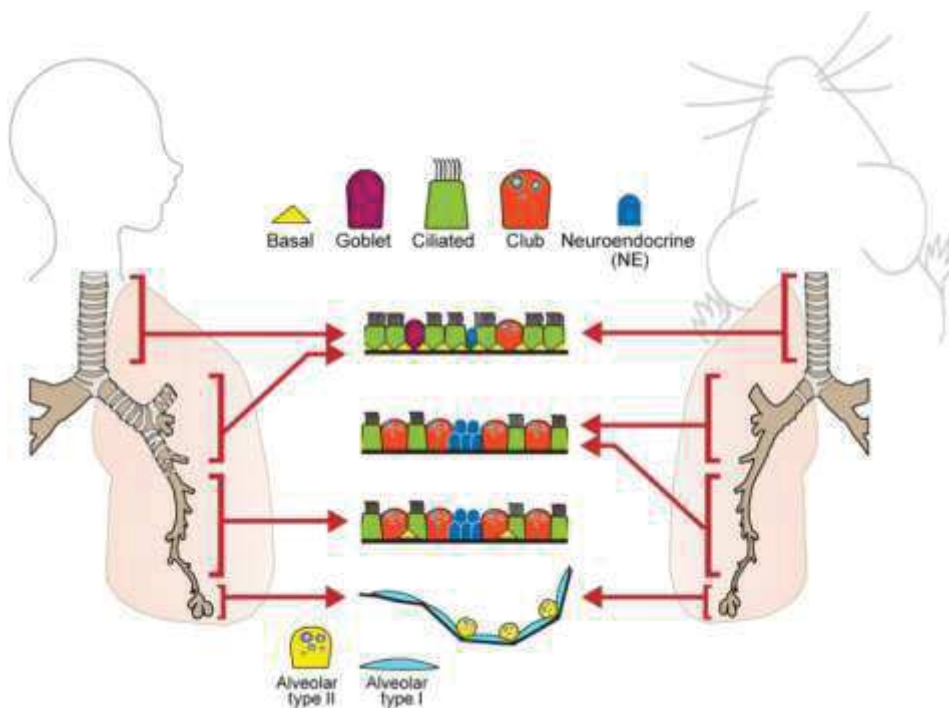


Figure 3 : Composition cellulaire des différentes divisions de l'arbre bronchique chez l'homme et la souris³⁵

II-3. Les différents types cellulaires composant l'épithélium des voies aériennes

Les cellules épithéliales retrouvées dans l'épithélium des voies aériennes se développent grâce à des voies de signalisations connues pour être impliquées dans le développement embryonnaire comme la voie Wnt³⁶ et la voie Notch^{35,37}. De ces voies de signalisations naissent les différents types cellulaires dont leur nombre dans l'épithélium différencié peut varier entre les sujets sains et les sujets malades. La modulation des voies de signalisation débouchant sur les différents types cellulaires sera abordée dans un prochain paragraphe.

a- Les cellules basales

Les cellules basales, de forme ovoïde, sont celles qui reposent sur la membrane basale sans jamais être en contact avec la lumière bronchique. Leur nombre va varier en fonction de l'épaisseur de l'épithélium. Elles sont considérées comme les cellules progénitrices de l'épithélium respiratoire c'est-à-dire qu'elles sont capables de proliférer et de se différencier dans tous les autres types cellulaires présents dans un épithélium différencié des voies aériennes^{38,39}. Elles assurent aussi la cohésion de l'épithélium respiratoire en se liant aux cellules voisines via des desmosomes et elles s'ancrent à la membrane basale grâce aux hémidesmosomes⁴⁰.

b- Les cellules ciliées

Les cellules ciliées, de forme prismatique, sont caractérisées par la présence à leur pôle apical de cils, environ 200 à 300 cils par cellule⁴¹. Ces cils forment un mouvement rotatoire synchrone pour assurer la fonction de clairance mucociliaire permettant d'éliminer les agents pathogènes ainsi que le mucus tapissant l'épithélium des voies aériennes. Ce sont les cellules les plus nombreuses dans l'épithélium à l'état physiologique avec un ratio estimé de cinq cellules ciliées pour une cellule caliciforme chez le sujet sain⁴². Mais, dans le cas de la BPCO, ce ratio cellules ciliées sur cellules caliciformes est réversé avec aussi bien une diminution du nombre de cellules ciliées qu'une augmentation du nombre de cellules caliciformes⁴³.

Les cellules ciliées ont été considérées pendant longtemps comme un stade ultime de différenciation de l'épithélium, issues de cellules progénitrices, comme les cellules basales⁴⁴ ou les cellules Club⁴⁵ et ne pouvant plus se différencier.

c- Les cellules caliciformes

Les cellules caliciformes, de forme prismatique, (aussi appelées cellules à mucus ou cellules en gobelet) sont des cellules sécrétrices⁴⁶ de l'épithélium des voies aériennes. Elles sont responsables de la production de mucus tapissant cet épithélium. Ce mucus est localisé dans des vésicules de sécrétion situées au pôle apical de la cellule. Il est composé principalement de

glycoprotéines de haut poids moléculaire appelées mucines (MUC) qui peuvent être de différents types dont les principales sont MUC5AC et MUC5B. Par contre, il existe aussi d'autres mucines qui n'interviennent pas dans la constitution du mucus comme MUC7 ou MUC19.

Le mucus joue un rôle de barrière physico-chimique notamment par le biais de la clairance des agents exogènes inhalés mais également dans l'immunité innée vis-à-vis des virus et des bactéries. Lors d'une agression des voies aériennes, ce mucus est produit plus rapidement et en plus grande quantité par les cellules caliciformes. Notamment, chez les patients atteints de BPCO, cette production de mucus est augmentée et le nombre de cellules à mucus est lui aussi augmenté comparé aux sujets sains notamment par la prolifération de ces cellules caliciformes^{47,48}.

d- Les cellules neuroendocrines

Les cellules neuroendocrines sont des cellules sécrétrices rares (1 pour 2500 cellules épithéliales) mais elles sont considérées comme prédominantes au niveau de l'épithélium bronchiolaire⁴⁹. Elles se retrouvent soit isolées, soit regroupées sous forme d'îlots innervés, nommés corpuscules neuro-épithéliaux (NEB)⁵⁰. Leurs sécrétions contiennent des amines bioactives et des peptides dont la sérotonine, la calcitonine, le peptide libérant la gastrine (GRP) ou encore la CGRP (calcitonine gene-related peptide). Ces produits de sécrétion ont pour cible les cellules adjacentes ou les structures sous-jacentes à la membrane basale. Par contre, lorsque l'épithélium bronchiolaire est chroniquement lésé, sa régénération est associée à une augmentation du nombre de cellules neuroendocrines regroupées sous forme de corpuscules NEB⁵¹.

e- Les cellules Club

Une prochaine partie sera consacrée aux cellules Club.

II-4. L'épithélium des voies aériennes dans la BPCO

L'épithélium des voies aériennes est composé des différents types cellulaires, présentés ci-dessus, mais leur nombre dans l'épithélium peut varier dans des cas pathologiques et notamment dans la BPCO. Dans cette maladie, l'agression chronique de l'épithélium par des agents irritants comme le tabac peut provoquer un processus inflammatoire exagéré et accru chez les patients, même après l'arrêt du tabac. Ces mécanismes physiopathologiques complexes sont encore méconnus, mais ils conduisent à des modifications physiopathologiques touchant l'épithélium des voies aériennes, le parenchyme pulmonaire et la vascularisation pulmonaire. Toutes ces modifications provoquent notamment le remodelage des voies aériennes avec des éléments caractéristiques de cette maladie comme l'hyperplasie des cellules à mucus, la diminution du nombre de cellules ciliées, le déficit en cellules Club, la métaplasie squameuse, une fibrose péribroncholaire, une destruction des parois alvéolaires et une inflammation chronique de type T1 ou T2 (Figure 4)^{52,53}.

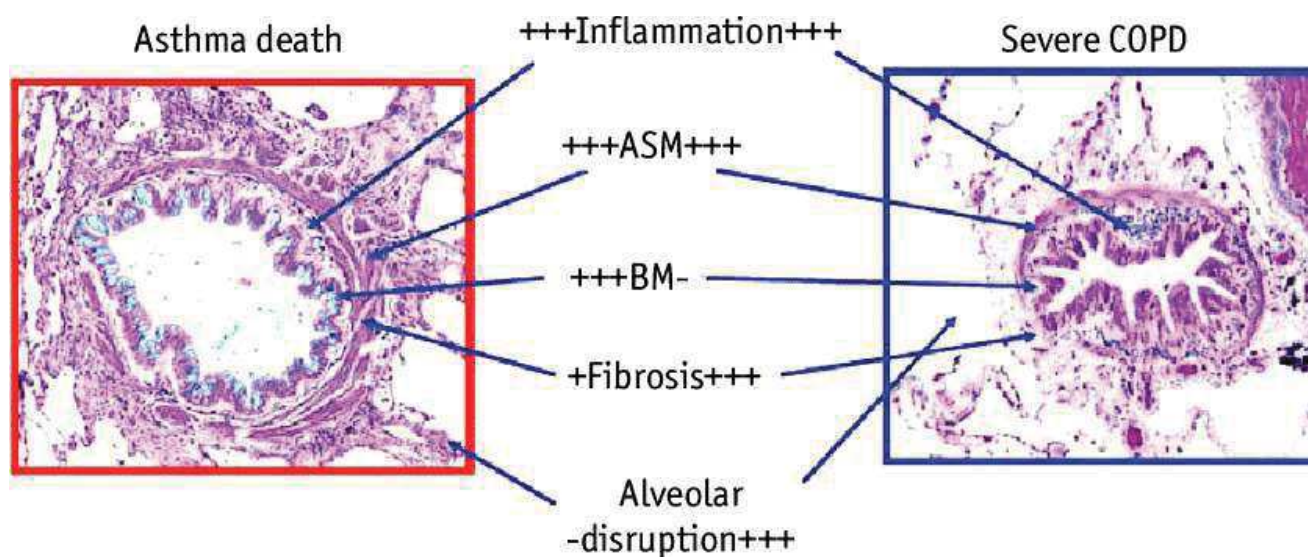


Figure 4 : Modifications physiopathologiques retrouvées dans la BPCO^{52,53}

Pour expliquer ces modifications physiopathologiques, l'agression des cellules épithéliales par la fumée de cigarette va provoquer un changement d'expression de certains gènes présents dans ces cellules épithéliales permettant ainsi la sécrétion de cytokines (type alarmines T1/T2) qui vont pouvoir indirectement provoquer des modifications au niveau de l'épithélium pulmonaire⁵⁴. Il a

aussi été mis en évidence que l'épaississement de l'épithélium contribuait à la diminution du diamètre de la lumière des voies aériennes et que cela était corrélé au déclin de la fonction respiratoire au cours du temps. De plus, l'épithélium squameux promeut la fibrose péribronchiolaire via la sécrétion d'interleukine-1 β (IL-1 β).

Une autre manifestation clinique présente chez les patients BPCO est l'hyperplasie des cellules caliciformes obtenue potentiellement par le biais de l'interleukine 13 (IL13), ou par des gènes tels que SPDEF, XBP1 et CREB3L1⁵⁵. Ce mucus sécrété contribuerait aussi à l'obstruction de la lumière bronchique par des exsudats muco-inflammatoires (Figure 5), d'autant plus qu'il est observé une diminution du nombre de cellules ciliées dans l'épithélium des voies aériennes. Ce changement de ratio cellulaire semble impliqué dans la baisse de la clairance mucociliaire et donc dans l'obstruction bronchique retrouvée chez ces patients.

De plus, pour expliquer le versant inflammatoire de la BPCO, les cellules épithéliales des petites voies aériennes agressées par la fumée de tabac et/ou la pollution sont capables de sécréter des cytokines notamment de type alarmines (TSLP, IL33, IL25 et IL8). Ces dernières favorisent le recrutement de cellules inflammatoires telles que les macrophages, les lymphocytes T CD8⁺, les ILC2, les neutrophiles et les éosinophiles formant un exsudat inflammatoire qui participe lui aussi à l'obstruction des voies aériennes distales.

Pour finir, le déficit en cellules Club peut contribuer à ce phénomène inflammatoire car la protéine CCSP (Club Cell Secretory Protein) qu'elle sécrète est aussi retrouvée diminuée chez les patients BPCO. Il a été montré au sein de l'équipe que le neutrophile est attiré par l'IL8 recombinant mais que ce chimiotactisme est réduit par l'addition de CCSP recombinant⁵⁶. De ce fait, le phénomène inflammatoire ne peut être inhibé chez les patients BPCO.

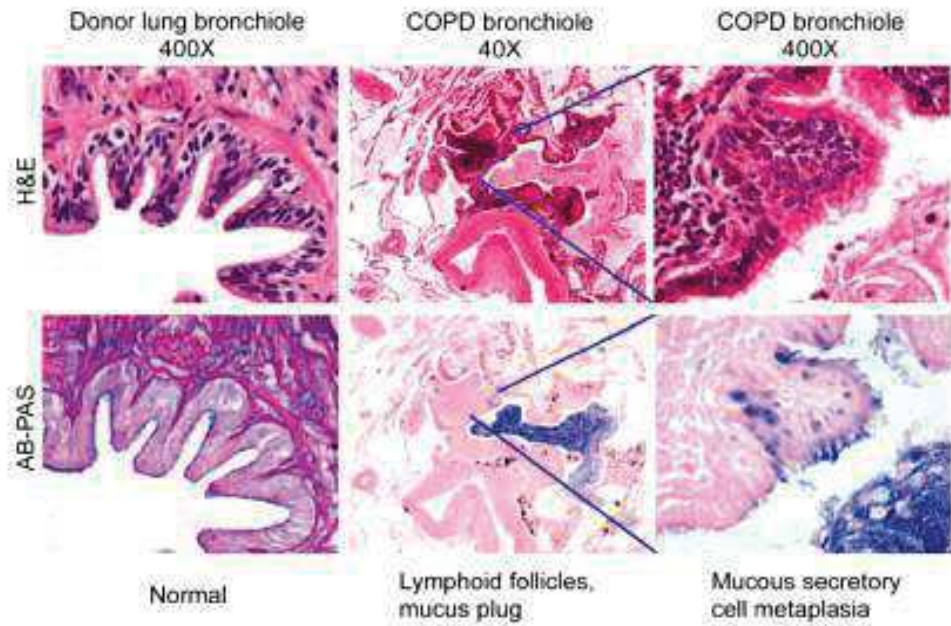


Figure 5 : Accumulation de mucus dans les bronchioles des patients BPCO⁵²

Pouvoir moduler ces changements de ratios cellulaires chez les patients atteints de BPCO est une potentielle piste thérapeutique car restaurer un épithélium sain avec le bon ratio de cellules ciliées, cellules à mucus et cellules Club pourrait limiter la progression de la maladie voire la réverser.

II-5. La modulation du phénotype épithélial dans les voies aériennes

a- Voie Notch

La voie de signalisation Notch est essentielle pour déterminer le devenir cellulaire dans de nombreux tissus, dont le poumon, au cours du développement et chez l'adulte (Figure 6). Dans le poumon en cours de développement, et notamment dans les voies aériennes supérieures, la voie de signalisation Notch contrôle le destin des cellules basales en cellules ciliées, sécrétoires et neuroendocrines en limitant le destin cilié et en favorisant le destin sécrétoire³⁷. Dans le poumon adulte, la voie Notch régule le choix du devenir cellulaire et le renouvellement des cellules basales⁵⁷ (Figure 6). Elle permet également de maintenir le statut de différenciation des cellules sécrétoires comme les cellules Club.

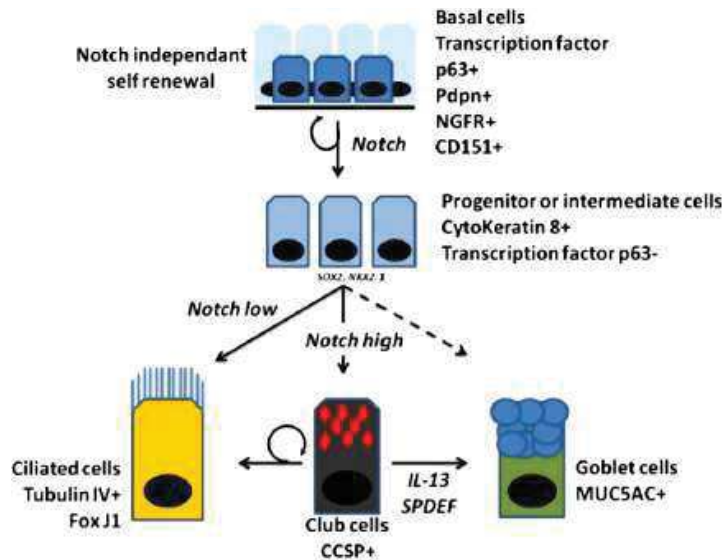


Figure 6 : Les étapes de différenciation des cellules épithéliales des voies aériennes⁵⁸

Par contre, lorsque l'on bloque la signalisation Notch-Jagged 1/ 2, on favorise la différenciation des cellules Club en cellules ciliées. Un anticorps monoclonal IgG1 qui se lie à Jagged-1 permet de réduire la différenciation des cellules caliciformes et induit une différenciation ciliée ce qui permet de reverser le remodelage de l'épithélium des voies aériennes murins modélisant la BPCO⁵⁹. Une molécule commercialisée permet le blocage de la voie Notch, le DapT, qui est un inhibiteur de la gamma-sécrétase (Figure 7).

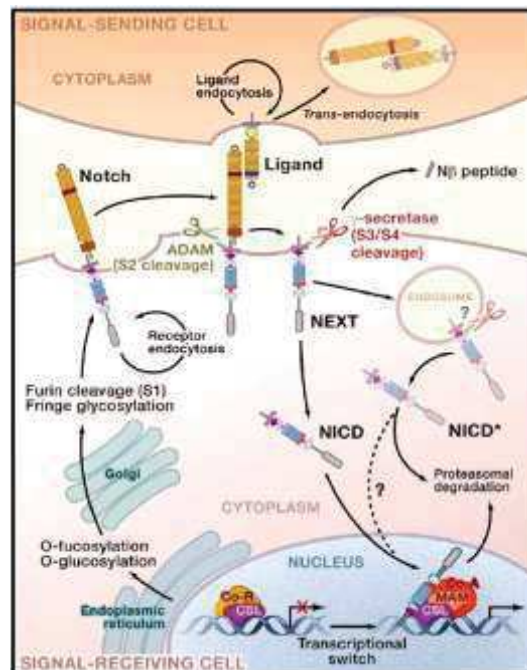


Figure 7 : Voie de signalisation Notch⁶⁰

L'inhibition de la voie Notch pourrait contribuer à augmenter le nombre de cellules ciliées au détriment des cellules sécrétoires comme les cellules à mucus dans l'épithélium des voies aériennes des patients BPCO.

b- Voie ROCK

La voie de signalisation ROCK semble jouer un rôle important dans cette différenciation épithéliale. Notamment l'inhibition de ROCK, par une molécule commercialisée, le Y27632, permet d'améliorer la prolifération des cellules épithéliales trachéales humaines et murines sans affecter le processus de différenciation en culture ALI⁶¹ (Air Liquid Interface). L'inhibition de cette voie pourrait permettre d'aider à la prolifération et donc au renouvellement des cellules épithéliales des voies aériennes.

c- Voie BMP

Les protéines morphogénétiques osseuses (BMP) sont un groupe de molécules de signalisation appartenant à la famille du TGF β (Figure 8). La voie BMP/TGF β régule notamment la prolifération cellulaire et la différenciation. Dans la voie de signalisation BMP, le BMP4 est une molécule impliquée dans le développement pulmonaire⁶². Au niveau distal, cette molécule pourrait être un régulateur négatif à la prolifération et à la différenciation des cellules épithéliales. Le LDN 193189 est un puissant inhibiteur de cette voie de signalisation BMP. Inhiber cette voie pourrait favoriser la différenciation cellulaire et ainsi aider à la restauration d'un épithélium « sain ».

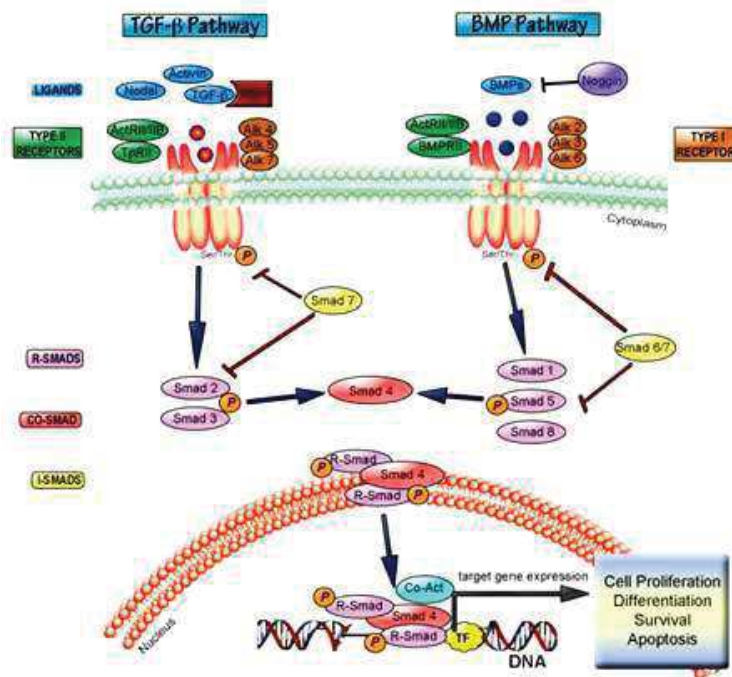


Figure 8 : Voie de signalisation TGFβ/BMP

Toutes ces voies de signalisations (Figure 9) jouent un rôle clé dans la modulation du destin des cellules composant l'épithélium des voies aériennes. Pouvoir moduler ces voies de signalisation, en les activant ou en les réprimant par les différentes molécules citées précédemment, pourrait être une piste thérapeutique dans la BPCO notamment en essayant de reformer un épithélium différencié « normal » comprenant les bons ratios cellulaires.

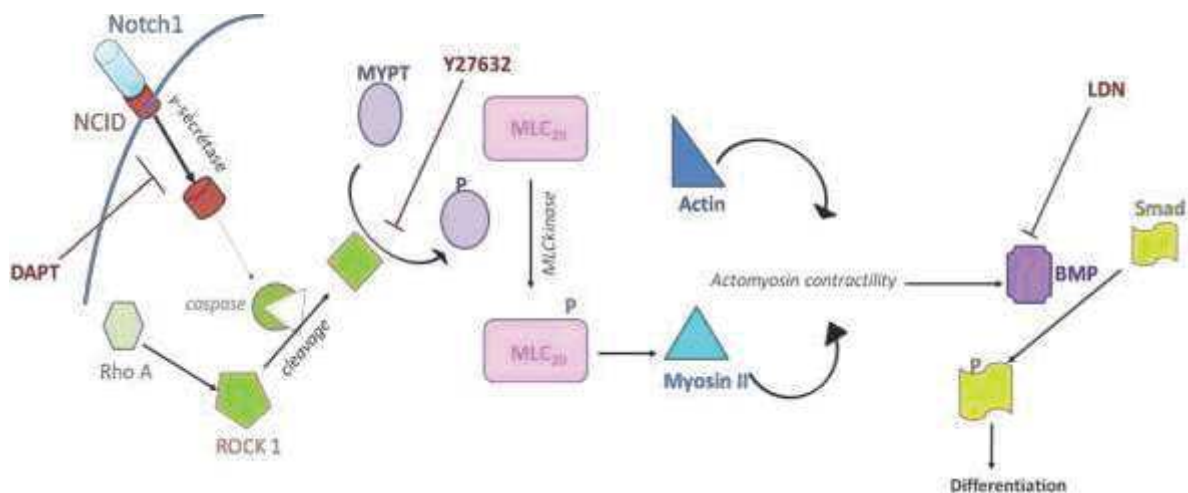


Figure 9 : Schéma récapitulatif des cibles des différents inhibiteurs commercialisés

III- Les cellules Club

Ces cellules ont été identifiées pour la première fois par Kölliker en 1881 comme étant un type cellulaire distinct, d'un point de vue morphologique et histochimique⁶³. Mais ce n'est qu'en 1937 que Max Clara décrit ce qui semble être le même type cellulaire que celui décrit en 1881 et lui donne ainsi son nom : cellules de Clara⁶³. Par contre, en 2013, un consortium scientifique décide de changer leur nom pour cellules « Club » pour des raisons éthiques.

III-1. L'origine des cellules Club

La plus grande proportion des études faites pour comprendre l'origine de ces cellules ont été réalisées sur le modèle murin car leur épithélium est constitué en grande partie de ces cellules⁶⁴. Par contre, il est à noter que l'épithélium murin est très différent de celui de l'humain par sa composition comme par sa proportion cellulaire.

Le développement de ces cellules dans l'épithélium des voies aériennes serait modulé par les voies de signalisation Wnt⁶⁵ et Notch⁶⁶. Notamment, des études ont montré que l'inhibition du récepteur Jagged par des ligands Jag1 et Jag2 induisait une différenciation ciliaire avec une perte presque complète des cellules Club⁵⁷. Ceci corrèle avec des résultats récents obtenus dans le modèle murin, par l'utilisation d'un anticorps anti-Jagged-1, qui permet de favoriser une différenciation ciliaire au détriment des autres types cellulaires comme les cellules Club⁵⁹. Pour la voie de signalisation Wnt, chez la souris, une forme stabilisée de la bêta-caténine est exprimée spécifiquement dans les cellules CCSP positives ce qui corrèle avec une maturation fonctionnelle par cette voie de signalisation durant le développement prénatal⁶⁵.

Par contre ces cellules Club se retrouvent déficitaires dans certaines pathologies, notamment dans la BPCO, donc impacter ces voies de signalisation importantes pour leur développement semblent être une piste prometteuse pour tenter de les restaurer dans l'épithélium des voies aériennes des patients BPCO⁶⁷.

III-2. Déficit des cellules Club dans l'épithélium bronchique des patients BPCO

Dans des cultures ALI (Air Liquid Interface) de cellules épithéliales bronchiques humaines, obtenues à partir de biopsies de patients atteints de BPCO, de fumeurs et de sujets sains, il a été montré qu'il existait une diminution de la quantité de ces cellules Club chez les sujets BPCO comparés aux sujets sains. Par contre, lorsque une culture de cellules épithéliales de sujet BPCO est supplémentée avec du CCSP recombinant, la libération d'IL8 induite par le tabac, caractéristique de la BPCO, est diminuée et retrouvée équivalente à celle des sujets sains et des fumeurs⁶⁸. De plus, dans l'épithélium des voies aériennes des patients atteints de BPCO, les cellules Club sont déficitaires comparés aux sujets sains⁶⁹ (Figure 10)

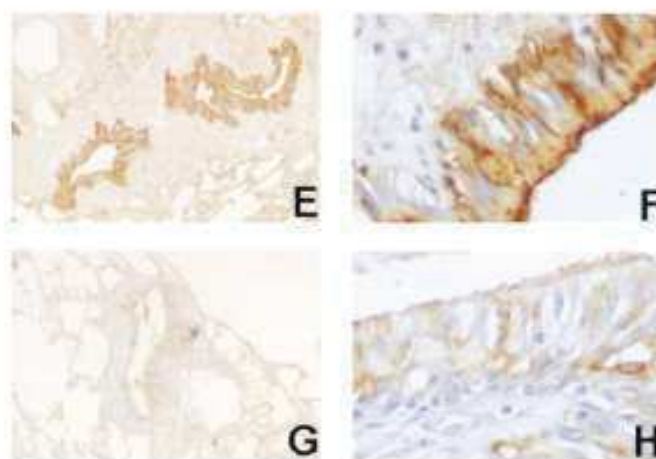


Figure 10 : Expression de la protéine CCSP au niveau des petites voies aériennes de sujets témoins (E, F) et de patients BPCO (G,H)⁶⁹

Au niveau du LBA (Lavage Broncho Alvéolaire) et du sang, la libération de CCSP est diminuée chez les sujets fumeurs comparés aux non fumeurs⁷⁰. Cette différence pourrait s'expliquer par des modifications épigénétiques, notamment une étude a montré que la fumée de cigarette altérait la méthylation de l'ADN des petites voies aériennes⁷¹. Le gène CCSP, lui, est retrouvé hyper méthylé chez les fumeurs ce qui pourrait contribuer au faible taux de CCSP retrouvé dans le LBA et dans le sang des fumeurs et des patients BPCO. Ce déficit en protéine CCSP est aussi mis en évidence dans les surnageants d'expectorations induites des patients BPCO comparés à des fumeurs sans trouble ventilatoire obstructif⁷². Par ailleurs, il a été montré chez les fumeurs souffrant ou non de la BPCO, qu'il existait une corrélation positive entre le déficit en CCSP dosé

dans les expectorations induites et le déficit du nombre de cellules Club dans l'épithélium bronchiolaire de ces mêmes sujets. Pour finir, dans l'étude ECLISPE, le déclin accéléré de la fonction respiratoire était corrélé au taux de protéine CCSP dans le serum⁷³.

Toutes ces données suggèrent que la BPCO est caractérisée par un déficit en cellules Club et en sa protéine CCSP. Son rôle anti-inflammatoire serait une potentielle arme thérapeutique dans cette pathologie où il existe une inflammation chronique accrue et exagérée.

Pouvoir restaurer ces cellules dans l'épithélium des patients BPCO pourrait être une aide pour réverser ou tout du moins limiter la progression de cette maladie.

III-3. Fonctions des cellules Club

La proportion de ces cellules ainsi que leur fonction varient avec leur localisation dans l'arbre bronchique humain. Au niveau des bronches et des bronchioles terminales, ces cellules représentent 11 % à 22 % des cellules épithéliales⁷⁴. Elles sont, de forme cubique, dépourvues de cils, avec une région apicale de forme arrondie remplie de granules de sécrétion, formant un dôme caractéristique de ces cellules.

a- Fonction de prolifération/différenciation

Les cellules Club ont un rôle dans la prolifération/différenciation épithéliale mais leur contribution est variable en fonction de leur localisation dans l'arbre bronchique. Au niveau distal, elles contribuent à la prolifération épithéliale de l'ordre de 15 à 44 % durant le renouvellement normal des voies aériennes⁷⁴. Dans ce processus, on dit que ces cellules ont un rôle de progéniteur accessoire c'est-à-dire qu'à l'état basal, elles jouent leur rôle de cellules Club mais, si nécessaire elles seraient capables de changer de phénotype pour rentrer dans un état prolifératif et se différencier dans les autres types cellulaires constituant l'épithélium des voies aériennes (phénomène de transdifférenciation). Ce processus de prolifération permettrait de maintenir le pool de cellules progénitrices accessoires, autrement dit de « s'auto-renouveler » mais aussi de restaurer les autres cellules différenciées (notamment les cellules ciliées et les cellules à mucus) dans l'épithélium des voies aériennes⁵⁸. Par contre, au niveau proximal, la cellule Club contribue directement comme progéniteur à la réparation de l'épithélium^{45,75}.

b- Fonction de métabolisme des xénobiotiques

Au niveau bronchique, les cellules Club ont aussi un rôle de protection de l'épithélium face aux agents toxiques grâce à leur contenu cellulaire constitué de taux importants de glutathion (GHS)⁷⁶ et de cytochrome (CYP) P450⁷⁷. De nombreuses études réalisées, dans le modèle murin, ont montré le rôle de ces cellules dans le métabolisme des toxiques via son activité Cyp2f2^{78,79}. Notamment, ce rôle a été démontré dans des modèles de souris exposés au naphthalène provoquant la déplétion des cellules Club. Les cellules Club sont capables de biotransformer le naphthalène en formant des espèces réactives qui entraînent une peroxydation lipidique, une oxydation de l'ADN provoquant une vacuolisation, une exfoliation et une nécrose de ces cellules Club. Cependant Cyp2f2 n'existe pas chez l'homme, c'est Cyp2f1 qui possède une activité métabolique semblable à Cyp2f2 mais moins forte⁸⁰, ne permettant pas de réaliser des modèles de déplétion de ces cellules Club pour étudier l'impact de leur perte dans l'épithélium des voies aériennes humaine.

c- Fonction de sécrétion

Les cellules Club sécrètent plusieurs types de protéines comme les protéines du surfactant (SP)-A, SP-B et SP-D, ou encore SCGB3A2⁸¹, possédant des propriétés tensio-actives, anti-inflammatoires et d'immunité innée. Elles sécrètent également des protéines jouant un rôle de protection de l'intégrité pulmonaire⁸², notamment des médiateurs endogènes anti-inflammatoires contenus dans des granules denses, comme la protéine CCSP⁸¹ (Club Cell Secretory Protein), encore appelée Club Cell (CC)-10⁸³ ou Secretoglobin(SCGB)1A1. Par ces sécrétions protéiques, ces cellules participent à la protection des voies respiratoires notamment grâce à leur capacité de détoxification des substances xénobiotiques mais aussi par leur rôle anti-inflammatoire. Ce rôle de modulation des processus inflammatoires peut aussi s'expliquer par la localisation du gène codant pour le CCSP au niveau du locus 11q12.3-q13.1, région où il existe d'autres gènes impliqués dans la régulation de l'inflammation. Enfin, ces cellules semblent également impliquées dans la sécrétion de mucines⁸¹.

Pour finir, des données récentes de single-cell RNA seq réalisées à partir de cellules épithéliales bronchiques humaines ont permis de mettre en évidence d'autres potentielles fonctions de ces cellules comme des fonctions antibactériennes (Lipocaline 2, Lysozyme), des fonctions

immunitaires (CD (Cluster Differentiation)⁵⁵, CD46, C3), des sécrétions de cytokines (CXCL(C-X-C motif ligand)¹⁷, CXCL1, CXCL6), des fonctions antiprotéases (SLPI (Secretory Leukocyte Peptidase Inhibitor), SERPINA1 (Serpine peptidase inhibitor, clade A (alpha-1 antiprotease, antitrypsin), member 1)) et une fonction de barrière (Claudin 1 et 4, Catenine, MUC5B)⁸⁴.

III-4. La protéine CCSP

Actuellement, le CCSP est la seule protéine qui permet de définir spécifiquement les cellules Club. Par contre, cette protéine possède différents noms en fonction du compartiment où elle a été découverte (blastokinine⁸⁵, utéroglobine⁸⁶) mais aussi en fonction de son poids moléculaire (CC10, CC16). De ce fait, une nomenclature internationale a été mise en place pour définir le nom unique de cette protéine : la SCGB1A1.

C'est un homodimère constitué de sous-unités de 70 acides aminés, jointes de façon antiparallèle par deux ponts disulfures stabilisant le dimère et permettant la formation d'une poche centrale, hydrophobe⁸⁷⁻⁸⁹. Dans cette poche, des molécules peuvent être piégées comme la progestérone⁹⁰, les polychlorobiphényles (PCB)⁹¹, le rétinol, la prostaglandine (PG) D2 ou la PG F2 α . Par conséquent, il serait possible que cette protéine séquestre des substances toxiques dans cette poche ce qui permettrait de réduire leur toxicité cellulaire et faciliterait leur élimination dans la lumière bronchique.

Dans le poumon humain, la sécrétion de CCSP se fait principalement par les cellules Club avec un taux de CCSP dans le LBA de l'ordre de 4 mg/mL⁹² chez les sujets sains. Mais cette protéine est aussi sécrétée dans d'autres compartiments de l'organisme comme l'endomètre et la prostate mais aussi dans le sérum avec un taux de l'ordre de 15 à 40 μ g/mL chez les sujets sains. Le taux de CCSP n'est pas modifié par le sexe, l'indice de masse corporelle⁹³ ou la quantité de lipides mais il est influencé par le statut tabagique^{70,94} et le rythme nyctéméral.

III-5. Modèles d'études des cellules Club et de sa protéine

Plusieurs modèles murins ont été mis en place pour tenter d'étudier et comprendre le rôle de la protéine CCSP dans cet épithélium constitué principalement de cellules Club.

Un premier modèle murin CCSP^{-/-}, déficient en protéine CCSP, est associé à des changements structuraux au niveau des cellules Club. Ces cellules ont une diminution du nombre de granules de sécrétion, une réduction du réticulum rugueux, des altérations au niveau de l'appareil de Golgi. De plus, la composition du liquide de surface des voies respiratoires de ces souris⁹⁵ semble altérée ce qui peut suggérer une plus grande susceptibilité des cellules épithéliales aux agressions extérieures. Lorsque ces souris sont exposées à une infection virale ou à des pathogènes extérieurs tels que *Pseudomonas aeruginosa*, leur réponse inflammatoire est plus importante avec un taux de cytokines pro-inflammatoires et chimiokines augmentées^{96,97}. Ceci contribue à évoquer un rôle anti-inflammatoire endogène de CCSP.

Un autre modèle de souris C57BL/6 CCSP^{-/-} a permis d'appréhender un peu plus les mécanismes de la BPCO. Notamment, après une exposition à la fumée de cigarette, ces souris présentent une inflammation exagérée avec une métaplasie et une apoptose cellulaire bronchique et alvéolaire augmentée. Mais un traitement, par inhalation de la protéine CCSP, a permis de corriger les effets néfastes de la fumée de cigarette. Avec ce modèle, il a été montré que cette protéine CCSP peut modifier le risque de développer les caractéristiques de la BPCO⁹⁸.

En parallèle de ces modèles, les cellules épithéliales de souris et notamment les cellules Club ont été caractérisées par une méthode de Single-cell RNA seq. A l'aide de cette méthode, la carte d'identité de ces cellules a été obtenue notamment différents marqueurs de surface qui permettent d'isoler les cellules Club viables⁹⁹. L'épithélium murin et humain sont différents ce qui fait que les marqueurs obtenus chez la souris ne peuvent pas forcément être transposés à l'humain ce qui signifie que la carte d'identité de la cellule Club murine sera différente de la cellule Club humaine.

Les cellules Club semblent être une potentielle cible thérapeutique dans la BPCO. Mais chez l'homme peu d'étude ont été réalisées. Actuellement, les études ayant permis d'obtenir la carte d'identité des cellules Club chez la souris ainsi que leur déplétion spécifique par le naphthalène ne peuvent être transposées chez l'homme. La seule protéine permettant de définir des cellules Club humaine est sa protéine intracellulaire, le CCSP, mais l'utilisation de ce marquage ne permet pas d'obtenir des cellules Club viables. Pour cela, des études de single cell-RNA seq à

partir de cellules épithéliales humaines ont été réalisées^{100,101}. Ces études ont eu pour but de définir la carte d'identité des cellules Club par l'expression de l'ARNm et possiblement trouver un marqueur de surface qui permettrait d'isoler ces cellules Club viables. Mais à partir de ces données, il a été montré que la totalité des cellules épithéliales semblent exprimer l'ARNm CCSP donc trouver la carte d'identité spécifique des cellules Club semble difficile à obtenir¹⁰⁰.

De plus, utiliser l'expression de l'ARNm CCSP signifie de supposer une parfaite corrélation entre l'expression de la protéine CCSP et de son ARNm. Pour autant, cette protéine est très active biologiquement, il est donc préférable de les caractériser par sa protéine et non par son ARNm. Des études transcriptomiques des cellules Club par l'expression de leur protéine CCSP sont donc essentielles pour obtenir la carte d'identité de ces cellules dans l'épithélium des voies aériennes.

III-6. Potentiel thérapeutique

En plus d'avoir des effets anti-inflammatoires dans les différents modèles d'études citées précédemment, le CCSP a aussi des effets « directs » sur les neutrophiles, cellules retrouvées augmentées dans les poumons des patients BPCO. Il a été montré au sein de l'équipe que le CCSP inhibait de manière dose-dépendante le chimiotactisme des neutrophiles stimulés par le fMLP^{56,102}. De plus, des études réalisées chez les chevaux, présentant une obstruction des voies aériennes similaire à de l'asthme, montrent que l'incubation des neutrophiles sanguins et du LBA de chevaux malades avec du CCSP permet de réduire le stress oxydant et leur activité phagocytaire¹⁰³.

Réaliser la carte d'identité des cellules Club par leur expression protéique CCSP est essentielle pour comprendre leurs différentes fonctions et savoir si restaurer cette cellule aurait effectivement un potentiel thérapeutique. En plus de ces fonctions, il serait intéressant de trouver un marqueur de surface pour pouvoir les isoler de manière viable afin d'étudier leurs rôles et sécrétions dans l'épithélium des voies aériennes. Mais, il serait aussi intéressant de tester l'action de CCSP sur le versant T2 retrouvé chez certains patients BPCO car le CCSP possède un rôle plus que certain sur le chimiotactisme des neutrophiles (versant T1).

IV- Pattern inflammatoires dans les voies aériennes

La BPCO est caractérisée par une réponse inflammatoire accrue et exagérée des cellules épithéliales des voies aériennes des patients face à une exposition à la fumée de cigarette, à la pollution, avec une perte de la balance entre tolérance et inflammation ce qui suggère une dérégulation des alarmines sécrétées par les cellules épithéliales. Cette maladie est caractérisée par une inflammation (infiltration des cellules immunitaires) et un remodelage des voies aériennes^{7,10,104}. Ce versant inflammatoire peut être de différents types : T1 avec la sécrétion d'IL8, IL17¹⁰⁵ et la présence de neutrophiles ; ou T2 avec la sécrétion d'alarmines T2 (IL33, TSLP et IL25) et la présence d'ILC2 et d'éosinophiles (Figure 11)¹⁰⁶.

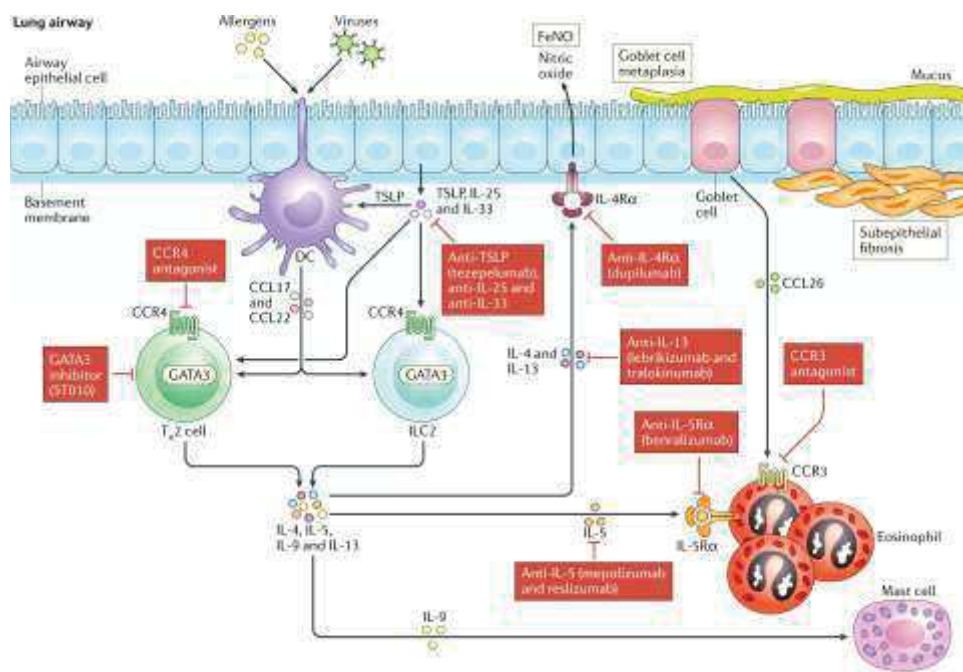


Figure 11 : Versant T2 dans la BPCO¹⁰⁶

Par contre, cette inflammation n'est pas stoppée après l'arrêt du tabac en particulier chez les patients très sévères même s'ils ont arrêté le tabac depuis plusieurs années¹⁰⁷. La raison de cette persistance n'est pas complètement comprise mais ceci pourrait être lié à une augmentation du nombre de cellules T activées incluant les lymphocytes T mémoires qui peuvent perpétuer cette réponse inflammatoire chronique⁵⁴. De plus, il existe une diminution du nombre de lymphocytes T régulateurs (CD4⁺CD25⁺FoxP3) chez les patients BPCO ayant fumé comparé aux sujets sains ce qui peut aussi jouer un rôle dans cette inflammation chronique¹⁰⁸.

Par contre, chez les patients développant une BPCO sans n'avoir jamais fumé, la nature de la réponse inflammatoire n'est pas connue même si des mécanismes comme le stress oxydatif et l'excès de protéases dans les poumons semblent liés à l'inflammation pulmonaire¹⁰⁹.

IV-1. Endotypes T1/T2 dans la BPCO

Chez les patients BPCO, l'endotype inflammatoire correspond à des profils de patients¹¹⁰ c'est-à-dire qu'après une agression, les réponses inflammatoires vont être de différents types : T1, T2.

a- Endotype T1

Le scénario majeur est qu'après une agression, les cellules épithéliales bronchiques vont libérer des médiateurs inflammatoires comme le TNF, IL1 β , IL6 et IL8. La présence d'IL8 et/ou de DAMPs (Damage Associated Molecular Patterns) va faciliter le recrutement des neutrophiles¹⁰. En réponse, les neutrophiles vont libérer un taux important de protéases qui vont causer des dommages épithéliaux. Puis, le système immunitaire adaptatif va se mettre en place avec le recrutement de lymphocytes T de type Th1 et Th17 avec la production respectivement d'IFN γ et d'IL17-A et d'IL17-F. Ceci correspond au versant T1 de la réponse inflammatoire chez les patients BPCO.

On retrouve ce versant T1 chez les patients dont le nombre de neutrophiles est augmenté dans le sputum⁹⁴. De plus, dans les cultures ALI de cellules épithéliales bronchiques humaines, après une stimulation par du CSE (Cigarette Smoke Extract), le taux d'IL8 sécrété est augmenté chez les patients BPCO comparés aux sujets sains⁶⁸.

Cependant, des essais cliniques ont tenté de bloquer cette voie (avec des anticorps anti-CXCR2) sans avoir de résultats thérapeutiques concluants¹¹¹. Ceci suggère que même si ce versant T1 est prédominant chez les patients, d'autres pistes thérapeutiques doivent être explorées.

b- Endotype T2

Chez 10 à 40 % des patients BPCO¹¹², il existe un profil de type T2. Il a été montré que l'augmentation du taux d'éosinophiles aussi bien dans le sputum que dans le sang des patients BPCO est associée à un risque élevé de développer une exacerbation sévère¹¹³. Pour expliquer cette margination des éosinophiles dans les poumons, plusieurs hypothèses peuvent être considérées. Notamment après une agression, l'épithélium sécrète des alarmines T2 de type IL33, IL25 et TSLP¹¹⁴. En réponse, ces cytokines attirent des cellules immunitaires : ILC2 ou cellules dendritiques (DC). Notamment, les ILC2 sont augmentées dans les poumons des patients BPCO¹¹⁵. En réponse, ces cellules sécrètent des cytokines de type T2 comme l'IL5³⁰ et l'IL13, molécules elles aussi retrouvées augmentées chez les patients BPCO. L'IL5 sécrétée, attire à son tour les éosinophiles d'où leur augmentation dans le sputum des patients.

Des essais cliniques dans l'asthme et la BPCO ont ciblé l'IL5 et l'IL13. Dans la BPCO les anti-IL5 n'ont pas donné de résultats définitivement concluants sans être totalement négatifs. La piste des alarmines T2 (IL33, IL25 et TSLP) peut être envisagée pour bloquer en amont de cette cascade immunitaire.

c- Autres endotypes

Les patients BPCO peuvent présenter d'autres endotypes : soit mixte avec à la fois des neutrophiles et des éosinophiles soit pauci granulocytaire sans présence de neutrophiles et d'éosinophiles.

Tout ceci illustre l'hétérogénéité des patterns inflammatoires qui existent dans cette maladie. De plus, des patients avec des données cliniques similaires ne répondent pas toujours de la même manière notamment au niveau du type et du taux de cytokines sécrétées.

IV-2. Alarmines

a- IL33-ST2

IL33 est une cytokine de type IL-1. Elle a été décrite comme une protéine nucléaire nommée NF-HEV (Nuclear Factor from High Endothelial Venules)¹¹⁶. *In vivo*, l'IL33 est une cytokine nucléaire associée à la chromatine. Elle possède un domaine N terminal nécessaire et suffisant pour cette localisation nucléaire¹¹⁷ et son association avec la chromatine mais ce domaine est aussi important pour sa régulation et sa fonction (Figure 12). Pour mieux comprendre le rôle de ce domaine N terminal, conservé au cours de l'évolution, des souris knocked-out pour ce domaine ont été réalisées. Dans le sérum de ces souris, il y a eu une augmentation du taux d'IL33¹¹⁷. Ceci permet de montrer le rôle de ce domaine dans la régulation de l'activité pro-inflammatoire de l'IL33 notamment en agissant contre une libération inappropriée de cette cytokine.

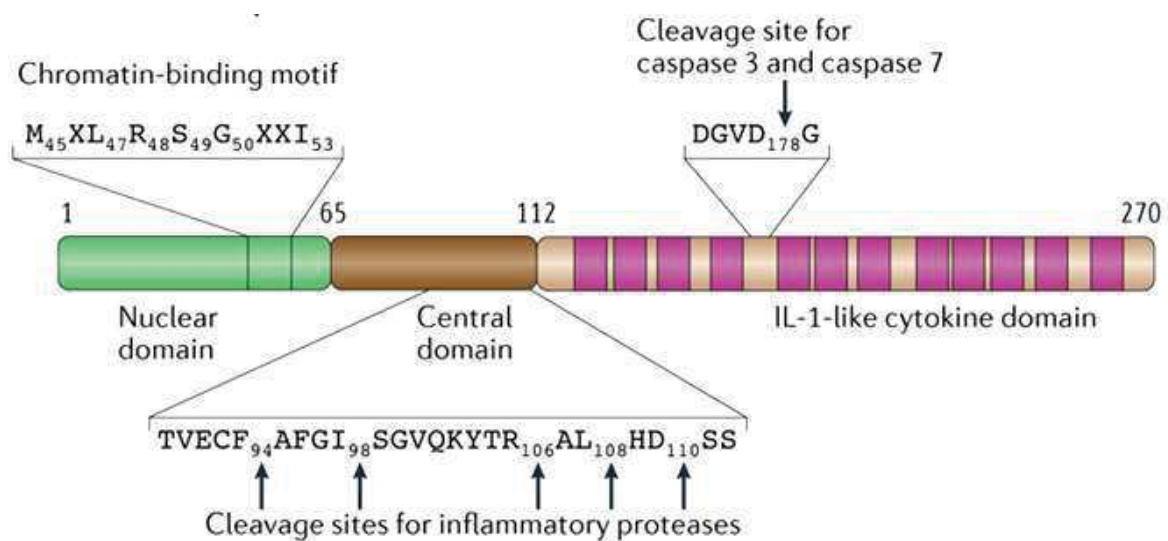


Figure 12 : La séquence de l'IL33¹¹⁸

L'IL33 possède une forme longue et courte¹¹⁹. La forme longue de l'IL33 est présente à l'état basal dans les tissus humains de manière constitutive et abondante, en particulier dans le noyau de différents types cellulaires comme ceux de l'endothélium et des voies aériennes (Figure 13). Par contre, cette cytokine ne contient pas de séquence signal pour permettre sa libération donc

différentes stimulations sont possibles pour permettre sa libération comme une agression, un mécanisme de stress, la mort cellulaire par nécrose¹¹⁶ ou l'activation de la voie ATP^{120,121}. Par exemple, dans le modèle murin, après administration d'un allergène type *Alternaria*, le taux d'IL33 est augmenté dans les lavages nasaux et bronchoalvéolaire¹¹⁷.

Une fois la forme longue libérée dans le milieu extracellulaire, plusieurs mécanismes se produisent. Soit la forme longue libérée va agir sur les cellules possédant son récepteur, soit dans l'autre cas, elle peut être clivée par les protéases inflammatoires notamment celles des neutrophiles et des mastocytes qui transforment la forme longue en la forme courte mature. Cette forme a une action 10 à 30 fois supérieure à celle de la forme longue sur l'activation des ILC2 et des mastocytes¹²² (Figure 13).

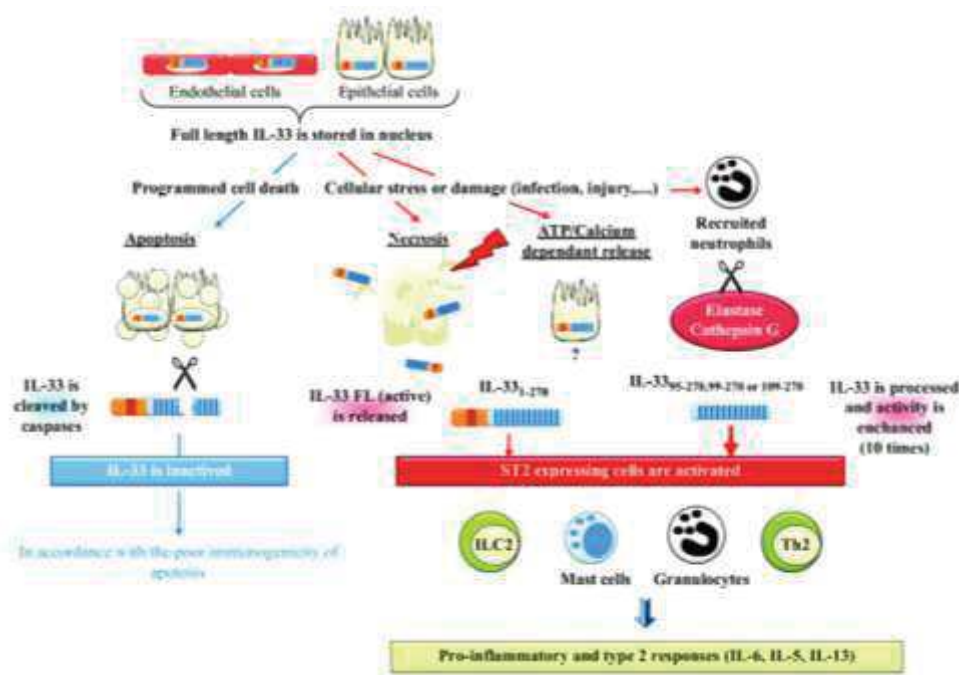


Figure 13 : De la forme longue dans le noyau des cellules à la forme active sur les cellules ST2⁺¹²³

En parallèle, des mécanismes pour limiter l'action de l'IL33 sont aussi connus car sa localisation nucléaire et sa rétention semblent importantes pour l'homéostasie immunitaire notamment en limitant les effets pro-inflammatoires de cette cytokine¹²⁴. Pour cela, il existe dans la séquence de l'IL33, un domaine spécifique situé dans la boucle $\beta 4$ - $\beta 5$ ¹²⁴, qui n'existe pas dans les autres cytokines de la famille de l'IL1. Ce domaine contient des sites d'action de caspases notamment les caspases 1, 3 et 7 (Figure 14) qui vont pouvoir générer deux formes biologiquement inactives

permettant d'inhiber l'action de l'IL33¹²⁴. Pour argumenter cela, chez la souris, une étude a montré le rôle important de la caspase 7 pour limiter les réponses de type T2 dans les poumons en inactivant potentiellement l'IL33¹²⁵. De plus, l'IL33 libérée dans le milieu extracellulaire est rapidement inactivée par l'oxydation de ces résidus cystéines notamment par les protéases inflammatoires¹²⁶.

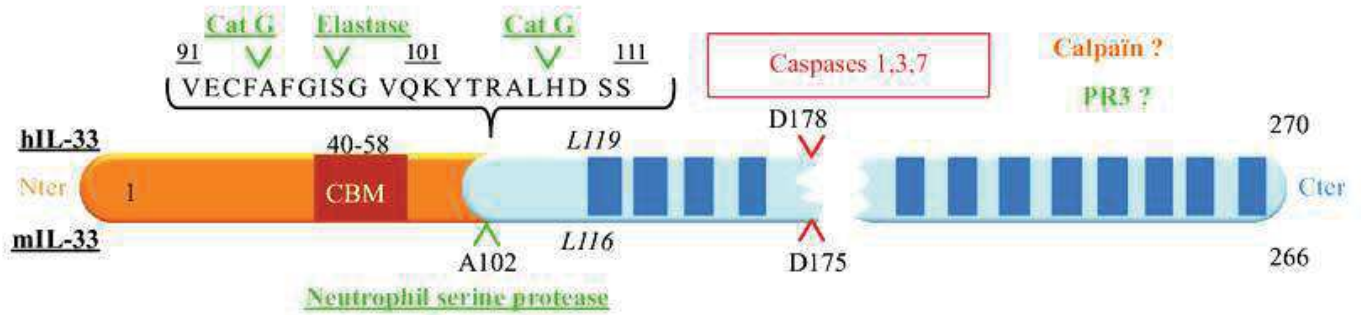


Figure 14 : Rôle des caspases dans l'inactivation de l'IL33¹²³

Une fois l'IL33 libérée dans le milieu extracellulaire, elle est capable de se fixer sur son récepteur hétérodimérique ST2 (Suppression of Tumorigenicity 2 aussi appelé IL-1RL1 et IL33-R) lié à son co-récepteur IL1RAcP (IL-1 Receptor Accessory Protein)¹²⁴. ST2 est un récepteur jouant un rôle clé dans l'inflammation et dans les maladies cardiaques¹²⁷. Ce récepteur possède plusieurs isoformes notamment un récepteur membranaire (ST2L) (Figure 15) présent de manière constitutive sur les cellules immunitaires effectrices en particulier sur les cellules Th2 mais aussi sur des cellules non hématopoïétiques notamment les cellules épithéliales pulmonaires^{128,129}.



Figure 15 : La forme ST2 membranaire¹³⁰

Puis, l'IL33 libérée va se lier au récepteur ST2 présent à la surface des cellules ST2⁺ notamment les ILC2. Ce complexe ST2-IL1RAcP-IL33 recrute Myd88, IRAK (IRAK 1 et 4) et TRAF6 ce qui va activer les voies de signalisation MAPKs et NF-KB¹¹⁹ (Figure 16). Il est à noter que l'expression de l'ARNm ST2 est augmentée dans les cellules présentes dans le sputum des patients BPCO et d'autant plus chez les patients BPCO avec une inflammation éosinophilique¹³¹, ce qui corrèle avec le versant T2 de la BPCO.

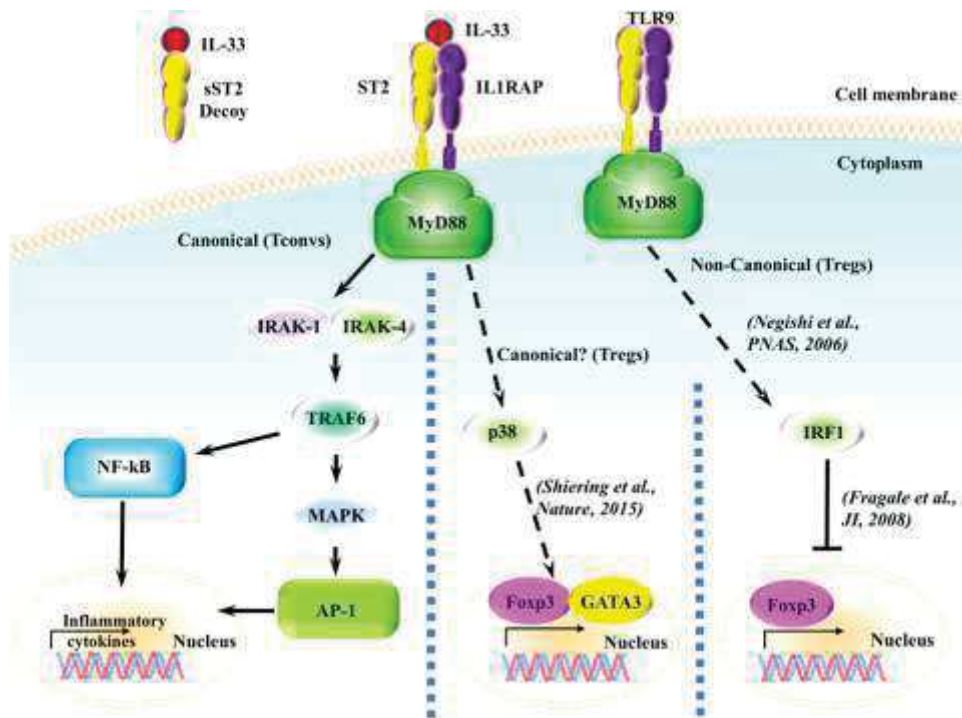


Figure 16 : Voie de signalisation ST2/IL33¹²⁹

Il existe d'autres formes du récepteur ST2, une forme soluble sST2 qui a un effet négatif sur l'axe IL33-ST2¹³² et une forme ST2V retrouvée dans les organes gastro-intestinaux mais aussi dans les stades tardifs de l'embryogénèse¹²⁹ (Figure 17).

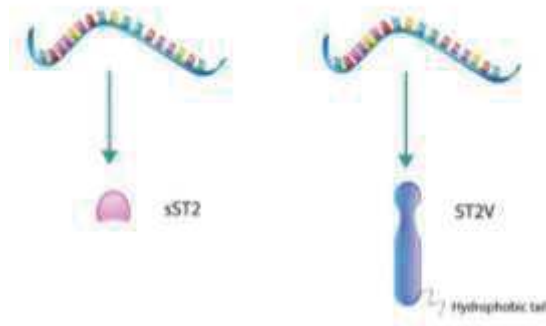


Figure 17 : Les autres formes du récepteur ST2¹³⁰

Cet axe ST2-IL33 joue un rôle important dans la BPCO : il a pu être montré que le nombre d'éosinophiles est corrélé avec le taux d'IL33 dans le sérum des patients BPCO stables. Cette cytokine est aussi augmentée dans le sérum des patients BPCO comparé aux sujets sains¹³³. De plus, le taux d'ARNm et de sa protéine IL33 sont augmentés dans les poumons des patients atteints de BPCO comparé aux sujets non BPCO¹³². Ceci permet de mettre en évidence la présence de cette alarmine chez les patients BPCO et donc son rôle potentiel dans la maladie. Par contre, l'IL33 peut être régulée par des miR. Le miR-543 a été montré comme pouvant réguler l'IL33 et notamment la diminution de ce miR dans le plasma est liée à une progression de la BPCO¹³⁴.

Pour finir, dans un modèle de souris BPCO induit par le tabac, le taux d'IL33 et de son récepteur ST2 sont augmentés dans les poumons de ces souris¹³¹. Mais les traits pathologiques caractéristiques de la BPCO sont réversées en ajoutant un anticorps anti-IL33¹³³. De plus, des souris traitées par de l'IL33 recombinant développent des changements histopathologiques dans leurs poumons comme une hyperplasie des cellules à mucus et une hypersécrétion de mucus mimant des caractéristiques de la BPCO¹³⁵. Pour finir, l'utilisation d'anticorps anti-IL33 réduit la production de cytokines T2 par les ILC2¹³⁵.

Tous ces éléments montrent l'impact de cette cytokine sur les voies aériennes des patients et son potentiel lien dans le développement de cette maladie. Un élément prometteur est que l'anticorps anti-IL33 permet de réverser les traits pathologiques chez la souris. Peut être qu'inhiber cette cytokine chez les patients BPCO pourrait être une piste thérapeutique.

b- TSLP

Le TSLP est une cytokine de la famille de l'IL2. Chez l'humain, il existe deux isoformes de cette cytokine, une forme courte exprimée à l'état basal et une forme longue exprimée en réponse à des stimuli inflammatoires¹³⁶. Durant ce phénomène inflammatoire, elle est produite par les cellules des voies aériennes et les cellules stromales¹³⁶.

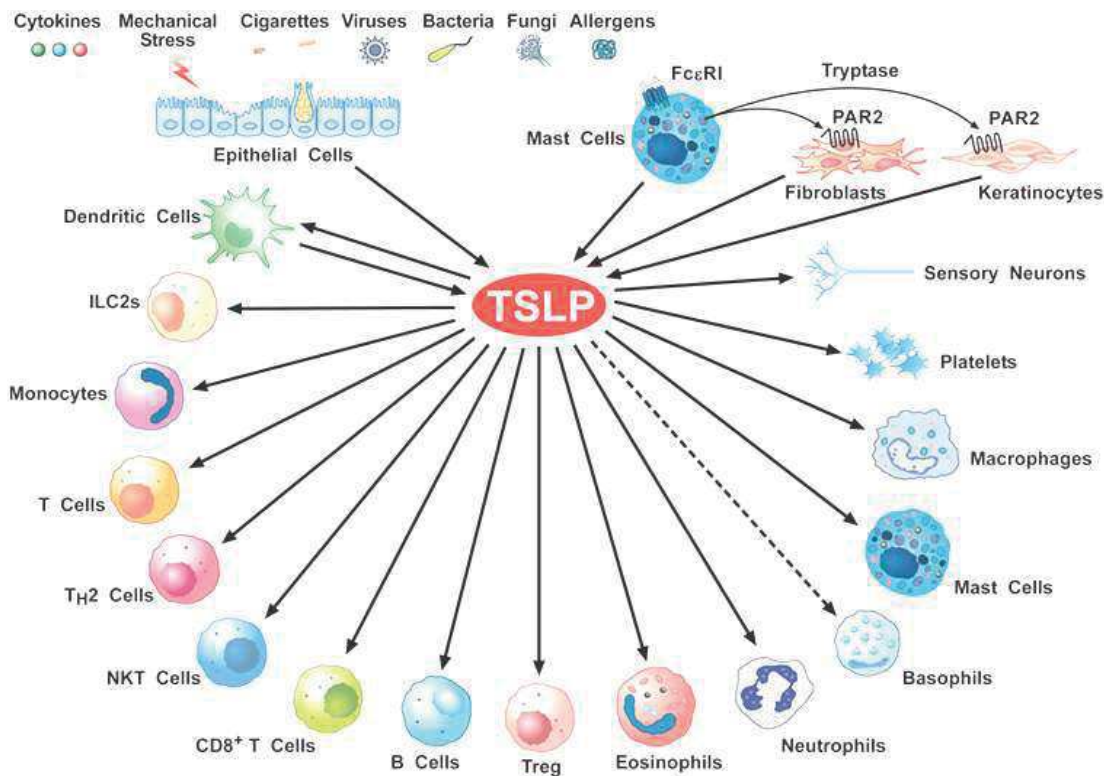


Figure 18 : Action du TSLP sur les différents types cellulaires¹³⁶

Les éléments déclenchant la production de ce TSLP par les cellules épithéliales des voies aériennes chez les patients BPCO sont l'exposition à des virus respiratoires, de l'ARN double brin, des extraits de cigarette et des cytokines pro-inflammatoires¹³⁷. Le TSLP sécrété va orchestrer la réponse de l'épithélium par l'activation notamment de cellules de type B, CD4, CD8, ILC2, mastocytes, basophiles et éosinophiles (Figure 18).

La protéine TSLP ainsi que son ARN messenger sont augmentés dans l'épithélium bronchique des patients BPCO comparés aux sujets sains²⁶. Il a été proposé que dans la BPCO, l'activation de NF-KB par le stress oxydant (induit par le biais d'exposition à des extraits de cigarette) permet d'augmenter la production de TSLP¹³⁷. Le rhinovirus (RV16) et l'ARN double brin permettent

aussi une induction de l'expression de TSLP par la voie du TLR3 dans l'épithélium des patients BPCO¹³⁸. De plus, les cytokines pro-inflammatoires (TNF, IL1 β), l'infection bactérienne ou virale, le stress oxydatif induit par la fumée de cigarette peuvent contribuer de manière synergique à l'élévation du TSLP retrouvée dans le LBA des patients BPCO¹³⁹. Pour finir, le TSLP est augmenté dans les cellules épithéliales des patients BPCO.

Toutes ces données suggèrent que le TSLP joue un rôle potentiel dans la cascade inflammatoire caractéristique des patients BPCO¹⁴⁰. Dans l'asthme, le TSLP est connu pour jouer un rôle clé dans cette maladie avec actuellement en cours d'essai, un anticorps anti-TSLP qui semble donner des résultats prometteurs^{139,141}. Pouvoir tester cette molécule dans la BPCO semble prometteur.

c- IL25

Cette cytokine est associée à une réponse immunitaire de type T2¹⁴² et est sécrétée par les cellules épithéliales^{142,143}. Elle a été décrite comme un amplificateur de l'inflammation T2 (ILC2, Th2) et permettant la production de cytokines (IL4, IL5 et IL13). Le taux d'IL25 est augmenté dans les poumons des patients asthmatiques comparé aux sujets sains et est inversement corrélé à la fonction pulmonaire. De plus, l'expression d'IL25 est augmentée dans les cellules des voies aériennes des patients BPCO et est corrélée avec une augmentation de la réponse Th2. Son mécanisme d'action et son récepteur restent peu connus.

IV-3. Futures thérapies

Plusieurs essais cliniques sont en cours pour cibler l'IL33 et son récepteur dans l'asthme comme dans la BPCO¹⁴⁴. Dans la BPCO, deux essais cliniques ciblant l'axe IL33/ST2 sont en cours⁸⁰. Un premier évalue l'effet d'un anticorps monoclonal anti-IL33 comparé à un placebo chez les patients BPCO modérée à sévère. Le second essai évalue l'efficacité d'un anticorps anti-ST2 versus un placebo sur la fréquence des exacerbations de modérées à sévères chez les patients BPCO.

Chez les patients asthmatiques, un anticorps anti TSLP est testé¹³⁹. Il réduit les exacerbations et augmente la fonction pulmonaire. Il permet également de réduire le nombre d'éosinophiles dans

le sang avec ou sans éosinophilie avant traitement. Actuellement, un essai clinique avec un anticorps anti-TSLP dans la BPCO (NCT04039113) est en cours.

Toutes ces données montrent que ces alarmines jouent un rôle dans cette pathologie donc agir sur ces dernières semblent être une piste thérapeutique.

B- OBJECTIFS

Actuellement, il n'existe pas de traitement curatif impactant l'histoire naturelle de la BPCO mais simplement des traitements préventifs et symptomatiques visant à diminuer les symptômes. Par contre, on observe des différences au niveau pulmonaire entre sujets sains et sujets BPCO incluant la composition et la structure épithéliale ainsi que leurs réponses face aux agressions environnementales. Ces différences observées sont notamment un déficit en cellules Club, une diminution du nombre de cellules ciliées, une augmentation du nombre de cellules à mucus, et une réponse inflammatoire accrue et exagérée. Il serait donc intéressant de pouvoir moduler ces différentes observations pour trouver de nouvelles perspectives thérapeutiques dans cette maladie.

Le but de ce travail de thèse a été d'étudier ces différences afin de trouver de nouvelles cibles thérapeutiques dans la BPCO.

Tout d'abord, il sera présenté une revue de la littérature sur les différents modèles disponibles aujourd'hui pour l'étude des maladies chroniques des voies aériennes (« les organoïdes pulmonaires »). Au sein du laboratoire, nous utilisons le modèle ALI (Air Liquid Interface).

La première partie de mon travail de thèse a été consacrée à l'étude des cellules Club avec pour objectif de mettre en évidence leur carte d'identité afin de mieux comprendre leurs fonctions dans l'épithélium respiratoire et plus particulièrement dans la BPCO. Actuellement, les cellules Club sont définies spécifiquement par un marqueur intracellulaire, la protéine CCSP. Un tel marqueur intracellulaire ne permet pas de trier les cellules Club viables afin de les isoler pour les étudier spécifiquement. Mieux identifier leur carte d'identité permettrait non seulement de mieux comprendre leur rôle mais aussi de trouver un marqueur de surface spécifique. Pour répondre à cette question, un protocole de tri cellulaire par la protéine CCSP a été mis en place pour obtenir le transcriptome de ces cellules. Ce protocole a nécessité de nombreuses mises au point notamment de fixation, perméabilisation, marquage anticorps, extraction ARN et a fait l'objet d'un manuscrit présenté ci-après (« Microarray protocol for intracellular-target-sorted, formalin-fixed human bronchial epithelial cells »). Une fois ce protocole mis au point, il a été réalisé la carte d'identité de ces cellules Club à partir de cultures ALI de cellules épithéliales bronchiques humaines et d'un broyage de cellules épithéliales humaines par différentes méthodes (Single Cell RNA-seq et puces à ADN). Ceci fait l'objet de l'écriture d'un manuscrit (« Different Club cells in human bronchial epithelium »).

La deuxième partie de mon travail s'est focalisée sur le remodelage des voies aériennes en supervisant la différenciation des cellules épithéliales grâce au modèle de culture ALI. Les

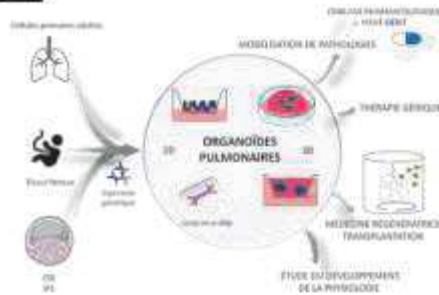
patients BPCO possèdent un épithélium avec un déficit en cellules Club, une hyperplasie des cellules à mucus et une diminution des cellules ciliées. Pouvoir restaurer le bon ratio de cellules dans l'épithélium des patients BPCO pour se rapprocher au plus près d'un épithélium « physiologique » pourrait être une opportunité thérapeutique. A partir du modèle de cultures ALI de cellules épithéliales commerciales (NHBE) ou obtenues à partir de biopsies humaines (HBEC), nous avons utilisé différents inhibiteurs des voies de signalisation, jouant un rôle dans le développement embryonnaire, afin de voir s'il est possible de superviser la différenciation épithéliale et ainsi rétablir un épithélium différencié « sain » (« Supervising differentiation for tailoring the airway epithelial cell phenotype »).

Dans la dernière partie de mon travail, nous avons étudié la réponse inflammatoire exagérée et accrue des patients BPCO. Les échecs thérapeutiques dans la BPCO sont potentiellement liés à l'hétérogénéité des réponses inflammatoires des patients et les cibles des médicaments actuels n'agissent pas sur l'histoire naturelle de la maladie. Des traitements ciblant les cytokines ou leurs récepteurs ont vu le jour dans l'asthme et sont aujourd'hui testés dans la BPCO. Nous avons émis l'hypothèse que cibler la cascade immunitaire plus en amont en bloquant les alarmines serait un potentiel thérapeutique (« What is the rationale for targeting alarmins to treat chronic obstructive pulmonary disease? »).

Afin d'étudier le rôle de ces cytokines dans les maladies chroniques des voies aériennes, des cultures ALI de cellules épithéliales de patients ont été obtenues à partir de biopsies humaines (patients BPCO, Asthmatiques et Témoins). Nous avons dosé les alarmines (IL8, IL25, IL33 et TSLP) dans les sousnageants de cultures et regroupé les patients en fonction du type de réponse observée. Ceci fait l'objet de l'écriture d'un manuscrit (« Alarmin secretions by human bronchial epithelial cells in air liquid interface model correlate with blood eosinophils in chronic airways diseases »).

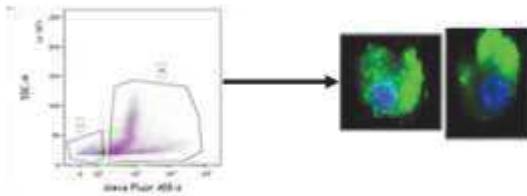
Partie I

Article 1 :
Les organoïdes pulmonaires
Soumis revue Med et Sciences

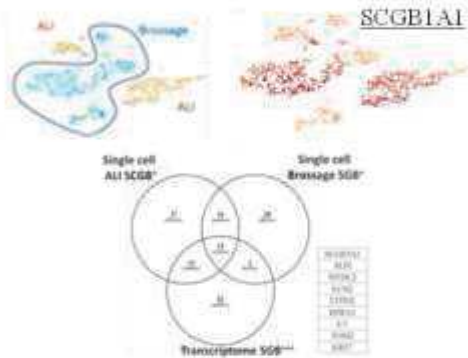


Partie II

Article 2 :
Microarray protocol for intracellular-target-sorted, formalin-fixed human bronchial epithelial cells
Soumis Scientific report



Article 3 :
Different Club cells in human bronchial epithelium
En cours d'écriture



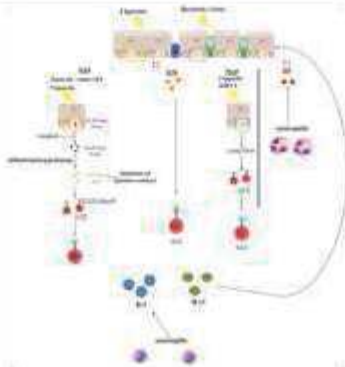
Partie III

Article 4 :
Supervising differentiation for tailoring the airway epithelial cell phenotype
En cours d'écriture

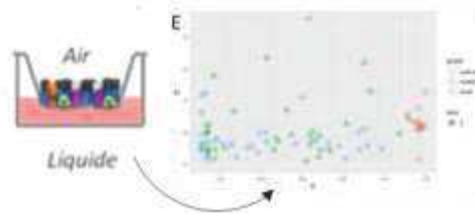


Partie IV

Article 5 :
What is the rationale for targeting alarmins to treat chronic obstructive pulmonary disease?
En cours d'écriture



Article 6 :
Alarmins secretions by human bronchial epithelial cells in air liquid interface model correlate with blood eosinophils in chronic airway disease
En cours d'écriture



C- RESULTATS

I- Les modèles d'étude des maladies chroniques des voies aériennes

Résumé

Actuellement, les résultats des études de physiopathologie pulmonaire ont été obtenus en partie sur des modèles de reconstitution d'épithélium bronchique *in vitro* à partir de cultures primaires en 2D ou d'organoïdes en 3D. Ces modèles ont pour but de mimer la structure et la fonction des cellules épithéliales pulmonaires. Mais récemment, ces modèles *in vitro* ont connu un nouvel essor notamment grâce aux organoïdes pulmonaires issus de cellules souches pluripotentes mais aussi grâce aux outils d'édition du génome.

L'ensemble de ces apports technologiques offrent de nouvelles perspectives dans la compréhension de la physiopathologie pulmonaire des maladies chroniques des voies aériennes. Ceci pourra amener, à terme, à de nouvelles pistes thérapeutiques et peut être dans le futur ouvrir de nouvelles portes dans le domaine de la médecine régénératrice pulmonaire.

Cette revue fait une synthèse des modèles disponibles pour étudier les maladies chroniques des voies aériennes ainsi que leurs possibles applications. Cette revue est publiée dans la revue « Médecine/Science ».

Les organoïdes pulmonaires

Lung organoids

Chloé Bourguignon¹, Charlotte Vernisse², Joffrey Mianné¹, Mathieu Fieldès¹, Engi Ahmed^{1,3}, Aurélie Petit², Isabelle Vachier², Thierry Lavabre Bertrand⁴, Said Assou¹, Arnaud Bourdin^{2,3}, John De Vos^{1,5}

¹ IRMB, Univ Montpellier, CHU de Montpellier, Inserm, Montpellier, France

² PhyMedExp, Univ Montpellier, CHU de Montpellier, Inserm, Montpellier, France

³ Département de Pneumologie, CHU de Montpellier, Montpellier, France

⁴ Unité de génétique médicale et cytogénétique, CHU de Nîmes, Montpellier, France

⁵ Département d'ingénierie cellulaire et tissulaire, CHU de Montpellier, Montpellier, France

Correspondance : Arnaud Bourdin, Département de Pneumologie, Hôpital Arnaud de Villeneuve, 371 avenue du doyen Gaston Giraud, 34090 Montpellier, France, a-bourdin@chu-montpellier.fr et John De Vos, Institut de Médecine Régénératrice et de Biothérapies de Montpellier, Hôpital Saint Eloi, 80, avenue Augustin Fliche, 34295 Montpellier, France, john.devos@inserm.fr

Mots-clés : organoïde, poumon, IPS, 2D/3D

Key-words: organoid, lung, IPS, 2D/3D

RESUME

L'impact en santé publique des pathologies respiratoires chroniques ne cesse de croître. Dans ce contexte, il paraît indispensable d'améliorer les modèles d'études du poumon afin de reproduire au plus proche l'architecture pulmonaire complexe, garante des fonctions d'oxygénation et d'épuration du gaz carbonique. Les connaissances actuelles en physiopathologie respiratoire résultent en partie des études de modèles de reconstitution d'épithélium bronchique *in vitro* à partir de cellules primaires, en 2D sur des inserts ou en organoïdes 3D, mimant jusqu'à l'arborescence pulmonaire. Le développement de ces modèles *in vitro* a connu un nouvel essor grâce aux organoïdes pulmonaires issus de cellules souches pluripotentes et la démocratisation des outils d'édition du génome. Ces apports technologiques récents offrent de nouvelles perspectives en matière de thérapeutiques ou de compréhension physiopathologique et pourraient, dans le futur, ouvrir les portes de la médecine régénératrice pulmonaire.

SUMMARY

As burden of chronic respiratory diseases is constantly increasing, improving *in vitro* lung models appears to be essential in order to reproduce as closely as possible the complex pulmonary architecture, responsible for oxygen uptake and carbon dioxide clearance. The study of diseases that affect the respiratory system has benefited from *in vitro* reconstructions of the respiratory epithelium with inserts in air/liquid interface (2D) or in organoids able to mimic up to the arborescence of the respiratory tree (3D). Recent development in the fields of pluripotent stem cells derived organoids and genome editing technologies has provided new insights to better understand pulmonary diseases and to find new therapeutic perspectives.

Introduction

Les pathologies pulmonaires chroniques comme l'asthme, la bronchopneumopathie chronique obstructive (BPCO) ou la fibrose pulmonaire primitive, représentent un lourd tribut en santé publique avec plus de 3 millions de morts par an [1]. Mais il n'existe aucun traitement curatif à ce jour. La mise au point de modèles pouvant reproduire la complexité architecturale et les fonctionnalités du poumon sont donc un enjeu médical majeur.

Les premiers modèles qui ont contribué à la connaissance du développement, de l'homéostasie et des pathologies du système respiratoire, en dehors des modèles animaux, ont été les cultures organotypiques *in vitro* de tissu pulmonaire [2]. L'avènement plus récent des organoïdes offre un modèle supplémentaire qui pourrait constituer un tournant dans la modélisation des pathologies pulmonaires chroniques et pourrait très significativement accélérer le développement de nouvelles thérapies. Les organoïdes sont de petits systèmes biologiques structurés en 3D, résultats de l'auto-organisation de cellules. Ces structures miment *in vitro*, au moins en partie, le développement et la fonction d'un organe en miniature. Ils reproduisent la complexité des types cellulaires et l'organisation de l'organe.

Les premiers organoïdes pulmonaires ont été obtenus à partir de cellules fœtales [3] mais c'est grâce aux cellules souches pluripotentes (CSP) [4] et notamment aux cellules souches pluripotentes induites humaines (IPS), que leur utilisation a été popularisée, offrant de nouvelles perspectives.

Bien que la définition des organoïdes implique une structure en 3D, la fonction pulmonaire d'interface ouverte sur le milieu extérieur peut être modélisée en 2D de façon légitime puisque cette organisation est inscrite dans l'architecture de la paroi de la trachée, des bronches, des bronchioles ou des alvéoles. C'est pourquoi cette revue décrira non seulement les organoïdes pulmonaires 3D mais également les épithélia bronchiques cultivés en 2D, dont les mises au point ont précédé et accompagné celui des structures en 3D.

Structure et développement pulmonaire : quand complexité rime avec nécessité

L'arbre respiratoire intra thoracique adulte se divise en deux zones de compositions architecturales et cellulaires bien distinctes qui répondent à deux impératifs fonctionnels différents : i) les voies aériennes de conduction (trachée, bronches et bronchioles) pour le transport et la filtration de l'air, et ii) la zone des échanges gazeux (bronchioles respiratoires, canaux alvéolaires, alvéoles) pour l'apport d'oxygène et l'élimination de gaz carbonique. Ces fonctions requièrent un haut degré de spécialisation cellulaire. La trachée, les bronches et les bronchioles constituent des epithelia cylindriques à cubiques formant les voies aériennes. Elles

garantissent l'humidification de l'air et la protection des zones distales contre les particules inhalées et les agents pathogènes grâce i) aux cellules à mucus (ou caliciformes) sécrétant du mucus qui capte ces mêmes particules, et ii) aux cellules ciliées qui assurent la clairance de ce mucus. Les cellules basales sont les progéniteurs de cet épithélium pseudostratifié, les cellules neuroendocrines, moins nombreuses, régulent la réponse épithéliale face à des stimuli physiologiques tels que l'hypoxie, tandis que les ionocytes, nouvellement découverts, sont responsables d'une forte activité CFTR, protéine membranaire impliquée dans le transport d'ions chlorures [5]. La fonction de l'épithélium est modulée par la proportion de ces différents types cellulaires, qui varie le long de l'arbre bronchique avec une augmentation de certaines populations rares au niveau des bronchioles terminales comme les cellules club qui sécrètent des glycosaminoglycanes et des peptides antimicrobiens. La fonction ventilatoire est régulée finement au niveau des sacs alvéolaires grâce aux pneumocytes de type 1 qui tapissent l'alvéole et permettent les échanges gazeux par diffusion avec les capillaires sous-jacents. Les pneumocytes de type 2 synthétisent le surfactant, essentiel pour réduire la tension de surface au niveau des alvéoles mais jouent également le rôle de cellules souches et sont capables de se différencier en pneumocyte de type 1.

Cette organisation étagée et complexe est le fruit d'un développement long qui débute dès les prémices de la période embryonnaire et s'étend jusqu'à plusieurs années après la naissance. Il peut être découpé en 5 phases : embryonnaire, pseudo-glandulaire, canaliculaire, sacculaire et alvéolaire, chacune correspondant à des degrés de ramification supérieurs de l'arbre respiratoire. La compréhension de la phase embryonnaire est particulièrement critique pour la mise au point des protocoles de différenciation des CSP en épithélium bronchique. Cette phase débute par la mise en place de l'endoderme définitif, qui devient l'intestin primitif et se subdivise en 3 sections selon un axe antéro-postérieur. L'activation de la voie Activine/Nodal est essentielle pour cette étape. Puis, une invagination se forme au niveau de l'intestin primitif antérieur et ce bourgeon endodermique envahit le mésoderme environnant avec lequel il entretiendra des relations étroites tout au long du développement pulmonaire. Ce bourgeon apparaît dans la partie ventrale de l'intestin primitif antérieur, région caractérisée par l'expression du facteur de transcription NKX2.1, sous l'influence de l'inhibition des voies de signalisation de TGF- β et des protéines morphogénétiques osseuses (BMPs). Les progéniteurs pulmonaires NKX2.1+ suivent ensuite un schéma de différenciation selon un gradient proximo-distal sous l'effet de facteurs de croissance tels que BMP4, FGFs et WNTs pour donner naissance à l'arbre bronchique proximal et aux alvéoles en distalité [6]. Le processus d'alvéolisation débute quelques semaines avant la naissance pour s'achever après l'adolescence [7].

Les modèles animaux ont longtemps été la méthode de choix pour étudier le développement pulmonaire, simuler et prédire la réponse biologique face à des agressions externes afin d'anticiper des succès pharmacologiques chez l'homme. Ils ont permis des avancées considérables dans ce domaine [8] mais ces modèles, en plus d'être coûteux, longs et fastidieux à mettre en place, ne sont pas toujours prédictifs des réponses chez l'être humain [9]. En effet, il existe des différences structurelles entre le poumon humain et celui des rongeurs. Par exemple, les cellules basales qui permettent le renouvellement épithélial tout au long des voies aériennes chez l'homme, ne sont présentes que dans la trachée chez la souris [10]. Les cellules à mucus sont également moins fréquentes dans les modèles murins [11]. Chez les souris et les rats, la production de surfactant apparaît déjà en place dès le stade sacculaire [12] alors que la maturation des pneumocytes de type 2 dont le surfactant est issu est bien plus tardive chez l'homme.

Cellules primaires in vitro : de la 2D vers les débuts des organoïdes

Cellules primaires bronchiques en interface air-liquide : 2 dimensions

La culture *in vitro* de cellules primaires épithéliales bronchiques humaines (CEBH) en interface air-liquide (ALI) est un très bon modèle pour étudier les phénomènes physiopathologiques des voies aériennes : à partir d'une biopsie ou d'un brossage bronchique réalisée lors d'une fibroscopie, les CEBH en ALI permettent de reconstituer un épithélium complet et différencié (Figure 1) [13]. Après dissociation mécanique des biopsies, les cellules basales sont amplifiées puis transférées sur une membrane poreuse tendue sur un insert (Transwell™). Le milieu nutritif se trouve au pôle baso-latéral, alors que le pôle apical des cellules est au contact de l'air. Les cellules basales, ainsi positionnées à l'interface air-liquide physiologique, se différencient en cellules ciliées et cellules à mucus notamment. Ainsi, en 28 jours de culture ALI, un épithélium différencié et fonctionnel est produit à partir de biopsies de sujets sains ou de patients atteints de pathologies respiratoires. Ce système a été utilisé avec succès pour étudier l'asthme ou les infections virales, par exemple [14]. L'introduction récente d'un nouveau milieu de culture (Pneumacult™) a permis de mieux développer les cultures de CEBH en conditions ALI, dans une architecture pseudostratifiée proche de l'architecture 3D de la bronche [15].

La troisième dimension

Bien que ce modèle permette de reproduire un épithélium pseudo-stratifié *in vitro* et qu'il puisse être enrichi par co-culture avec d'autres types cellulaires [16], il ne reproduit pas l'architecture tri-dimensionnelle essentielle pour assurer des interactions et des fonctions cellulaires fidèles

aux processus *in vivo* [4]. Certaines équipes ont proposé de combiner ce modèle à une matrice pour créer une 3^e dimension : broncho-sphères [17], trachéo-sphères [18] ou alvéolosphères en isolant des pneumocytes de type 2 par tri cellulaire [19], voire des structures mimant *in vitro* la ramification des bronches au cours du développement et réalisant ainsi les premiers organoïdes [20]. Les matrices utilisées sont des hydrogels, le plus souvent le Matrigel. C'est une préparation solubilisée extraite du sarcome murin d'Engelbreth-Holm-Swarm (EHS), une tumeur riche en laminine (60%) collagène IV (30%) et entactine (8%), ce dernier contribuant à l'organisation structurale en liant la laminine et le collagène. Il contient également des protéoglycanes héparane sulfate et des facteurs de croissance. Ses propriétés de polymérisation à température ambiante en font une matrice biologiquement et physiquement active semblable à la matrice basale. Il faut noter l'influence favorable de l'ajout de cellules d'origine mésodermiques (fibroblastes, cellules endothéliales) pour la structuration et la maturation de ces structures en 3D. Ce type de modèle a pu permettre à Gao et al. [17] grâce à des outils d'édition génomique, d'identifier deux facteurs de transcription impliqués dans les processus de ciliogenèse (ZNF750), de différenciation et de coordination des fonctions de barrière (GRHL2). Un autre exemple d'utilisation de ce modèle, couplé à une approche haut débit en plaques 384 puits, a montré que l'interleukine-13 induit la production de mucus tandis que le blocage du récepteur NOTCH2 par un anticorps diminue la proportion de cellules à mucus par rapport aux cellules ciliées [21].

Organoïdes issus de cellules fœtales

Les cultures en 2 ou 3 dimensions de cellules primaires adultes sont très intéressantes pour étudier les mécanismes physiologiques ou pathologiques survenant à l'âge adulte mais, du fait du stade de différenciation avancé des cellules prélevées et malgré des processus de transdifférenciation, ces modèles ne sont pas pertinents pour la compréhension des phénomènes intervenant lors du développement pulmonaire. A ce titre, bien que l'accès à ces cellules soit délicat, certains auteurs ont rapporté l'utilisation de cellules pulmonaires fœtales [22,23]. Les informations issues de ces études sont précieuses. Ainsi, des cellules pulmonaires fœtales prélevées au stade canaliculaire peuvent générer l'ensemble des cellules de l'arbre respiratoire adulte [22]. Ces tissus immatures peuvent être utilisés pour comprendre le développement pulmonaire ou pour mimer *in vitro* la dysplasie broncho-pulmonaire [23].

Lung on a chip : quand la bio-ingénierie s'en mêle

Afin de contrôler le plus finement possible le micro-environnement cellulaire *in vitro*, l'équipe de Donald Ingber a développé un système micro-fluidique mimant l'interface air liquide

alvéolaire en 3D. Il s'agit d'une fine membrane poreuse et flexible de polydiméthylsiloxane (PDMS), recouverte sur la face supérieure d'une matrice extra-cellulaire sur laquelle repose une couche de cellules épithéliales alvéolaires au contact de l'air, et sur la face inférieure, d'une couche de cellules endothéliales immergée dans un milieu de culture [24]. Ce « lung on a chip » reproduit dans quelques millimètres carrés la complexité et la diversité de l'épithélium pulmonaire. Grâce à un système de pressions négatives mimant les mouvements respiratoires, il a été utilisé pour mettre en évidence l'importance des contraintes mécaniques dans la réponse inflammatoire liée aux nanoparticules de silice. En effet, dans ce modèle, le stress mécanique augmente la capture endothéliale et épithéliale des particules, accentuant ainsi les réponses toxiques et inflammatoires induites par les nanoparticules. Cependant, cette technologie n'est, pour le moment, maîtrisée que par une équipe.

Toutefois, les cellules primaires bronchiques issues de tissus adultes ou fœtaux ont un inconvénient majeur : elles ne sont disponibles qu'en quantité très limitée. En effet, elles ne peuvent être obtenues qu'à partir de procédures médicales invasives (fibroscopie) et/ou dans des cadres éthiques restreints (utilisation de tissus fœtaux à visée de recherche). De plus, leur durée de culture limitée, leur faible potentiel de pré-amplification *in vitro* et la grande variabilité interindividuelle sont des limites qui justifient de rechercher d'autres sources cellulaires pour produire des organoïdes.

Organoïdes dérivés de cellules souches pluripotentes humaines

Les CSP, cellules souches embryonnaires humaines ou cellules souches pluripotentes induites humaines (iPS), sont une source alternative très prometteuse [25]. En effet, les CSP ont un potentiel d'auto-renouvellement illimité et peuvent se différencier vers tous les types cellulaires, y compris ceux du système respiratoire. Ainsi, plusieurs protocoles de culture 2D d'épithélia respiratoires dérivés de CSP ont été publiés [26–28]. Ces protocoles reproduisent *in vitro* les conditions du développement embryonnaire du système respiratoire, via les étapes d'endoderme définitif, d'intestin primitif antérieur ventralisé, puis de progéniteurs pulmonaires (Figure 2) et permettent d'obtenir des épithélia comportant les principaux types cellulaires bronchiques ou alvéolaires. Ils ont fait précédemment l'objet d'une synthèse [7].

Les CSP permettent également de produire des organoïdes 3D. Certaines équipes réalisent les premières étapes de différenciation en culture monocouche 2D [29–32] puis les progéniteurs pulmonaires NKX2.1⁺ sont purifiés grâce à des marqueurs membranaires spécifiques (CPM⁺ ou CD47^{high}/CD26^{low}) avant d'être mise en culture en 3D dans du Matrigel. D'autres équipes

préfèrent induire la culture en 3D juste après le stade d'endoderme définitif passant par un stade de précurseurs organisés en sphéroïdes avant d'induire la structure organoïde [33–35]. L'une des grandes difficultés rencontrée par les équipes travaillant sur la différenciation des CSP en tissu bronchique réside dans le degré de maturité de l'épithélium obtenu : l'aspect morphologique et les données transcriptomiques montrent souvent des résultats équivalents à ceux de poumons fœtaux [36]. Cet écueil peut-être résolu par une transplantation de ces cellules dans une souris immunodéficiente pour achever la maturation de ces organoïdes *in vivo*, à condition d'associer une niche bioartificielle synthétique en PLG (poly(lactide-co-glycolide)) avant la greffe dans le cas des organoïdes [34]. L'implémentation *in vitro* du milieu commercial Pneumacult™, initialement destiné à la culture de cellules primaires bronchiques en ALI, permet également d'obtenir des organoïdes avec des cellules multi-ciliées nombreuses et suffisamment matures pour étudier les battements ciliaires [30].

D'autres protocoles se concentrent sur la différenciation du compartiment alvéolaire au sein des organoïdes [29,32]. Ces alvéolosphères produisent du surfactant (SFPC) et les cellules qui les composent ont des profils d'expression génique proches des pneumocytes de type 2 et possèdent des corps lamellaires.

Cependant certaines problématiques restent à résoudre comme l'absence de modélisation de l'interface entre l'épithélium et le tissu sous-jacent (cellules endothéliales et fibroblastiques/mésenchymateuses) au sein de ces organoïdes. Même si un compartiment de nature mésenchymateuse est parfois représentée dans ces modèles, il n'atteint jamais le stade de cellule endothéliale, y compris après greffe *in vivo* [33,36]. Il sera ainsi très utile de complexifier le modèle en intégrant un véritable compartiment mésenchymateux.

Les organoïdes pulmonaires au service de la médecine...

D'aujourd'hui

Les organoïdes pulmonaires dérivés de CSP sont des outils puissants. Ils sont capables de modéliser de manière pertinente des maladies génétiques rares touchant le poumon, telles que la mucoviscidose [38] ou le syndrome de Hermansky-Pudlak [39]. L'avènement de la technologie CRISPR/Cas9 démultiplie les possibilités de modélisation de ces pathologies et permet d'imaginer de possibles thérapies géniques [40].

Les virus à tropisme respiratoire sont à l'origine de lésions majeures à plus ou moins long terme au niveau de l'épithélium bronchique. Ces lésions peuvent être reproduites et étudiées sur ces

organoïdes, comme par exemple celles induites par un virus parainfluenza, le virus respiratoire syncytial et le virus de la rougeole [41]. Enfin, la modélisation en 2D ou 3D ouvre une voie majeure pour l'innovation dans le traitement des pathologies respiratoires, en particulier les pathologies chroniques telles que la BPCO ou la fibrose pulmonaire. En effet, la génération à grande échelle d'organoïdes dérivés d'iPS modélisant ces pathologies, devrait permettre le criblage pharmacologique massif de petites molécules. De plus, ces stratégies de criblages pourraient tenir compte du terrain génétique en sélectionnant des génotypes de patients susceptibles [7].

Et de demain

Les travaux sur les matrices pulmonaires décellularisées et l'ingénierie pulmonaire ex vivo pourraient être à terme une alternative au don d'organe issu de patients en état de mort encéphalique [42], seule option thérapeutique actuelle pour les patients atteints d'insuffisance respiratoire chronique en attente de transplantation pulmonaire. Mais les protocoles de décellularisation des matrices et d'amplification/fonctionnalisation des cellules en bioréacteurs pour produire un organe complet, n'en sont qu'à leur balbutiement.

Conclusion

Le poumon est un organe complexe et diversifié tant sur le plan cellulaire que sur le plan structurel. Cette revue des différents modèles d'organoïdes pulmonaires en est le reflet : diversité des sources cellulaires, diversité des architectures, diversité des applications (Figure 3). Les modèles en 2D sont privilégiés pour leur facilité d'utilisation et de monitoring, ceux en 3D pour leur pertinence histologique. Par rapport aux autres sources cellulaires, les CSP donnent accès à tous les stades développementaux et permettent une production quasi infinie d'organoïdes pulmonaires. Enfin, associées à la technologie CRISPR, les CSP offrent une palette de modèles essentiellement illimitée. Les pistes d'amélioration de ces organoïdes pulmonaires se dirigeront certainement vers une complexification du modèle avec l'implémentation de vaisseaux, de nerfs, de cellules immunitaires *etc.* pour tendre à un système *in vitro* le plus complet possible. En effet, le rôle architectural et paracrine joué par les vaisseaux au cours du développement [43] et de la réparation du poumon est majeur. Outre les « lung on a chip » évoqués ci-dessus, les co-cultures avec des cellules mésenchymateuses et endothéliales avant greffe chez l'animal immunodéprimé [44] pourraient être une solution. L'amélioration continue des matériaux biocompatibles, notamment des hydrogels modulables à souhait et photo-polymérisables, permettra très probablement la production de vaisseaux dans ces organoïdes pulmonaires [45]. L'ensemble de ces avancées technologiques seront, sans conteste, à l'origine de grands progrès en pneumologie.

REMERCIEMENTS

Nous remercions la FRM pour son soutien (financement FDM20170638083).

LIENS D'INTERET

Les auteurs déclarent n'avoir aucun lien d'intérêt concernant les données publiées dans cet article.

REFERENCES

1. GBD 2017 Causes of Death Collaborators. Global, regional, and national age-sex-specific mortality for 282 causes of death in 195 countries and territories, 1980-2017: a systematic analysis for the Global Burden of Disease Study 2017. *Lancet Lond. Engl.* 2018 ; 392 : 1736–1788.
2. Ekelund L, Arvidson G, Emanuelsson H, *et al.* Effect of cortisol on human fetal lung in organ culture: a biochemical, electron-microscopic and autoradiographic study. *Cell Tissue Res.* 1975 ; 163 : 263–272.
3. Zimmermann B. Lung organoid culture. *Differ. Res. Biol. Divers.* 1987 ; 36 : 86–109.
4. Nadkarni RR, Abed S, Draper JS. Organoids as a model system for studying human lung development and disease. *Biochem. Biophys. Res. Commun.* 2016 ; 473 : 675–682.
5. Plasschaert LW, Žilionis R, Choo-Wing R, *et al.* A single-cell atlas of the airway epithelium reveals the CFTR-rich pulmonary ionocyte. *Nature* 2018 ; 560 : 377–381.
6. Dye BR, Miller AJ, Spence JR. How to Grow a Lung: Applying Principles of Developmental Biology to Generate Lung Lineages from Human Pluripotent Stem Cells. *Curr. Pathobiol. Rep.* 2016 ; 4 : 47–57.
7. Ahmed E, Sansac C, Assou S, *et al.* Lung development, regeneration and plasticity: From disease physiopathology to drug design using induced pluripotent stem cells. *Pharmacol. Ther.* 2017 ; .
8. Morrissey EE, Hogan BLM. Preparing for the first breath: genetic and cellular mechanisms in lung development. *Dev. Cell* 2010 ; 18 : 8–23.
9. Hardin-Pouzet H, Morosan S. [Animal research models and regulations]. *Med. Sci. MS* 2019 ; 35 : 153–156.
10. Boers JE, Ambergen AW, Thunnissen FB. Number and proliferation of clara cells in normal human airway epithelium. *Am. J. Respir. Crit. Care Med.* 1999 ; 159 : 1585–1591.
11. Rock JR, Randell SH, Hogan BLM. Airway basal stem cells: a perspective on their roles in epithelial homeostasis and remodeling. *Dis. Model. Mech.* 2010 ; 3 : 545–556.
12. Jobe AH. Animal Models, Learning Lessons to Prevent and Treat Neonatal Chronic Lung Disease. *Front. Med.* 2015 ; 2 : 49.
13. Gras D, Petit A, Charriot J, *et al.* Epithelial ciliated beating cells essential for ex vivo ALL culture growth. *BMC Pulm. Med.* 2017 ; 17 : 80.
14. Kast JI, McFarlane AJ, Głobińska A, *et al.* Respiratory syncytial virus infection influences tight junction integrity. *Clin. Exp. Immunol.* 2017 ; 190 : 351–359.
15. Rayner RE, Makena P, Prasad GL, *et al.* Optimization of Normal Human Bronchial Epithelial (NHBE) Cell 3D Cultures for in vitro Lung Model Studies. *Sci. Rep.* 2019 ; 9 : 500.

16. Gras D, Martinez-Anton A, Bourdin A, *et al.* Human bronchial epithelium orchestrates dendritic cell activation in severe asthma. *Eur. Respir. J.* 2017 ; 49 .
17. Gao X, Bali AS, Randell SH, *et al.* GRHL2 coordinates regeneration of a polarized mucociliary epithelium from basal stem cells. *J. Cell Biol.* 2015 ; 211 : 669–682.
18. Rock JR, Gao X, Xue Y, *et al.* Notch-dependent differentiation of adult airway basal stem cells. *Cell Stem Cell* 2011 ; 8 : 639–648.
19. Barkauskas CE, Crouse MJ, Rackley CR, *et al.* Type 2 alveolar cells are stem cells in adult lung. *J. Clin. Invest.* 2013 ; 123 : 3025–3036.
20. Franzdóttir SR, Axelsson IT, Arason AJ, *et al.* Airway branching morphogenesis in three dimensional culture. *Respir. Res.* 2010 ; 11 : 162.
21. Danahay H, Pessotti AD, Coote J, *et al.* Notch2 is required for inflammatory cytokine-driven goblet cell metaplasia in the lung. *Cell Rep.* 2015 ; 10 : 239–252.
22. Rosen C, Shezen E, Aronovich A, *et al.* Preconditioning allows engraftment of mouse and human embryonic lung cells, enabling lung repair in mice. *Nat. Med.* 2015 ; 21 : 869–879.
23. Sucre JMS, Vijayaraj P, Aros CJ, *et al.* Posttranslational modification of β -catenin is associated with pathogenic fibroblastic changes in bronchopulmonary dysplasia. *Am. J. Physiol. Lung Cell. Mol. Physiol.* 2017 ; 312 : L186–L195.
24. Huh D, Matthews BD, Mammoto A, *et al.* Reconstituting organ-level lung functions on a chip. *Science* 2010 ; 328 : 1662–1668.
25. De Vos J, Bouckenheimer J, Sansac C, *et al.* Human induced pluripotent stem cells: A disruptive innovation. *Curr. Res. Transl. Med.* 2016 ; 64 : 91–96.
26. Firth AL, Dargitz CT, Qualls SJ, *et al.* Generation of multiciliated cells in functional airway epithelia from human induced pluripotent stem cells. *Proc. Natl. Acad. Sci. U. S. A.* 2014 ; 111 : E1723-1730.
27. Huang SXL, Green MD, Carvalho AT de, *et al.* The in vitro generation of lung and airway progenitor cells from human pluripotent stem cells. *Nat. Protoc.* 2015 ; 10 : 413–425.
28. Wong AP, Bear CE, Chin S, *et al.* Directed differentiation of human pluripotent stem cells into mature airway epithelia expressing functional CFTR protein. *Nat. Biotechnol.* 2012 ; 30 : 876–882.
29. Gotoh S, Ito I, Nagasaki T, *et al.* Generation of alveolar epithelial spheroids via isolated progenitor cells from human pluripotent stem cells. *Stem Cell Rep.* 2014 ; 3 : 394–403.
30. Konishi S, Gotoh S, Tateishi K, *et al.* Directed Induction of Functional Multi-ciliated Cells in Proximal Airway Epithelial Spheroids from Human Pluripotent Stem Cells. *Stem Cell Rep.* 2016 ; 6 : 18–25.
31. McCauley KB, Hawkins F, Kotton DN. Derivation of Epithelial-Only Airway Organoids from Human Pluripotent Stem Cells. *Curr. Protoc. Stem Cell Biol.* 2018 ; 45 : e51.

32. Yamamoto Y, Gotoh S, Korogi Y, *et al.* Long-term expansion of alveolar stem cells derived from human iPS cells in organoids. *Nat. Methods* 2017 ; 14 : 1097–1106.
33. Chen Y-W, Huang SX, Carvalho ALRT de, *et al.* A three-dimensional model of human lung development and disease from pluripotent stem cells. *Nat. Cell Biol.* 2017 ; 19 : 542–549.
34. Dye BR, Dedhia PH, Miller AJ, *et al.* A bioengineered niche promotes in vivo engraftment and maturation of pluripotent stem cell derived human lung organoids. *eLife* 2016 ; 5 .
35. Miller AJ, Hill DR, Nagy MS, *et al.* In Vitro Induction and In Vivo Engraftment of Lung Bud Tip Progenitor Cells Derived from Human Pluripotent Stem Cells. *Stem Cell Rep.* 2018 ; 10 : 101–119.
36. Dye BR, Hill DR, Ferguson MAH, *et al.* In vitro generation of human pluripotent stem cell derived lung organoids. *eLife* 2015 ; 4 .
37. Ronaldson-Bouchard K, Ma SP, Yeager K, *et al.* Advanced maturation of human cardiac tissue grown from pluripotent stem cells. *Nature* 2018 ; 556 : 239–243.
38. McCauley KB, Hawkins F, Serra M, *et al.* Efficient Derivation of Functional Human Airway Epithelium from Pluripotent Stem Cells via Temporal Regulation of Wnt Signaling. *Cell Stem Cell* 2017 ; 20 : 844-857.e6.
39. Strikoudis A, Cieślak A, Loffredo L, *et al.* Modeling of Fibrotic Lung Disease Using 3D Organoids Derived from Human Pluripotent Stem Cells. *Cell Rep.* 2019 ; 27 : 3709-3723.e5.
40. Mianné J, Ahmed E, Bourguignon C, *et al.* Induced Pluripotent Stem Cells for Primary Ciliary Dyskinesia Modeling and Personalized Medicine. *Am. J. Respir. Cell Mol. Biol.* 2018 ; 59 : 672–683.
41. Porotto M, Ferren M, Chen Y-W, *et al.* Authentic Modeling of Human Respiratory Virus Infection in Human Pluripotent Stem Cell-Derived Lung Organoids. *mBio* 2019 ; 10 .
42. Gilpin SE, Wagner DE. Acellular human lung scaffolds to model lung disease and tissue regeneration. *Eur. Respir. Rev. Off. J. Eur. Respir. Soc.* 2018 ; 27 .
43. Peng T, Tian Y, Boogerd CJ, *et al.* Coordination of heart and lung co-development by a multipotent cardiopulmonary progenitor. *Nature* 2013 ; 500 : 589–592.
44. Takebe T, Sekine K, Enomura M, *et al.* Vascularized and functional human liver from an iPSC-derived organ bud transplant. *Nature* 2013 ; 499 : 481–484.
45. Grigoryan B, Paulsen SJ, Corbett DC, *et al.* Multivascular networks and functional intravascular topologies within biocompatible hydrogels. *Science* 2019 ; 364 : 458–464.

FIGURES

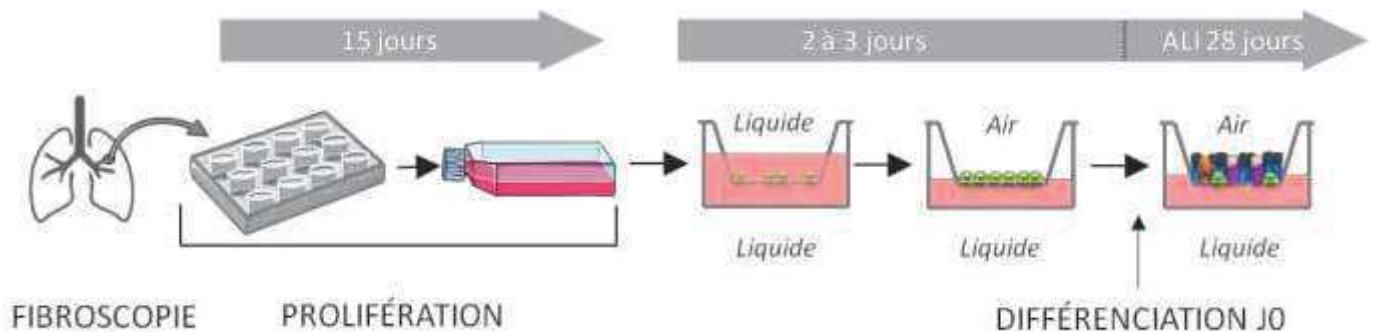


Figure 1.

Culture ALI obtenue à partir de biopsies bronchiques.

Les biopsies sont dissociées mécaniquement puis repiquées en plaque 12 puits afin d'isoler les cellules basales par adhésion préférentielle. Ces cellules basales prolifèrent pendant plusieurs semaines, puis une phase de différenciation débute lorsqu'on les dépose sur un Transwell - une membrane poreuse tendue sur un insert - où elles sont recouvertes de milieu de culture au niveau apical et basolatéral. Après adhésion des cellules, l'interface Air Liquide est mise en place en aspirant le milieu de culture au niveau apical, exposant à l'air libre la face apicale des cellules, tout en leur permettant de continuer à être nourries par le milieu présent en basolatéral. Ce système ALI reproduit ainsi en culture les conditions naturelles des cellules bronchiques. Une fois le système ALI établi, les cellules basales se différencient et l'épithélium bronchique constitué notamment les cellules ciliées, les cellules caliciformes et les cellules club apparait.

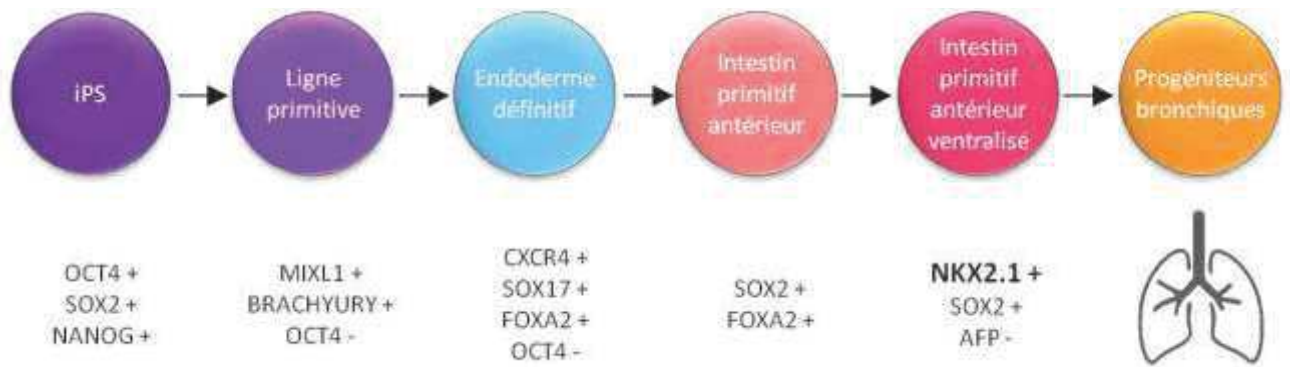


Figure 2.

Etapes-clés des protocoles de différenciation pulmonaire à partir de cellules souches pluripotentes, mimant *in vitro* le développement de l'épithélium respiratoire. iPS : cellules souches pluripotentes induites.

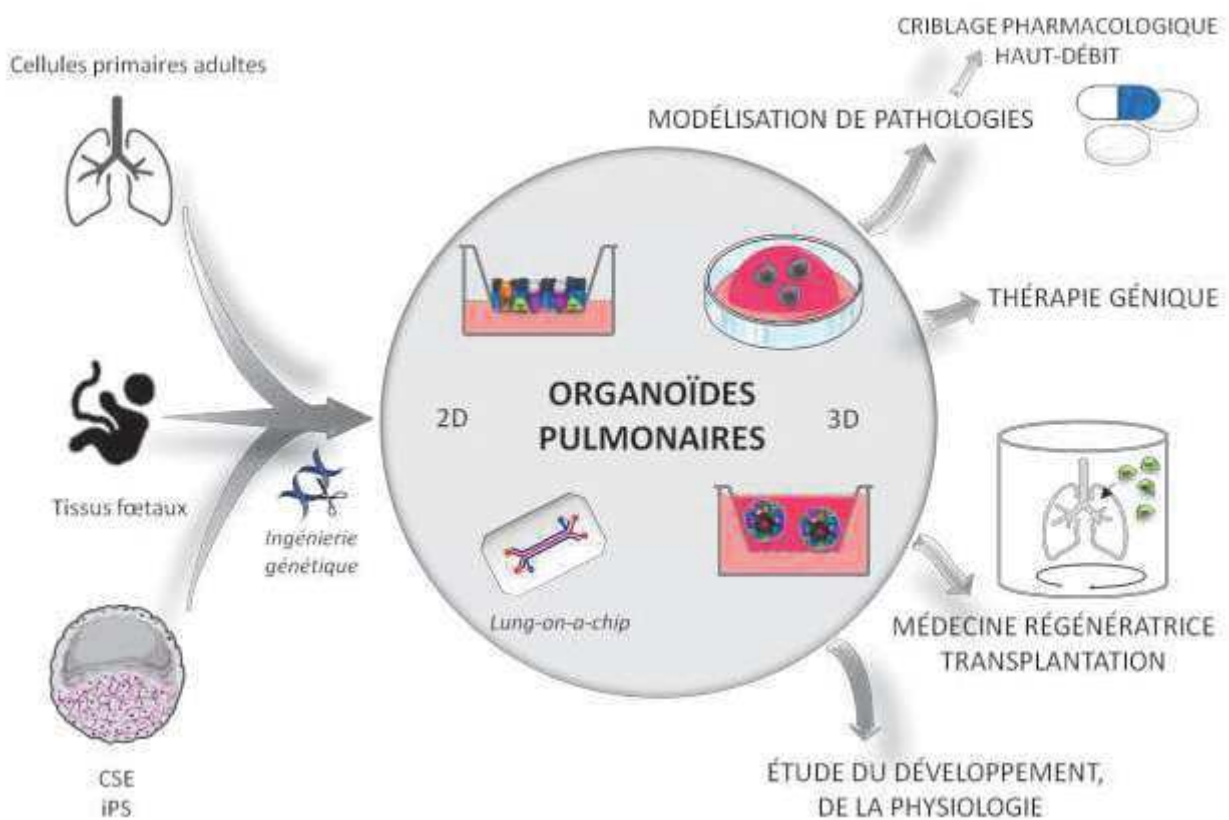


Figure 3.

Sources cellulaires, types et applications des organoïdes pulmonaires. CSE : cellules souches embryonnaires ; iPS : cellules souches pluripotentes induites.

Conclusion

Plusieurs modèles d'études de l'épithélium bronchique sont à notre disposition pour tenter de comprendre les mécanismes physiopathologiques des maladies chroniques des voies aériennes. Mais le poumon est un organe complexe et diversifié sur le plan structurel et cellulaire. Notamment, la diversité des modèles d'études disponibles en est le reflet : diversité des sources, architecture et applications. Par contre, ces modèles tendent toujours vers l'amélioration et la complexification du modèle pour se rapprocher au plus près de l'architecture et de la fonction du poumon.

Au sein du laboratoire, les études sont réalisées sur un modèle en 2D de reconstitution de l'épithélium bronchique *in vitro*, à partir de cellules primaires humaines, le modèle ALI (Air Liquid Interface). Ce modèle permet l'étude de l'épithélium bronchique dans les maladies pulmonaires, notamment la BPCO, afin de mieux comprendre les changements de ratios cellulaires (cellules ciliées/cellules à mucus) et l'absence de certain type cellulaire (cellules Club), observés dans l'épithélium des patients atteints de la BPCO.

II- La plasticité des cellules Club dans l'épithélium bronchique humain

II-1. Protocole pour obtenir la carte d'identité des cellules Club à partir de cultures primaires de cellules épithéliales bronchiques humaines en modèle ALI

Résumé

La composition de l'épithélium bronchique d'un patient BPCO est différente de celle d'un sujet sain notamment au niveau des ratios cellulaires. Par exemple, les cellules Club sont des cellules déficitaires dans l'épithélium des patients atteints de BPCO. Néanmoins, elles possèdent divers rôles dont un anti-inflammatoire et un de progéniteur accessoire. Restaurer la proportion physiologique de ces cellules dans l'épithélium bronchique des patients atteints de BPCO semble être une piste thérapeutique potentielle dans cette pathologie inflammatoire où le remodelage des voies aériennes est prédominant. Pour confirmer cette hypothèse, il convient de réaliser leur carte d'identité afin d'étudier leur rôle.

Actuellement, il n'existe pas de marqueur de surface permettant d'isoler spécifiquement ces cellules par une méthode de tri. Il est donc incontournable de réaliser un marquage intracellulaire dirigé contre son marqueur spécifique, la protéine CCSP. Par contre, ce marquage intracellulaire ne permet pas d'isoler les cellules Club viables ce qui rend l'étude de leur rôle quasi impossible. De plus, ce marquage intracellulaire endommage aussi le matériel génétique nécessaire pour réaliser la carte d'identité de ces cellules. Par conséquent, des études récentes tentent de contourner ce marquage intracellulaire en se basant sur l'analyse de l'expression de l'ARNm de ces cellules par la méthode de Single Cell-RNA seq. Cependant, cette méthode ne tient pas compte de la fonctionnalité de ces cellules liée à l'expression de sa protéine, sauf si on suppose une corrélation parfaite entre l'expression de l'ARNm et de sa protéine, sans régulation post transcriptomique. De plus, les données actuelles de Single Cell-RNA seq semblent montrer que la quasi-totalité des cellules épithéliales *in vivo* et/ou *in vitro* en modèle de culture ALI expriment l'ARNm de CCSP, ce qui rend d'autant plus difficile l'identification de leur spécificité par cette méthode.

Par conséquent, nous avons mis en place un protocole qui permettra de trier spécifiquement, par cytométrie en flux, les cellules Club, par le marquage intracellulaire de la protéine CCSP, à partir de cultures de cellules épithéliales bronchiques humaines en modèle ALI. Pour optimiser le protocole, nous avons testé l'efficacité de toutes les étapes : fixation (éthanol, formaline), perméabilisation (saponine et/ou triton) et marquage par l'anticorps CCSP (anticorps primaire et secondaire). Une fois le protocole de tri cellulaire validé, nous avons dû tester les protocoles d'extraction d'ARN (extraction RNeasy mini kit, extraction FFPE) des cellules Club triées pour obtenir la plus grande quantité d'ARN tout en préservant sa qualité. Enfin, des puces à ADN sont réalisées pour obtenir la carte d'identité de ces cellules.

Nous avons montré que :

- La fixation et la perméabilisation sont des étapes essentielles pour l'obtention d'un marquage intracellulaire, mais il faut cependant essayer de conserver le plus possible l'intégrité du matériel génétique. Pour cela, il est essentiel d'inhiber les enzymes présentes dans les tissus différenciés mais aussi dans les milieux environnants comme les RNases.
- La méthode d'extraction du matériel génétique doit être choisie et adaptée en fonction du tissu étudié et de la fixation utilisée. Une fixation par la formaline nécessite une extraction de type FFPE (Formaldehyde-Fixed Paraffin-Embedded) comprenant une digestion par des protéases permettant d'éliminer les fixations créées par la formaline entre les protéines et l'ARN.
- Enfin une étape d'amplification est nécessaire pour des échantillons fixés-perméabilisés avec une faible quantité de matériel génétique extraite.

Ce travail est actuellement soumis à la revue « Scientific Report ».

Microarray protocol for intracellular-target-sorted, formalin-fixed human bronchial epithelial cells

Vernisse C¹, Petit A², Pantesco V³, Chanez P⁴, Gras D⁴, Duperray C³, Vachier I², Bourdin A^{1,2}

1. PhyMedExp, University of Montpellier, INSERM U1046, CNRS UMR9214, France
2. Department of Respiratory Diseases and Addictology, Hospital Arnaud de Villeneuve, CHU Montpellier, France
3. IRMB, University of Montpellier, INSERM, CHU Montpellier, Montpellier, France
4. Department of Respiratory Medicine, Assistance Publique Hôpitaux de Marseille, UMR INSERM U1067 CNRS 7333, Aix Marseille University, Marseille, France

Correspondence:

Prof Arnaud Bourdin

Department of Respiratory Diseases

Hospital Arnaud de Villeneuve

371 avenue Doyen Giraud 34295 Montpellier Cedex 5, France

a-bourdin@chu-montpellier.fr

Tel: +33 4 67 33 61 26

Abstract

Certain cell types can only be recognized by intracellular markers, and intracellular staining (as opposed to surface marker staining) for subsequent cell sorting is challenging. The fixation and permeabilization steps for intracellular staining notably hinder preservation of high mRNA quality. We report more than 2-years of optimization work that was necessary for the development of a successful protocol for intracellular target-sorted, formalin-fixed, human bronchial epithelial cells with sufficient nucleic acid quality for microarray analysis. Cells obtained from differentiated ALI (Air Liquid Interface) cultures were stained with intracellular markers to sort club (SCGB1A1⁺) and goblet cells (MUC5AC⁺), respectively. A benchmarked intracellular staining protocol was applied before flow cytometry. The primary outcome was the presence of mRNA of sufficient quality as assessed by a bioanalyzer to perform microarray assays. PFA 4% Fixation coupled with triton 0.1%/saponin 0.1% permeabilization gave the best results for SCGB1A1 staining (negative and positive cells). Addition of RNase inhibitors dramatically improved mRNA quality after all along the process, resulting in samples eligible for microarray analysis. The provided protocol results in successful cell sorting according to specific intracellular markers (and while not using cell surface markers). The protocol also preserves nucleic acid quality sufficient for subsequent microarray transcriptomic analysis.

Introduction

Sorting cells that are identified only by intracellular proteins, especially in cases where no surface marker is known¹, is challenging. The multiple steps required to achieve reliable intracellular staining are well described², albeit subject to personalization. The first two critical steps are fixation and permeabilization using different chemical agents, the challenge of which increases to discouraging levels when the aim is to subsequently assay nucleic acids. For example, mRNA is supposedly degraded by the procedures required for intracellular staining and cell sorting^{3,4}, though many single cell RNAseq pipelines⁵ have overcome most such aggressive staining/sorting issues. In this context⁶, it is important to note that sorting cells using an RNA-based method implies a nearly perfect correlation in expression levels between a given mRNA and its encoded protein, and this argument is used to defend single cell proteomic techniques⁷⁻⁹. However, the latter assumption can be a pitfall as concerns the airway epithelium because: 1) the airway epithelium is heterogeneous, including diverse cells such as ciliated, goblet, club, tuft, neuroendocrine and basal cells and 2) in humans, the difficulty of sorting and keeping club and goblet cells alive is linked to the intracellular localization of their specific markers (SCGB1A1¹⁰ and MUC5AC). To date, no specific surface marker for these cells has been identified, thus hindering cytometry cell sorting without intracellular staining. Additionally, both SCGB1A1 and MUC5AC are highly biologically active in the airways and their expression levels are subject to strong variation, which creates a further dimension of difficulty for single cell RNAseq techniques.

The goal of the present study was to develop a reliable protocol for sorting club cells based on their intracellular characteristic protein SCGB1A1, without compromising RNA quantity and quality. Specifically, we aimed at describing a method for the permeabilization of SCGB1A1 stained cells obtained from human bronchial epithelial cells cultivated at the air-liquid interface, and subsequently sorting them using flow cytometry for further RNA extraction and subsequent cDNA microarray analyses.

Results

Fixation and permeabilization tests. In general, strategically varied protocols of fixation (Figure 1A) and permeabilization (Figure 1B) were performed in order to determine the most optimal SCGB1A1 staining for both flow cytometry cell sorting (Figure 1C) and subsequent mRNA extraction. Microarray analysis was performed after validation of the resulting Bioanalyzer profile (Figures 1D, E, F and G).

At the fixation step, different previously published epithelial cell fixation protocols were tested (Figure 1A). Ethanol 70%, used as previously described¹¹, did not work and resulted in cell loss (supplementary data). Further tests were performed at different concentrations of PFA and incubation temperatures¹². At PFA concentrations of 1%-2% (regardless of temperature), the cells were poorly fixed and loss was observed (supplementary data). The best results were achieved only with the highest PFA concentrations (3%-4%). Stained cells appeared to be better discriminated (compared to the negative control) during sorting with PFA 4% (assay repeated twice with 3% vs. more than 16 times with 4%). This concentration was finally kept for all subsequent assays (Figure 1C). As concerns RNA degradation, Bioanalyzer profiles were the same for all PFA concentration and temperature combinations (Figure 1D, 1E, 1F, 1G).

Using the PFA 4% fixation protocol, different permeabilization reagents were tested (Figure 1B); this step allows a specific antibody access to intracellular vesicles¹³. At first, triton 0.1% (assays repeated twice) or saponin 0.1% (assays repeated twice) permeabilizations were not adequate, resulting in non-positive staining on the flow cytometry profile (Supplementary data). We then successfully tested the combination of triton 0.1% followed by saponin 0.1% as shown on Figure 2C (assay repeated 16 times with PFA 4%).

Antibody tests. Before carrying out any antibody staining, antigen saturation was deemed necessary to eliminate non-specific sites. For this purpose, we performed saturation using a donkey serum for one hour at RT. The anti-SCGB1A1 antibody used was not marketed with a fluorescent probe. Therefore, a secondary antibody (anti-primary antibody) coupled to a fluorescent molecule was also required. Different incubation times (2h at room temperature (to reduce method time) (supplementary data) or overnight at 4°C) for the primary antibody were tested to optimize SCGB1A1 staining. The optimal primary antibody concentration was determined to be 1/1000, overnight at 4 °C and the best secondary antibody coupled with alexa fluor 488 was 1/2000, 1h at RT (Figure 2A) (as performed in the routine lab)¹⁴.

These successive protocols successfully sorted SCGB1A1⁺ fluorescent cells from negative ones (Figure 2A).

Validation of SCGB1A1 staining. SCGB1A1 positive and negative cell populations were recovered (Figure 2A). Then, RNA was extracted and reverse transcribed for further PCR experiments (Figure 2B). As expected, the levels of mRNA for SCGB1A1 were increased in the SCGB1A1 positive populations in

the three different assays (Figure 2B). Moreover, sorted cells mounted on a slide confirmed sorting efficiency (Figure 2C).

RNA Extraction protocol. Before DNA microarray analysis, all the genetic material was extracted, and the integrity of RNA was verified using a Bioanalyzer. For this purpose, sorted cells were recovered in two different solutions associated with different extraction kits. First, sorted cells were recovered in RLT buffer (Qiagen) with beta-mercaptoethanol (350 μ L cell solution: 200 μ L beta-mercaptoethanol in 20mL RLT buffer) to lyse cells and extract genetic material. Then, RNA was extracted with a standard kit (RNeasy mini kit, Qiagen) according to the manufacturer's instructions (Figure 3B). After this first extraction, both 18S and 28S peaks were absent from the Bioanalyzer profile, suggesting that all genetic material was degraded or absent from cellular extracts. This was further confirmed by very late Ct (Cycle Threshold) for GAPDH and SCGB1A1 during PCR (Figure 3E). An extraction of the cells before cell sorting showed that the RNA was also degraded (Figure 3A).

We therefore tested a second extraction technique specifically for mRNA extraction from fixed tissues (RecoverAll Total Nucleic Acid Isolation kit, ThermoFisher). This extraction process added a protease digestion step (Figure 3C). This digestion is supposed to eliminate the protein-genetic material binding caused by formalin fixation¹⁵. The resulting Bioanalyzer profile showed not only the absence of peaks but also a very limited amount of genetic material extracted. The absence of a suitable profile using Bioanalyzer in the two previous tests cannot be fully explained by the formalin fixation only, suggesting RNA was degraded.

RNase inhibitor solution (RNasin plus Rnase Inhibitor, 100 to 1000U, ref N261B, Promega) was then added to solutions during all steps of the intracellular staining protocol and FFPE tissue extraction was carried out (Figure 3D) to prevent genetic material degradation. By associating FFPE extraction and RNase inhibitors, a multitude of peaks due to the presence of genetic material was recorded, but the limited quantity suggested the persistence of RNA damage. This was further confirmed by improvement of Ct for GAPDH and SCGB1A1 at PCR (Figure 3E). The FFPE tissue extraction protocol was optimized by increasing protease digestion to 1h at 50 °C to obtain the best yield of genetic material recovery.

Microarray protocol. The absence of suitable distinct 18S and 28S peaks on the bioanalyzer profile and limited genetic material (on the order of picograms) prevented us from performing microarrays at this stage. An amplification procedure was deemed required and then applied (GeneChip™ IVT Pico Amplification Kit). Nanodrop (Figure 4A) revealed higher RNA concentrations (on the order of milligrams). These samples were then deemed suitable for DNA microarray procedures (GeneChip™ Human Gene 2.0 ST Array). Before interpreting microarrays, a validation step was performed 1) to exclude bacterial contamination or absence of conserved genetic material and 2) to confirm that the samples were homogeneous, with the remaining variation due to between sample differences (Figure 4B).

Figure 5 summarizes the different steps shown to be critical for successfully achieving the two aims of staining and sorting cells with an intracellular antibody without compromising future RNA-based analysis.

Discussion

The present protocol development study demonstrates that it is possible to isolate the genetic material required for describing the transcriptome of intracellular-target-sorted, formalin-fixed, human bronchial epithelial cells. RNA was successfully extracted from cells and used for PCR.

Similar results have been previously achieved, but with slightly different protocols. For example, the MARIS method¹⁶ is known to generate high quality RNA for transcriptome profiling following cellular fixation, intracellular immunofluorescent staining and FACS. However, the latter method was performed with a different cell type (human embryonic stem cell) and required adaptation for the bronchial epithelial cells used in the present study. In another study on HBEC cultures, the cells underwent a protocol similar to that of the present study, but with a different staining technique¹⁷.

Our protocol was validated by both confocal microscopy and PCR. It was highly reproducible, and it was used to sort other intracellular marker-defined bronchial epithelial cells (Tubulin IV and Mucin5AC, data not shown). This protocol also results in sufficient DNA quality for microarray analysis on fixed-permeabilized cells. However, the weakness of the protocol is that despite all the precautions taken, the remaining RNA amounts and quality are limited, and an amplification step is required prior to microarray preparation.

The lessons learned from this study focus on certain key points (Figure 6) that require careful consideration when designing an intracellular staining protocol. The first is proper cell fixation, without which intracellular contents may leak and result in staining failure. Fixation¹⁸ also alters RNA extraction, making it an especially determinant step for transcriptomics. PFA is the most efficient fixation method, but also the hardest on genetic material. This is why we tested the alternative ethanol (70%) method, which is known to better preserve nucleic acids. When PFA is nevertheless required, the subsequent RNA extraction¹⁵ can require adjustment. Protease digestion should be considered and can require optimization as a function of cell type, PFA percentage and PFA fixation time.

Permeabilization is a second crucial step to consider when creating an intracellular staining protocol (Figure 6) and has to be more or less “aggressive” according to the location of the molecule targeted for staining. The more the target is hidden within the intracellular space (behind several membranes for example), the more permeabilization is required. However, once the cell is permeabilized, the genetic material present becomes more vulnerable to the environment, in particular to degrading enzymes such as DNases and RNases. In this case, the use of enzyme inhibitors can help preserve genetic materials. If the profile of the RIN bioanalyzer is too low, amplification will be required to produce a DNA microarray.

In conclusion, microarray analysis of intracellular target-sorted, formalin-fixed human bronchial epithelial cells is validated in this study.

Methods

Human Bronchial Epithelial Cell (HBEC) cultures. Air-liquid interface cultures of Primary Human Bronchial Epithelial Cells (HBEC) were derived from bronchial biopsy specimens obtained during fiberoptic bronchoscopy. All donors signed a consent form after being informed about the biomedical research on airway epithelium performed thanks to their donation. The protocol was approved by the institutional ethics commission of Sud Méditerranée III (CHRU Montpellier-AOI 9244–NCT02354677). All experiments and methods were performed in accordance with relevant guidelines and regulations. HBEC were then cultured as previously described¹⁴. Briefly, cells were dissociated mechanically from biopsies and cultivated in 12 well plates (ref 353043, Falcon) and then in 75cm² flasks (ref 353136, Falcon) in PneumaCult-Ex Plus medium (cat #05041, Stemcell Technologies, Grenoble, France) for 15 days. After an expansion phase, differentiation was initiated by seeding 110000 cells on the polyester membrane of Transwell^R permeable supports (ref 3460, Corning, Kennebunk, United States) in Pneumacult-Ex Plus medium until confluence. After confluence, an ALI culture was established by the aspiration of the medium of the apical chamber (D0, day 0). Basolateral medium was replaced every two days with the PneumaCult ALI maintenance medium (cat #05002, Stemcell Technologies, Grenoble, France), while cells were maintained at 37°C, 5% CO₂ until day 28 of culture (referred as to D28). At D28, after trypsin (ACF enzymatic dissociation solution, cat #05247, Stemcell Technologies, Grenoble, France)/ACF enzymatic inhibition solution, cat #05428, Stemcell Technologies, Grenoble, France) addition, the cell suspension was recovered for further analyses (Figure 7).

Intracellular Staining. Multiple protocols were benchmarked at all mandatory steps required for successfully achieving intracellular staining without compromising RNA quality. At day 28 of culture, cells were trypsinized (ACF Enzymatic Dissociation solution and ACF Enzymatic Inhibition solution, Stemcell technologie, France) at 37°C for 7 minutes. The cell suspension was centrifuged at 1500 rpm for 5 minutes. The supernatant was discarded, and cells were resuspended in fixative solution. To determine the most appropriate methods for fixation, permeabilization and antibody staining, the following steps were carried out.

Fixation. Different reagents and/or concentrations and/or temperatures were tested: ethanol 70% (Ethanol absolute anhydrous, ref 4146072) for 15 minutes at room temperature and PFA 1% to 4% (Formaldehyde solution, F8775, Sigma) for 15 minutes at room temperature or 4°C.

Permeabilization. The cells were centrifuged and resuspended in triton 0.1% (ref 93443, sigma) and/or saponin 0.1% (ref 93443, Sigma) in PBS (PBS w/o Magnesium w/o calcium, L0615, Dutscher) for 10 minutes at room temperature.

Antibody Staining. After a blocking step with donkey serum 10% (D9663, Sigma) (in 1% BSA PBS) for 1 hour at room temperature, cells were labeled with an anti-SCGB1A1 primary antibody (club cell protein CC16 human, rabbit polyclonal antibody, 1/10000, ref RD181022220-01, Biovender) for 2 hours at room

temperature or overnight at 4°C. Finally, the cells were incubated with a secondary antibody (Alexa Fluor 488 donkey anti rabbit IgG (H+L), ref A21206, 1/2000, Invitrogen) for 1 hour at room temperature.

During all these processes (fixation, permeabilization and antibody staining steps), solutions were kept in sterile conditions and various regimens of supplementation (or not) with RNasin Ribonuclease Inhibitor (RNasin plus Rnase Inhibitor, 100 to 1000U, ref N261B, Promega) were tested.

Finally, cells were sorted according to the presence/absence of the intracellular marker SCGB1A1 using Aria IIIu becton Dickinson cytometer. Sorted cells were recovered in PBS with or without RNasin Ribonuclease inhibitor (1000U, ref N261B, Promega).

RNA Extraction. The RNA was extracted from sorted cells using the RNeasy plus mini kit (ref 74134, Qiagen) with RLT + beta mercaptoethanol (Buffer RLT Lysis Buffer, Mat No 1015750, Qiagen) or the FFPE (“Formaldehyde-Fixed Paraffin-Embedded”) RecoverAll Total Nucleic Acid Isolation kit (AM1975, Thermofisher) in combination with the Recover All™ kit (ref 00641531, Thermofisher).

RNeasy plus mini kit extraction was performed according to the manufacturer’s instructions and an elution step was performed in 30µL of Rnase free water (RNeasy plus mini kit, ref 74134, Qiagen). When using the FFPE extraction kit, cells were digested with protease buffer at 50°C for 1 hour and the protease digestion step was stopped at 80°C for 15 min. Then, RNA extraction was performed according to the manufacturer’s instructions. RNA was eluted in 20µL of “elution solution” (RecoverAll Total Nucleic Acid Isolation kit, AM1975, Thermofisher).

RNA integrity. RNA integrity was visualized using an Agilent 2100 Bioanalyzer (Agilent RNA 6000 PICO reagents kit, ref 5067-1514, Agilent Technologies). The Bioanalyzer profile demonstrated the state of degradation and quantified the amount of RNA present.

Real time RT-PCR analysis. After total RNA extraction from ALI cells, 0.4µg of RNA was reverse transcribed with verso one step RT-PCR kit (Verso cDNA synthesis kit, ref AB-1453/B, Thermofisher Scientific). Real time PCR was performed using a light cycler DNA master SYBR Green (light cycler 480 Syber Green I master, ref 1457 1520, Roche Applied Science). The comparative Ct (Cycle Threshold) method for relative quantification of gene expression was used ($2^{\Delta Ct}$, where ΔCt represents the difference in the threshold cycle between the target and control genes). Data were normalized to GAPDH mRNA levels. Primer sequences are detailed in Table 1

Amplification and Microarray. The GeneChip™ IVT Pico Amplification Kit (ref 902622, WT Pico 12 RNA, Life Technologies SAS) was used according to manufacturer’s instructions. Then, mRNA was applied to Nanodrop and Bioanalyzer in order to assess qualitatively and quantitatively the amplification procedure.

Finally, DNA microarray analysis (GeneChip™ Human Gene 2.0 ST Array, Ref 902112, Life Technologies SAS) was used to study the transcriptome of sorted cells according to the manufacturer’s instructions.

References

1. Paik, E. J., O'Neil, A. L., Ng, S.-Y., Sun, C. & Rubin, L. L. Using intracellular markers to identify a novel set of surface markers for live cell purification from a heterogeneous hPSC culture. *Sci Rep* **8**, 804 (2018).
2. Sadick, J. S., Boutin, M. E., Hoffman-Kim, D. & Darling, E. M. Protein characterization of intracellular target-sorted, formalin-fixed cell subpopulations. *Scientific Reports* **6**, 1–12 (2016).
3. Liu, L. *et al.* Maintaining RNA Integrity for Transcriptomic Profiling of Ex Vivo Cultured Limbal Epithelial Stem Cells after Fluorescence-Activated Cell Sorting (FACS). *Biol Proced Online* **19**, 15 (2017).
4. Nilsson, H., Krawczyk, K. M. & Johansson, M. E. High salt buffer improves integrity of RNA after fluorescence-activated cell sorting of intracellular labeled cells. *Journal of Biotechnology* **192**, 62–65 (2014).
5. Treutlein, B. *et al.* Reconstructing lineage hierarchies of the distal lung epithelium using single-cell RNA-seq. *Nature* **509**, 371–375 (2014).
6. Travaglini, K. J. *et al.* A molecular cell atlas of the human lung from single cell RNA sequencing. *bioRxiv* 742320 (2019) doi:10.1101/742320.
7. Li, Y., Liu, G., Zhang, J., Zhong, X. & He, Z. Identification of key genes in human airway epithelial cells in response to respiratory pathogens using microarray analysis. *BMC Microbiol* **18**, (2018).
8. McCauley, K. B. *et al.* Single-Cell Transcriptomic Profiling of Pluripotent Stem Cell-Derived SCGB3A2+ Airway Epithelium. *Stem Cell Reports* **10**, 1579–1595 (2018).
9. Zuo, W.-L. *et al.* Ontogeny and Biology of Human Small Airway Epithelial Club Cells. *Am. J. Respir. Crit. Care Med.* **198**, 1375–1388 (2018).
10. Barnes, P. J. Club cells, their secretory protein, and COPD. *Chest* **147**, 1447–1448 (2015).
11. Togo, S. *et al.* Hepatic growth factor (HGF) inhibits cigarette smoke extract induced apoptosis in human bronchial epithelial cells. *Exp. Cell Res.* **316**, 3501–3511 (2010).
12. Bussolati, G., Annaratone, L., Medico, E., D'Armento, G. & Sapino, A. Formalin fixation at low temperature better preserves nucleic acid integrity. *PLoS ONE* **6**, e21043 (2011).

13. Scheffler, J. M., Schiefermeier, N. & Huber, L. A. Mild fixation and permeabilization protocol for preserving structures of endosomes, focal adhesions, and actin filaments during immunofluorescence analysis. *Meth. Enzymol.* **535**, 93–102 (2014).
14. Gras, D. *et al.* Epithelial ciliated beating cells essential for ex vivo ALI culture growth. *BMC Pulm Med* **17**, 80 (2017).
15. Gouveia, G. R., Ferreira, S. C., Ferreira, J. E., Siqueira, S. A. C. & Pereira, J. Comparison of Two Methods of RNA Extraction from Formalin-Fixed Paraffin-Embedded Tissue Specimens. *BioMed Research International* <https://www.hindawi.com/journals/bmri/2014/151724/> (2014) doi:10.1155/2014/151724.
16. Hrvatin, S., Deng, F., O'Donnell, C. W., Gifford, D. K. & Melton, D. A. MARIS: Method for Analyzing RNA following Intracellular Sorting. *PLOS ONE* **9**, e89459 (2014).
17. Wang, Z. *et al.* TRRAP is a central regulator of human multiciliated cell formation. *J. Cell Biol.* **217**, 1941–1955 (2018).
18. Thavarajah, R., Mudimbaimannar, V. K., Elizabeth, J., Rao, U. K. & Ranganathan, K. Chemical and physical basics of routine formaldehyde fixation. *J Oral Maxillofac Pathol* **16**, 400–405 (2012).

Table 1. Sequences of the primers used for PCR

Primers	Sequences (5' to 3')
GAPDH	Forward : CCA TCT TCC AGG AGC GAG Reverse : CTT GAG GCT GTT GTC ATA CT
SCGB1A1	Forward : CAT GAA ACT CGC TGT CAC CC Reverse : GAT GAC ACG CTG AAA GCT CG

Figures

Figure 1

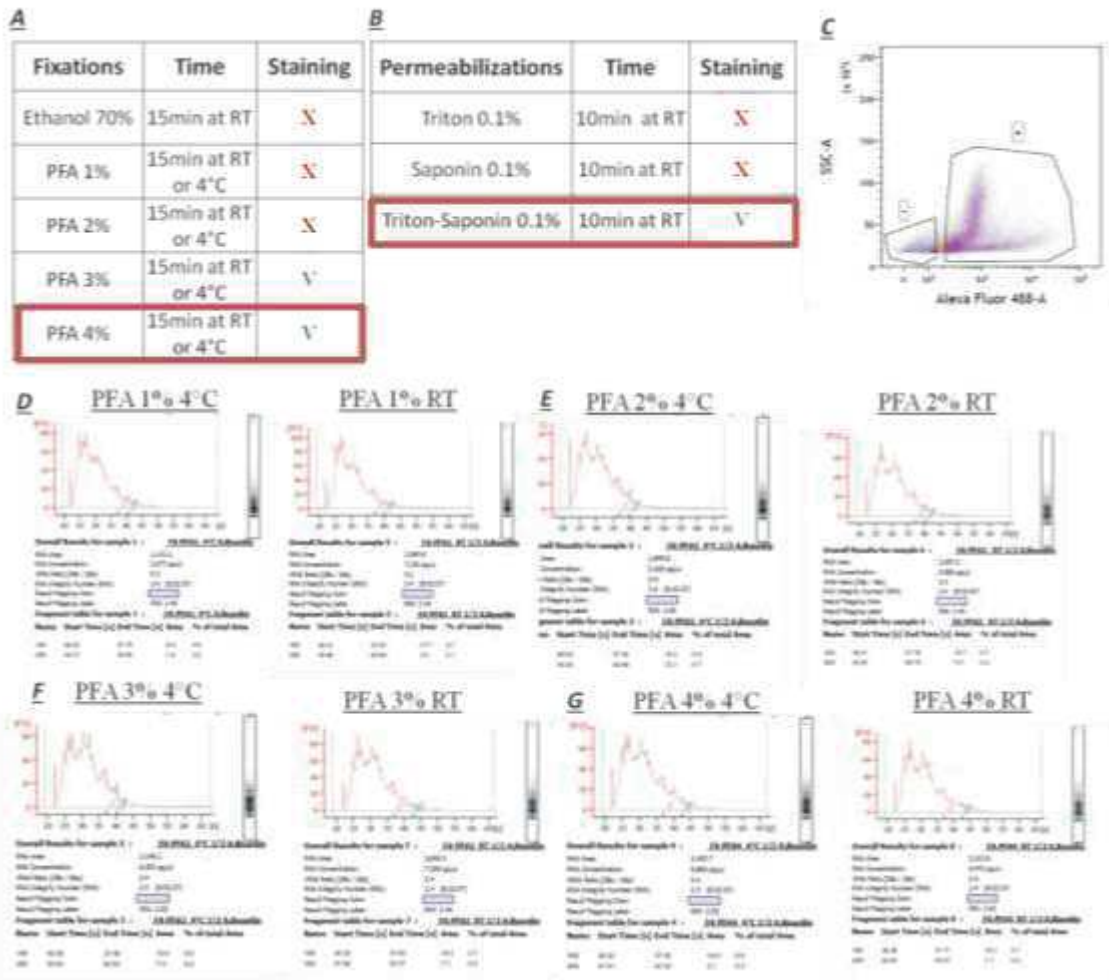


Figure 2

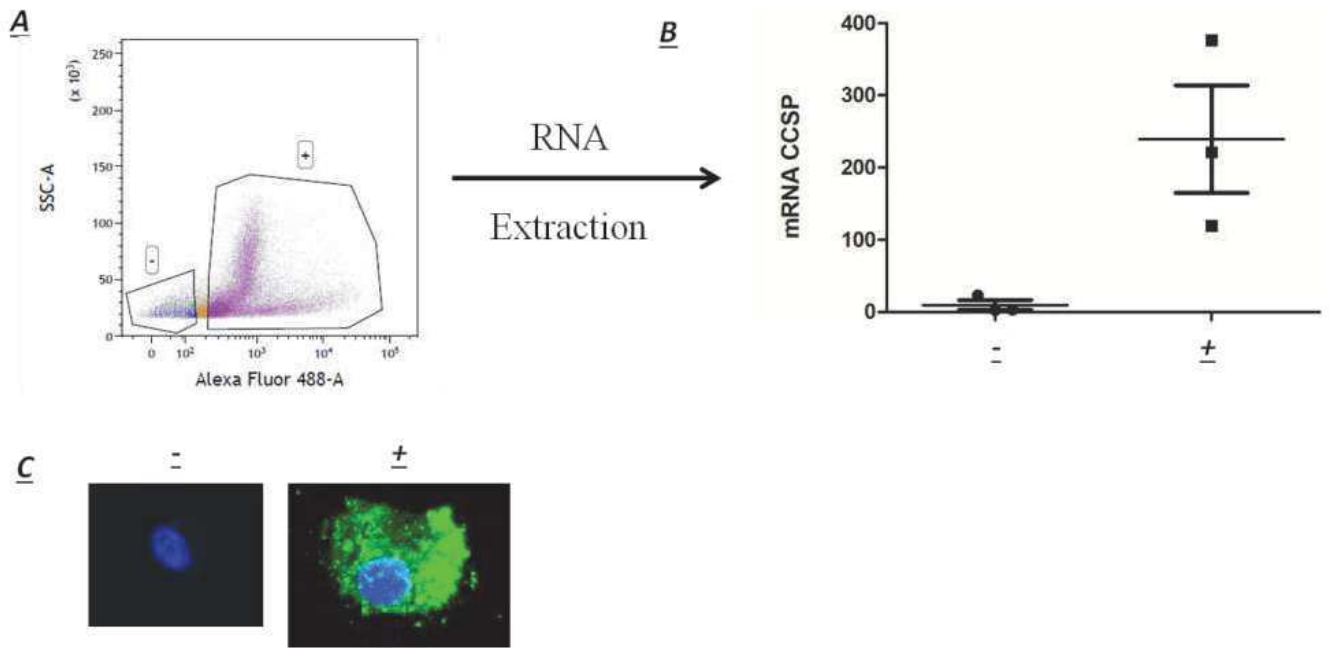


Figure 3

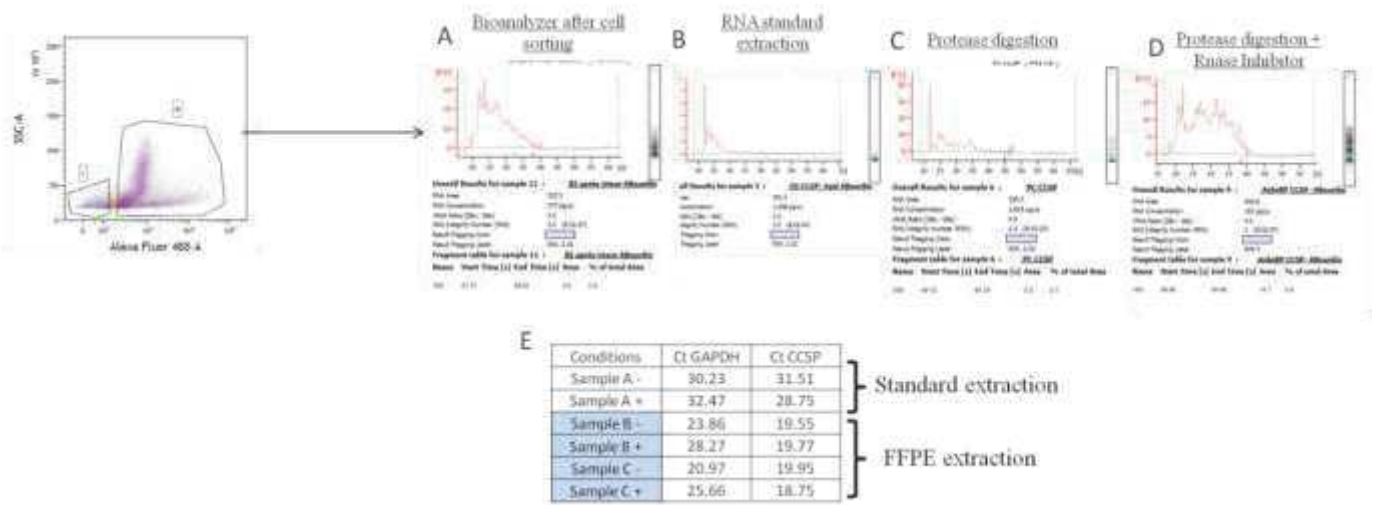


Figure 4

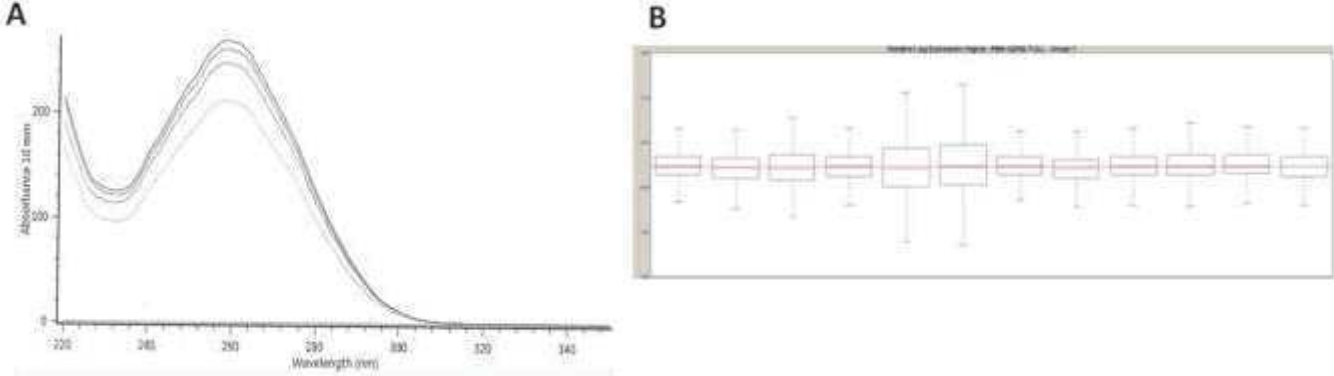


Figure 5

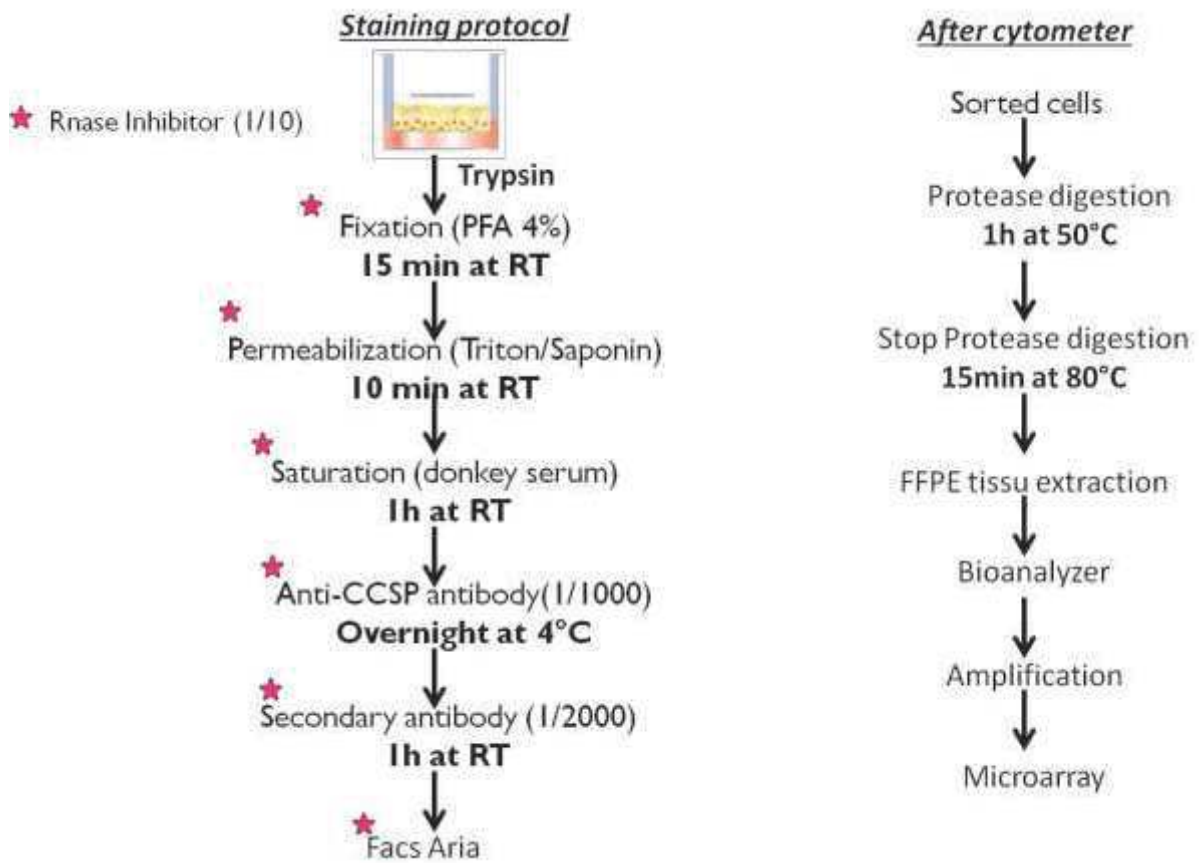


Figure 6

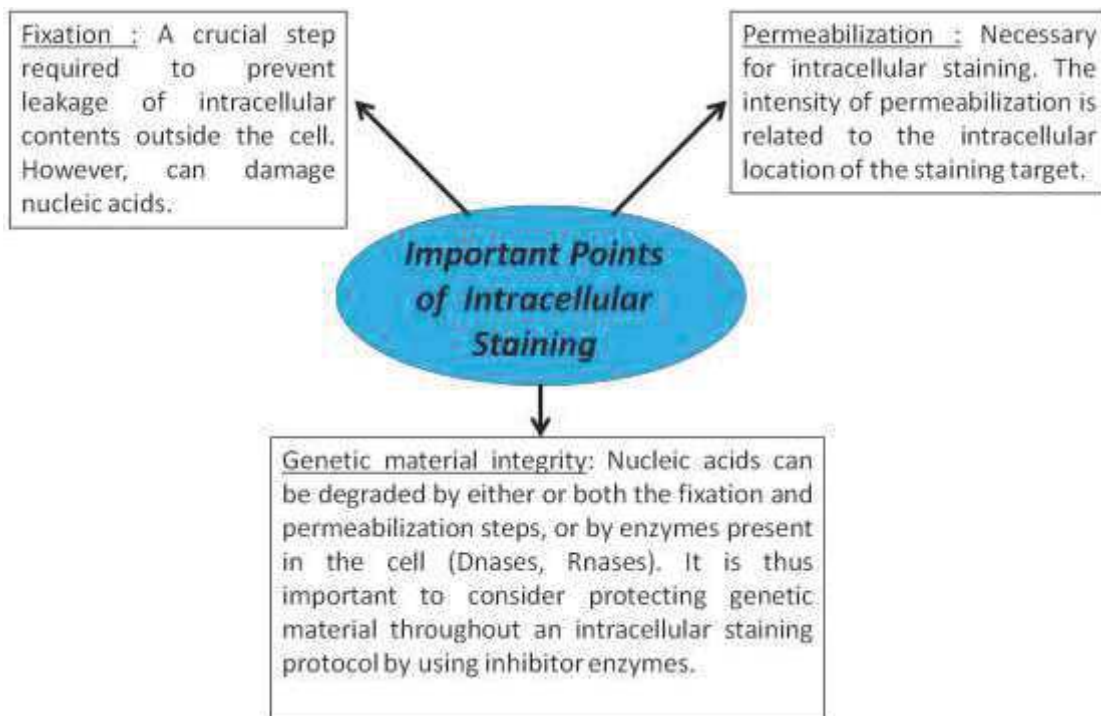


Figure 7

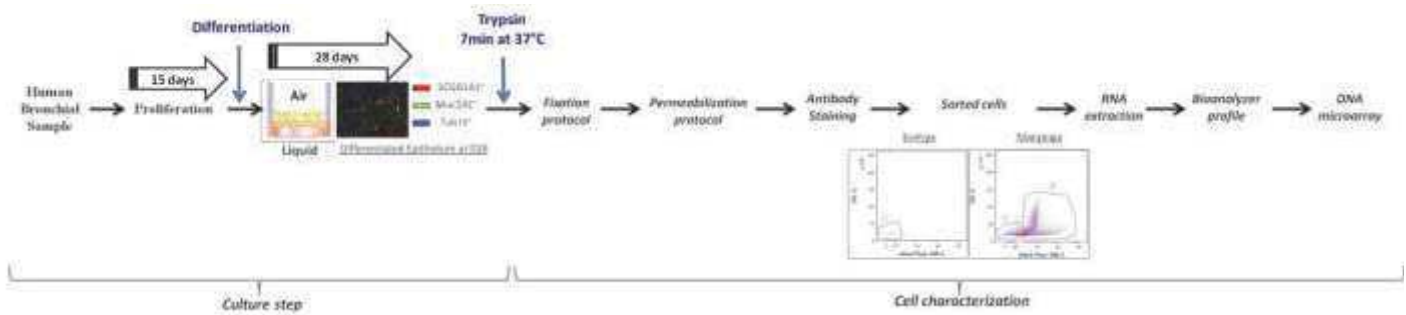


Figure legends

Figure 1: Fixation and permeabilization protocols in preparation for SCGB1A1 staining. A- Fixation assay table for optimal SCGB1A1 staining. The cells are trypsinized. Ethanol 70% or PFA (1% to 4%) fixations were tested for 15 min at RT (Room Temperature) or 4°C. The staining with SCGB1A1 antibody was carried out: overnight at 4 ° C or 2 hours at RT. After, cells are passed through a cytometer to visualize SCGB1A1 staining (supplementary data). The red 'X' indicates poor staining; the green 'V' corresponds to good staining. The red frame indicates the best fixation technique for SCGB1A1 staining. B- Permeabilization assay table for optimal SCGB1A1 staining because SCGB1A1 is an intracellular target. Permeabilizations with triton 0.1% and/or saponin 0.1% were carried out for 10 min at RT. Cells are passed through a cytometer to visualize SCGB1A1 staining (supplementary data). The red 'X' indicates poor staining; the green 'V' corresponds to good staining. The red frame gives the best permeabilization technique for SCGB1A1 staining. C- SCGB1A1 staining obtained from an ALI culture. Cells were trypsinized, fixed with PFA 4% (15min at RT) and permeabilized with Triton 0.1% /Saponin 0.1% (10min at RT). The staining was carried out overnight at 4 °C. Cells were passed through a cytometer to visualize SCGB1A1 staining. D-E-F-G: Fixation tests were repeated to confirm lack of RNA degradation. The cells were trypsinized and PFA1% (D) or 2% (E) or 3% (F) or 4% (G) fixation was performed for 15 min at 4°C or RT. The cells were then permeabilized for 10 min at RT with Triton 0.1%/Saponin 0.1%. Staining with SCGB1A1 antibody was carried out overnight at 4 °C and secondary antibody for 1 hour at RT. Cells were then passed through a cytometer to visualize staining. RNA was extracted and Bioanalyzer profiles generated.

Figure 2: Validation of intracellular staining. A- Staining obtained from an ALI culture. Cells were trypsinized at D28. They were then fixed with PFA 4% (15min at RT) and permeabilized with Triton 0.1%/Saponin 0.1% (10min at RT). Staining with SCGB1A1 antibody was carried out overnight at 4 °C and secondary antibody (anti-primary antibody) 1 hour at RT. Cells were passed to a cytometer to visualize staining. Two populations (- and +) were obtained according to their fluorescence (n=1). B- At the end of cell sorting (protocol to figure 2-A), the two populations (- and +) were recovered in different tubes. RNA extraction (by FFPE extraction kit) was then performed. A part of the RNA was retrotranscribed into DNA. PCR was performed on DNA to validate the expression of SCGB1A1 and GAPDH in the different populations (n=3). Data were normalized to GAPDH mRNA levels. C- Microscopy of sorted cells. At cell sorting output, SCGB1A1-positive (green staining) and -negative cells were recovered in different tubes. Cells were then placed on a slide and mounted for confocal microscopy (n=1).

Figure 3: Extraction protocol after cell sorting. Preserving genetic material as much as possible is necessary for subsequent studies. In this context, different extraction tests were carried out to optimize genetic material recovery. A- Prior to cell sorting, the cells were put in RLT + beta-mercaptoethanol and a standard RNA extraction was carried out (RNeasy mini kit, Qiagen). To visualize RNA integrity, a

Bioanalyzer profile was performed (n=1). B- At the end of cell sorting, the cells were put in RLT + beta-mercaptoethanol and a standard RNA extraction was carried out (RNeasy mini kit, Qiagen). To visualize RNA integrity, a Bioanalyzer profile was performed (n=1). C- At the end of cell sorting, the cells underwent protease digestion and FFPE tissue extraction was performed (RecoverAll Total Nucleic Acid Isolation kit, Thermofisher). To visualize RNA integrity, a Bioanalyzer profile was performed (n=1). D- Before cell sorting, all the steps of intracellular staining-formalin fixed protocol were completed with RNase inhibitor solution (RNasin plus Rnase Inhibitor, ref N261B, Promega). After cell sorting, the cells underwent protease digestion and FFPE tissue extraction was carried out. To visualize RNA integrity, a Bioanalyzer profile was performed (n=1). E- At the end of cell sorting, the cells were recovered in different tubes corresponding to SCGB1A1-positive and -negative populations according to SCGB1A1 fluorescence. Sample A, a standard extraction (RNeasy mini kit, Qiagen) was performed. Then the RNA was retrotranscribed into DNA and PCR was performed. Samples B and C, before cell sorting, all the solutions were supplemented with RNase inhibitor solution. At the end of cell sorting, the cells were recovered. A specific fixed tissue extraction (Recoverall Total Nucleic Acid Isolation kit, Thermofisher) was performed. Then the RNA was retrotranscribed into DNA and PCR was performed.

Figure 4: Amplification and Microarray. A- A Nanodrop profile from 10ng of RNA (obtained by a formalin fixed- intracellular staining protocol) after an amplification step (GeneChip™ IVT Pico Amplification Kit) (n=4). The Nanodrop Profile shows that the amplification worked with the OD (Optical Density) at 260nm. One curve corresponds to one sample. B- Relative Log expression signal-RMA-GENE-FULL of 12 RNA (RiboNucleic Acid) from sorted cellular populations (GeneChip™ Human Gene 2.0 ST Array). All samples have the same level of expression.

Figure 5: Final protocol from culture to DNA chip. After all adjustments, the final protocol is presented with essential points: RNase inhibitor solution, fixation, permeabilization and extraction steps.

Figure 6: Essential points during intracellular staining. Fixation and permeabilization are necessary for preserving intracellular contents and then subsequently staining them, but they also result in nucleic acid degradation. Therefore, it is necessary to implement the correct fixation and permeabilization while using techniques to avoid the degradation of genetic material.

Figure 7: Study Method. Human bronchial tissues were biopsied during fiberoptic bronchoscopy. Cells from the latter were first cultured in a proliferation phase (for 15 days) in Pneumacult-Ex Plus medium (Stemcell Technologies). Cells were then dropped on transwell^R permeable supports and then transferred to an Air Liquid Interface Model (in PneumaCult ALI maintenance medium, Stemcell Technologies) where the cells are able to organize into a differentiated epithelium (during 28 days) with club cells (SCGB1A1⁺, Secretoglobulin1A1), goblet cells (Muc5AC⁺, mucin5AC) and ciliated cells (TUB IV⁺, tubulin IV). At D28 (day 28), the differentiated epithelium is trypsinized (ACF enzymatic dissociation solution and ACF enzymatic inhibition solution, Stemcell Technologies) and bronchial epithelial cells recovered.

A formalin-fixed, intracellular-staining (SCGB1A1+ antibody) procedure was then performed to tag cells. These stained cells were sorted according to the marker and RNA extraction was performed on the resulting marker-positive and marker-negative cell populations. Finally, a Bioanalyzer profile was performed to validate DNA quality prior to microarray analysis.

Supplementary Data

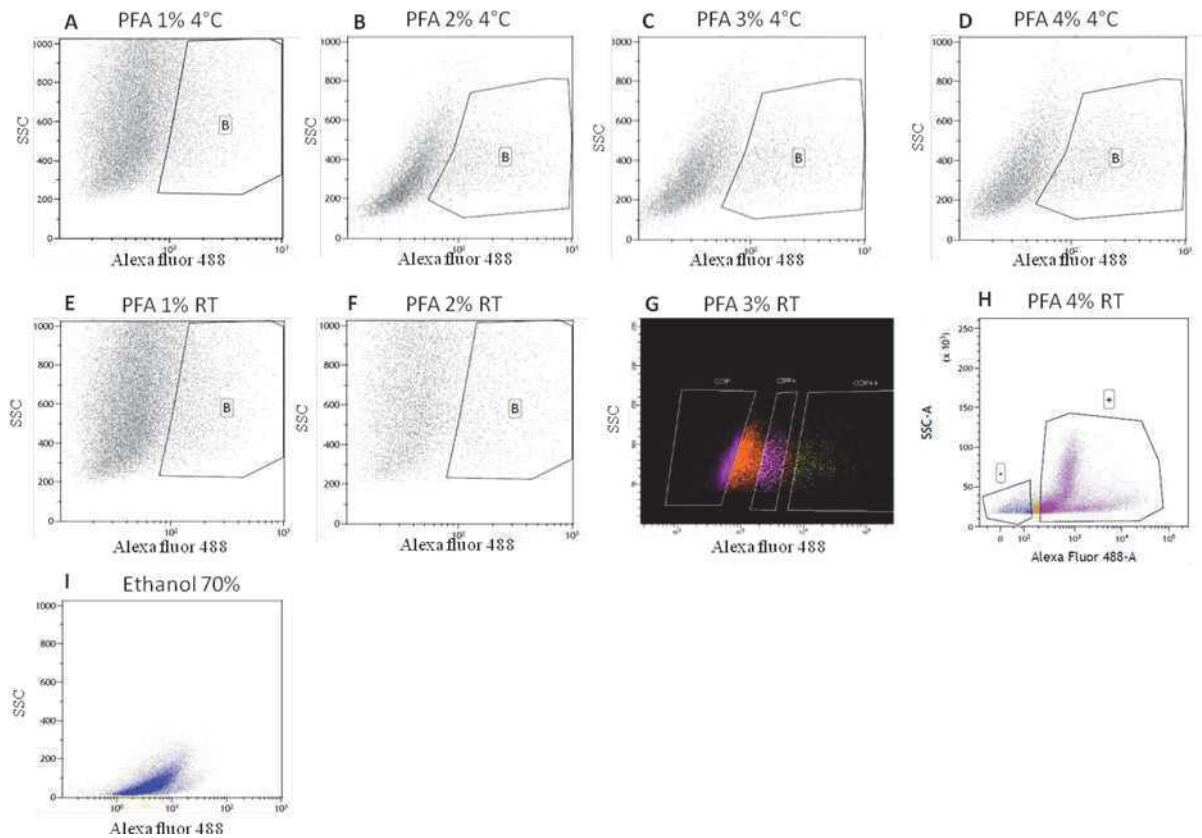


Figure S1: Fixation protocols in preparation for SCGB1A1 staining A- Fixation assay for optimal SCGB1A1 staining. The cells are trypsinized. PFA (1% to 4%) were tested for 15 min at 4°C (A, B, C and D) or RT (Room temperature) (E, F, G and H). Ethanol 70% fixations was tested for 15 min at RT (Room Temperature). The cells were permeabilized with Triton 0.1% /Saponin 0.1% (10min at RT). The staining with SCGB1A1 antibody was carried out: overnight at 4 °C. Cells were passed through a cytometer to visualize SCGB1A1 staining

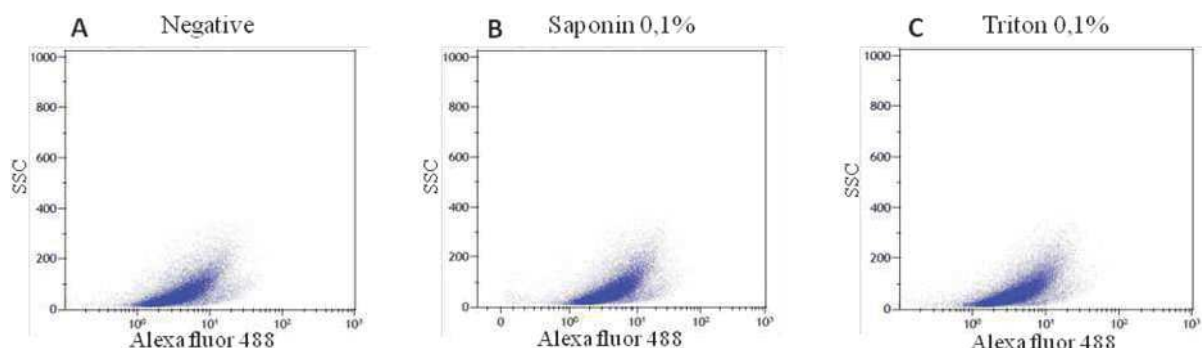


Figure S2: Permeabilization protocols in preparation for SCGB1A1 staining. Cells were trypsinized, fixed with PFA 4% (15min at RT). Then Permeabilization assay for optimal SCGB1A1 staining is performed because SCGB1A1 is an intracellular target. Permeabilizations with saponin 0.1% (B) or triton 0,1% (C) were carried out for 10 min at RT. Cells are passed through a cytometer to visualize SCGB1A1 staining (supplementary data).

Acknowledgements

This work was supported by the PHRC (IR 2013-14), and CHU Montpellier approval number: 2013 11 05; NCT02354677.

Author contributions

CV performed assays and experiments and interpreted the data and drafted the manuscript. AP helped design the assays and reviewed the manuscript. VP helped design the Microarray protocol and performed microarrays. CD helped design the Cell Sorting Protocol and performed cell sorting. DG and PC helped design the assays and reviewed the manuscript. IV supervised experiments and reviewed the manuscript. AB designed the study, interpreted the results and wrote the manuscript.

Competing interests

The authors declare no competing interest.

Discussion

Plusieurs études de single cell-RNA seq ont été réalisées afin d'obtenir la carte d'identité des cellules Club. Mais, ces études reposent sur l'expression de l'ARNm codant pour le CCSP dans l'ensemble des cellules épithéliales bronchiques humaines et non de celles exprimant la protéine CCSP. De plus, les données actuelles de Single cell-RNA seq semblent montrer que tous les types de cellules épithéliales bronchiques humaines *in vivo* et *in vitro* en modèle de culture ALI expriment l'ARNm de CCSP (données présentées dans le paragraphe suivant, II-2). Par conséquent, il est difficile de définir les cellules Club par l'expression de l'ARNm CCSP. C'est pourquoi, nous avons mis en place le protocole de tri cellulaire sur la protéine intracellulaire CCSP afin d'obtenir leur carte d'identité génétique et éventuellement trouver un marqueur alternatif (préférentiellement de surface) de ces cellules.

Actuellement, des protocoles pour réaliser des puces à ADN à partir de tissus fixés-perméabilisés ont été mis en place notamment à l'aide de la méthode MARIS. Mais, il est nécessaire d'adapter cette méthode au marquage souhaité et au tissu étudié. Le protocole de tri cellulaire que nous avons mis au point pour le marquage de CCSP, à partir des cultures de cellules épithéliales bronchiques humaines en modèle ALI, fonctionne aussi pour le marquage d'autres types cellulaires : cellules à mucus (marquage Muc5AC) et cellules ciliées (marquage TUBIV).

Dans ce protocole de tri, les étapes de fixation et de perméabilisation sont deux étapes essentielles pour obtenir un marquage intracellulaire CCSP en cytométrie en flux mais ces étapes ont aussi des effets délétères. En conséquence, il est essentiel d'utiliser des inhibiteurs des enzymes pouvant dégrader le matériel génétique notamment les RNAses présentes dans les tissus et le milieu environnant qui deviennent accessibles à cause de la perméabilisation. De plus, l'étape d'extraction du matériel génétique doit être adaptée à la fixation utilisée. La fixation par la formaline permet le marquage des cellules épithéliales par l'anticorps CCSP mais il induit aussi la formation de liaisons entre les protéines et le matériel génétique (ADN, ARN). Par conséquent afin de rompre ses liaisons, il est nécessaire de réaliser une digestion protéase au début de l'extraction à l'aide du kit d'extraction FFPE spécifique des tissus fixés.

Ce protocole mis en place a été validé par des techniques complémentaires. Il a été montré par PCR que l'expression de l'ARNm CCSP est bien augmentée dans la population de cellules CCSP positive en cytométrie en flux comparée à la population négative. Ceci permet aussi de valider la présence de matériel génétique après extraction des cellules Club triées. De plus, grâce

à la microscopie confocale, nous avons démontré l'intensité du marquage CCSP après le tri cellulaire. Les cellules triées CCSP positives en cytométrie en flux étaient bien marquées par l'anticorps anti-CCSP en immunofluorescence confocale (et inversement les triées négatives étaient bien non marquées). Ce sont deux validations par deux techniques différentes qui permettent de confirmer la séparation des populations par le protocole de tri cellulaire réalisé sur des cellules épithéliales humaines fixées et perméabilisées.

Avec l'utilisation d'échantillons fixés et perméabilisés, les étapes d'analyse par le Bioanalyzer sont essentielles pour suivre et valider la quantité et la qualité du matériel génétique à chaque étape. Pour finir, l'amplification avant la réalisation des puces à ADN est une étape clé dans la réalisation du transcriptome à cause de la faible quantité de matériel génétique obtenue après les étapes de tri.

Conclusion

Nous avons réussi à mettre au point un protocole qui permet de trier les cellules Club, par leur protéine CCSP, à partir de cultures ALI de cellules épithéliales bronchiques humaines. A l'aide de ce protocole, il a été possible de réaliser l'analyse transcriptomique de ces cellules triées par l'utilisation de puces à ADN (n=3). Ce protocole est reproductible et il peut être utilisé pour d'autres types cellulaires notamment les cellules à mucus et les cellules ciliées.

II-2. Identité des cellules Club dans l'épithélium des voies aériennes

Résumé

Les cellules Club sont déficitaires dans l'épithélium des voies aériennes des patients BPCO. Elles possèdent notamment des rôles de progéniteur accessoire et anti-inflammatoire qui peuvent être essentiels dans cette maladie. Les caractériser est donc primordial pour mieux appréhender leur potentiel thérapeutique.

Tout d'abord, à partir de cultures ALI de cellules épithéliales bronchiques humaines, des études morphologiques et « phénotypiques » ont été réalisées à l'aide de techniques de microscopie. Puis, grâce au protocole mis en place dans la partie précédente (II-1), les cellules Club sont triées, sur leur protéine CCSP, à partir de cultures ALI de cellules épithéliales bronchiques humaines (n=3), pour réaliser leur carte d'identité à l'aide d'une technique de puces à ADN. Les données obtenues sont confirmées par une technique de single cell-RNA seq à partir d'une culture ALI de cellules épithéliales bronchiques humaines (n=1) et d'un brossage de cellules épithéliales humaines (n=1).

Cette étude a permis d'obtenir l'identité des cellules Club dans différents modèles (*in vivo* et *in vitro*) et à l'aide de différentes techniques d'études (Single Cell-RNA seq, puces à ADN).

Nous avons montré que :

- Les cellules Club retrouvées en culture ALI ont une forme de dôme et elles possèdent des doubles marquages avec les cellules à mucus.
- Les données de single cell-RNA seq obtenues à partir d'une culture ALI ou d'un brossage montrent que la totalité des cellules épithéliales humaines expriment l'ARNm de CCSP.
- Les données de cytométrie en flux montrent qu'il y a plusieurs populations positives au marquage CCSP. Ces différentes populations possèdent une granulométrie et une fluorescence différentes.

-L'analyse des données des puces à ADN obtenues à partir des populations CCSP triées montrent que les différentes populations CCSP positives possèdent un profil ARN différents : profil de « type multicilié », profil de type « Club classique », profil de type « transition ». La population avec le profil de « type multicilié » est retrouvée déficitaire chez les patients BPCO tout comme la population de « type Club classique ».

-Il n'existe pas une mais des cellules Club.

-La carte d'identité des cellules Club par différentes méthodes a pu être réalisée.

Le papier est en cours d'écriture.

Different Club cells in human bronchial epithelium

Vernisse C¹, Assou S³, Petit A², Fieldes M³, De Vos J³, Vachier I², Bourdin A^{1,2}

1. PhyMedExp, University of Montpellier, INSERM U1046, CNRS UMR9214, France
2. Department of Respiratory Diseases and Addictology, Hospital Arnaud de Villeneuve, CHU Montpellier, France
3. IRMB, University of Montpellier, INSERM, CHU Montpellier, Montpellier, France

Address for Correspondence

Prof Arnaud Bourdin

Department of Respiratory Diseases

Hospital Arnaud de Villeneuve

371 avenue Doyen Giraud 34295 Montpellier Cedex 5 France

a-bourdin@chu-montpellier.fr

tel +33 4 67 33 61 26

Introduction

A decrease number of Club cell and its CCSP (Club Cell Secretory Protein) have been reported at small airway to COPD patient and this contributes to COPD development. Club cells are characterized in mice models and not in human. But, mice airway presents major differences with human so we cannot transpose mice data to humans. Currently, it is possible to study airway epithelium by using ALI (Air Liquid Interface) model and Club cells study can be performed in this model. A better understanding of these roles in particular progenitor and anti-inflammatory roles is essential. COPD is also defined by a decrease number of ciliated cells and an increase number of goblet cells. Club cell has accessory progenitor role that could help to restore missing cells in bronchial epithelium. So, their identity card is essential to better understand their potential therapeutic role in COPD. In human, it is possible to isolate them only by their intracellular marker, the secretoglobin1A1 (SCGB1A1 or CCSP for Club Cell Secretory Protein). A major problem of this marker is its localization. It is an intracellular marker which means that CCSP stained cells are not viable after CCSP staining protocol. To find cells roles and to understand a little more about what these cells are able to do, the genetic identity card of Club cells by different methods were performed in different subjects (COPD, control and smoker).

Methods

HBEC (Human Bronchial Epithelial Cells) cultures

Bronchial biopsies from controls, smokers and COPD subjects were collected during endobronchial bronchoscopy. Subjects were recruited at Arnaud de Villeneuve hospital, Montpellier, France, under a study protocol approved by ethics committee (RRR study, NCT02354677) of our institution, and all patients agreed to participate by reading and signing written consent forms. Human bronchial epithelial cells (HBECs) were obtained from endobronchial biopsies and cultured under air-liquid interface conditions, as described previously. Two method of culture are used.

Cultures to microscopy analysis: Bronchial epithelial biopsies were mechanically dissociated and suspended in Bronchial Epithelial Growth Medium (BEGM, Lonza). After seeding in multiwell plates coated with a solution of fibronectin and collagen, cells were expanded in a flask (0.75 cm²) and then plated (250,000 cells per well) on polyester membrane of Transwell^R in a 1:1 mixture of BEGM and DMEM (Dulbecco Modified Eagle Medium, Lonza) applied at the basal chamber only to establish air-liquid interface. Cells were maintained in culture for 28 days to obtain differentiated cells with a pseudostratified mucociliary epithelium. Cell cultures were maintained at 37 °C under 5 % CO₂. At day 28, cells were fixed for microscopy analysis.

Cultures to Microarray and Single cell-RNAseq analysis: Cells were dissociated mechanically from biopsies and cultivated in 12 well plate (ref 353043, Falcon) and then in 75 cm² flask (ref 353136, Falcon) in PneumaCult-Ex Plus medium (cat #05041, Stemcell Technologies, Grenoble, France) during 15 days. After an expansion phase, differentiation was initiated by seeding 110,000 cells on polyester membrane of Transwell^R (ref 3460, Corning, Kennebunk, United States) in Pneumacult-Ex Plus medium until confluence. After confluence, ALI culture was established by the aspiration of the apical chamber milieu (D0, day 0). Basolateral medium was replaced every two days with PneumaCult ALI maintenance medium (cat #05002, Stemcell Technologies, Grenoble, France), while cells were maintained at 37 °C, 5% CO₂ until day 28 of culture (referred as to D28).

Club cell Isolation to transcriptome analysis

At day 28 of HBEC culture (in stemcell medium), cells were trypsinized (ACF Enzymatic Dissociation solution and ACF Enzymatic Inhibition solution, Stemcell technologie, France) at 37 °C for 7 minutes. Cell suspension was centrifuged at 1500 rpm for 5 minutes. Supernatant was discarded and cells were resuspended in fixative solution. PFA 4 % (Formaldehyde solution, F8775, Sigma) fixation for 15 minutes at room temperature was performed. Then, cells were centrifuged and resuspended in triton 0.1% (ref 93443, sigma) and saponin 0.1 % (ref 93443, Sigma) in PBS (PBS w/o Magnesium w/o calcium, L0615, Dutscher) for 10 minutes at room temperature. After blocking step with donkey serum 10 % (D9663, Sigma) (in 1 % BSA PBS) for 1 hour at room temperature, cells were labeled with anti-SCGB1A1 primary antibody (Club cell protein CC16 human, rabbit polyclonal antibody, 1/10000, ref RD181022220-01, Biovendor) overnight at 4 °C. Finally, the cells were incubated with secondary

antibody (Alexa Fluor 488 donkey anti rabbit IgG (H+L), ref A21206, 1/2000, Invitrogen) for 1 hour at room temperature. During all these processes (fixation, permeabilization and antibody staining steps), solutions kept in sterile condition and supplemented with RNasin Ribonuclease Inhibitor (RNasin plus Rnase Inhibitor, 1000U, ref N261B, Promega). Finally, cells were sorted for intracellular marker SCGB1A1 using Aria IIIu becton Dickinson cytometer. Sorted cells were recovered in PBS with RNasin Ribonuclease inhibitor (1000U, ref N261B, Promega).

Extraction of SCGB1A1 sorted cells

RNA extraction of sorted cells was performed using the FFPE (“Formaldehyde-Fixed Paraffin-Embedded”) RecoverAll Total Nucleic Acid Isolation kit (AM1975, Thermofisher) with Recover All™ kit (ref 00641531, Thermofisher). During FFPE extraction kit, cells were digested with protease buffer at 50 °C for 1 hour and protease digestion step was stopped at 80 °C for 15 min. Then, RNA extraction was performed according to the manufacturer’s instruction. RNA was eluted in 20 µL of “elution solution” (RecoverAll Total Nucleic Acid Isolation kit, AM1975, Thermofisher).

RNA integrity

To evaluate RNA integrity, RNA solution was proceeded using Agilent 2100 Bioanalyzer (Agilent RNA 6000 PICO reagents kit, ref 5067-1514, Agilent Technologies). The Bioanalyzer profile allowed to evaluate the degradation and the RNA quantification.

Amplification and Microarray

The GeneChip™ IVT Pico Amplification Kit (ref 902622, WT Pico 12 RXN, Life Technologies SAS) was used according to manufacturer’s instructions. Then, Nanodrop and Bioanalyzer were used to qualitatively and quantitatively assess the amplification procedure.

Finally, DNA microarray (GeneChip™ Human Gene 2.0 ST Array, Ref 902112, Life Technologies SAS) were used to study the transcriptome of sorted cells according to manufacturer’s instructions.

Single cell-RNAseq procedure

The brush is placed in 5mL eppendorf containing 1mL of culture milieu. The tube is vortexed vigorously and then centrifuged for 2 min at 150g. Brush is removed and the cells are passed through 21G needles syringe 5 times every 5 minutes. The cells are centrifuged at 400 g for 5 min. The supernatant is removed and the cells are resuspended in 500 µL HBSS / 0.05 % BSA and 2.250 mL of 0.8 % ammonium chloride is added to lyse the red blood cells. After 10 min of incubation, the cells are centrifuged (400g for 5min). The supernatant is removed and the cells are resuspended in 1mL HBSS 0.05 % BSA and passed through 40 µm porosity Flowmi™ Cell Strainer. The supernatant is removed and the cells are taken up in HBSS 0.05 % BSA at a concentration of 1000 cells/µL. The same thing is done from an ALI culture.

Immunofluorescence and confocal microscopy

HBECs (in Lonza Medium) were fixed with 10% formalin for 15min followed by permeabilisation in PBS-0.1 % Triton for 15min. Nonspecific binding sites were blocked for 1h with 10 % donkey serum diluted in PBS-1 % BSA. Then cells were incubated overnight at 4 °C with rabbit anti-CCSP antibody at

1:1000; mouse anti-tubulinIV antibody at 1:400; mouse anti-MUC5AC antibody at 1:100; goat anti-P63 antibody at 1:50 and mouse anti-Ki-67 antibody at 1:200. As a negative control, the primary antibody was omitted. After several rinses in PBS-0.025 % Triton, the cells were incubated for 1h with Alexa Fluor secondary antibodies at 1:2000 (Invitrogen), proceeding in the darkness, and counterstained for nuclei with 4,6-diamidino-2-phenylindole (DAPI) at 1:5000 for 1 min. The coverslips were mounted using Fluoroshield mounting medium (Abcam). Stained cells were visualized under a Zeiss Axio Imager fluorescence microscope and a Zeiss LSM 780 confocal microscope. All images were processed with Axio Vision Software and Image J software for image analysis.

Ultrastructural evaluation

Inserts with *ex vivo* differentiated epithelial cells were immersed in a solution of 2.5 % glutaraldehyde in PHEM buffer (pH 7.4) overnight at 4 °C. They were then rinsed in PHEM buffer and post-fixed in a 0.5% osmic acid for 2 h at dark and room temperature. After 2 rinses in PHEM buffer, the cells were dehydrated in a graded series of ethanol solutions (30-100 %). The cells were embedded in EmBed 812 using an Automated Microwave Tissue Processor for Electronic Microscopy, Leica EM AMW. Then sections (70 nm; Leica-Reichert Ultracut E) were collected at different levels of each block. These sections were counterstained with uranyl acetate 1.5 % in 70% ethanol and lead citrate and observed using a Tecnai F20 transmission electron microscope at 200KV in the CoMET MRI facilities, INM France.

Scanning electron microscopy

PBS washed-bronchial epithelial cells cultured in ALI were fixed with 2.5 % glutaraldehyde in PHEM buffer (pH 7.2) for 1 h at room temperature, followed by washing in PHEM buffer. Fixed samples were dehydrated using a graded ethanol series (30-100 %), followed by 10 min in graded ethanol – hexamethyldisilazane and then hexamethyldisilazane alone. Subsequently, the samples were sputter coated with an approximative 10 nm thick gold film and then examined under a scanning electron microscope (Hitachi S4000, at CoMET,MRI-RIO Imaging, Biocampus, INM Montpellier France) using a lens detector with an acceleration voltage of 10KV at calibrated magnifications.

Statistical analyses

Data were expressed as mean \pm SEM. Paired comparisons were made using Mann-Whitney tests and were considered statistically significant at p-value<0.05. All graphical data and statistical analyses were generated with GraphPAD Prism software (Version 6.0).

Results

Club Cell in ALI culture

In ALI culture, epithelium was differentiated, we find Club and ciliated cells (Figure 1A). Moreover, you can see that CCSP secretion forms spans in the culture (Figure 1B). We visualize, by transmission microscopy, cilia (Figure 1C) but also dome cells (Figure 1D and E) which colocalize with CCSP labeling (Figure 1F). Dome cells in ALI culture was Club cells. Finally, double labeling was performed, we notice that CCSP (Club cell) and Muc5AC label (goblet cell) are found in the same cell, which allows us to visualize progenitor role of Club cells.

Club cell depletion in ALI cultures of human bronchial epithelial cells were performed by using naphthalene and paraquat. You can see that these two tests do not deplete Club cells in ALI cultures (Figure S1). Moreover, identity card of Club cells were defined in mice by using the single cell RNA seq technique. CHAD is a surface marker found characteristic of these cells. This marker was tested on human bronchial biopsies but it was negative (Figure S2).

Club cell profile with Single Cell-RNA seq

A single cell-RNA seq technique was performed on human bronchial epithelial cells culture and human epithelial cell brushing. The tSNE representation shows that cells from ALI culture and brushing made distinct groups (Figure 2A). You can see that CCSP mRNA is present in all epithelial cells but with different expression level (Figure 2B). For ciliated cells, FoxJ1 expression (Figure 2C) is found in both samples and fairly well localized, as goblet cells (Figure 2D) and basal cells (Figure 2E). Unsupervised clustering of ALI culture was carried out in order to find different differentiated cell groups. There are 5 different clusters (Figure 2F) but gene expression is different between clusters. We notice that cluster 1 (Figure 2G) corresponds to ciliated cells; cluster 2 (Figure 2H), cluster 4 (Figure 2J) and cluster 5 (Figure 2K) correspond to Club cells; cluster 3 (Figure I) to basal cells. We do not find a single cluster of Club cells. It is confirmed when we look at the functions of these different clusters (Figure 2H) where it is difficult to see various functions of differentiated cell.

Club cell transcriptome

CCSP protein is biologically active. You have set up a technique to sort Club cells by their specific intracellular marker. Clusters of Single cell-RNA seq sorted three groups of Club cells. We wanted to see what was happening with CCSP protein expression. Protocol for sorting Club cells by their CCSP protein has been set up. You obtain 4 distinct cell populations according to their granularity and fluorescence (Figure 3A). These cells are sorted and they are recovered to visualize their labeling by confocal microscopy. You can see that cells have different fluorescence according to sorted populations (Figure

3B). The proportion of different CCSP populations in different “disease” (smokers, COPD and controls) is different; you can see that cell populations are not present in the same quantity. The very positive CCSP population (CCSP +++) is found to be decreased in COPD patients and smokers compared to controls. CCSP++ population is decreased in COPD patients compared to controls. CCSP+ population is increased in COPD patients. Transcriptomic analyses were performed by using DNA microarrays to understand what the different sorted populations are. It was noted that the very positive CCSP cells have specific marker of Club cells (Figure 3D) and these functions seem to correspond to the "classical" roles of Club cells (Figure 3G). CCSP++ population have ciliated cell markers (Figure 3D), which is confirmed by their functions that are related to cilia (Figure 2F). CCSP+ population profile shows a transient state (Figure 3D) with signaling functions (Figure 2E). These three different types of CCSP cells still have common markers that seem to correlate with mucus cells (Figure 2D). It is confirmed by double CCSP/MUC labeling showing that mucus is dispersed in these different cell types.

“Homology” between single cell-RNA seq and microarray

The data obtained in two methods (Single cell-RNA seq and DNA microarray) were compared to see if sorted CCSP populations can be found in single cell-RNA seq cluster. You see that cluster 1 resembles to sorted CCSP++ population; cluster 3 corresponds to sorted CCSP- population; clusters 2, 4 and 5 correspond to sorted CCSP+++ population (Figure 4). CCSP- population is not found in the clusters of the single cell RNA seq.

Identity card of Club cells

It is possible to define Club cell identity card by using single cell-RNA seq technique in an ALI culture (Figure 5A). They have characteristic markers such as SCGB, XBP1, and markers found in literature (SLPI, BPIFB1). These data were also extracted from human epithelial cell brushing. They have classical Club cell markers such as SCGB, CYP2F1, XBP1, and other markers found in the literature (Figure 5B). The two conditions are cross-matched to obtain Club cell identity card, they have characteristic Club cell markers such as SCGB, Cyp2f1, XBP1 and other markers found in the literature (LYPD2, C3, SLPI) (Figure 5C). CCSP+++ cells transcriptomic analysis are compared with Club cells data obtained from single cell-RNA seq data, there have characteristic Club cell markers such as XBP1, Cyp2f1, XBP1 and other markers from the literature (C3, LCN2) (Figure 5D). Club cell identity card from all data includes 15 common markers but no surface markers as if these cells had only secretory role.

Discussion

There is not one but various Club cells with different RNA profiles: ciliated RNA, Club RNA and transient RNA. These populations are not present in same quantity, especially the "classical Club" cells, and "ciliated" cells are decreased in COPD patients whereas "transient" cells are increased. "Ciliated cells" are decreased and this seems to correlate with literature data showing decrease of ciliated cells in COPD patients.

It is possible to think that Club cells can give ciliated cells except in case of COPD where the level of these cells is decreased compared to controls. We have shown that DapT, a gamma secretase inhibitor, can reverse the effects of smoking by increasing the number of ciliated cells. We can think that these cells are impacted in COPD patients and be able to act on these cells could have a therapeutic potential to fight the mucociliary clearance deficit. Modulating different Club cell types could be therapeutic potential in COPD

Figures

Figure 1

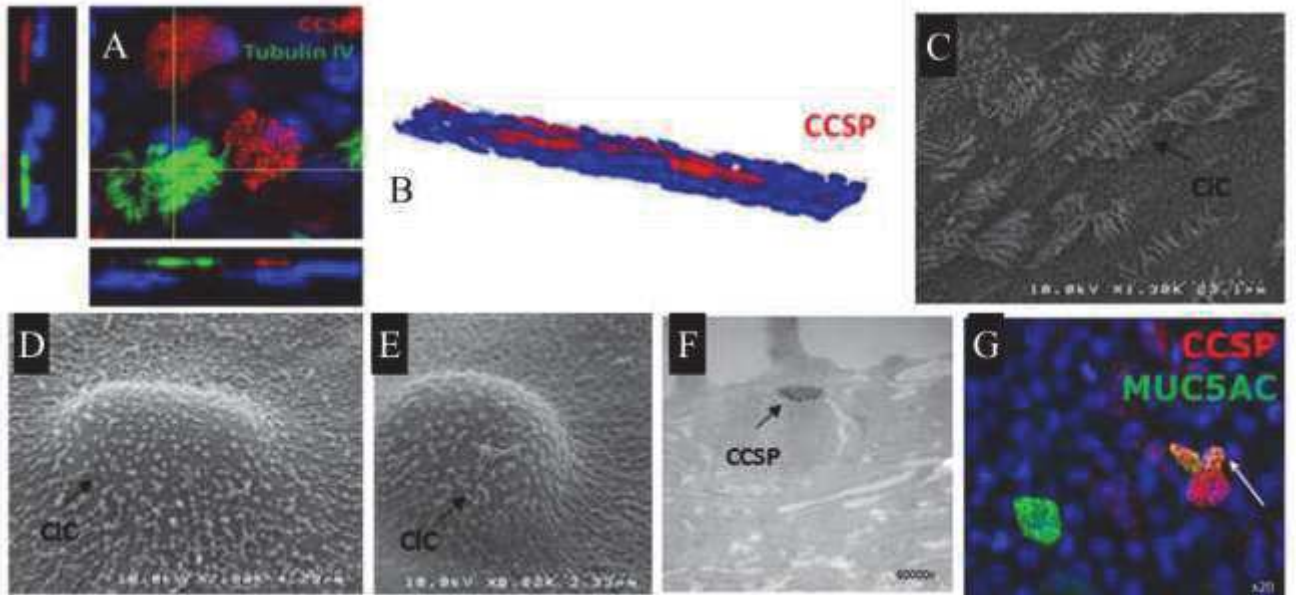


Figure 2

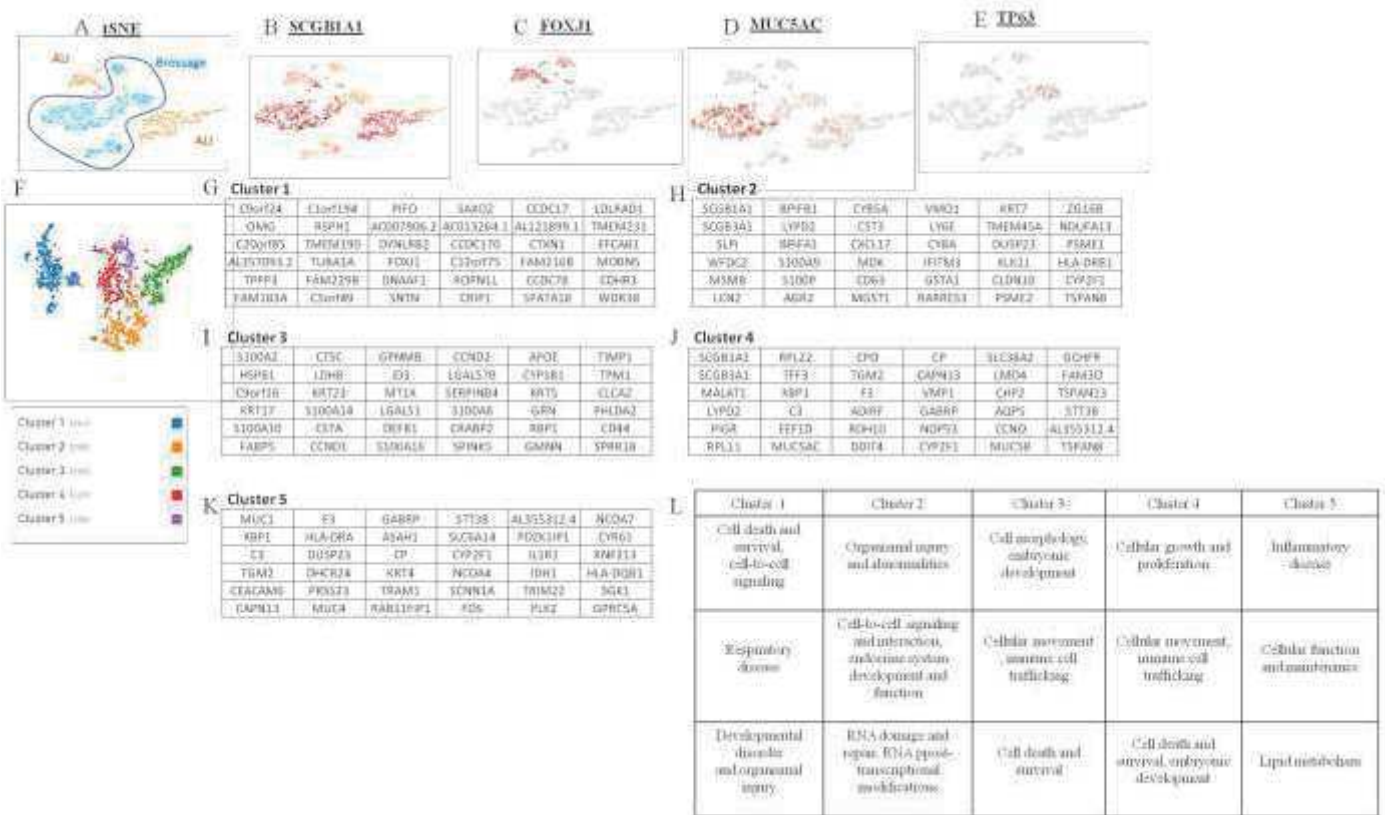


Figure 3

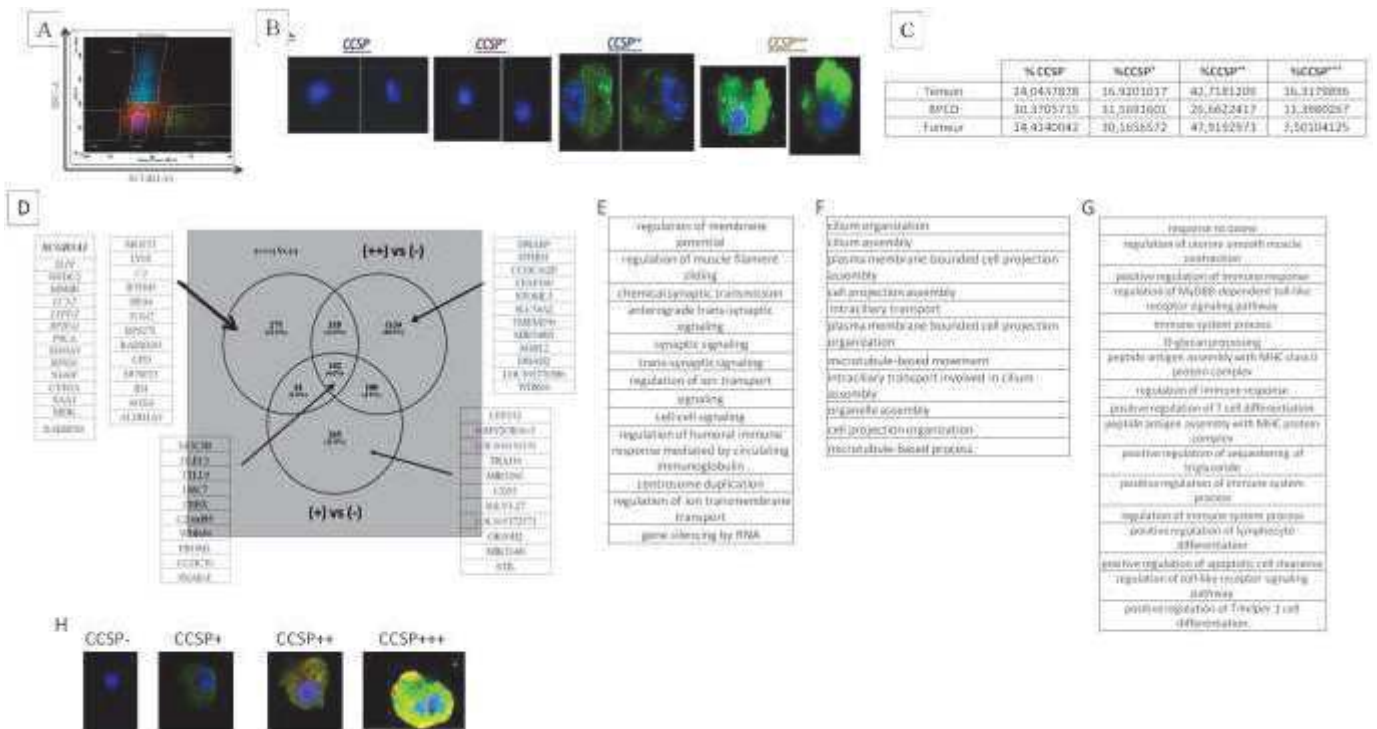
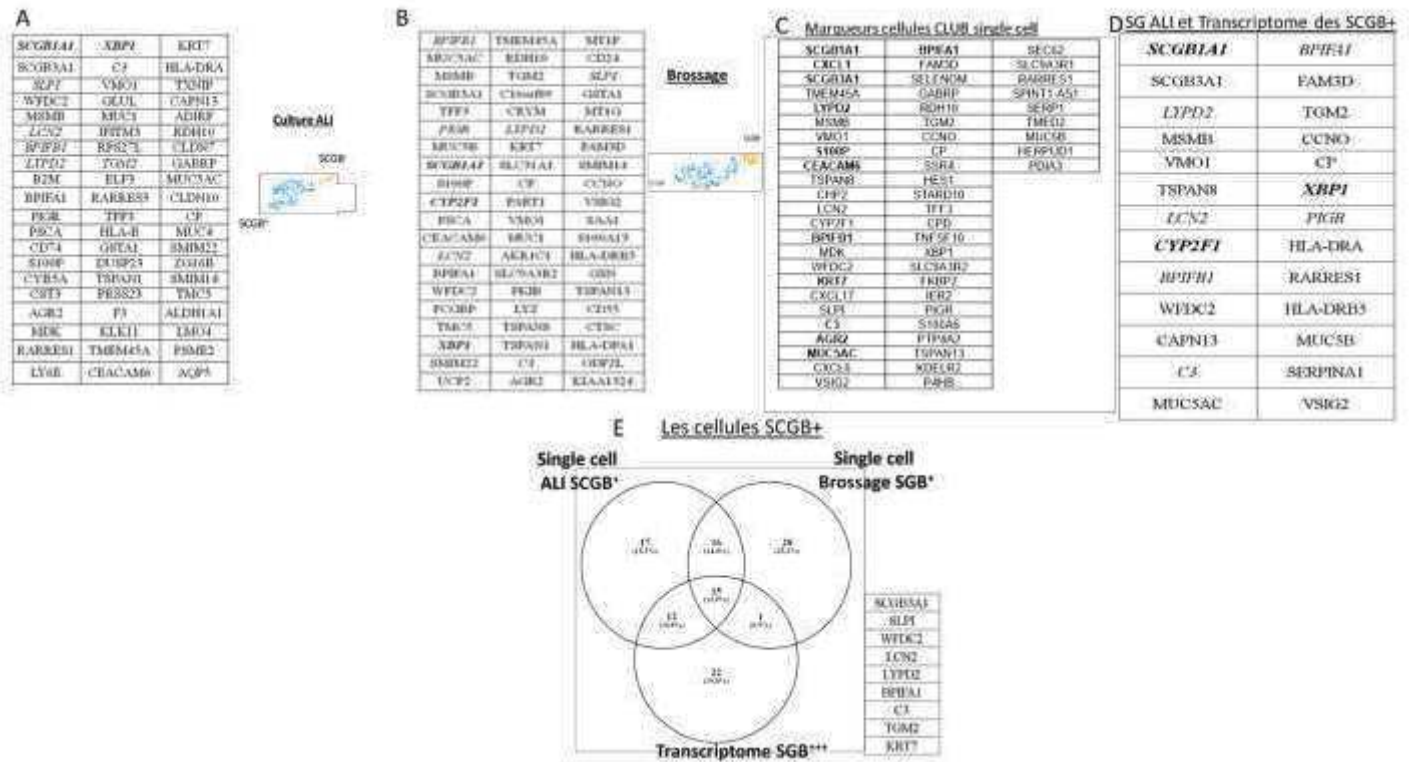


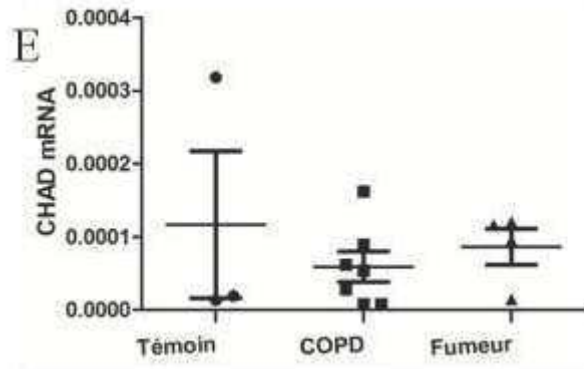
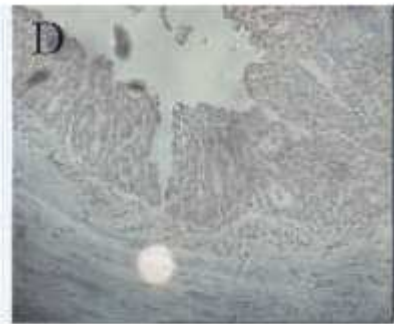
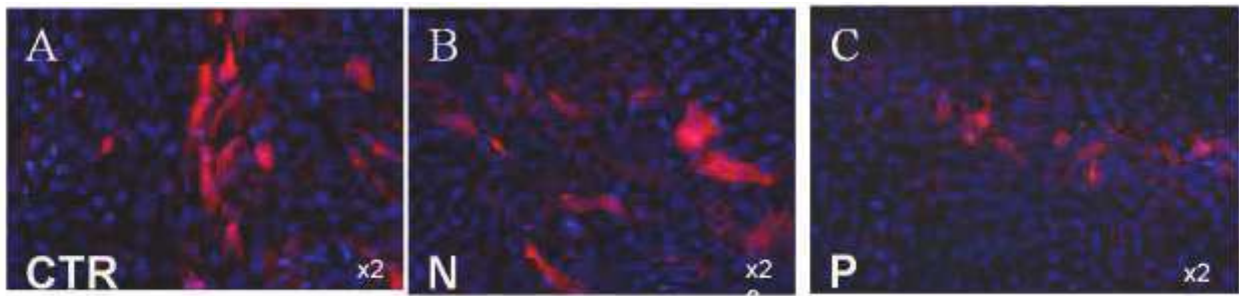
Figure 4

Cluster 1 SG et CCSP++	Cluster 2 SG et CCSP+++	Cluster 3 SG et CCSP-	Cluster 4 SG et CCSP+++	Cluster 5 SG et CCSP+++
Name	Name	Name	Name	Name
C9orf24	SCGB1A1	S100A2	SCGB1A1	MUC1
OMG	SCGB3A1	HSP91	SCGB3A1	XBP1
C20orf85	SLPI	C9orf16	MALAT1	C3
AL357093.2	WFDC2	KRT17	LYPD2	TGM2
TPPP3	M5MB	S100A10	PIGR	CEACAM6
FAM183A	LCN2	FABP5	RPL11	CAPN13
C1orf194	BPIFB1	CTSC	RPL22	F3
RSPH1	LYPD2	LDHB	TFF3	HLA-DRA
TMEM190	8P1FA1	KRT23	XBP1	DUSP23
TUBA1A	S100A9	S100A14	C3	DHCR24
FAM229B	S100P	CSTA	EEF1D	PRSS23
C5orf49	AGR2	CCND1	MUC5AC	MUC4
PIFO	CYB5A	GFNMB	CPD	GABRP
ACC07906.2	CST3	ID3	TGM2	ASAH1
DYNLRB2	CXCL17	MT1X	F3	CP
FOXJ1	MDK	LGALS1	ADIRF	KRT4
DNAAF1	CD63	DEFB1	RDH10	TRAM1
SNTN	MGST1	S100A16	DDIT4	RAB11FIP1
SAXO2	VMO1	CCND2	CP	STT3B
AC013264.1	LY6E	LGALS7B	CAPN13	SLC6A14
CCDC170	CYBA	SERPINB4	VMP1	CYP2F1
C12orf75	IFITM3	S100A8	GABRP	NCOA4
ROPN1L	GSTA1	CRABP2	NOP53	SCNN1A
CRIP1	RARRES3	SPINK5	CYP2F1	FOS
CCDC17	KRT7	APOE	SLC38A2	AL355312.4
AL121899.1	TMEM45A	CYP1B1	LMO4	PDZK3IP1
CTXN1	DUSP23	KRT5	CHP2	IL1R1
FAM216B	KLK11	GRN	AQP5	IDH1
CCDC78	CLDN10	RBP1	CCNO	TRIM22
SPATA18	PSME2	GMNN	MUC5B	PLK2
LDLRAD1	ZG16B	TIMP1	GCHFR	NCOA7
TMEM231	NDUFA13	TPM1	FAM3D	CYR61
EFCAB1	PSME1	CLCA2	TSPAN13	RNF213
MORN5	HLA-DRB1	CD44	STT3B	HLA-DQB1
CDHR3	CYP2F1	SPRR1B	AL355312.4	SGK1
WDR38	TSPAN8	BTG2	TSPAN8	GPRC5A
LRRC10B	PSMB1	GSTA4	BPIFA2	CLIC6
FAM92B	PI3	SFN	ELOVL5	STEAP4
PPIL6	PSMB3	ITGAV	SLC15A2	VWTR1
FAM166B	TMEM205	KRT13	FOXN3	ASS1
C22orf15	COPE	TM4SF1	PTM5	PHACTR2
ACC04832.1	SERPINF1	ATP1B3	RHOV	MET
WDR78	PSMB6	CDK6	DHR53	C15orf48
TUBA4B	RNF183	FAM162A	SLC12A2	NTN4
ENKUR	VSIG2	JAG1	CDC42EP5	CHPT1
	HLA-DRB5	KRT15	STEAP4	TNFAIP2
	DCXR	ITGB6	ST6GAL1	CX3CL1
	MYDGF	PHLDA3	CRACR2B	DTX4
	MGST2	CDKN2B	SRRM1	C1orf116
	SERPINA1		SELENBP1	NOTCH2

Figure 5



Supplementary data



Discussion

Les cellules Club ont été assez bien caractérisées chez la souris mais chez l'homme leur caractérisation est plus difficile. En particulier, la déplétion de ces cellules dans des cultures ALI de cellules épithéliales bronchiques humaines n'est pas possible par l'utilisation du naphthalène et leur caractérisation repose sur l'utilisation de leur marqueur intracellulaire, le CCSP.

Cette étude a permis de montrer que les cellules Club en culture ALI possèdent des co-marquages avec Muc5AC. Ceci corrèle avec les données de la littérature qui montrent le rôle de progéniteur accessoire de ces cellules Club. En parallèle, il a été testé sur des échantillons humains, des marqueurs spécifiques des cellules Club chez la souris, en particulier CHAD (Chondroadhérine), mais les marqueurs présents chez la souris ne peuvent pas être transposés chez l'humain.

Plusieurs études de Single cell-RNA seq ont été réalisées à partir de cellules épithéliales humaines afin d'obtenir la carte d'identité de ces cellules. Nos données montrent que la totalité des cellules épithéliales bronchiques humaines dans une culture ALI ou dans un broyage de cellules épithéliales humaines expriment l'ARNm de CCSP. Ceci corrèle avec des données de la littérature montrant la plasticité et le rôle de progéniteur de ces cellules Club. Mais avec cette technique, il semble difficile de distinguer les cellules Club d'autant plus que la protéine CCSP est une protéine très active biologiquement donc une méthode d'étude des cellules Club par leur protéine est essentielle.

Les données obtenues en cytométrie en flux montrent que plusieurs populations expriment la protéine CCSP mais avec une granulosité et fluorescence différentes. Les résultats des puces à ADN obtenues à partir des populations triées CCSP montrent que les différentes populations CCSP positives ne possèdent pas le même profil d'expression ARNm, un type « multicilié », un type « Club classique » et un type plutôt de « transition ». Ceci corrèle avec les données de la littérature qui montrent une grande plasticité de ces cellules.

Par contre, la proportion des différentes populations cellulaires CCSP positives n'est pas la même en fonction des maladies. Les populations « type multicilié » et « type Club classique » sont déficitaires dans la BPCO par contre on a une augmentation de la population « type transition » dans cette maladie. Cette population CCSP « type multiciliée » est potentiellement celle qui est destinée à se différencier en cellules ciliées. Cela semble corrélérer avec les données de la littérature puisque le déficit en cellules ciliées dans la BPCO a été rapporté à de nombreuses

reprises. Nous avons pu montrer dans un autre papier (paragraphe III), que le DapT, un inhibiteur de la gamma secretase dans la voie Notch, pouvait réverser ces changements favorisés par la fumée de cigarette. On peut donc penser qu'il existe un effet spécifique du tabac ou de la maladie, la BPCO (sans pouvoir dire à ce stade la part respective de l'un ou de l'autre) sur ce sous type de cellule qui représente une cible thérapeutique pour lutter contre le déficit de clairance mucociliaire, et peut être donc l'obstruction.

Toutes ces données montrent qu'il n'existe pas une mais des cellules Club avec un profil ARNm différent en fonction de leur granulosité et leur fluorescence, pour le marquage CCSP en cytométrie en flux, ce qui renforce l'idée de la plasticité de ces cellules. Par contre, on remarque que les cellules CCSP avec un profil ARN « type Club classique » ne possèdent pas de marqueur de surface comme si elles ne possédaient qu'un profil sécrétoire. Si on souhaitait trier ces cellules Club, il serait donc nécessaire de réaliser un tri négatif en ôtant les autres populations cellulaires.

Par contre les données obtenues à partir des puces à ADN devront être validées soit sur des brossages soit sur des biopsies pour valider la présence des différents types de cellules Club ainsi que leur déficit dans la BPCO.

Conclusion

On ne retrouve pas un type de cellules Club mais des cellules Club ce qui corrèlent avec les données de la littérature qui parle de « plasticité » des cellules Club. A partir des données des puces à ADN, on peut envisager que les cellules Club peuvent se différencier en plusieurs types cellulaires avec un profil d'expression ARNm ciblant un type cellulaire particulier (ciliée, Club). Ceci permet d'envisager de moduler les différents types de cellules Club dans la BPCO pour restaurer le « bon type » de cellules Club dans l'épithélium. Notamment agir sur la population « type multiciliée » pour lutter contre le déficit en clairance mucociliaire et peut être l'obstruction caractéristique des patients BPCO, est une piste thérapeutique dans cette maladie.

Pouvoir moduler les cellules présentes dans l'épithélium des patients BPCO est une piste thérapeutique à envisager.

III- Superviser la différenciation pour adapter le phénotype des cellules épithéliales bronchiques humaines en culture ALI

Résumé

La proportion de chaque type de cellules épithéliales spécifiques dans l'épithélium des voies aériennes est relativement bien déterminée et leurs rapports sont assez caractéristiques des différentes maladies chroniques des voies aériennes. Notamment, au niveau de l'épithélium des patients atteints de BPCO, il y a une diminution de la quantité de cellules Club, une augmentation du nombre de cellules à mucus et une diminution du nombre de cellules ciliées. Cette hyperplasie des cellules à mucus semble impliquée dans la réduction de la clairance mucociliaire. Le tabac serait la principale cause de ces changements chez les patients BPCO.

Nous posons donc l'hypothèse que superviser la différenciation cellulaire pour rétablir un épithélium dit « normal » pourrait être une piste thérapeutique dans les maladies chroniques des voies aériennes. L'objectif est notamment de restaurer le rapport cellules ciliées/cellules à mucus et le nombre de cellules Club dans l'épithélium. Pour confirmer cette hypothèse, il est possible d'activer ou de réprimer des voies de signalisation (voies Rho, Notch et BMP) connues dans le développement embryonnaire pour impacter le phénotype cellulaire. Pour cela, nous avons étudié l'effet de différentes molécules (Y27632, DapT et LDN193189), connues pour activer ou inhiber ces voies de signalisation, sur la différenciation de deux modèles de cultures cellulaires (NHBE et HBEC). De plus, nous avons vérifié l'impact de ces drogues sur les effets du tabac modélisés par la présence de CSE (Cigarette Smoke Extract) mais aussi sur le remodelage induit par une agression mécanique de type scratch.

Nous avons montré que :

- Y27632, un inhibiteur de la voie Rho, augmente l'expression de l'ARNm CCSP et la quantité de cellules Club dans les cultures HBEC et NHBE.

- DapT, un inhibiteur de la γ -secretase présente dans la voie de signalisation Notch, inhibe la différenciation des cellules Club et des cellules à mucus mais favorise le développement des cellules ciliées et des cellules basales dans les cultures HBEC et NHBE.
- LDN193189, un inhibiteur de la voie BMP, augmente la quantité de cellules à mucus dans les cultures NHBE.
- Le ratio d'ARNm des cellules ciliées/cellules à mucus est restauré par l'ajout de DapT dans les cultures NHBE ou HBEC.
- La stimulation par le CSE permet d'augmenter la quantité de cellules à mucus dans les cultures HBEC mais l'ajout de DapT reverse l'action du CSE sur l'épithélium.
- DapT ralentit la réparation cellulaire, dans les cultures HBEC, lors d'une agression mécanique induite par un scratch.

Cet article est actuellement en cours d'écriture pour une soumission à l'AJRCCM.

Supervising differentiation for tailoring the airway epithelial cell phenotype

Charlotte Vernisse^{1§} and Noemie Drappier^{1§}, Aurelie Petit², Lucie Knabe², John de Vos³, Said Assou³, Mathieu Fieldes³, Chloe Bourguignon³, Joffrey Mianne³, Jeremy Charriot^{1,2}, Isabelle Vachier², Delphine Gras⁴, Pascal Chanez⁴, Arnaud Bourdin^{1,2§} and Engi Ahmed^{2,3§}.

§ both authors equally contributed to this work

- 1 PhyMedExp, University of Montpellier, INSERM U1046, CNRS UMR9214, France
- 2 Department of Respiratory Diseases and Addictology, Hospital Arnaud de Villeneuve, CHU Montpellier, France
- 3 IRMB, University of Montpellier, INSERM, CHU Montpellier, Montpellier, France
- 4 Department of Respiratory Medicine, Assistance Publique Hôpitaux de Marseille, UMR INSERM U1067 CNRS 7333, Aix Marseille University, Marseille, France

Address for Correspondence

Prof Arnaud Bourdin

Department of Respiratory Diseases

Hospital Arnaud de Villeneuve

371 avenue Doyen Giraud 34295 Montpellier Cedex 5 France

a-bourdin@chu-montpellier.fr

tel +33 4 67 33 61 26

Author's contribution to this work

CV and ND perform assays and experiments, interpreted the data and drafted the manuscript

LK performs experiments

AP and JDV supervised, designed assays and experiments and reviewed the manuscript

MF, CB, JM, JC, SA and IV helped in interpreting the data and improved the manuscript

DG and PC helped in designed the assays and reviewed the manuscript

AB and EA designed the study, interpreted the results and wrote the manuscript.

Running title: DapT supervises goblet cell hyperplasia

In function of drugs, cell fate is tailored in airway epithelium. DapT allows to supervise goblet cell hyperplasia which is a therapeutic opportunity in COPD.

Abstract

Rationale: Promoting high ciliated to goblet cell ratios would prevent impaired mucociliary clearance commonly associated with progression of chronic airway diseases.

Objective: We aimed at testing whether the goblet or ciliated cells fates could be pharmacologically tailored in NHBE and to which extent the CSE induced goblet cell hyperplasia could be prevented in ALI cultures.

Methods: HBEC and NHBE cultures were cultivated with different drugs (Y, DapT, LDN), known to impact signalling pathways.

Measurements and Main results: At day 7 either in NHBE and ALI cultivated-HBEC, CCSP upregulation by the p160ROCK inhibitor, Y27632 (2 fold increase in NHBE and 3 fold in HBEC) was accompanied by a parallel increase in density of Muc5AC expressing cells and Muc5AC mRNA (4 fold increase in NHBE). An increase of Muc5AC cells were observed in NHBE when supplementing the milieu with the BMP inhibitor, LDN. In contrast, inhibiting the Notch gamma secretase with DapT specifically increased the respective FoxJ1 ciliated cell marker (3 fold increases in HBEC and 2 fold in NHBE) and p63 basal cell marker while hampering CCSP and Muc5AC mRNA, protein and density of positive cells. These data have been confirmed by single cell-RNAseq, DapT promotes basal and ciliated phenotypes and reduces secretory cells. Moreover, in ALI HBEC cultures, DapT was able to prevent CSE-induced goblet cell hyperplasia by increasing differentiation toward ciliated cells without inducing excess of mortality.

Conclusion: Tailoring the airway epithelial cell phenotype is achievable in human primary BEC cultures spontaneously and after injuries.

Keywords: Cell fate, Goblet Cells Hyperplasia, Tailoring cell phenotype

Introduction

Changes in airway epithelial phenotypes are hallmarking chronic airway diseases and this was observed as early as the 19th century. Indeed, decreased Club cell rates and progressive replacement of ciliated by goblet cells were consistently reported in COPD (Chronic Obstructive Pulmonary Disease) but also in Cystic Fibrosis (CF) and severe asthma^{1,2,3}. Reduced mucociliary clearance and mucoid impactions are thought to be the consequences of these changes whereas defective innate immune response related to Club cell deficiency may lead to excessive airway neutrophilic inflammation⁴ and potentially to an increased susceptibility to inhaled noxious agents^{5,6,7,8}. Cigarette smoke is the most likely responsible of cellular imbalance particularly, Goblet Cell hyperplasia found in COPD patients. At a glance, tailoring the differentiation process likely represent a great therapeutic opportunity in chronic airway diseases to restore the ciliated to goblet cell imbalance and protect club cells to improve and maintain airway homeostasis.

Drivers ruling the cell fates are incompletely understood and many hypotheses are still debated^{9,10,11,12,13,14}. Rainbow assays dramatically improved our understanding of the airway epithelial cell fate in mice^{10,11}. Conversely, not obvious are the discrepancies reported between human and mice airways and cautions are claimed before extrapolations can be trusted. In mice, Club cells and basal cells are acknowledged airway epithelial stem cells whereas ciliated cells may also be able to play this role¹⁵. In humans, basal cells are the main airway epithelial stem cells and club cells accessory only^{16,17,18,19}. Progenitors are supposed to express both Nkx2.1 and CCSP early together with Sox2 and 9 but most of these markers are later lost^{20,21,22,23}.

In developing lung, ligand-activated Notch signalling controls cell fates in the upper airways by restricting ciliated fate and promoting secretory fates²⁴. In adult lung, Notch regulates cell fate decision, basal cell renewal and drives differentiation of stem cells into goblet cells²⁵. Notch signalling is required to maintain differentiated state of secretory cells in the upper airways and blocking Notch-Jagged1/2 signalling led to transdifferentiation of club cells into ciliated cells²⁶. DapT is a Notch pathway inhibitor. Y27632, ROCK inhibitor, has been shown to improve proliferation rates of human and mouse tracheal epithelial cells without affecting subsequent ALI differentiation²⁷. Bone Morphogenetic Proteins (BMPs) are group of signalling molecules that belongs to Transforming Growth Factor- β (TGF- β) superfamily. BMP4 is a prominent signalling molecule in lung development²⁸. LDN193189 is a potent inhibitor of BMP pathway, inhibiting ALK.

We aimed at modifying human airway epithelial phenotype by activating or repressing pathways identified during development to affect cell fates in order to promote differentiated cells in ALI cultures spontaneously and after injuries. For this purpose, we develop cell models in NHBE and CSE-exposed ALI human bronchial epithelial cell cultures.

Methods

NHBE and HBEC cultures

NHBE and HBEC were cultivated according to manufacturer's instructions. See in data supplement.

Cell stimulation in ALI cultures

The basolateral medium of NHBE culture (n=6) or HBEC culture (n=5) were supplemented all along the differentiation process (i.e. until day 7 or until day 14) with Y27632 (5 μ M) or DapT (10 μ M) or LDN-193189 (250 nM) or with combination of molecules: Y27632 (5 μ M) plus LDN-193189 (250 nM) and Y27632 (5 μ M) plus DapT (10 μ M) or not supplemented.

Immunofluorescence for ALI culture

At day 7 (NHBE and HBEC) or day 14 (HBEC) of ALI culture, cells were fixed with 10% formalin solution followed by permeabilization using PBS 0.1% Triton X-100 (Sigma). Non-specific binding sites were blocked with 10% donkey serum (Sigma) diluted in PBS 1% BSA (Bovine Serum Albumin) at room temperature. Then, cells were incubated overnight at 4°C with rabbit polyclonal anti-CCSP (Club Cell Secretory Protein) antibody (Biovendor, Brno, Czech Republic) or mouse monoclonal anti-Muc5AC (Mucin 5AC) antibody (clone 45M1, Abcam, UK) or mouse monoclonal anti- β Tubulin IV antibody (sigma, Missouri, United states) or mouse monoclonal p63 antibody (sigma, Missouri, United States). Cells were incubated with Alexa Fluor secondary antibodies (Invitrogen, USA) at room temperature (RT) and counterstained for nuclei with DAPI (4,6-diamidino-2-phenylindole) before mounting. Finally, stained cells were visualized under a Zeiss AxioImager microscope and 4 randomly located pictures for each condition were analyzed using Image J Software.

Dot Blot Assays

CCSP and Muc5AC secretions were quantified at apical washes performed with 150 μ l (HBEC) or 500 μ l (NHBE) of PBS. 10 μ l of apical washes or different concentrations of CCSP recombinant protein (Santa Cruz, Germany, 0.5 to 1000ng/ml) or Muc5AC (standard sample) were spotted onto nitrocellulose membrane. After blocking, membranes were incubated with primary antibody (rabbit polyclonal anti-CCSP (Biovendor, Brno, Czech Republic) or mouse polyclonal anti-Muc5AC (ThermoFisher scientific, USA)) at RT. Immunodetection was carried

out using fluorescent secondary antibody revealed (Invitrogen) and analysed with Odyssey Infrared Imaging System (LI-COR Biosciences).

Real time RT-PCR analysis

Total RNA was extracted from ALI cells (D0, D7 and D14: stimulated and control conditions) by using All prep DNA/RNA/protein Mini kit (Qiagen) and 0.4 μ g of RNA was reverse transcribed with verso one step RT-PCR kit (Thermofisher Scientific). Real time PCR was performed using light cycler DNA master SYBR Green (Roche Applied Science). The comparative Ct method for relative quantification of gene expression was used ($2^{\Delta\text{Ct}}$, where ΔCt represents the difference in the threshold cycle between the target and control genes). Data was normalized to GAPDH mRNA levels. Primer sequences are detailed in Table 1.

Statistical analysis

Data were expressed as mean \pm SEM. Paired comparisons were made using Mann-Whitney tests and were considered statistically significant at $p\text{-value} < 0.05$. All graphical data and statistical analyses were generated with GraphPad Prism software.

Results

NHBE stimulation with Y, DapT and LDN

At D7 of ALI NHBE cell culture, CCSP and Muc5AC mRNA expression level were upregulated in comparison to D0 (Figure 1A and 1E) while FoxJ1 and p63 mRNA expression level were unchanged (Figure 1I and 1J). The number of Club and Goblet cells were quantified by immunofluorescent staining for CCSP (Figure 1C and 1D) and Muc5AC (Figure 1G and 1H). Consistent with mRNA expression (Figure 1A and 1E), ALI culture conditions increased the rate of CCSP (figure 1C and 1D) and Muc5AC (figure 1G and 1H) expressing cells. Moreover, released CCSP and Muc5AC quantified by Dot-Blot in the apical washes were also increased at D7 (Figure 1B and 1F). These data suggest that NHBE cultivated in ALI can differentiate into Club and Goblet cells in 7 days and Club and Goblet cells are functional because they secrete CCSP and Muc5AC protein.

Addition of Y27632 during 7 days showed an increase level of CCSP mRNA expression (Figure 1A). It was also observed a significant increased rate of the Club cells quantified by immunofluorescent staining (Figure 1C and 1D) as well as a non significant increased release of CCSP in the apical washes of NHBE (figure 1B). The increased expression of Muc5AC mRNA during the 7 days of ALI culture was amplified by the addition of Y27632 (figure 1E). Muc5AC immunostaining and released Muc5AC were in line with mRNA findings (Figure 1G and 1H). Moreover, Y induced an increase p63 mRNA expression. On the other cells, Y had no effect on FoxJ1 mRNA expression. These results suggest that Y27632 improves not only the expression of Club cells marker in NHBE ALI culture but also the expression of basal and Goblet cell marker.

DapT supplementation suppressed CCSP mRNA expression (figure 1A) and had no effect on Muc5AC mRNA expression (Figure 1E). These results persisted with the addition of Y27632 (Figure 1A and 1E). These data were further confirmed by immunofluorescent staining for CCSP (Figure 1C and 1D) and Muc5AC proteins (Figure 1G and 1H) as well as the released CCSP and Muc5AC levels measured by Dot Blot (figure 1B and 1F). In contrast, DapT considerably increased FoxJ1 (Figure 1I) and p63 (Figure 1J) mRNA expression after 7 days of culture. This increase persisted with the addition of Y27632. (Figure 1I and 1J). DapT positively affected FoxJ1 and p63 expression in NHBE cultures.

LDN-193189 alone had no significant impact on CCSP, Muc5AC, FoxJ1 or p63 markers whereas an increase was observed on Muc5AC mRNA expression level when Y27632 was added (condition D7+LDN+Y) (figure 1E). This was confirmed by Muc5AC immunostaining (Figure 1G and 1H) as well as an increased release of Muc5AC (Figure 1F). LDN-193189, on top of Y27632, positively affected MUC5AC expression.

It was assessed through the monitoring of lactate dehydrogenase (LDH) release every 48hrs in each condition throughout the differentiation process. There is no mortality induced by the molecules.

Y27632 improves the expression of Club and Goblet cells. DapT seems to have an effect toward basal and ciliated cells development. LDN associated to Y promotes Goblet cells.

HBEC stimulation with Y and DapT:

In order to confirm results, we reproduced the same stimulations on HBEC cultures. At D7 of HBEC ALI culture, mRNA expression of CCSP (Figure 2A), Muc5AC (Figure 2C), FoxJ1 (Figure 2E) and p63 (Figure 2G) were upregulated in comparison to D0. Consistent with mRNA expression data, ALI culture conditions increased the rate of CCSP (Figure 2B), Muc5AC (Figure 2D), FoxJ1 (Figure 2F) expressing cells quantified by immunostaining. These data were confirmed at day 14 of culture (data not shown).

Addition of Y27632 showed an increase level of CCSP mRNA expression (Figure 2A). Conversely, there is no change in Club cells rate of HBEC treated with Y27632 (figure 2B). Muc5AC mRNA expression level was increase at D7 compared to D0 and this was amplified by Y27632 (figure 2C). Muc5AC immunostaining was in line with mRNA data (Figure 2D). There was no significant difference on p63 (Figure 2G) and FoxJ1 (Figure 2E) mRNA expressions with milieu supplemented with Y in comparison to D7. TubIV immunostaining corresponded with mRNA data (Figure 2F). These results suggest that Y27632 improves not only the Club cells expression in HBEC ALI culture but also the expression of goblet cells marker.

DapT supplementation decreased CCSP and Muc5AC mRNA expression level (Figure 2A) (figure 2C) and the number of Club cells quantified by immunostaining (Figure 2B). This result persisted with the addition of Y27632 (Figure 2A and 2C) and confirmed by Club cells

immunofluorescent staining (Figure 2B). In contrast, DapT considerably increased FoxJ1 mRNA expression level at day 7 and this increase persisted with the addition of Y27632 (figure 2E). These data were confirmed by TUB-IV immunostaining (figure 2F). DapT also increased p63 mRNA expression (Figure 1G) and this trend persisted with the addition of Y27632 (Figure 2G). These data suggest that DapT positively affected FoxJ1 and p63 expression in HBEC cultures.

Y27632 improves Club cells and Goblet cells expression. DapT seems to have an effect toward basal and ciliated cells development.

Modulation of goblet/ciliated cells ratio in NHBE and HBEC cultures:

It was shown that molecules could play a role on cell fate and thus pushes towards one differentiated cell type compared to another. The main problem in chronic airways diseases is the balance of ciliated and goblet cells. The ratio of FoxJ1 mRNA to Muc5AC mRNA was examined to see if one cell type was increased to the other in cultures and if the drugs could play on this ratio. Muc5AC and FoxJ1 mRNA expressions were plotted in order to obtain a ratio of ciliated cell (FoxJ1) to goblet cell (Muc5AC) expression for NHBE (Figure 3A) and HBEC cultures (Figure 3B). These data showed that Y does not promote ciliated cells and goblet cells. DapT increased FoxJ1/Muc5AC ratio (Figure 3A and 3D). This increase persisted with the addition of Y27632 (Figure 3A and 3D). DapT modulates FoxJ1/Muc5AC ratio.

CSE and Scratch stimulations in HBEC cultures:

We have implemented aggression models (CSE and Scratch) that reflect COPD disease. Our goal is to restore the good quantity of ciliated cells compared to goblet cells in patients with chronic airway disease. CSE stimulation (CSE induced Muc5AC) increased goblet cells expression. Inversely, when DapT (DapT prevent) was added to the basolateral medium, we showed a decrease of Muc5AC mRNA expression. Finally, we demonstrated that DapT was able to prevent CSE-induced Muc5AC.

In ALI culture condition, the cell repair is 0.5 at 24 h and complete at 48h. Addition of DapT showed a slower repair process which remains incomplete at 48h (around 30%). DapT inhibits repair process

Single cell-RNAseq Analysis of DapT impact in HBEC cultures

tSNE representation shown distinct mRNA expression between DapT and control conditions (Figure 4A). Addition of DapT showed no CCSP (Figure 4B) and Muc5AC (Figure 4C) mRNA expression but there is p63 (Figure 4D), FoxJ1 (Figure 4E) and TubIV (Figure 4F) mRNA expression. In control condition, there is CCSP (Figure 4B), Muc5AC (Figure 4C) and p63 (Figure 4D) mRNA expression but there is not FoxJ1 (Figure 4E) and TubIV (Figure 4F) mRNA expression. These difference in mRNA profiles were visualized by using a heat map (Figure 4G) (List of mRNA expression was in the supplementary data). (Figure S1 and S2). These data confirmed results obtained in HBEC and NHBE cultures (PCR, Immunostaining).

Clustering method gave 6 clusters with different mRNA profiles (Figure 5A). Cluster 1 had basal cell markers (figure 5B), cluster 3 (Figure 5C) had club and goblet cell markers, and cluster 5 (figure 5D) and 4 (Figure 5E) had ciliated cell markers. In ciliated cells, there are two clusters. Cluster 4 is common at control and DapT conditions whereas cluster 5 is specific to DapT condition. Cluster 5 seems to be more “complex”, “structured” than cluster 4 (Figure S3). Clusters obtained showed that DapT gives ciliated cells and inhibits secretory cells because Custer 3 was specific to control condition.

Discussion

We demonstrated that it is achievable tailoring differentiation of NHBE and HBEC cells toward CCSP and MUC5AC producing cells or ciliated and basal cells under ALI culture condition allowing an imbalance study of epithelial cell. Affecting the Rho, Notch and BMP pathways respectively by Y27632, DapT and LDN-193189 in NHBE and HBEC cultures had the potential to modify the airway epithelial phenotype preventing or encouraging specific bronchial epithelial cell type in culture.

NHBE and HBEC expositions to Y27632 induced CCSP and Muc5Ac upregulation and no changed FoxJ1 expression. This suggests that Notch prevents ciliated cell phenotype development and has beneficial effects on Goblet and Club cell phenotype development. In the two models, these effects were seen both at the intracellular and mRNA levels. Benchmarking protocols aiming at differentiating iPSC into airway epithelial cells allowed for a better understanding of the main drivers involved in these processes. We took advantage from these progresses by modulating these critical pathways. The Rho kinase inhibitor Y27632 is a key molecule in iPSC for maintenance of pluripotency – even though the loss of Y27632 dependence is seen with adaptation. The huge increase of club cell density and CCSP release promoted by Y27632 in NHBE suggests that Rho inhibition promotes Club cell self renewal, potentially, but also promotes the differentiation toward mucus producing cells. These data were confirmed in HBEC cultures with an increase CCSP and Muc5AC mRNA expression level with Y27632.

BMP inhibition also promoted mucus producing cell fate, on top of Y27632 in NHBE culture. This is not a surprise as many other teams observed these results but at different levels using different inhibitors. The exact mechanism by which LDN-193189 inhibits BMP is not perfectly known and studies dedicated to assess key members of this very large family are required even though BMP4 looks as the best candidate²⁹. Noteworthy, LDN-193189 in NHBE cultures also didn't promote acquisition of ciliated cell features and this is a confirmation of the key role of BMP in this real imbalance likely through Smad phosphorylation³⁰. This is an argument that fits with the frequent observations of colocalized MUC5AC/CCSP+ve cells in the airway epithelium. Whether all MUC5AC+ve cells expressed CCSP early in their life and progressively lost this expression at the benefit of mucin, is an interesting concept that may explain why club cells are reduced in COPD whereas goblet cells are increased by acceleration of this process. Whether slowing down this process, it will restore the club cell pool and will decrease the goblet cell rate in the sick airway epithelium is one first question. Whether, it will be clinically

beneficial is another one. Moreover, recent study demonstrated that local growth factors (included FGF10) and mechanical forces synergistically control alveolar epithelial cell differentiation³¹. In parallel, osteoblastogenesis and osteogenic differentiation were promoted by both chemical factors (included BMP and Notch signaling³² and physical signal (mechanical forces)³³. Furthermore, FGF10 and BMP4 have combinatorial roles in branching morphogenesis of the lung³⁴. This is another argument for the potential implication of BMP and Notch pathways in airway epithelial phenotype and potential cell fate drivers.

In contrast, inhibition of the Notch gamma secretase promoted ciliated cell differentiation as expected. DapT targets are not perfectly known but it seems that it may increase DLL1 while suppressing HES1³⁵. In addition, AMG430 antibody, a monoclonal IgG1 antibody, binds Notch ligand, Jagged-1, and prevents Jagged-1-induced Notch activation. This antibody reduces the goblet cells differentiation and induces ciliated cells differentiation in human airways epithelium. These give similar results to those obtained in our cultures by using DapT³⁶. These results have been confirmed by the fact that AMG430 antibody reduces goblet cells differentiation, and reverses airway epithelium remodelling in obstructive pulmonary disease mouse models³⁷. Unfortunately we didn't assess Notch levels in our cells as insufficient amount of proteins could be collected. Notch was already suspected as a key ciliated cell driver. That it worked in NHBE cells cultivated at the ALI was unknown as large induction of cell death could be suspected. We were unable to promote differentiation until cilia beating. After day 7 mortality rates tended to increase and we stopped these experiments. These datas were confirmed in HBEC culture where DapT induced ciliated cell (day 14 of ALI culture without cells death). All our experiments could be repeated a large number of time and we were confident in observing concordant results at the protein and mRNA levels. Alternative techniques for achieving these goals exist but they are not easy to modulate in humans. These data were confirmed by single cell-RNA seq. Addition of DapT decreased CCSP and Muc5AC mRNA expression and promoted FoxJ1, TubIV and p63 mRNA expression. DapT promotes ciliated and basal cells and inhibits secretory cells. This is an advantage because we want to increase the number of ciliated cells compared to goblet cells. We have seen that DapT can reverse the cigarette effect by decreasing goblet cell hyperplasia but also other differentiated cells. Inhibiting other cells is a problem because we don't have a differentiated epithelium. However, in repair process, DapT decreases the repair process which suggests that it is also a disadvantage in our model where cellular damage is found.

DapT is a good candidate to act on hyperplasia of goblet cells, but molecule doses should be adapted to obtain a differentiated epithelium with ciliated cells but also Club cells which are completely inhibited by this molecule.

Our results also deserve a few comments. Firstly, cell culture medium composition is not perfectly known and it means that results may have been different with different medium. Secondly and in line with this comment, it means that the plasticity of the airway epithelium can be engaged even in differentiated normal bronchial cells. Likewise, persistence of underlying disease features in ALI cultures is questionable even though our group and others found consistent results. But this may largely rely on the medium composition and this implies that “ALI cultures” are not always comparable and merged for meta-analysis only cautiously. Finally, induced-goblet cell hyperplasia model is essential to modulate the pathways and cell fate. CSE stimulation and exacerbation model may be a promising model to induce disease.

In conclusion, some airway epithelial cell fate drivers were confirmed in differentiated airway epithelium. Y27632 and LDN-193189 are promoting differentiation toward club and goblet cells whereas DapT promotes cell fate toward ciliated and basal differentiation. Tailoring the airway epithelial cell phenotype is achievable.

REFERENCES

1. Burney, P. G. J., Patel, J., Newson, R., Minelli, C. & Naghavi, M. Global and regional trends in COPD mortality, 1990–2010. *Eur. Respir. J.* **45**, 1239–1247 (2015).
2. Rycroft, C. E., Heyes, A., Lanza, L. & Becker, K. Epidemiology of chronic obstructive pulmonary disease: a literature review. *Int J Chron Obstruct Pulmon Dis* **7**, 457–494 (2012).
3. Vijayan, V. K. Chronic obstructive pulmonary disease. *Indian J. Med. Res.* **137**, 251–269 (2013).
4. Knabe, L. *et al.* CCSP counterbalances airway epithelial-driven neutrophilic chemotaxis. *European Respiratory Journal* **54**, (2019).
5. Pauwels, R. A. *et al.* Global strategy for the diagnosis, management, and prevention of chronic obstructive pulmonary disease. NHLBI/WHO Global Initiative for Chronic Obstructive Lung Disease (GOLD) Workshop summary. *Am. J. Respir. Crit. Care Med.* **163**, 1256–1276 (2001).
6. Pathophysiology of airflow limitation in chronic obstructive pulmonary disease. - PubMed - NCBI. <https://www.ncbi.nlm.nih.gov/pubmed/15325838>.
7. Puchelle, E., Zahm, J.-M., Tournier, J.-M. & Coraux, C. Airway Epithelial Repair, Regeneration, and Remodeling after Injury in Chronic Obstructive Pulmonary Disease. *Proc Am Thorac Soc* **3**, 726–733 (2006).
8. Stănescu, D. *et al.* Airways obstruction, chronic expectoration, and rapid decline of FEV1 in smokers are associated with increased levels of sputum neutrophils. *Thorax* **51**, 267–271 (1996).
9. Ahmed, E. *et al.* Lung development, regeneration and plasticity: From disease physiopathology to drug design using induced pluripotent stem cells. *Pharmacol. Ther.* **183**, 58–77 (2018).
10. Samadikuchaksaraei, A. & Bishop, A. E. Effects of growth factors on the differentiation of murine ESC into type II pneumocytes. *Cloning Stem Cells* **9**, 407–416 (2007).
11. Ali, N. N. *et al.* Derivation of type II alveolar epithelial cells from murine embryonic stem cells. *Tissue Eng.* **8**, 541–550 (2002).
12. Rippon, H. J. *et al.* Embryonic stem cells as a source of pulmonary epithelium in vitro and in vivo. *Proc Am Thorac Soc* **5**, 717–722 (2008).
13. Coraux, C. *et al.* Embryonic stem cells generate airway epithelial tissue. *Am. J. Respir. Cell Mol. Biol.* **32**, 87–92 (2005).
14. Ameri, J. *et al.* FGF2 specifies hESC-derived definitive endoderm into foregut/midgut cell lineages in a concentration-dependent manner. *Stem Cells* **28**, 45–56 (2010).
15. Rackley, C. R. & Stripp, B. R. Building and maintaining the epithelium of the lung. *J. Clin. Invest.* **122**, 2724–2730 (2012).
16. Hajj, R. *et al.* Basal cells of the human adult airway surface epithelium retain transit-amplifying cell properties. *Stem Cells* **25**, 139–148 (2007).
17. Masuda, S. Evidence for human lung stem cells. *N. Engl. J. Med.* **365**, 464–465; author reply 465–466 (2011).

18. Shiyu, S. *et al.* Polydatin up-regulates clara cell secretory protein to suppress phospholipase A2 of lung induced by LPS in vivo and in vitro. *BMC Cell Biology* **12**, 31 (2011).
19. Boers, J. E., Ambergen, A. W. & Thunnissen, F. B. Number and proliferation of clara cells in normal human airway epithelium. *Am. J. Respir. Crit. Care Med.* **159**, 1585–1591 (1999).
20. Lazzaro, D., Price, M., de Felice, M. & Di Lauro, R. The transcription factor TTF-1 is expressed at the onset of thyroid and lung morphogenesis and in restricted regions of the foetal brain. *Development* **113**, 1093–1104 (1991).
21. Minoo, P., Su, G., Drum, H., Bringas, P. & Kimura, S. Defects in tracheoesophageal and lung morphogenesis in Nkx2.1(-/-) mouse embryos. *Dev. Biol.* **209**, 60–71 (1999).
22. Mahoney, J. E., Mori, M., Szymaniak, A. D., Varelas, X. & Cardoso, W. V. The hippo pathway effector Yap controls patterning and differentiation of airway epithelial progenitors. *Dev. Cell* **30**, 137–150 (2014).
23. Hashimoto, S. *et al.* β -Catenin-SOX2 signaling regulates the fate of developing airway epithelium. *J. Cell. Sci.* **125**, 932–942 (2012).
24. Giuranno, L. *et al.* NOTCH signaling promotes the survival of irradiated basal airway stem cells. *Am. J. Physiol. Lung Cell Mol. Physiol.* **317**, L414–L423 (2019).
25. Rock, J. R. *et al.* Notch-dependent differentiation of adult airway basal stem cells. *Cell Stem Cell* **8**, 639–648 (2011).
26. Lafkas, D. *et al.* Therapeutic antibodies reveal Notch control of transdifferentiation in the adult lung. *Nature* **528**, 127–131 (2015).
27. Eenjes, E. *et al.* A novel method for expansion and differentiation of mouse tracheal epithelial cells in culture. *Sci Rep* **8**, 7349 (2018).
28. Wang, R. N. *et al.* Bone Morphogenetic Protein (BMP) signaling in development and human diseases. *Genes Dis* **1**, 87–105 (2014).
29. Weaver, M., Yingling, J. M., Dunn, N. R., Bellusci, S. & Hogan, B. L. Bmp signaling regulates proximal-distal differentiation of endoderm in mouse lung development. *Development* **126**, 4005–4015 (1999).
30. Tadokoro, T., Gao, X., Hong, C. C., Hotten, D. & Hogan, B. L. M. BMP signaling and cellular dynamics during regeneration of airway epithelium from basal progenitors. *Development* **143**, 764–773 (2016).
31. Li, J. *et al.* The Strength of Mechanical Forces Determines the Differentiation of Alveolar Epithelial Cells. *Dev. Cell* **44**, 297–312.e5 (2018).
32. Marie, P. J. Osteoblast dysfunctions in bone diseases: from cellular and molecular mechanisms to therapeutic strategies. *Cell. Mol. Life Sci.* **72**, 1347–1361 (2015).
33. Wang, J. *et al.* Mechanical stimulation orchestrates the osteogenic differentiation of human bone marrow stromal cells by regulating HDAC1. *Cell Death Dis* **7**, e2221 (2016).

34. Weaver, M., Dunn, N. R. & Hogan, B. L. Bmp4 and Fgf10 play opposing roles during lung bud morphogenesis. *Development* **127**, 2695–2704 (2000).
35. Konishi, S. *et al.* Directed Induction of Functional Multi-ciliated Cells in Proximal Airway Epithelial Spheroids from Human Pluripotent Stem Cells. *Stem Cell Reports* **6**, 18–25 (2016).
36. In Vitro Characterization of the Anti-Jagged-1 Antibody AMG 430 Using Human Airway Organoid Cultures to Study the Role of Jagged-1 in Normal and Diseased Human Airway Epithelial Cell Differentiation | A62. MUCUS, MUCINS, MUCOCILIARY UNIT IN LUNG DISEASE. https://www.atsjournals.org/doi/abs/10.1164/ajrccm-conference.2019.199.1_MeetingAbstracts.A2154.
37. Phillips, J. e. *et al.* Anti-Jagged1 Antibody AMG 430 Reduces Airway Mucus in Mouse Models of Obstructive Pulmonary Disease. in *B63. ANIMAL MODELS OF COPD* A3839–A3839 (American Thoracic Society, 2019). doi:10.1164/ajrccm-conference.2019.199.1_MeetingAbstracts.A3839.
38. Gras, D. *et al.* Epithelial ciliated beating cells essential for ex vivo ALI culture growth. *BMC Pulm Med* **17**, 80 (2017).
39. Gamez, A. S. *et al.* Supplementing defect in club cell secretory protein attenuates airway inflammation in COPD. *Chest* **147**, 1467–1476 (2015).

Figure legends:

Figure 1. Y, DapT and LDN effects in NHBE ALI cultures

Cells were cultured in absence (D7) and presence of 5 μ M Y27632 (D7+Y), 10 μ M of DapT (D7+DapT), 250 nM of LDN-193189 (D7+LDN), or combinations of molecules LDN-193189+Y27632 (250nM, 5 μ M) (D7+LDN+Y) or DapT+Y27632 (10 μ M, 5 μ M)(D7+DapT+Y) for 7 days in ALI culture conditions. (A) CCSP, (E) Muc5AC, (I) FoxJ1, (J) p63 mRNA levels normalized to GAPDH mRNA levels in 6 NBHE ALI cultures at D0 and D7 with or without drugs. (B) CCSP concentration in NHBE apical lavages measured by Dot-Blot at D0 and D7 of NHBE ALI cultures supplemented with or without drugs (n=6). (C) On D0 and D7 of NHBE ALI cultures supplemented with or without drugs, cells were immunostained for CCSP (red) (n=6). (D) Quantification of CCSP positive cell area shown in 1C. (F) Muc5AC release in NHBE apical lavages measured by Dot Blot at D0 and D7 of NHBE ALI cultures supplemented with or without drugs (n=6). (G) On D0 and D7 of NHBE ALI cultures supplemented with or without drugs, cells were immunostained for Muc5AC (green) (n=6). (H) Quantification of Muc5AC positive cells area shown in 1G. The mean +/- SEM are shown.

Figure 2. DapT and Y effects in HBEC ALI cultures

Cells were cultured in absence (D7) and presence of 5 μ M Y27632 (D7+Y), 10 μ M of DapT (D7+DapT) or combination of molecules DapT+Y27632 (10 μ M, 5 μ M) (D7+DapT+Y) for 7 days in ALI culture conditions. (A) CCSP, (C) Muc5AC, (E) FoxJ1, (G) p63 mRNA levels normalized to GAPDH mRNA levels in 5 ALI cultures at D0 and D7 with or without drugs. (B) On D0 and D7 of NHBE ALI cultures supplemented with or without drugs, cells were immunostained for CCSP. (C) Quantification of CCSP positive cell area with or without drugs (n=5). (D) On D0 and D7 of NHBE ALI cultures supplemented with or without drugs, cells were immunostained for Muc5AC. Quantification of Muc5AC positive cell area with or without drugs (n=5). (F) On D0 and D7 of NHBE ALI cultures supplemented with or without drugs, cells were immunostained for TUBIV. Quantification of TUBIV positive cell area with or without drugs (n=5). The mean +/- SEM are shown.

Figure 3. DapT supplementation in ALI culture medium improves expression of FoxJ1 compared to Muc5AC in NHBE and HBEC cultures and reverses Goblet cell Hyperplasia and inhibits cell repair in ALI cultures.

Cells were cultured in absence (D7) and presence of 5 μ M Y27632 (D7+Y), 10 μ M of DapT (D7+DapT) or combination of molecules DapT+Y27632 (10 μ M, 5 μ M) (D7+DapT+Y) for 7

days in ALI culture conditions. FoxJ1 and Muc5AC mRNA levels normalized to GAPDH mRNA levels in ALI cultures at D7 with or without drugs. (A) Ratio mRNA FoxJ1/Muc5AC in NHBE cultures (n=6). (B) Ratio mRNA FoxJ1/Muc5AC in HBEC cultures (n=5). (C) Cells were cultured in absence (D14 or CSE induced MUC5AC) or presence of 10 μ M of DapT (DapT prevent) for 14 days in ALI culture conditions with (CSE induced Muc5AC, DapT prevent) or without (D14) CSE apical stimulation (n=10). Muc5AC mRNA levels normalized to GAPDH mRNA levels in HBEC ALI cultures (n=10) at D14 with or without drugs or CSE stimulation. (D) HBEC were cultured for 21 days in ALI culture conditions (without stimulation). At D21, the cells are scratched and incubated with (DapT) or without (basal) 10 μ M of DapT. The repair was quantified at H0, H6, H24 and H48. The mean +/- SEM are shown.

Figure 4. DapT supplementation in HBEC ALI culture improves FoxJ1 and TUB IV expression compared to others mRNA expressions of differentiated cell.

Cells were cultured in absence or presence of 10 μ M of DapT for 14 days in ALI culture (n=1). After, cells were collected and single cell-RNAseq was performed. (A) tSNE representation of single cell-RNA seq data obtained to HBEC cultures stimulated with or without DapT. (B) SCGB1A1, (C) MUC5AC, (D) TP63 (E) FoxJ1 and (F) TUBIV mRNA expressions were analysed in HBEC cultures. (G) Heat map of HBEC cultures in absence or presence of DapT was performed to visualize DapT impact to signalling pathways.

Figure 5. Clusters were specific to cell type. (A) Clustering method of single cell-RNAseq data obtained from HBEC cultures stimulated with or without DapT. The different cluster ((B) Cluster 1, (C) Cluster 3, (D) Cluster 5 and (E) Cluster 4) has been achieved to visualize mRNA expression profile of epithelial cell.

Figure 6. Proposed model for epithelial cell type modulation in NHBE and HBEC cells.

DapT (Notch Inhibitor) prevents Club cell and Goblet cell phenotype development improves ciliated and basal cells. In contrast Y (Rho Inhibitor) and LDN (BMP inhibitor) improves Club and Goblet cell phenotype development.

Tables

Primers	Sequences (5' to 3')
GAPDH	Forward : CCA TCT TCC AGG AGC GAG Reverse : CTT GAG GCT GTT GTC ATA CT
CCSP	Forward : CAT GAA ACT CGC TGT CAC CC Reverse : GAT GAC ACG CTG AAA GCT CG
FOXJ1	Forward : TCG TAT GCC ACG CTC ATC TG Reverse : CTT GTA GAT GGC CGA CAG GG
MUC5AC	Forward : TAC TCC ACA GAC TGC ACC ACC TG Reverse : CGT GTA TTG CTT CCC GTC AA
p63	Forward : ACC CCG AGA TGA GTG GAA TG Reverse : AGG AGT GCT TTT AGG GGG CT

Table 1: Primers for PCR

Figures

Figure 1

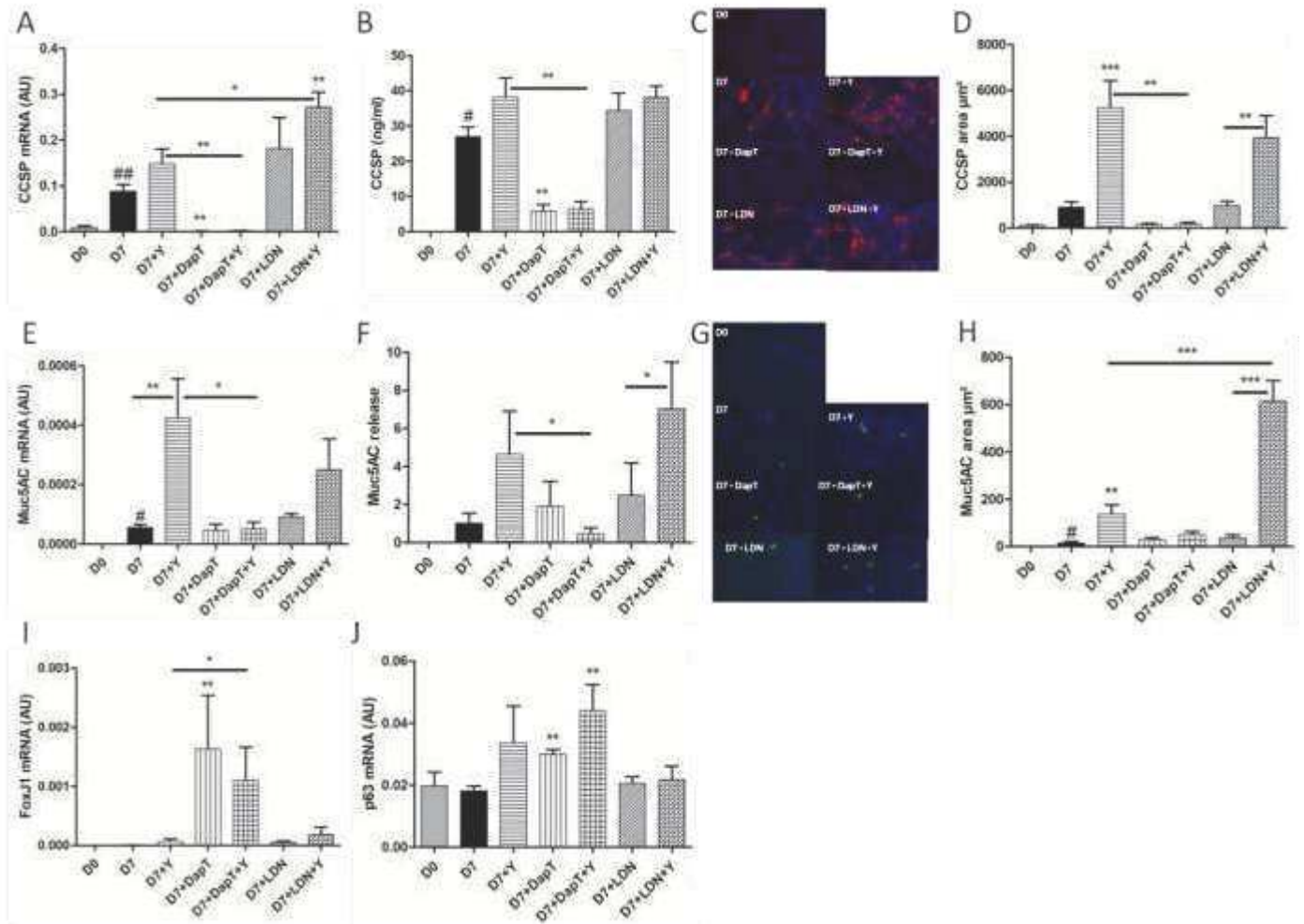


Figure 2

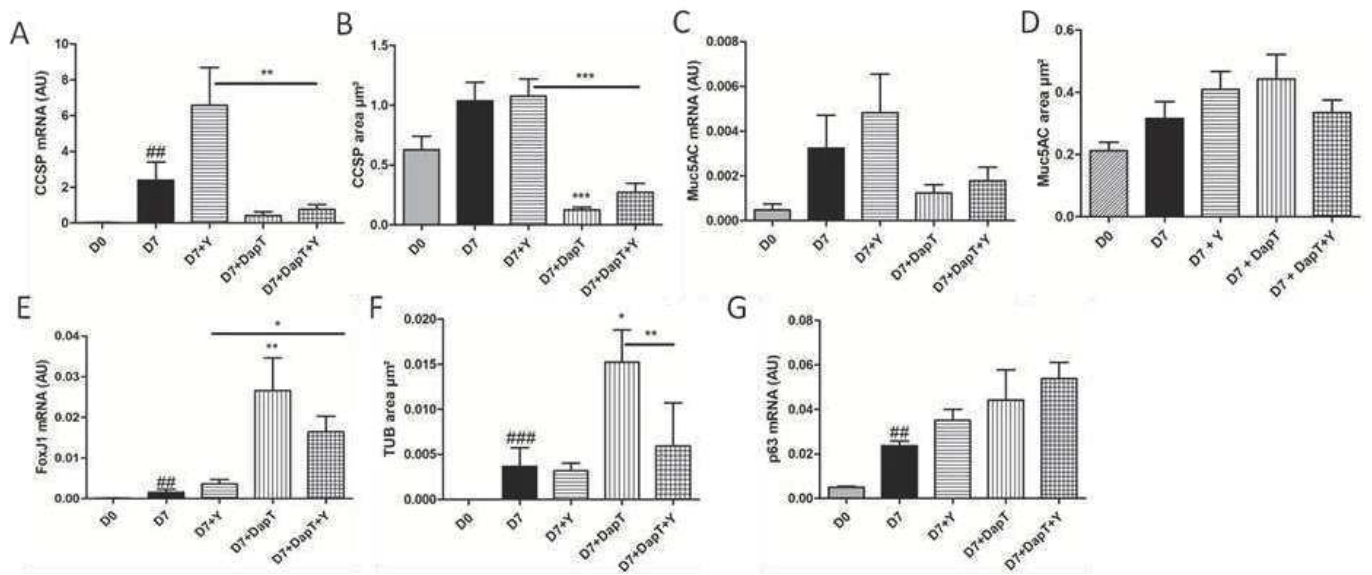


Figure 3

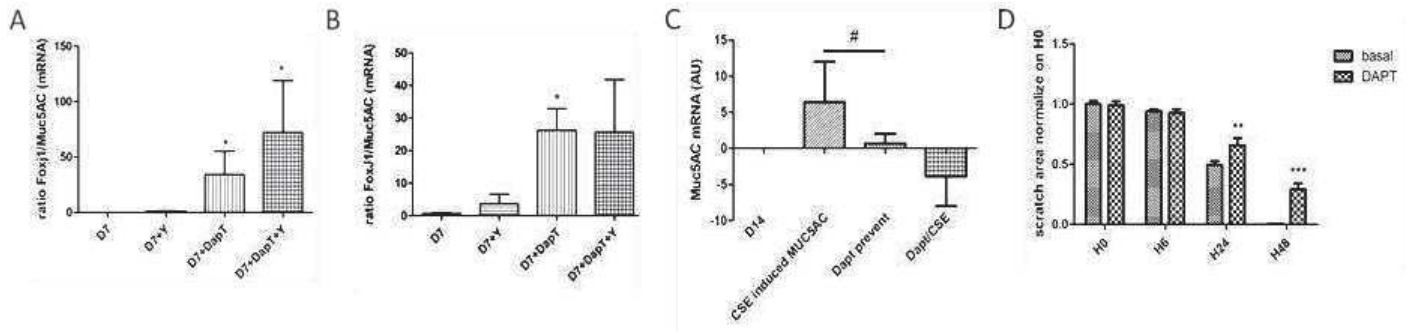


Figure 4

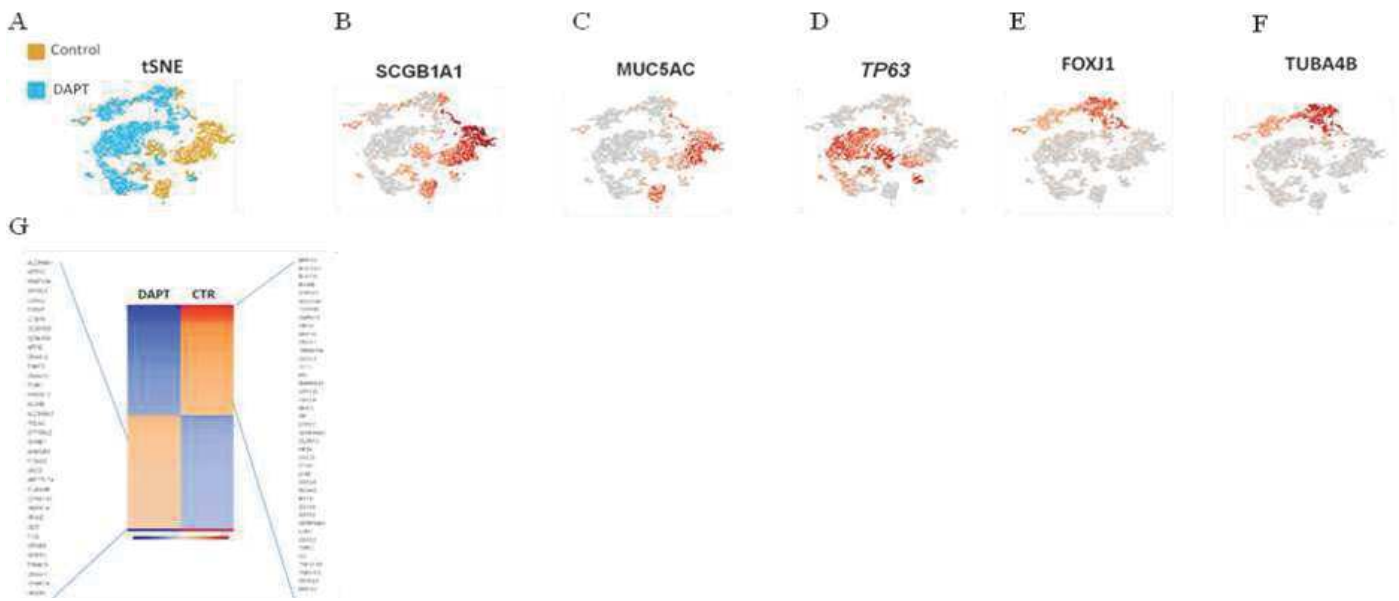


Figure 5

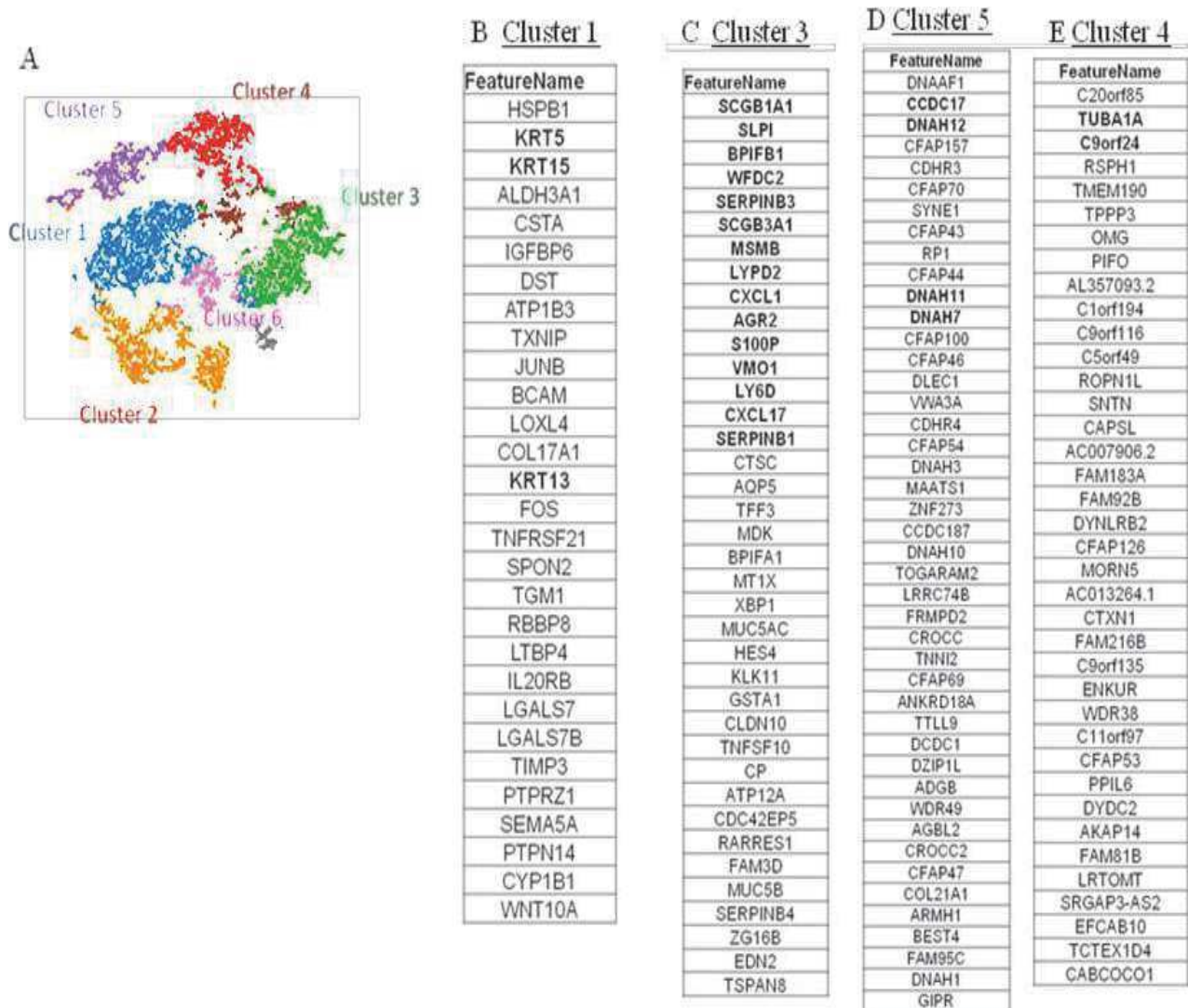
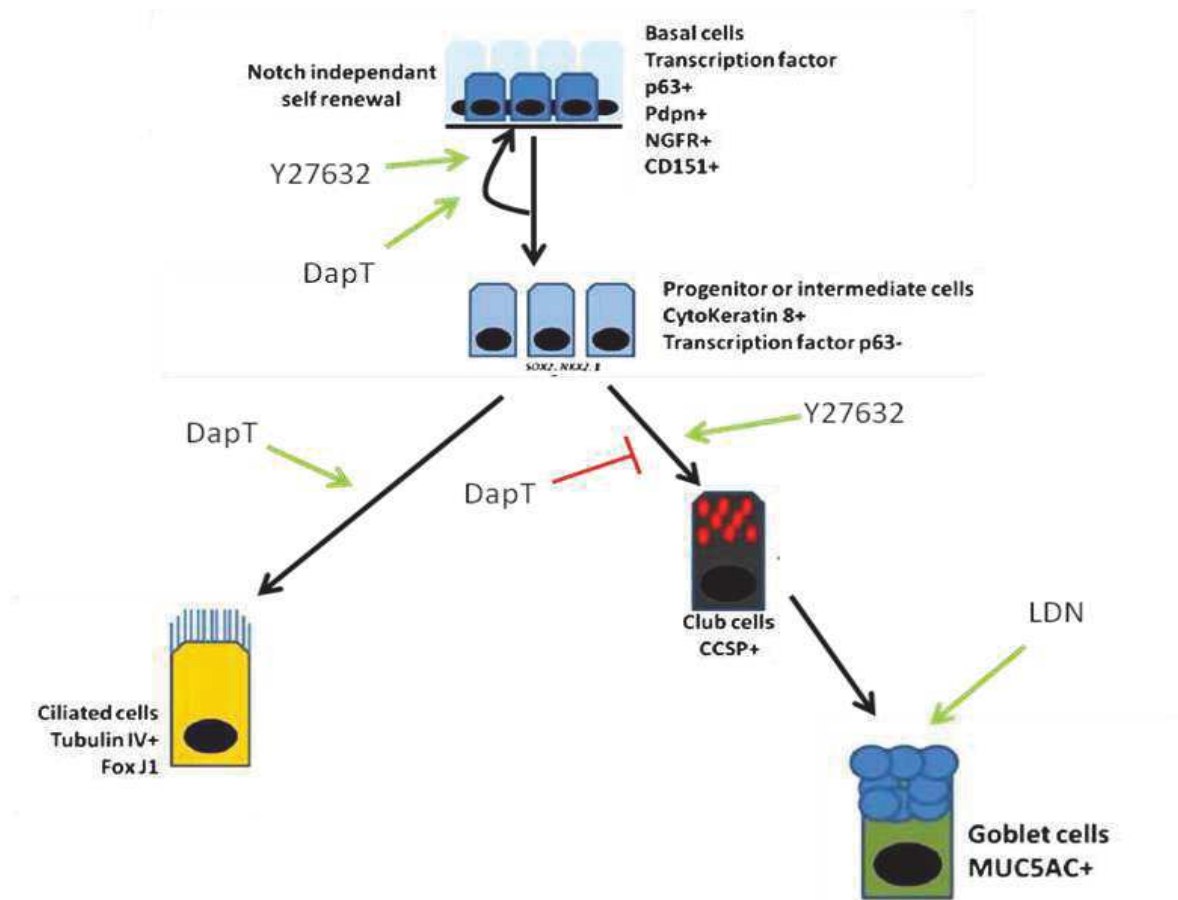


Figure 6



Supplementary data

Figure S1. Up-regulated genes in DAPT.

HBEC cultures were cultivated with DapT. Then, cells were collected and single cell-RNAseq method was performed. mRNA expression of HBEC cultures was studied to visualize impact of DapT on signaling pathway.

FeatureID	FeatureName	ND_DAPT_Log2 FC	ND_DAPT_P- Value
ENSG00000108602	ALDH3A1	3,1	0
ENSG00000135925	WNT10A	2,2	0
ENSG00000171346	KRT15	2,2	0
ENSG00000159674	SPON2	2	0
ENSG00000265972	TXNIP	1,9	0
ENSG00000138131	LOXL4	1,9	0
ENSG00000090006	LTBP4	1,9	0
ENSG00000091986	CCDC80	1,8	0
ENSG00000169715	MT1E	1,7	0
ENSG00000112902	SEMA5A	1,7	0
ENSG00000007174	DNAH9	1,7	0
ENSG00000092295	TGM1	1,6	0
ENSG00000105877	DNAH11	1,6	0
ENSG00000100234	TIMP3	1,6	0
ENSG00000164099	PRSS12	1,6	0
ENSG00000091409	ITGA6	1,6	0
ENSG00000072210	ALDH3A2	1,5	0
ENSG00000187244	BCAM	1,5	0
ENSG00000152518	ZFP36L2	1,5	0
ENSG00000206199	ANKUB1	1,5	0
ENSG00000131018	SYNE1	1,5	0
ENSG00000164379	FOXQ1	1,5	0
ENSG00000185432	METTL7A	1,5	0
ENSG00000184916	JAG2	1,5	0
ENSG00000243910	TUBA4B	1,4	0

ENSG00000160401	CFAP157	1,4	0
ENSG00000166592	RRAD	1,4	0
ENSG00000204389	HSPA1A	1,4	0
ENSG00000151914	DST	1,3	0
ENSG00000152582	SPEF2	1,3	0
ENSG00000204389	HSPA1A	1,4	0
ENSG00000151914	DST	1,3	0
ENSG00000152582	SPEF2	1,3	0
ENSG00000197057	DTHD1	1,3	0
ENSG00000170345	FOS	1,3	0
ENSG00000137699	TRIM29	1,3	0
ENSG00000156042	CFAP70	1,3	0
ENSG00000118997	DNAH7	1,3	0
ENSG00000128536	CDHR3	1,3	0
ENSG00000157423	HYDIN	1,3	0
ENSG00000172831	CES2	1,3	0
ENSG00000196344	ADH7	1,3	0
ENSG00000104237	RP1	1,3	0
ENSG00000272398	CD24	1,3	0
ENSG00000155761	SPAG17	1,3	0
ENSG00000261150	EPPK1	1,3	0
ENSG00000152104	PTPN14	1,3	0
ENSG00000159588	CCDC17	1,3	0
ENSG00000185361	TNFAIP8L1	1,2	0
ENSG00000133640	LRR1Q1	1,2	0
ENSG00000065618	COL17A1	1,2	0
ENSG00000138061	CYP1B1	1,2	0
ENSG00000151023	ENKUR	1,2	0
ENSG00000186710	CFAP73	1,2	0
ENSG00000197748	CFAP43	1,2	0
ENSG00000171223	JUNB	1,2	0
ENSG00000188659	SAXO2	1,2	0
ENSG00000130707	ASS1	1,2	0

ENSG00000132470	ITGB4	1,2	0
ENSG00000132821	VSTM2L	1,2	0
ENSG00000159713	TPPP3	1,2	0
ENSG00000069849	ATP1B3	1,2	0
ENSG00000178965	ERICH3	1,2	0
ENSG00000158023	WDR66	1,2	0
ENSG00000165309	ARMC3	1,2	0
ENSG00000206530	CFAP44	1,2	0

Figure S2. Up-regulated genes in CTR

HBEC cultures were cultivated. Then, cells were collected and single cell-RNAseq method was performed. mRNA expression of HBEC cultures was studied.

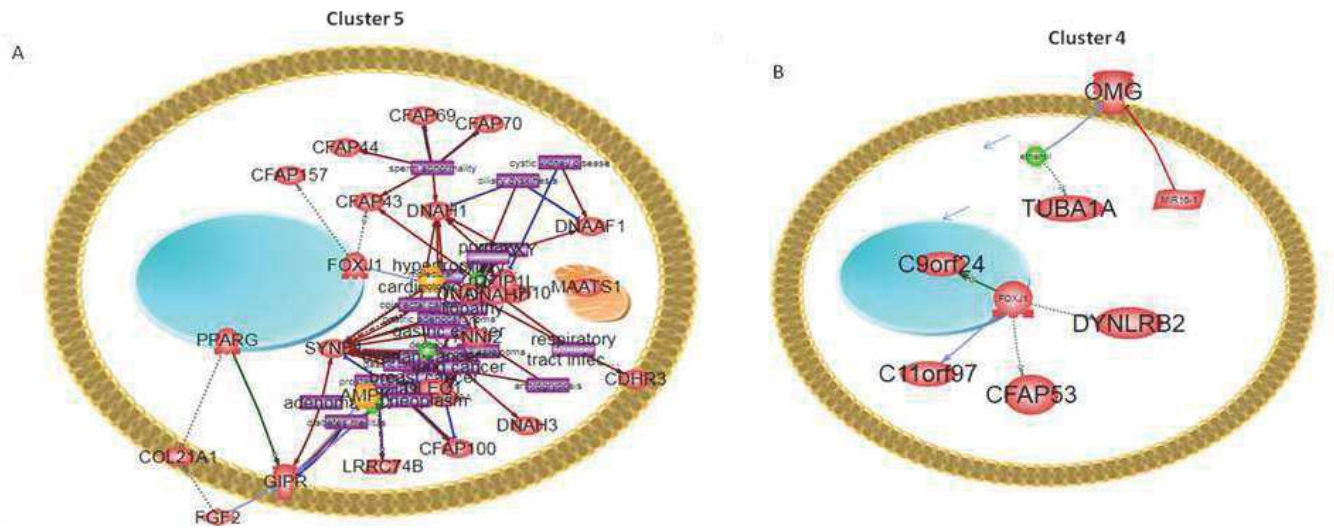
FeatureID	FeatureName	P-Value	
		FC (CTR)	(CTR)
ENSG00000149021	SCGB1A1	15,2	0
ENSG00000215182	MUC5AC	8,1	0
ENSG00000263639	MSMB	7,1	0
ENSG00000117983	MUC5B	7,5	0
ENSG00000161055	SCGB3A1	6,8	0
ENSG00000197446	CYP2F1	7,1	0
ENSG00000182853	VMO1	6,2	0
ENSG00000127324	TSPAN8	6,6	0
ENSG00000162949	CAPN13	6,1	0
ENSG00000198183	BPIFA1	7,8	0
ENSG00000125999	BPIFB1	5,2	0
ENSG00000163739	CXCL1	4,6	0
ENSG00000181458	TMEM45A	4,6	0
ENSG00000075673	ATP12A	4,2	0
ENSG00000163734	CXCL3	4,3	0
ENSG00000118849	RARRES1	4,2	0
ENSG00000169429	CXCL8	4	0
ENSG00000047457	CP	3,9	0
ENSG00000104140	RHOV	3,9	0
ENSG00000160180	TFF3	4,2	0
ENSG00000197353	LYPD2	3,9	0
ENSG00000188290	HES4	3,6	0
ENSG00000057149	SERPINB3	3,7	0
ENSG00000134873	CLDN10	3,6	0
ENSG00000115009	CCL20	3,5	0
ENSG00000109861	CTSC	3,3	0
ENSG00000187193	MT1X	3,2	0

ENSG00000167656	LY6D	3,3	0
ENSG00000159200	RCAN1	3,1	0
ENSG00000243955	GSTA1	3	0
ENSG00000162078	ZG16B	3	0
ENSG00000124102	PI3	4,2	0
ENSG00000124875	CXCL6	3,2	0
ENSG00000081041	CXCL2	2,8	0
ENSG00000115594	IL1R1	2,8	0
ENSG00000121858	TNFSF10	2,6	0
ENSG00000206073	SERPINB4	2,8	0
ENSG00000125730	C3	2,6	0
ENSG00000198959	TGM2	2,6	0
ENSG00000185215	TNFAIP2	2,6	0
ENSG00000110492	MDK	2,5	0
ENSG00000006210	CX3CL1	2,5	0
ENSG00000101443	WFDC2	2,4	0
ENSG00000131050	BPIFA2	2,5	0
ENSG00000162896	PIGR	2,4	0
ENSG00000167772	ANGPTL4	2,4	0
ENSG00000100219	XPB1	2,3	0
ENSG00000189377	CXCL17	2,3	0
ENSG00000167617	CDC42EP5	2,2	0
ENSG00000268104	SLC6A14	2,2	0
ENSG00000117525	F3	2,2	0
ENSG00000127129	EDN2	2,4	0
ENSG00000175130	MARCKSL1	2,2	0
ENSG00000090339	ICAM1	2,2	0
ENSG00000167757	KLK11	2,1	0
ENSG00000163993	S100P	2,1	0
ENSG00000124107	SLPI	2	0
ENSG00000021355	SERPINB1	2	0
ENSG00000143320	CRABP2	2	0
ENSG00000145632	PLK2	2	0

ENSG00000106541	AGR2	1,9	0
ENSG00000118503	TNFAIP3	1,9	0
ENSG00000170477	KRT4	1,9	0
ENSG00000150687	PRSS23	1,9	0
ENSG00000148926	ADM	1,9	0

Figure S3. Two ciliated profiles.

Schema of mRNA profile of Cluster 5 (A) and Cluster 4 (B) obtained from single cell-RNA seq of HBEC cultures.



Supplementary method

NHBE and HBEC cultures

Normal Human Bronchial Epithelial cells (NHBE) (Lonza, Walkersville, MD) were from two anonymous females, non-smoking donors, free of any respiratory disease. NHBE were cultivated according to manufacturer's instructions. Briefly, cells were cultivated in 75cm² flask in Bronchial Epithelial Growth Medium (BEGM, Walkersville, MD). Differentiation was initiated by seeding 350000 cells on Transwell^R (Corning, Kennebunk, United States) coated previously with fibronectin and collagen. Cells were cultivated in a 1:1 mixture of BEGM and Dulbecco's Modified Eagle's Medium (DMEM, Lonza, Walkersville, MD). Air Liquid Interface (ALI) culture was established by aspiration of apical chamber medium when cells reached confluence (referred to as D0). Basolateral medium was replaced every two days, while cells were maintained at 37°C, 5 % CO₂ until day 7 of culture (referred to as D7).

Primary Human Bronchial Epithelial Cells (HBEC) (n=5) were obtained from subjects recruited at Arnaud de Villeneuve Hospital, Montpellier, France under a protocol approved by an independent ethic committee and all patients gave their written informed consent (approval number: 2013 11 05; NCT02354677). HBEC were cultured as previously described³⁸. Briefly, cells were dissociated mechanically and cultivated in 12 well plate and then in 75cm² flask in PneumaCult-Ex Plus medium (Stemcell Technologies, Grenoble, France). After an expansion phase, differentiation was initiated by seeding 110000 cells on Transwell^R in Pneumacult-Ex Plus medium until confluence. After confluence, ALI culture was established by the aspiration of the apical chamber medium (referred to as D0). Basolateral medium was replaced every two days with the PneumaCult ALI maintenance medium (Stemcell Technologies, Grenoble, France), while cells were maintained at 37°C, 5% CO₂ until day 14 of culture (referred as to D14)

Cell cytotoxicity

Cell cytotoxicity was assessed through the monitoring of lactate deshydrogenase (LDH) release every 48hrs in each condition (Cytotoxicity detection kit, Roche, Mannheim, Germany).

Smoke production

CSE was prepared as previously described³⁹. Briefly, the smoke of three commercial cigarettes (Marlboro) was drawn into a Pasteur pipette and bubbled into 30 mL of PBS. CSE was adjusted to pH 7.4 and sterilized through a 0.22 μm filter. We obtained a 100% stock solution of CSE diluted to 5% for experiments. HBEC cultures were incubated every two days with 150 μL of PBS or CSE (5% at the apical pole) during 6 hours (day 2 until day 14).

Epithelial repair

Cells were cultivated in ALI conditions (referred as to D21) without any stimulation. At D21, cells were scratched with a pipette tip and cultured in presence or absence of 10 μM DapT. Wound images were recorded using microscope, immediately after wounding (0H) then at 6H, 12H and 24H. Wound area of each epithelium was measured using image J analysis software.

Single-cell-RNAseq

At D14 of HBEC cultivated in presence (10 μM) or absence of DapT, cells were trypsinized (ACF Enzymatic Dissociation or inhibition solution, Stemcell technologie, France) at 37°C for 7 minutes. Cell suspension was centrifuged at 1500 rpm for 5 minutes. Supernatant was discarded. Then, cells were resuspended in 1mL HBSS 0.05% BSA and passed through 40 μm porosity Flowmi™ Cell Strainer. Then, cell suspension was centrifuged at 1500 rpm for 5 minutes. The supernatant was removed and the cells were resuspended in HBSS 0.05% BSA at a concentration of 1000 cells/ μL .

Discussion

Impacter les voies de signalisation Rho, Notch et BMP respectivement par les molécules Y27632, DapT et LDN193189, en les supplémentant ou non dans les milieux de cultures NHBE et HBEC, aurait le potentiel de modifier le phénotype épithélial des voies respiratoires en modulant la différenciation d'un type cellulaire spécifique par rapport aux autres.

Les expositions des cultures NHBE et HBEC avec le Y27632 ont induit une régulation positive des cellules exprimant le CCSP et le MUC5AC au niveau ARNm et protéine mais elles n'ont pas modifié l'expression des cellules ciliées. Ceci suggère que la voie Rho joue un rôle sur la différenciation des cellules à mucus et des cellules Club. L'augmentation des cellules Club et de la libération de CCSP favorisées par le Y27632 dans les modèles NHBE et HBEC suggèrent que l'inhibition de la voie Rho favorise l'auto-renouvellement des cellules Club mais aussi la différenciation vers les cellules productrices de mucus.

L'inhibition de la voie BMP (par le LDN193189) a favorisé le destin cellulaire vers une différenciation des cellules à mucus dans le modèle NHBE. Ces résultats ont été montrés par d'autres études mais le mécanisme exact par lequel le LDN193189 inhibe la voie BMP n'est pas parfaitement connu. Il est à noter que dans le modèle NHBE, cette molécule n'a pas permis l'acquisition de cellules ciliées ce qui confirme le rôle de la voie BMP dans le déséquilibre cellulaire probablement dû à la phosphorylation du facteur de transcription SMAD. C'est un argument qui corrèle avec les observations fréquentes, dans les cellules de l'épithélium des voies respiratoires, de colocalisation de CCSP et MUC5AC. De plus, nous remarquons aussi que les cellules MUC5AC positives qui ont exprimé le CCSP au début, l'ont progressivement perdu. Ceci peut expliquer pourquoi les cellules Club sont réduites dans la BPCO alors que les cellules à mucus sont augmentées par l'accélération de ce processus de différenciation. Ralentir ce processus permettrait de restaurer le pool de cellules Club et réduire celui des cellules à mucus dans l'épithélium des voies aériennes mais le bénéfice clinique reste à prouver.

L'inhibition de la voie Notch par le DapT a favorisé la différenciation des cellules ciliées. Cependant, les cibles du DapT ne sont pas parfaitement connues mais il semble que cela puisse augmenter DLL1 tout en supprimant HES1. Des données récentes ont montré que l'anticorps AMG430, se liant au ligand Jagged-1, empêche l'activation de Notch, réduisant ainsi celle-ci et permettant d'augmenter la différenciation des cellules ciliées dans l'épithélium des voies respiratoires. De plus, l'inhibition de la gamma-sécrétase permet la différenciation des cellules basales. Ces données suggèrent que cette molécule est capable de promouvoir les cellules

progénitrices et ciliées en inhibant la différenciation des autres cellules. Ceci peut présenter un avantage pour augmenter le nombre de cellules ciliées par rapport aux cellules à mucus notamment dans la BPCO.

Pour finir, le DapT a permis de reverser l'effet du tabac en diminuant l'hyperplasie des cellules à mucus. Par contre il a aussi permis d'inhiber la différenciation des cellules Club et des cellules à mucus. L'inhibition des autres types cellulaires est un problème car nous avons besoin d'un épithélium différencié « normal » possédant la bonne composition et proportion cellulaire. En parallèle, dans le processus de réparation après un scratch, le DapT diminue la réparation ce qui serait également un inconvénient dans notre modèle où les dommages cellulaires sont importants.

Le DapT est un candidat pour agir contre l'hyperplasie des cellules à mucus et permettre l'augmentation de la différenciation des cellules ciliées mais il faut adapter les doses de cette molécule pour obtenir un épithélium différencié et cohésif avec tous les types cellulaires.

Conclusion

Nous avons montré que certaines voies de signalisation sont déterminantes pour le devenir des cellules épithéliales des voies aériennes. Par conséquent, il est possible d'adapter la différenciation des cellules provenant de cultures ALI NHBE et HBEC vers des cellules ciliées, cellules à mucus, cellules Club ou cellules basales. Ceci permet de jouer sur le déséquilibre des cellules épithéliales retrouvées dans certaines pathologies chroniques des voies aériennes comme la BPCO. Notamment, le Y27632 et le LDN193189 favorisent la différenciation vers les cellules Club et les cellules à mucus tandis que le DapT favorise le destin cellulaire vers les cellules ciliées et les cellules basales. A partir des données obtenues, il est possible d'envisager de personnaliser le phénotype des cellules épithéliales des voies aériennes. Cependant, ce déséquilibre de rapport cellulaire n'est pas le seul responsable dans cette maladie. Notamment la dérégulation du système immunitaire est aussi en cause.

IV-Le rôle des alarmines dans les maladies chroniques des voies aériennes

IV-1. La place des cytokines dans les maladies chroniques des voies aériennes

Résumé

La réponse des cellules épithéliales des patients atteints de BPCO face à une agression de l'environnement est exagérée avec une perte de la balance entre tolérance et inflammation ce qui suggère la dérégulation de certaines molécules de type T2 appelées alarmines (IL33, IL25 et TSLP). Ces dernières sont sécrétées par l'épithélium en réponse à une stimulation, notamment l'IL33 est augmentée chez les patients atteints de BPCO alors que le TSLP, lui, est retrouvé augmenté chez les asthmatiques.

Actuellement, les thérapies sont basées sur l'utilisation de bronchodilatateurs et d'anti-inflammatoires, mais ceux-ci n'ont pas d'effet sur le développement de la maladie car ils ne ciblent pas la réponse exagérée du système immunitaire inné. De plus, il existe une forte hétérogénéité des phénotypes et à l'heure actuelle il n'existe pas de biomarqueur identifié dans cette maladie ce qui rend difficile la compréhension de la maladie et la mise en place de traitements.

Cependant, des essais cliniques ont tenté de cibler les cellules effectrices de la cascade immunitaire activée par les alarmines, en inhibant notamment l'IL4, l'IL5 et l'IL13 dans l'asthme et la BPCO. Aujourd'hui dans la BPCO, ces études cliniques n'ont pas donné de résultats totalement concluants. D'autres essais cliniques ont ciblé l'inhibition de l'IL8 pour bloquer le versant T1 mais cette piste n'est actuellement pas poursuivie. De ce fait, il serait nécessaire d'agir en amont de cette cascade de type T2 notamment en impactant les alarmines. Ces molécules de type T2 sont augmentées chez les patients BPCO et sont capables d'attirer les cellules du système T2 notamment les ILC2. Ces cellules sont retrouvées en plus grand nombre dans les poumons des patients BPCO. Ce sont des cellules intermédiaires produisant des cytokines de type IL13 et IL5 permettant d'attirer les éosinophiles.

Par cette revue de la littérature, nous avons voulu démontrer l'enjeu de cibler le haut de la cascade immunitaire c'est-à-dire les alarmines dans la BPCO, pour tenter d'agir ainsi sur l'histoire naturelle de la maladie.

Cet article sera soumis à la revue *Respiratory Medicine and Research*.

What is the rationale for targeting alarmins to treat chronic obstructive pulmonary disease?

C Vernisse¹, AS Bedin², A Petit³, P Chanez⁴, D Gras⁴, I Vachier³, J Charriot^{1,3}, E Ahmed³, E Tuailon², A Bourdin^{1,3}

1. PhyMedExp, University of Montpellier, INSERM U1046, CNRS UMR9214, France
2. UMR 1058, Pathogenesis & control of chronic infection, France
3. Department of Respiratory Diseases and Addictology, Hospital Arnaud de Villeneuve, CHU Montpellier, France
4. Department of Respiratory Medicine, Assistance Publique Hôpitaux de Marseille, UMR INSERM U1067 CNRS 7333, Aix Marseille University, Marseille, France

Correspondence

Prof Arnaud Bourdin

Department of Respiratory Diseases

Hospital Arnaud de Villeneuve

371 Avenue Doyen Giraud 34295 Montpellier Cedex 5 France

a-bourdin@chu-montpellier.fr

tel +33 4 67 33 61 26

Author's contribution to this work

CV drafted the manuscript

ASB, AP, DG, IV reviewed the manuscript

PC, JC, EA, ET defined profile of “anti-alarmin” patient

AB wrote the manuscript

1.Introduction

Chronic Obstructive Pulmonary Disease (COPD) progresses and became in 2020 the 3rd leading cause of death worldwide¹. In developed country, the main cause of this disease is cigarette smoking. But, it is not the only factor because non smokers may also develop chronic airflow limitation. Consequently, it seems to be rather a combination of several factors that will cause diseases development, such as genetic or epigenetic factors, environment exposure (pollution, particles), paediatric origin, age, sex¹. The response of epithelial cells of COPD patient to environment exposure is exaggerated with the loss of balance between tolerance and inflammation which suggests alarmins dysregulation (IL33, TSLP, and IL25). Thereby, alarmins can be secreted by epithelial cells in response to stimulation and cause immune cascade. This disease is characterized within the small airways of COPD patients by inflammation (immune cells infiltration)² and airway remodelling^{3,4}. These mechanisms lead to reduce the diameter of the airways, increase the resistance to the flow and cause the decline of respiratory function^{5,3}.

Currently, pharmacological therapies are bronchodilators and anti-inflammatory drugs⁶. These treatments are merely for symptoms. They have no effects on the development of the disease itself¹ because of the susceptibility, exaggerated and failing engagement of innate immune system that are implicated in this pathology, it makes sense that existing treatments do not work. Moreover, because of poor disease knowledge and heterogeneity phenotypes⁷, in addition to the lack of specific biomarkers, the current therapies failed to treat the disease. Therefore, the better knowledge of pathophysiological mechanisms involving upstream signals may highlight other therapeutic targets that have to be considered⁸. Notably, asthma and some cases of COPD are mainly driven by type 2 immune responses involving the secretion of IL-4, IL-5⁹ and IL-13¹⁰. Clinical trials of antibodies that block these interleukins have shown reduced acute exacerbations, oral corticosteroid use and improvements in lung function and symptoms in selected patients^{11,12}. Notably, specific antibodies have been approved for severe asthmatics patients¹³ and this can be a track to find a solution in COPD. Unfortunately, either IL5 or IL13 monoclonal antibody failed in COPD and demonstrated heterogeneity results in asthma.

Therefore, it is necessary to target upstream T2 orientating cytokines called alarmins^{8,11,14}, cytokines who are increased in COPD patients. These secreted alarmins are able to attract T2 immune cells such as ILC2. These cells are found increased in COPD lung patients compared to controls¹⁵ and it is intermediate cells to arrive to IL5 and IL13 cytokines secretions. In parallel,

there is also the T1 type with the production of IL8 in response to the epithelial cells stimulation. This will attract neutrophils.

The heterogeneity of COPD patient's response and the clinical trials failures suggest that it is necessary to target the top of the cascade to have effects on the disease.

2.Inflammation in COPD

COPD is an airway disease associated by chronic inflammation of the respiratory tract. An association of factors (cigarette smoke, toxic particles and others) seems to be the cause of this lung inflammation. This inflammation is a normal response against an aggression, but it seems to be amplified in COPD patients, which leads to the development of the pathology¹⁶. This chronic inflammation causes parenchymal destruction, dysfunction of reparation and defence mechanisms, structural changes in airways (metaplasia, goblet cell hyperplasia and peribroncholar fibrosis)^{15,17}. These changes are thought to be largely irreversible and often progressive.

Mechanisms leading to the development of COPD are poorly known but theories are advanced. Currently, it is unknown how irritants, such as cigarette smoke, trigger an innate immune response, but "danger hypothesis" is a plausible explanation¹⁸. Matzinger and all¹⁹ suggested that it was not the presence of a microbe itself that warned the immune system to respond, but rather the cellular stress or tissue damage (danger signals) resulting from an infection. For COPD, each puff of cigarette contains more than 2000 xenobiotic compounds and 1014 free radicals that damage lung epithelial cells²⁰. Products derived from lung epithelial cell injury may act as ligands for TLR4 and TLR2 (TLR expressed by epithelial cells). When one product is cross-linked by its corresponding ligand, it will activate the nuclear factor κ B (NF- κ B), and induce the epithelial cells to produce upstream mediators of inflammation, notably alarmins (IL33, TSLP, IL25) or IL8. This inflammation response to epithelial cell stimulation has many guises and phenotyping this heterogeneity has revealed different patterns. Depending on secreted mediators in response to stimulation, we will either neutrophil-associated COPD with IL8 secretion, T1 immunity, the most common phenotype or either eosinophil-associated COPD with T2-mediated immunity with alarmins, ILC2 and eosinophils, the minority phenotype²¹. This inflammatory response in airways of COPD patients is not resolved by stopping smoking and in particular in patients who have very severe disease even though they stopped smoking for several years²². The

reason for the persistence of inflammation is not completely known but it may be due to an increase number of activated T cells, including memory T cells that can perpetuate this chronic inflammatory response. In addition, this is further complemented by the low numbers of regulatory T cells (CD4⁺ CD25⁺ foxp3) in COPD patients who have smoked, compared to controls²³. These data reveal a significant heterogeneity response to patients and COPD concepts still uncertain such as eosinophilic group of this disease. Moreover, currently, it is not possible to give the potential effect of treatment to COPD patient when you touch the bottom of inflammation cascade (IL5, IL13) notably because of you haven't biomarker and poor knowledge on COPD development.

3.COPD Endotypes: The T1/T2 paradigm

In COPD patients, inflammatory endotype depends on the patient²⁴. Consequently, after lung injury, there are different inflammatory responses for COPD patients. In the main scenario, after aggression the epithelial cells release inflammatory mediators such as Tumor Necrosis Factor (TNF), IL-1 β , IL-6 and IL-8. With the presence of IL8 and/or DAMPs (Damage Associated Molecular Patterns), neutrophils are recruited². In response, they release a significant amount of proteases and doing airway damage. Then, the adaptative immune response is also involved with recruitment of T1 and T17 cells, which produce IFN- γ , IL-17A and IL-17F respectively, with a later predominance of CD8⁺ T-cells²⁴. To argue this immune response, neutrophil levels are increased within the sputum of COPD subjects compared to controls and correlated with the GOLD stage²⁵. Using ALI (Air Liquid Interface) epithelial cell culture, IL8 is increased in COPD patients compared to healthy donors when stimulated by CSE²⁶. Neutrophils and pro-inflammatory cytokines involved in COPD have been targeted²⁷. But the treatment efficacy and cytokines inhibition have not yielded the expected results because disease is not resolved²⁸. This suggests that other targets need to be found.

Although the neutrophil phenotype is the most common inflammatory endotype found in COPD patients, other inflammatory patterns exist. There are 10-40% of COPD patients²⁹ with increased eosinophil in the sputum and blood, correlated with an increased T2-transcriptome signature. It has been shown that in blood and sputum samples of COPD patients, increasing of eosinophils were associated with a higher risk to develop severe exacerbation³⁰.

To explain the margination of eosinophils within the lung, several hypotheses have been considered. One of them is that with an aggression, the epithelium can secrete IL33, IL25 and TSLP alarmins. These cytokines are able to attract the immune cells, ILC2 or DC. In turn, notably ILC2 will be activated and then release T2 cytokines, IL5 and IL13 cytokines, which attract eosinophils^{31,9}. IL5 and IL13 levels are increased in COPD patients² and ILC2 are also found increased in lung of COPD patients. But, it remains two relative failures with mepolizumab and with benralizumab, especially benralizumab with the absence of trend and answer dose.

COPD patients also presented other endotypes: patients who presented either both neutrophils and eosinophils within the lung, either patient with neither these cell types called paucigranulocytic.

All these studies show the problem of heterogeneity inflammatory patterns that exists in this pathology because clinical trials have failed. Moreover, even patients who have similar clinical data will not respond in the same way especially at the type and level of cytokine secretion. Therefore this is a problem because choosing the right treatment for the patient is a challenge in this pathology where there is no cure.

Taken together, blocking the end of the immune cascade including IL5, IL13 failed to achieve significant results in COPD. These observations may suggest the importance of therapies targeting upstream signals like alarmins, suggesting that treating on the top of the cascade with anti-alarmins should more efficient than treating only with anti-cytokines at the bottom of the inflammatory cascade. If the beginning of inflammatory cascade is stopped, the follow will also be stopped notably ILC2 (increased in COPD lung).

Currently, most clinical trials using cytokine inhibitors failed in COPD notably due to the heterogeneity of the disease¹² but also because we should target upstream the inflammatory cascade (IL33, IL25 and TSLP)¹¹. Finally finding a biomarker specific to the responses of these therapies, other than eosinophil number should add pathophysiologic efficacy criteria in addition to clinical data. Moreover, finding the “bon répondeur” to treatment is a challenge in this heterogeneous disease where it is difficult to predict patient’s response and profile.

4. Alarmins and their potential implication in COPD

4.1. IL33 – ST2 axis

IL33 is an IL1-type alarmin with different forms (long form, short form)³². This cytokine has been described as a nuclear protein called "Nuclear Factor from High Endothelial Venues" (NF-HEV)³³. *In vivo*, IL33 is a nuclear cytokine associated with chromatin. This is allowed by its amino-terminal nuclear domain (N terminal domain), which is necessary and sufficient for nuclear localization and its association with chromatin³⁴. Evolutionary conservation of this N terminal domain suggests that nuclear localization and its chromatin binding are important for IL33 regulation and function. To better understand the role of this N terminal domain knocked out mouse model showed increased level of IL33 levels in the serum³⁸. This brings us to conclude that this domain has a role in the regulation of its own pro inflammatory activity but also to avoid an inappropriate liberation of IL33.

IL33 long form is constitutively and abundantly expressed at steady state in human tissues and in particular in the nuclei of different cell types, endothelium and airway epithelium for example. IL33 doesn't contain a secretion signal sequence as there is for other cytokines. In order to release this alarmin in the extracellular medium, different mechanisms are possible such as aggression or stress mechanisms or necrotic cell death³³. When allergen type *Alternaria* is administered intranasally in a mouse model, the level of IL33 is increased in the bronchoalveolar and nasal lavages³⁴. Moreover, cellular activation via ATP pathway can induce the release of IL33 in the absence of cell death^{35,36}

After an aggression, IL33 long form is released in the extracellular space. This form can be processed by inflammatory proteases from neutrophils or mast cells. These inflammatory cells are able to process the long form into a mature short form which is 10 to 30 fold more potent for activating ILC2 and mast cells³⁷. *In vivo*, this short form of IL33 is detected after acute lung injury associated with neutrophilic infiltration in mice.

In contrast, mechanisms to limit IL33 activity are also known. Its nuclear location and retention seems important for immune homeostasis by limiting the pro-inflammatory effects³⁸. In IL33 sequence at the β 4- β 5 loop, there is an insertion of 100 residues which is not found in the other cytokines of IL1 family³⁸. This insertion contains caspase domains and in particular caspase 3 and 7 which generates two inactive biological forms³⁹. To argue, a study performed in mice

showed the important role of caspase 1 and 7 by limiting type 2 immune responses in lung and potentially inactivating IL33⁴⁰.

Once released, IL33 binds a heterodimeric receptor ST2 (Suppression of Tumorigenicity 2) also called IL-1RL1 and IL-33R, and its co-receptor IL1RAcP (IL-1 Receptor Accessory Protein)³⁸. ST2 was identified as an orphan receptor in 1989. This receptor was found to play a role in inflammatory and cardiac diseases⁴¹. There are different isoforms of the ST2 receptor, such as ST2L form (membrane form), which is constitutively expressed on effectors immune cells, in particular Th2 cells, but also found on non hematopoietic cells notably lung epithelial cells^{42,43}. This molecule seems to play a critical role in inflammatory process, especially those involving T2 cells and in production of their T2 cytokines. Pro-inflammatory stimuli increase the expression of ST2 mRNA. ST2 is expressed by various cell types including Th2 cells, ILC2, CD8⁺ T cells, natural killer and non hematopoietic cells (endothelial cells, epithelial cells, and fibroblasts)⁴⁴.

IL33 is able to promote T2 response, notably when IL33 binds ST2 receptor on ILC2. This complex (IL33-ST2-IL1RAcP) recruits MyD88, IRAK (IRAK1, IRAK4) and TRAF6 to activate signalling pathway (MAPKs and NF-KB)³². ST2 mRNA is overexpressed in PBMC (Peripheral Blood Mononuclear cells) and sputum from COPD subjects compared to healthy donors. ST2 mRNA expression was significantly higher in sputum cells from COPD patients with eosinophilic airway inflammation compared to patients without⁴⁵.

However, sST2, the soluble form of ST2 receptor, has a negative effect on the IL33-ST2 axis⁴⁶. There are also other ST2 forms such as ST2V found in gastrointestinal organs or the ST2LV found in the late states of embryogenesis⁴³.

In the extracellular medium, IL33 is rapidly inactivated (about 2 hours) by the oxidation of cysteine residues, done by inflammatory proteases which may also have a role in the inactivation of IL33⁴⁷.

To argue the importance of IL33-ST2 axis in COPD, in plasma of stable COPD patients, the number of eosinophils is significantly correlated with the level of IL33. Patients with high levels of IL33 have chronic bronchitis⁴⁸. In the serum, IL33 was increased in COPD patients compared to healthy subjects⁴⁵. Moreover, the levels of IL33 mRNA and protein are increased in the lungs of COPD subjects compared to non-COPD patients⁵⁴. However, MiR-543 has been shown to

regulate IL33, when decreasing in plasma it enhanced the progression of COPD⁴⁹. In addition, in mouse model of cigarette smoke-induced COPD, both IL-33 and ST2 receptor expressions were increased in lungs⁴⁴. The pathogenic changes induced by extracts of tobacco are reversed when adding anti-IL33 antibodies⁴⁵. Furthermore, mice treated with IL-33 developed histopathological changes within the lungs such as goblet cell hyperplasia, and mucus hypersecretion, which are typical features of COPD⁵⁰. The murine models of both asthma and COPD suggest that IL-33 and ST2 might be prominent new therapeutic targets for these chronic inflammatory respiratory diseases. The use of anti-IL-33 antibody reduced Th2 cytokines production by ILC2⁵¹.

Model	Compartment	Disease	Datas
human	plasma	COPD	IL33 correlate with number of eosinophils
human	lung	COPD	IL33 protein and mRNA increased in COPD patients to non COPD subjctcs
human	plasma	COPD	MiR-543 regulate IL33
mouse	lung	COPD	IL33 and ST2 increased in mouse model of cigarette smoke induced COPD
mouse	lung	COPD	Anti-IL33 reverse histopathological changes

Figure: IL33/ST2 axis in COPD

Several clinical trials targeting either IL-33 or its receptor in asthma and COPD are ongoing at present⁵². In COPD, two trials concerning IL-33/ST2 have been reached⁴⁴. One investigates the effects of anti-IL-33 monoclonal antibody compared to placebo, on the annualized rate of moderate to severe acute exacerbations of COPD. The second evaluates the efficacy of anti-ST2 antibody vs. placebo on the frequency of moderate to severe exacerbations of COPD. Moreover, a clinical trial (anti-ST2) is underway in COPD patients with moderate to severe disease to block the IL33 / ST2 signalling pathway¹¹.

Diseases	Antibody	phase	clinical trials
COPD	Anti-IL33 monoclonal antibody	2	NCT0354690
COPD	Anti-ST2 antibody	2	NCT03615040
Asthma	Anti-IL33 receptor monoclonal antibody	2	NCT0320724
Asthma	Anti-IL33 monoclonal antibody	1	NCT03112577

Figure: Clinical trials on IL33/ST2 axis in COPD and asthma

IL33 is a cytokine that seems fairly well regulated and has all the mechanisms to be activated in the right conditions and inactivate when needed. Yet it seems to play an important role in the development of COPD.

4.2.TSLP

TSLP is a member of the IL2 family cytokines. It is produced by airway and stromal cells during inflammation⁵³. In human, there are two isoforms. A short isoform is expressed at basal conditions whereas the longer one is expressed in response of inflammatory stimuli⁵³. TSLP orchestrates the response to epithelial aggression by activating CD4, CD8, B cells, mast cells, basophil, ILC2 and eosinophil. TSLP mRNA and protein are overexpressed in the bronchial epithelium of COPD patients compared to controls⁸. Activators of airway epithelial cells such as respiratory viruses, double-stranded RNA, cigarette smoke extracts, and pro-inflammatory cytokines can stimulate the production of TSLP in COPD patients⁷⁰. It was proposed recently that the activation of NF- κ B by oxidative stress from cigarette smoke may underlie the elevated TSLP production in the bronchial mucosa in COPD⁵⁰. Furthermore, repeated intranasal exposure to CSE was found to increase the lung TSLP expression, predominantly through oxidative stress and TNFR (TNF receptor) activation, linking CSE and TSLP expression in lung for the first time⁵⁴. Rhinovirus (RV16) or dsRNA was shown to induce TSLP expression in COPD epithelium in a TLR3-dependent manner⁵⁵. Altogether, it is plausible that the pro-inflammatory cytokines (TNF- α , IL-1 β), bacterial/viral infections and oxidative stress from cigarette smoke contribute synergistically towards elevated TSLP expression in BAL fluid of COPD patients⁷³.

Model	Compartment	Disease	Datas
human	lung	COPD	protein and mRNA TSLP increased
human	lung	COPD	production of TSLP stimulate by activators of airway epithelial cells
human	lung	COPD	TSLP expression increase in BAL fluid by synergy of pro-inflammatory cytokines, infections and oxidative stress

Figure: TSLP in COPD

A clinical study is currently ongoing in asthmatic patients with anti-TSLP antibodies (Tezepelumab)⁵⁶. It reduces asthma exacerbations and increases lung function. Moreover, it reduces the number of eosinophil in the blood with or without a high eosinophilia before treatment. This allows to show the complexity of immune response. Currently, it is considered that alarmins are related to a high level of eosinophils and neutrophils are linked to IL8 secretion. But this previous study shows that even without high eosinophilia, the patient can have TSLP because anti-TSLP antibody function. The alarmins, the immune cascade are complicated to understand and to try to touch by treatments especially without biomarkers or knowledge on disease development. Yet, alarmin treatments seem promising for patients. Currently, there is no current studies perform in COPD patients. TSLP has been found increased within the epithelial cells of COPD patients suggesting that TSLP plays a role in the inflammatory cascade in COPD patients⁵⁷.

4.3.IL25 in COPD

This cytokine is associated with a type 2 immune response⁵⁸. It was described as an amplifier of Th2 inflammation with the induction of cytokines (IL4, IL5 and IL13). It is expressed constitutively in lung epithelial cells in asthmatics patients⁵⁹. The levels of IL25 are higher in lung of asthmatic patient compared to healthy patients and IL25 expression is inversely correlated with lung function. It is mostly secreted by epithelial cells and is able to regulate the Th2 and ILC2 cells functions⁵⁸. Moreover, IL25 expression is increased in airway epithelial cells of COPD patients and is correlated with increased Th2 response. Combination of IL33 and IL25 can promote the development of type 2 innate lymphoid cells⁶⁰. But its mechanism of action and the receptor allows its function, are not really known. This cytokine is described to play a role in homeostasis but it is found deregulate in chronic airway disease and particularly linked to alarmin such as IL33. To act on this cytokine with an anti-IL25 antibody would put back the

right level of IL25 and regulate the other alarmins including IL33. Currently, there is no current studies perform in COPD patients.

5.Future therapies

Given by the poor response to actual classical anti-inflammatory drugs in COPD patients and moreover with some anti-neutrophilic targeting drugs (such as anti CXCR2 or anti TNF), it is necessary to start exploring other cytokines involved in the immunity T2 system and eosinophilic inflammation¹². The use of cytokine inhibitors has shown encouraging results, especially with anti-IL5 in selected asthma patient. But a small proportion of COPD patients responded to these cytokine inhibitors because it is necessary to go upstream of the cascade or the need to find a potential biomarker to better define the target group to treat^{50,61}. Patients answer differently to a same injury by secreting different cytokines, alarmins and others. The reason of these differential answers remains unknown but probably epigenetic or genetic markers may be in cause. However, targeting the upstream inflammatory cascade may allow us to act on a larger spectrum of answers and so may be benefit to more patients. On the other hand, acting at this upstream cascade must be performed with more knowledge of mechanism of action because these alarmins are not found only within the lung and so can cause dangerous side effects. Finally, to have the better chance to find the best therapy for an individual, it is essential to find predictive biomarkers to response to this new therapy.

6.Conclusion

Recent works have led to major advances in our understanding of mechanisms by which epithelial cells interact with environmental stimuli and with other cells in the airway in patient with chronic airway diseases. Developing new therapeutic strategies to target alarmins, IL33, IL25 or TSLP has already been move forward with ongoing clinical trials.

Besides eosinophils target, other chronic airways endotypes are less well understood, but studies of airway epithelial cells are helping to identify individuals with activation of other pathways including which may help identify new approaches for personalized prevention and treatment.

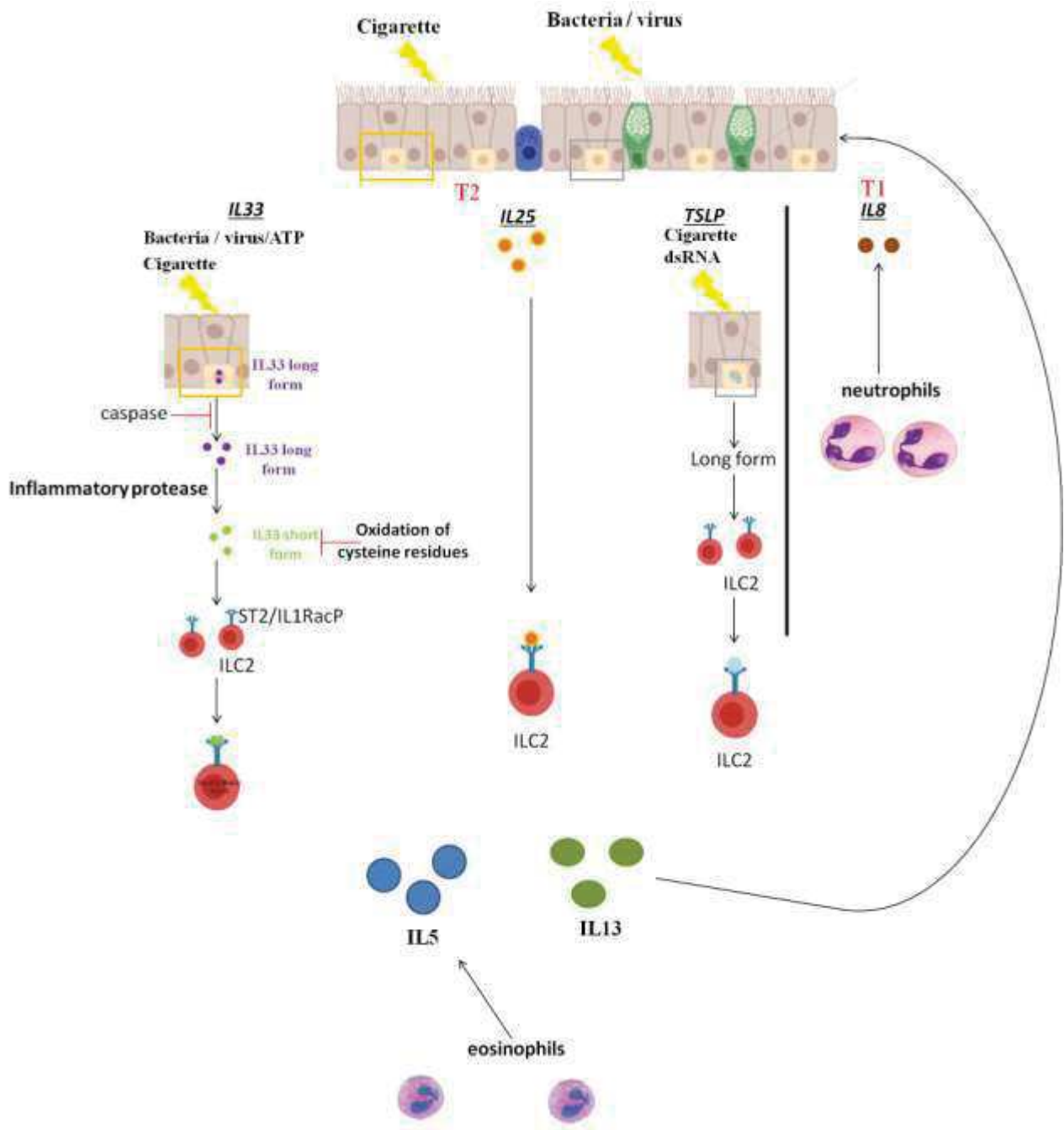


Figure : Alarmins in COPD

REFERENCES

1. Gold Reports for Personal Use - Global Initiative for Chronic Obstructive Lung Disease - GOLD. <https://goldcopd.org/gold-reports/>.
2. Barnes, P. J. Inflammatory mechanisms in patients with chronic obstructive pulmonary disease. *J. Allergy Clin. Immunol.* **138**, 16–27 (2016).
3. Baraldo, S., Turato, G. & Saetta, M. Pathophysiology of the small airways in chronic obstructive pulmonary disease. *Respiration* **84**, 89–97 (2012).
4. Wang, Y., Xu, J., Meng, Y., Adcock, I. M. & Yao, X. Role of inflammatory cells in airway remodeling in COPD. *Int J Chron Obstruct Pulmon Dis* **13**, 3341–3348 (2018).
5. Rabe, K. F. & Watz, H. Chronic obstructive pulmonary disease. *The Lancet* **389**, 1931–1940 (2017).
6. Candela, M., Costorella, R., Stassaldi, A., Maestrini, V. & Curradi, G. Treatment of COPD: the simplicity is a resolved complexity. *Multidisciplinary Respiratory Medicine* **14**, 18 (2019).
7. Mirza, S. & Benzo, R. COPD Phenotypes - implications for care. *Mayo Clin Proc* **92**, 1104–1112 (2017).
8. Yousuf, A. & Brightling, C. E. Biologic Drugs: A New Target Therapy in COPD? *COPD: Journal of Chronic Obstructive Pulmonary Disease* **0**, 1–9 (2018).
9. Narendra, D. K. & Hanania, N. A. Targeting IL-5 in COPD. *Int J Chron Obstruct Pulmon Dis* **14**, 1045–1051 (2019).
10. Brightling, C. E., Saha, S. & Hollins, F. Interleukin-13: prospects for new treatments. *Clin Exp Allergy* **40**, 42–49 (2010).
11. Barnes, P. J. Targeting cytokines to treat asthma and chronic obstructive pulmonary disease. *Nat. Rev. Immunol.* **18**, 454–466 (2018).
12. Yousuf, A., Ibrahim, W., Greening, N. J. & Brightling, C. E. T2 Biologics for Chronic Obstructive Pulmonary Disease. *J Allergy Clin Immunol Pract* **7**, 1405–1416 (2019).
13. Chung, K. F. Targeting the interleukin pathway in the treatment of asthma. *Lancet* **386**, 1086–1096 (2015).
14. Caramori, G., Adcock, I. M., Di Stefano, A. & Chung, K. F. Cytokine inhibition in the treatment of COPD. *Int J Chron Obstruct Pulmon Dis* **9**, 397–412 (2014).
15. Silver, J. S. *et al.* Inflammatory triggers associated with exacerbations of COPD orchestrate plasticity of group 2 innate lymphoid cells in the lungs. *Nat. Immunol.* **17**, 626–635 (2016).
16. Chung, K. F. & Adcock, I. M. Multifaceted mechanisms in COPD: inflammation, immunity, and tissue repair and destruction. *European Respiratory Journal* **31**, 1334–1356 (2008).
17. Cornwell, W. D., Kim, V., Song, C. & Rogers, T. J. Pathogenesis of Inflammation and Repair in Advanced COPD. *Semin Respir Crit Care Med* **31**, 257–266 (2010).

18. Baraldo, S., Saetta, M. & Cosio, M. G. For Whom the “Alarm” Tolls. *Am J Respir Crit Care Med* **181**, 879–880 (2010).
19. Matzinger, P. The danger model: a renewed sense of self. *Science* **296**, 301–305 (2002).
20. Barnes, P. J., Drazen, J. M., Rennard, S. I. & Thomson, N. C. *Asthma and COPD: Basic Mechanisms and Clinical Management*. (Elsevier, 2009).
21. Brightling, C. & Greening, N. Airway inflammation in COPD- progress to precision medicine. *Eur. Respir. J.* (2019) doi:10.1183/13993003.00651-2019.
22. Hogg, J. C. *et al.* The nature of small-airway obstruction in chronic obstructive pulmonary disease. *N. Engl. J. Med.* **350**, 2645–2653 (2004).
23. Chiappori, A. *et al.* CD4(+)/CD25(high)/CD127(-) regulatory T-cells in COPD: smoke and drugs effect. *World Allergy Organ J* **9**, 5 (2016).
24. Garudadri, S. & Woodruff, P. G. Targeting Chronic Obstructive Pulmonary Disease Phenotypes, Endotypes, and Biomarkers. *Ann Am Thorac Soc* **15**, S234–S238 (2018).
25. Singh, D., Edwards, L., Tal-Singer, R. & Rennard, S. Sputum neutrophils as a biomarker in COPD: findings from the ECLIPSE study. *Respir. Res.* **11**, 77 (2010).
26. Gamez, A. S. *et al.* Supplementing defect in club cell secretory protein attenuates airway inflammation in COPD. *Chest* **147**, 1467–1476 (2015).
27. Butler, A., Walton, G. M. & Sapey, E. Neutrophilic Inflammation in the Pathogenesis of Chronic Obstructive Pulmonary Disease. *COPD* **15**, 392–404 (2018).
28. Jasper, A. E., Mclver, W. J., Sapey, E. & Walton, G. M. Understanding the role of neutrophils in chronic inflammatory airway disease. *F1000Res* **8**, (2019).
29. George, L. & Brightling, C. E. Eosinophilic airway inflammation: role in asthma and chronic obstructive pulmonary disease. *Therapeutic Advances in Chronic Disease* **7**, 34–51 (2016).
30. Yun, J. H. *et al.* Blood eosinophil count thresholds and exacerbations in patients with chronic obstructive pulmonary disease. *J. Allergy Clin. Immunol.* **141**, 2037-2047.e10 (2018).
31. Roan, F., Obata-Ninomiya, K. & Ziegler, S. F. Epithelial cell-derived cytokines: more than just signaling the alarm. *J. Clin. Invest.* **129**, 1441–1451 (2019).
32. Liew, F. Y., Girard, J.-P. & Turnquist, H. R. Interleukin-33 in health and disease. *Nat. Rev. Immunol.* **16**, 676–689 (2016).
33. Cayrol, C. & Girard, J.-P. Interleukin-33 (IL-33): A nuclear cytokine from the IL-1 family. *Immunological Reviews* **281**, 154–168 (2018).
34. Drake, L. Y. & Kita, H. IL-33: biological properties, functions, and roles in airway disease. *Immunol. Rev.* **278**, 173–184 (2017).

35. Kouzaki, H., Iijima, K., Kobayashi, T., O'Grady, S. M. & Kita, H. THE DANGER SIGNAL, EXTRACELLULAR ATP, IS A SENSOR FOR AN AIRBORNE ALLERGEN AND TRIGGERS IL-33 RELEASE AND INNATE TH2-TYPE RESPONSES. *J Immunol* **186**, 4375–4387 (2011).
36. Byers, D. E. *et al.* Long-term IL-33–producing epithelial progenitor cells in chronic obstructive lung disease. *J Clin Invest* **123**, 3967–3982 (2013).
37. Scott, I. C. *et al.* Interleukin-33 is activated by allergen- and necrosis-associated proteolytic activities to regulate its alarmin activity during epithelial damage. *Sci Rep* **8**, (2018).
38. Lingel, A. *et al.* The structure of interleukin-33 and its interaction with the ST2 and IL-1RAcP receptors – insight into the arrangement of heterotrimeric interleukin-1 signaling complexes. *Structure* **17**, 1398–1410 (2009).
39. Cayrol, C. & Girard, J.-P. The IL-1-like cytokine IL-33 is inactivated after maturation by caspase-1. *Proc Natl Acad Sci U S A* **106**, 9021–9026 (2009).
40. Molofsky, A. B., Savage, A. K. & Locksley, R. M. Interleukin-33 in Tissue Homeostasis, Injury, and Inflammation. *Immunity* **42**, 1005–1019 (2015).
41. Kakkar, R. & Lee, R. T. The IL-33/ST2 pathway: therapeutic target and novel biomarker. *Nat Rev Drug Discov* **7**, 827–840 (2008).
42. Pascual-Figal, D. A. & Januzzi, J. L. The Biology of ST2: The International ST2 Consensus Panel. *American Journal of Cardiology* **115**, 3B-7B (2015).
43. Griesenauer, B. & Paczesny, S. The ST2/IL-33 Axis in Immune Cells during Inflammatory Diseases. *Front Immunol* **8**, 475 (2017).
44. Gabryelska, A., Kuna, P., Antczak, A., Białasiewicz, P. & Panek, M. IL-33 Mediated Inflammation in Chronic Respiratory Diseases-Understanding the Role of the Member of IL-1 Superfamily. *Front Immunol* **10**, 692 (2019).
45. Tworek, D. *et al.* The association between airway eosinophilic inflammation and IL-33 in stable non-atopic COPD. *Respir. Res.* **19**, 108 (2018).
46. Zhao, J. & Zhao, Y. Interleukin-33 and its Receptor in Pulmonary Inflammatory Diseases. *Crit Rev Immunol* **35**, 451–461 (2015).
47. Cohen, E. S. *et al.* Oxidation of the alarmin IL-33 regulates ST2-dependent inflammation. *Nature Communications* **6**, 8327 (2015).
48. Kim, S. W. *et al.* Factors associated with plasma IL-33 levels in patients with chronic obstructive pulmonary disease. *Int J Chron Obstruct Pulmon Dis* **12**, 395–402 (2017).
49. He, H., Wang, H., Pei, F. & Jiang, M. MiR-543 Regulates the Development of Chronic Obstructive Pulmonary Disease by Targeting Interleukin-33. *Clin. Lab.* **64**, 1199–1205 (2018).
50. Qiu, C. *et al.* Anti-interleukin-33 inhibits cigarette smoke-induced lung inflammation in mice. *Immunology* **138**, 76–82 (2013).

51. Chen, W.-Y., Tsai, T.-H., Yang, J.-L. & Li, L.-C. Therapeutic Strategies for Targeting IL-33/ST2 Signalling for the Treatment of Inflammatory Diseases. *CPB* **49**, 349–358 (2018).
52. Garth, J., Barnes, J. W. & Krick, S. Targeting Cytokines as Evolving Treatment Strategies in Chronic Inflammatory Airway Diseases. *Int J Mol Sci* **19**, (2018).
53. Varricchi, G. *et al.* Thymic Stromal Lymphopoietin Isoforms, Inflammatory Disorders, and Cancer. *Front Immunol* **9**, 1595 (2018).
54. Nakamura, Y. *et al.* Cigarette smoke extract induces thymic stromal lymphopoietin expression, leading to T(H)2-type immune responses and airway inflammation. *J. Allergy Clin. Immunol.* **122**, 1208–1214 (2008).
55. Calvén, J. *et al.* Viral stimuli trigger exaggerated thymic stromal lymphopoietin expression by chronic obstructive pulmonary disease epithelium: role of endosomal TLR3 and cytosolic RIG-I-like helicases. *J Innate Immun* **4**, 86–99 (2012).
56. Corren, J. *et al.* Tezepelumab in Adults with Uncontrolled Asthma. *N. Engl. J. Med.* **377**, 936–946 (2017).
57. Ziegler, S. F. *et al.* The biology of thymic stromal lymphopoietin (TSLP). *Adv Pharmacol* **66**, 129–155 (2013).
58. Hallstrand, T. S. *et al.* Airway epithelial regulation of pulmonary immune homeostasis and inflammation. *Clin. Immunol.* **151**, 1–15 (2014).
59. Becerra-Díaz, M., Wills-Karp, M. & Heller, N. M. New perspectives on the regulation of type II inflammation in asthma. *F1000Res* **6**, (2017).
60. Nejman-Gryz, P., Górska, K., Paplińska-Goryca, M., Proboszcz, M. & Krenke, R. Epithelial derived cytokines IL-25, IL-33 and TSLP in obstructive lung diseases. *European Respiratory Journal* **50**, PA571 (2017).
61. Barnes, P. J. Targeting cytokines to treat asthma and chronic obstructive pulmonary disease. *Nature Reviews Immunology* **18**, 454–466 (2018).

Discussion

Les différentes alarmines de type T2 sont détectées dans les différents modèles d'études des maladies chroniques des voies aériennes et semblent jouer un rôle important dans ces maladies. Dans le modèle murin modélisant la BPCO, IL33 est augmentée. Lorsqu'on injecte un anticorps anti-IL33, les effets induits par le tabac sont reversés, notamment le remodelage des voies aériennes, ce qui laisse penser que cette cytokine joue un rôle clé dans cette maladie. Le TSLP, lui, joue un rôle clé dans l'asthme. Par contre dans la BPCO, cette cytokine est beaucoup moins connue même si des données récentes commencent à montrer un rôle potentiel de cette molécule. L'IL25 joue un rôle dans l'homéostasie tissulaire et peut réguler la sécrétion d'autres cytokines comme IL33 et le TSLP mais peu d'études ont été réalisées.

Actuellement, des protocoles d'essais cliniques sont en cours pour bloquer les cytokines telles que l'IL33 et le TSLP dans la BPCO. Pour l'IL25, actuellement aucune thérapie ou essai clinique ne ciblent cette molécule. Les résultats des essais cliniques dans la BPCO permettront de confirmer le rôle potentiel de ces molécules dans cette pathologie notamment savoir si les bloquer agit sur l'histoire naturelle de la pathologie ou ralentit sa progression. De plus, le potentiel thérapeutique de cibler en amont de la cascade immunitaire passe par le fait que les voies de signalisation qui vont de l'alarmine aux cellules immunitaires effectrices restent assez méconnues.

Conclusion

Toutes ces études montrent le rôle thérapeutique potentiel des anti-alarmines dans la BPCO. Mais trouver « les bons répondeurs » à ces traitements n'est pas simple à cause de l'hétérogénéité des profils cytokiniques dans cette pathologie. L'IL25 semble jouer un rôle central dans la sécrétion des cytokines et dans la cascade immunitaire. Mieux étudier le rôle de cette cytokine pourrait permettre de mieux comprendre la dérégulation des autres alarmines et cytokines et potentiellement entrevoir de nouvelles cibles.

IV-2. Les cytokines sécrétées par les cellules de l'épithélium bronchique dans les maladies chroniques des voies aériennes reconstituées en ALI

Résumé

Les alarmines sont des molécules clés sécrétées par l'épithélium des voies aériennes en réponse à une stimulation extérieure. Ces dernières sont notamment dérégulées dans des pathologies chroniques des voies aériennes comme la BPCO. Mais les traitements actuels de cette maladie ne permettent pas de stopper le développement de celle-ci car la cible de ces médicaments ne permet pas d'agir directement sur la dérégulation immunitaire.

Notre hypothèse est que le blocage en amont de la cascade immunitaire, notamment en bloquant les alarmines (IL33, IL25 et TSLP), serait un bénéfice et permettrait de stopper la cascade immunitaire qui en découle. Pour vérifier notre hypothèse, nous avons mis en place des cultures ALI de cellules épithéliales bronchiques humaines obtenues à partir de biopsies de patients (asthmatiques, BPCO et témoins). Le sous-nageant des cultures d'épithélium différencié obtenues est récupéré à J28. Les cytokines sont dosées dans ces sous-nageants de cultures ALI à l'état basal (sans stimulation).

Les résultats des dosages nous ont permis de démontrer que :

- Les alarmines sont bien sécrétées à l'état de base dans les sous-nageants de culture ALI des patients (asthmatiques, BPCO et témoins) et ce de façon différente en fonction des pathologies.
- L'IL33 est la cytokine la plus difficile à doser dans les sous-nageants des cultures.
- La sécrétion d'IL25 est la plus importante par les cellules épithéliales des patients asthmatiques.
- Les cellules épithéliales de patients BPCO sont capables de sécréter le TSLP comme celles des asthmatiques.
- La sécrétion des cytokines T2 est corrélée avec le taux d'éosinophiles sanguins.

Alarmins secretions by human bronchial epithelial cells in air liquid interface model correlate with blood eosinophils in chronic airways diseases

**C Vernisse¹, A Petit², C Suesh⁴, P Chanez³, D Gras³, N Molinari⁴, I Vachier²,
A Bourdin^{1,2}**

1. PhyMedExp, University of Montpellier, INSERM U1046, CNRS UMR9214, France
2. Department of Respiratory Diseases and Addictology, Hospital Arnaud de Villeneuve, CHU Montpellier, France
3. Department of Respiratory Medicine, Assistance Publique Hôpitaux de Marseille, UMR INSERM U1067 CNRS 7333, Aix Marseille University, Marseille, France
4. Department of Medical Information, Hôpital Arnaud de Villeneuve and University of Montpellier, Montpellier, France

Correspondence

Prof Arnaud Bourdin

Department of Respiratory Diseases

Hospital Arnaud de Villeneuve

371 avenue Doyen Giraud 34295 Montpellier Cedex 5 France

a-bourdin@chu-montpellier.fr

tel +33 4 67 33 61 26

Author's contribution to this work

CV performed assays and experiments, interpreted the data and drafted the manuscript

CS, NM helped in statistical analysis

AP, PC, DG, IV helped in interpreting the data and improved the manuscript

AB designed the study, interpreted the results and wrote the manuscript

Abstract

Objectives. Finding new therapeutic track is essential in COPD where currently therapeutic treatment target symptoms. Study aims was to measure alarmin level in order to visualize alarmin patient profile and know if it's possible to correlate it with clinical data.

Methods. HBEC (Human Bronchial Epithelial Cells) cultures were obtained from human bronchial epithelial cells of asthmatics, COPD (Chronic Obstructive Pulmonary Disease) and control subjects in ALI (Air Liquid Interface) condition. At 28 day of ALI culture, in basal state, cytokines (IL8, IL25, TSLP and IL33) were assayed by Elisa sandwich in basolateral medium culture.

Results. Alarmins were secreted by HBEC ALI cultures, in basal state, with different levels and profiles (T1 and/or T2) between diseases and also within the same disease. IL33 was secreted by only some COPD patients. TSLP was secreted by bronchial epithelial cells of COPD (0.008) and asthma patients (0.005). IL25 was secreted by the different groups with a decrease in COPD group (0.0125) compared to healthy (0.025) and asthmatic (0.05) groups. IL8 was more secreted by asthmatic patients (170) than controls (60) and COPD (35) subjects. Asthmatic patients are T2 and T1 High. COPD and controls subjects were combination of T1 and T2 profiles High and Low. T2 High profile is found to correlate with the highest blood eosinophils level.

Conclusions. Alarmins were present in basal state in HBEC ALI cultures, so inhibiting it, was a therapeutic option. But alarmins is present in different way in diseases so better understanding of signalling pathway was essential.

Keywords. Alarmins, Chronic airway disease, ALI culture

1.Introduction

Asthma and COPD (Chronic Obstructive Pulmonary Disease) are chronic airway diseases in progress. The response of COPD patients to environment exposure is exaggerated with the loss of balance between tolerance and inflammation which suggests alarmins dysregulation¹. These alarmins (IL33, IL25 and TSLP) can be secreted by epithelial cells in response to stimulation^{2,3,4,5} and contribute to disease development^{6,7}. Pharmacological therapies are currently bronchodilators and anti-inflammatory drugs⁸. However, because of susceptibility, exaggerated and failing engagement of innate immune system, that are implicated in this disease, it makes sense that existing treatments do not work. In addition, there are several inflammatory patterns in these chronic airway diseases. Asthma patients and some cases of COPD are mainly driven by type 2 immune responses involving at the end of cascade by IL-4, IL-5⁹, IL-13¹⁰ secretion. Unfortunately, either IL5 or IL13 mAbs clinical trials failed in COPD and demonstrated heterogeneous results in asthma. But in COPD patients, it exists type 2 inflammation in 10%-40% of patients associated with increased T2 transcriptome signature¹¹ and lung eosinophils; and type 1 inflammation with T1 signature and lung neutrophils¹². T2 profile corresponds at the bottom of cascade to IL33, IL25 and TSLP¹³ secretions whereas T1 profile corresponds to IL8 secretion.

IL33^{11,4} and TSLP^{15,5} is able to promote T2-type response and their expression were increased in airway epithelial cells of COPD and asthmatics patients^{3,18}. In mouse model, anti-IL33 antibodies reduced tobacco-induced inflammation⁴. Clinical trials are currently ongoing such as anti-TSLP and anti-IL33 monoclonal antibody in asthmatic or COPD patient¹⁶. IL25 would be involved to T2 inflammatory response³ and this expression was increased in airways epithelial cells of asthmatics patients correlated severity of disease¹⁷. But, IL25 contributes to homeostasis and clinical trials don't touch this unknown molecule. IL8 was secreted by airway epithelial cell of COPD patients¹² and clinical trials failed to target this molecule.

Cytokine inhibitors clinical trials are promising molecules to act on chronic airway diseases. But studies have shown that patient with similar clinical data had different cytokine profile⁷. The reason, why patients do not release same cytokines is not elucidate. Genetic and epigenetic factors may explain this difference. However, signaling pathways induced by these alarmins to attract eosinophils and neutrophils are not completely understood and signaling pathway used may be not the same for all patients. Patients groups defined to their cytokine's secretions linked to clinical data seem to be essential to understand the different profiles. Moreover, it is important

to choose a good patient profile to obtain a good response to treatment. As we don't know signaling pathways, studying cytokines present at the top of inflammatory cascade seems to be a good target.

Research goal is to find cytokine signatures associated with clinical data that will allow us to understand disease profile. We cultured bronchial epithelial cells of COPD, asthmatics and controls subjects in air liquid interface model. Then, we measured by Elisa sandwich T2 cytokines (IL25, IL33 and TSLP) and T1 cytokine (IL8) profiles in basolateral chamber at day 28 of ALI culture.

2. Methods

2.1. Patients

Primary Human Bronchial Epithelial Cells (HBEC) (31 controls subjects, 39 COPD patients and 21 asthmatics patients) were derived from bronchial biopsy specimens obtained during Fiberoptic Bronchoscopy at Arnaud Villeneuve Hospital, Montpellier, France. All donors signed a consent form after being informed about biomedical research on airway epithelium performed thanks to their donation. The protocol was approved by the institutional ethics commission of Sud Mediterranee III (CHRU Montpellier-AOI 9244- NTC02354677). All experiments and methods were performed in accordance with relevant guideline and regulations.

2.2 Cell Culture

HBEC were cultured as previously described¹⁸. Briefly, cells were dissociated mechanically and cultivated in 24 well plate and then in 75cm² flask in Bronchial Epithelial Growth Medium (BEGM, Lonza). After, differentiation was initiated by seeding 350000 cells on polyester membrane of Transwell^R (Corning, Kennebunk, United States). Cells were cultivated in a 1:1 mixture of BEGM (Lonza) and Dulbecco's Modified Eagle's Medium (DMEM, Lonza). Air Liquid Interface (ALI) culture was established by aspiration of medium of the apical chamber when cells reached to confluence (referred to D0). Basolateral medium was replaced every two days, while cells were maintained at 37°C, 5 % CO₂ until day 28 of culture.

2.3. Cytokines Detection

IL-25 (EK1179, Bioocean), IL-33 (435908, Biolegend), TSLP (434204, Biolegend) and IL-8 (851530005, Diaclone) concentrations were determined by using sandwich ELISA (Enzyme-Linked Immunosorbent Assay) system according to the manufacturer's instructions in medium culture at day 28 of ALI culture. The color change was detected spectrophotometrically at a wavelength of 450 nm. Samples concentrations were interpolated with the standard curve.

2.4. Statistical Method

R software is used to statistical tests. T1 profile is IL8 centered reduced. T1 high is when T1 cytokine level is superior of T1 profile average whereas T1 low is when T1 cytokine level is inferior of T1 profile average. T2 profile is centered reduced average of IL25, IL33 and TSLP. T2 high is when T2 cytokine level is superior of T2 profile average whereas T2 low is when T2 cytokine level is inferior of T2 profile average.

3. Results

3.1. Cytokine profiles in chronic airway diseases

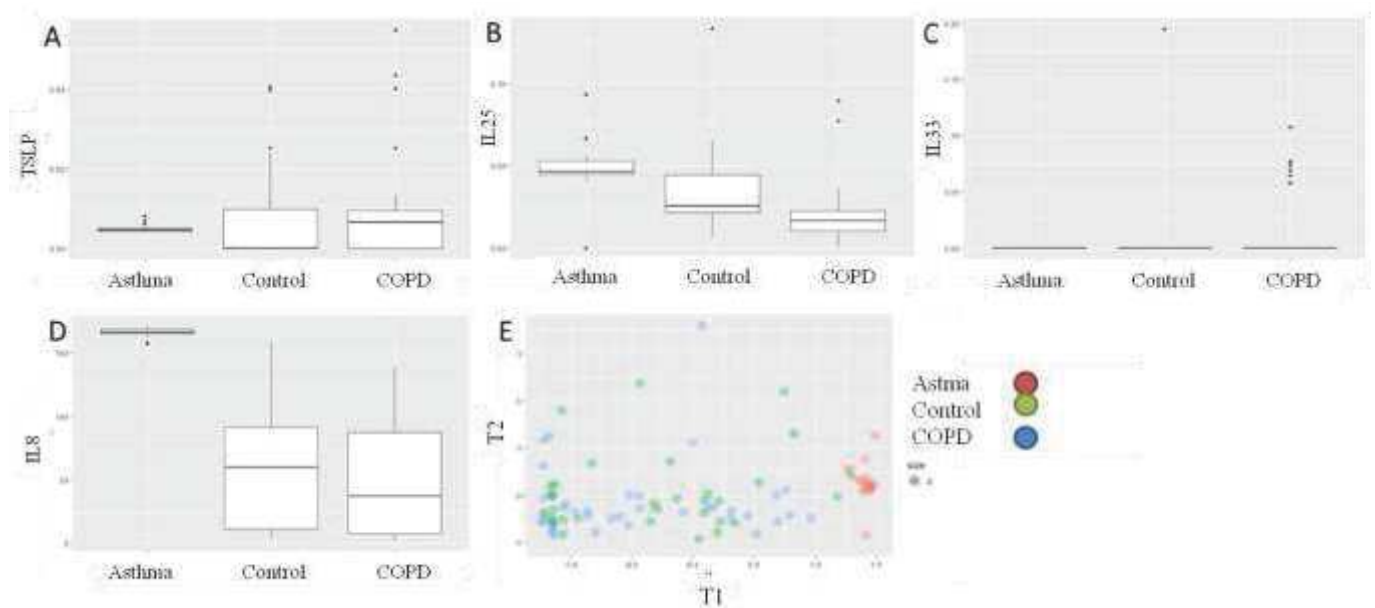


Figure 1: Cytokine profile of COPD (n=39), asthmatics (n=21) and controls (n=31) subjects. At D28 of ALI culture, TSLP (A), IL25 (B), IL33 (C) and IL8 (D) level of the different groups (asthma, COPD and controls groups) were dosed by sandwich Elisa in basolateral medium culture. E-T1/T2 signatures (asthma, COPD and controls groups) were represented: T1 is IL8 centered reduced while T2 is centered reduced average of IL25, IL33 and TSLP.

At “basal state” of ALI culture, TSLP quantity was similar for all groups (Figure 1A). IL25 quantity was not the same in function of disease (Figure 1B). We found the most quantity in asthma group (0.05) whereas the lowest level was in COPD group (0.0125). Control group was in the middle of the two diseases (0.025) (Figure 1B). IL33 level was zero for all groups. Only a few patients could be dosed in COPD group (Figure 1C). The largest amount of IL8 was in asthma group (170) whereas control (60) and COPD (35) groups were quite similar (Figure 1D). Differences between groups were IL8 and IL25 secretions.

Cytokine profiles of patients were realized to classify patients by their T1 and T2 profiles. At “basal state” of ALI culture, we found T1 and T2 profiles in the different groups (asthma, controls and COPD groups). Control and COPD groups were dispersed between T1 and T2 profiles whereas asthmatics group was T1 profile (Figure 1E). ALI model allows to give cytokine profile of patients groups.

3.2. T1/T2 profiles in chronic airways diseases

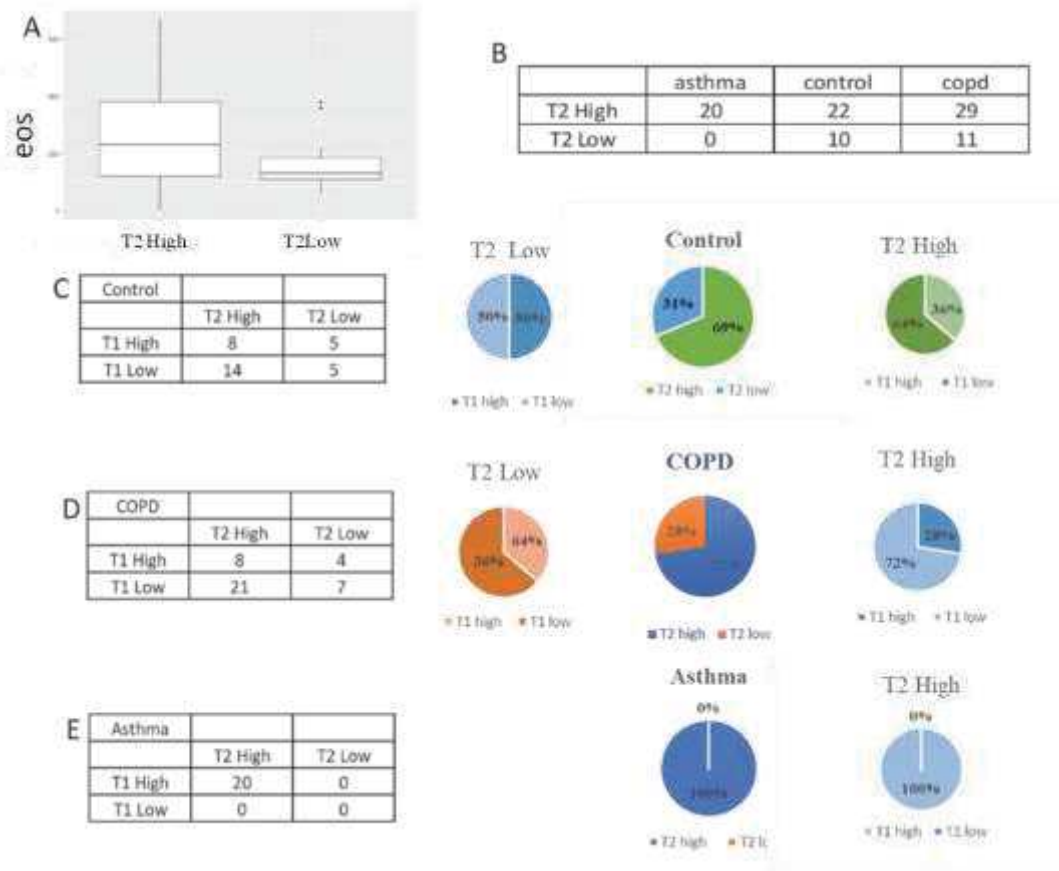


Figure 2: T2/T1 profiles to different groups (asthma (n=21), controls (n=31) and COPD (n=39) groups). A- Graphic to visualize T2 profile according to blood eosinophils level (groups taken together, n=91). T2 profile is centered reduced average of IL25, IL33 and TSLP. T2 high is when T2 cytokine level is superior of T2 profile average whereas T2 low is when T2 cytokine level is inferior of T2 profile average. B- Patients were ranked according to their T2 High and Low profile in the different disease groups. In controls group (C), COPD groups (D) and Asthma group (E), T1 and T2 profile classification were made. T1 profile is IL8 centred reduced. T1 high is when T1 cytokine level is superior of T1 profile average whereas T1 low is when T1 cytokine amount is inferior of T1 profile average. T2 profile is centered reduced average of IL25, IL33 and TSLP. T2 high is when T2 cytokine level is superior of T2 profile average whereas T2 low is when T2 cytokine amount is inferior of T2 profile average

T2 high profile correlates with higher blood eosinophil count (count >200) than T2 low profile (count <200) (Figure 2A). Then, different groups were separated to visualize T2 High and Low profiles in disease groups; we noticed that in asthma group, all patients were T2 High (Figure 2B). In control and COPD groups, there was more T2 High than T2 Low (Figure 2B). In addition, in T2 High of control group, we had more T1 Low than T1 High whereas in T2 Low profiles; there was as much T1 High as Low (Figure 1C). In T2 High and Low profiles of COPD group, there was more T1 Low than T1 High (Figure 2D). In asthma group, there is only T2 High which is only T1 High (Figure 2E). T1 and T2 profiles are different depending on groups.

4. Discussion

We have demonstrated by this study that cytokine profiles (T1, T2) were found at “basal state” in basolateral medium culture of human bronchial epithelial cells whereas epithelial cells haven’t seen “human environment” since 2 months. ALI culture is a model to study secretions.

IL8 was more present in medium of asthmatics patients than COPD patients and controls. This data is “strange” because COPD is linked with neutrophils and IL8 whereas asthmatics patients have rather T2 profile. But T2 profile in COPD patients with eosinophil is admitted. We didn’t find a high TSLP level, known to characterise asthmatic group¹⁹. The low detection is maybe due to TSLP degradation. COPD patients secreted TSLP. This data is not currently known. TSLP seems to have a potential role in COPD because bronchial epithelial cells can secrete it. In addition, different disease groups had very different IL25 secretion. Asthmatics had much more IL25 than other groups. COPD group had the lower IL25 amount. This cytokine is known to have a role in homeostasis. IL25 decrease in COPD may be at the origin of chronic inflammation. In addition, this cytokine is known to regulate other cytokines such as TSLP and IL33²⁰. IL25 reduction can’t block TSLP and IL33 secretions in COPD whereas in asthmatics group, IL25 level regulates alarmin secretions. Moreover, IL25 plays a pleiotropic role. In asthma, it seems to be associated with high neutrophils and lower eosinophils¹⁷. This suggests that IL25 inhibits T2 profile and “activates” T1 profile. This hypothesis may explain the high IL8 levels found in asthmatics group. IL33 secretion was zero except for some COPD patients. However, IL33 seems to have a significant impact in COPD disease. Detection threshold of Elisa kit should not fall low enough for this molecule secreted in very small quantities. Moreover, in mouse model, it had been shown that an anti-IL33 antibody could reverse effects caused by cigarette in COPD. This cytokine seems to play an essential role but its detection is difficult. It would be interesting to visualize IL33 polymorphism to explain IL33 secretion in some patients

The limit of our cytokines data is the lack of stimulation to reproduce smoking stimulation and exacerbation with normally increased cytokine levels. This would validate secreted cytokine profile to see if it changes or not. Immune system co-culture will also be a possibility to visualize cytokines action. But T2 High profile was correlated with blood eosinophil levels (groups taken together). This correlates with clinical data used in literature and clinical trials.

Clinical trials were targeted IL5, IL4 and IL13, failed in COPD and asthma. Other clinical trials are currently ongoing to aim at the top of the cascade (TSLP, IL33) in asthma and COPD patients. These cytokines secretions are detected in our culture medium of bronchial epithelial

cells of patients. But patient profiles (T1/T2 High and Low) are quite dispersed in the same disease. We don't know what happens between alarmin and end of the cascade even if T2 high alarmins profile is correlated to blood eosinophils level. We have to act at the top of the cascade even to inhibit it, as anti-Tslp in asthma or whatever the eosinophilia before treatment, this molecule works. This confirms that even if we consider TSLP as a T2 cytokine whether the patients have eosinophils or not, treatment works. This helps to understand the need to look for other clinical data found to correlate with these alarmins. But inhibiting these alarmins seems a good idea even if activation cascades are still unknown. Better understanding of the endotype disease seems to be a possibility to understand the cytokine secretion and to find the better treatment of patients.

In conclusion, alarmins seem to play a role in chronic airways diseases. Targeting IL33 or TSLP seem to be a lead in this disease but perhaps targeting a regulatory cytokine such as IL25 may be other lead. Inhibiting alarmins must be done correctly because these cytokines play other roles in the body.

REFERENCES

1. Sharma, G., Hanania, N. A. & Shim, Y. M. The Aging Immune System and Its Relationship to the Development of Chronic Obstructive Pulmonary Disease. *Proc Am Thorac Soc* **6**, 573–580 (2009).
2. Patel, N. N. *et al.* Sentinels at the wall: epithelial-derived cytokines serve as triggers of upper airway type 2 inflammation. *International Forum of Allergy & Rhinology* **9**, 93–99 (2019).
3. Nejman-Gryz, P., Górska, K., Paplińska-Goryca, M., Proboszcz, M. & Krenke, R. Epithelial derived cytokines IL-25, IL-33 and TSLP in obstructive lung diseases. *European Respiratory Journal* **50**, PA571 (2017).
4. Qiu, C. *et al.* Anti-interleukin-33 inhibits cigarette smoke-induced lung inflammation in mice. *Immunology* **138**, 76–82 (2013).
5. TSLP: A Key Regulator of Asthma Pathogenesis.
<https://www.ncbi.nlm.nih.gov/pmc/articles/PMC3859144/>.
6. Barnes, P. J. The cytokine network in asthma and chronic obstructive pulmonary disease. *J. Clin. Invest.* **118**, 3546–3556 (2008).
7. Barnes, P. J. Targeting cytokines to treat asthma and chronic obstructive pulmonary disease. *Nat. Rev. Immunol.* **18**, 454–466 (2018).
8. Candela, M., Costorella, R., Stassaldi, A., Maestrini, V. & Curradi, G. Treatment of COPD: the simplicity is a resolved complexity. *Multidisciplinary Respiratory Medicine* **14**, 18 (2019).
9. Narendra, D. K. & Hanania, N. A. Targeting IL-5 in COPD. *Int J Chron Obstruct Pulmon Dis* **14**, 1045–1051 (2019).
10. Brightling, C. E., Saha, S. & Hollins, F. Interleukin-13: prospects for new treatments. *Clin Exp Allergy* **40**, 42–49 (2010).
11. George, L. & Brightling, C. E. Eosinophilic airway inflammation: role in asthma and chronic obstructive pulmonary disease. *Therapeutic Advances in Chronic Disease* **7**, 34–51 (2016).
12. Nocker, R. E. *et al.* Interleukin-8 in airway inflammation in patients with asthma and chronic obstructive pulmonary disease. *Int. Arch. Allergy Immunol.* **109**, 183–191 (1996).
13. Yousuf, A. & Brightling, C. E. Biologic Drugs: A New Target Therapy in COPD? *COPD: Journal of Chronic Obstructive Pulmonary Disease* **0**, 1–9 (2018).

14. Kakkar, R. & Lee, R. T. The IL-33/ST2 pathway: therapeutic target and novel biomarker. *Nat Rev Drug Discov* **7**, 827–840 (2008).
15. Ziegler, S. F. *et al.* The biology of thymic stromal lymphopoietin (TSLP). *Adv Pharmacol* **66**, 129–155 (2013).
16. Gauvreau, G. M., White, L. & Davis, B. E. Anti-alarmin approaches entering clinical trials. *Curr Opin Pulm Med* (2019) doi:10.1097/MCP.0000000000000615.
17. Paplińska-Goryca, M. *et al.* Sputum interleukin-25 correlates with asthma severity: a preliminary study. *Postepy Dermatol Alergol* **35**, 462–469 (2018).
18. Gras, D. *et al.* Epithelial ciliated beating cells essential for ex vivo ALI culture growth. *BMC Pulm Med* **17**, 80 (2017).
19. Berraïes, A., Hamdi, B., Ammar, J., Hamzaoui, K. & Hamzaoui, A. Increased expression of thymic stromal lymphopoietin in induced sputum from asthmatic children. *Immunol. Lett.* **178**, 85–91 (2016).
20. Xu, G. *et al.* Opposing roles of IL-17A and IL-25 in the regulation of TSLP production in human nasal epithelial cells. *Allergy* **65**, 581–589 (2010).

Discussion

Dans cette étude, nous avons montré que les alarmines sont sécrétées à l'état basal dans les sousnageants de cultures de patients atteints de maladies chroniques des voies aériennes.

L'IL33 n'est dosée que chez certains patients BPCO. Pour les patients ayant la capacité de sécréter cette molécule, il serait intéressant d'analyser le polymorphisme^{145,146} de cette cytokine pour vérifier s'il existe une relation entre la sécrétion d'IL33 et la présence de son polymorphisme.

Le TSLP est une molécule dont le rôle dans l'asthme a été démontré. Dans notre étude, la quantité de TSLP sécrétée dans le sousnageant des cellules épithéliales est relativement faible chez les asthmatiques. Par contre, on remarque que le TSLP est une molécule retrouvée dans les sousnageants de cultures des patients BPCO ce qui est une donnée nouvelle.

L'IL25 est une cytokine jouant un rôle clé dans l'homéostasie. Elle se retrouve différemment sécrétée en fonction des maladies. Notamment chez les patients asthmatiques où la quantité d'IL25 est plus importante que chez les patients BPCO. Cette cytokine est connue pour réguler la sécrétion d'autres cytokines notamment les alarmines IL33 et TSLP. La quantité plus faible d'IL25 sécrétée dans la BPCO peut suggérer qu'elle ne permet pas de réguler correctement la sécrétion de l'IL33 et du TSLP.

Pour améliorer l'impact des résultats de cette étude et mieux caractériser les patients sur leur profil de sécrétion des cytokines, nous aurions aimé réaliser des stimulations de l'épithélium via des agresseurs tels que du tabac ou des stimulations virales et/ou bactériennes permettant de reproduire des phénomènes d'exacerbation. Cette étude permettrait de confirmer le profil cytokinique des patients en situation de stimulation et vérifier si celui-ci change par rapport à l'état de base. Une fois ce profil étudié, il aurait été intéressant d'analyser les polymorphismes connus des gènes codant pour ces protéines afin d'ouvrir une éventuelle piste pharmacogénétique.

Conclusion

En conclusion, le profil des cytokines T2 est analysable par la sécrétion des alarmines dans le sousnageant des cultures de cellules épithéliales bronchiques humaines en modèle ALI à l'état basal. De plus, nous avons démontré que le profil cytokinique est corrélé aux taux d'éosinophiles sanguins chez ces mêmes patients. La principale faiblesse de cette étude réside dans la non

stimulation des cellules au pôle apical ce qui auraient permis de mimer une exposition tabagique, bactériennes ou virales, retrouvées dans les maladies chroniques des voies aériennes.

D-CONCLUSIONS/PERSPECTIVES

Ce travail a eu pour but de répondre à trois objectifs :

- le premier était de réaliser la carte d'identité des cellules Club par l'utilisation de deux méthodes différentes (Single cell-RNA seq et puces à ADN) à partir de cultures ALI de cellules épithéliales bronchiques humaines ou à partir d'un brossage de cellules épithéliales humaines,
- le second était de superviser la différenciation pour adapter le phénotype des cellules épithéliales bronchiques humaines de cultures ALI pour tenter de réverser le ratio cellules ciliées/cellules à mucus qui se trouve modifié chez les patients BPCO,
- le dernier était d'étudier le rôle potentiel des alarmines de type T1/T2 dans les maladies chroniques des voies aériennes (BPCO, asthme).

Tout d'abord, dans la BPCO, plusieurs études ont montré que les cellules Club sont déficitaires chez les patients BPCO. Ce déficit en cellules Club serait notamment à l'origine de concentrations moindres en sa protéine spécifique, le CCSP, dans les voies aériennes des patients BPCO. De ce fait, dans la première partie de mon travail de thèse, nous avons réalisé la carte d'identité des cellules Club provenant de cultures ALI de cellules épithéliales bronchiques humaines ou d'un brossage de cellules épithéliales humaines par une méthode de Single cell-RNA seq afin de mieux comprendre leurs rôles et trouver un potentiel marqueur de surface spécifique à ces cellules. Les résultats obtenus par cette méthode montrent que la totalité des cellules épithéliales bronchiques humaines *in vivo* et *in vitro* expriment l'ARNm CCSP. De ce fait, il est difficile de définir la population de cellules Club et donc d'obtenir leur carte d'identité. Pour pallier à ce problème, nous avons mis au point un protocole de tri cellulaire des cellules Club, par leur protéine intracellulaire spécifique, le CCSP, à partir de cultures ALI de cellules épithéliales bronchiques humaines. Ceci permet d'isoler les cellules Club sur leur protéine et non plus sur leur ARNm. Par contre, ce protocole a nécessité de nombreuses mises au point (fixation par la formaline, perméabilisation triton/saponine, marquages, extraction ARN). Ce protocole a été validé par deux méthodes complémentaires : par la PCR pour vérifier l'expression génique du CCSP dans les différentes populations triées, par la microscopie confocale pour vérifier la fluorescence du marquage CCSP après le tri cellulaire. De plus, ce protocole a pu être validé pour son utilisation sur d'autres types cellulaires comme les cellules à mucus et les cellules ciliées. A partir de ce protocole de tri cellulaire validé, il a été réalisé la carte d'identité des cellules Club par une méthode de puces à ADN pour définir les fonctions de ces cellules Club et trouver un potentiel marqueur de surface. Les résultats obtenus par cytométrie en flux ont montré

qu'il y avait trois populations distinctes obtenues, en fonction de leur intensité de fluorescence et de leur granulosité qui sont différentes, cependant toutes expriment la protéine CCSP. Ceci corrèle avec les données de la littérature qui montrent une vraie plasticité des cellules Club. Par contre, avec les données des puces à ADN, on observe que les trois populations CCSP positives possèdent des rôles/fonctions qui sont différents : une population avec l'expression d'ARNm de « type multiciliée » (ciliogénèse), une population avec l'expression d'ARNm de « type Club classique » (métabolisme des xénobiotiques, prolifération, anti-inflammatoire) et une population avec l'expression des ARNm de « type transition », c'est-à-dire possédant des ARNm équivalents aux autres populations. Mais, trouver un marqueur de surface spécifique de ces cellules « type Club classique » semble compliqué comme si ces cellules Club n'avaient qu'une fonction sécrétoire. Pour contourner ce problème, la solution serait plutôt d'ôter les autres types cellulaires pour obtenir les cellules Club par un tri négatif.

Ces résultats permettent de mettre un peu plus en exergue la plasticité et le rôle progéniteur des cellules Club. Mais, ceci a permis aussi de montrer qu'en fonction du profil de maladie, les différentes populations CCSP positives ne sont pas présentes dans les mêmes proportions chez les patients BPCO, fumeurs et témoins. La population type « Club classique » est une population cellulaire diminuée chez les patients BPCO. Ceci corrèle avec les données de la littérature. A partir de ces données, il serait intéressant de récupérer cette population par tri pour les remettre en culture pour comprendre leurs rôles dans l'épithélium bronchique humain. La population « type multiciliée » est déficitaire elle aussi chez les patients BPCO ce qui permettrait d'expliquer le déficit en cellules ciliée retrouvé dans la BPCO. Mieux étudier cette population et comprendre son potentiel rôle dans cette maladie est essentiel.

Par contre, il est nécessaire de valider les populations obtenues en tri cellulaire sur des biopsies bronchiques de patients pour valider les résultats obtenus sur les cultures ALI. Une autre perspective intéressante serait de connaître le panel de protéines sécrétées par ces cellules notamment les cellules « type Club classique » pour envisager de les compléter dans les cultures ALI de patient BPCO afin d'étudier leur potentiel thérapeutique à réverser ou diminuer les problèmes physiopathologiques retrouvés dans cette maladie.

Un autre problème chez les patients BPCO est le ratio cellules ciliées/cellules à mucus qui se retrouve inversé comparé aux sujets sains. Le travail réalisé lors de la deuxième partie de ma thèse m'a permis de superviser la différenciation du phénotype épithélial pour tenter de réverser ce changement de ratio retrouvé chez les patients BPCO. Pour cela, des cultures ALI de cellules épithéliales bronchiques humaines (HBEC) ou des cultures de cellules commercialisées (NHBE)

ont été incubées avec différentes drogues connues pour impacter les différentes voies de signalisation (Rho, Notch, BMP) importantes dans le développement embryonnaire. Avec ces données, nous avons montré que le DapT permet de pousser la différenciation vers le phénotype cilié et basal au détriment des cellules Club et des cellules à mucus. Le DapT permet aussi de réverser l'hyperplasie des cellules à mucus induite par le tabac. Néanmoins, après le traitement par le DapT, nous n'avons pas obtenu un épithélium différencié avec tous les types cellulaires. Une adaptation de la dose pourrait permettre d'obtenir un épithélium différencié physiologique. De plus, la réparation n'est pas totale lorsque les cultures sont en contact avec le DapT comme si le DapT ralentissait la réparation normale de l'épithélium, ce qui est un inconvénient dans une maladie comme la BPCO où les dommages cellulaires sont importants. Par contre, le Y lui favorise les cellules Club et les cellules à mucus qui sont elles-mêmes poussées par la présence de LDN ce qui est un avantage pour restaurer la quantité de cellules Club dans l'épithélium des patients BPCO. Toutes ces molécules permettent de superviser la différenciation de l'épithélium vers un type cellulaire ou un autre. Le DapT semble la meilleure piste thérapeutique dans la BPCO notamment en réversant l'hyperplasie des cellules à mucus. Par contre adapter la dose et passer sur le modèle animal permettrait d'affiner le traitement par le DapT.

Pour finir, la dernière partie de mon travail a permis d'étudier les sécrétions des alarmines T1/T2 dans les maladies chroniques des voies aériennes. Pour cela, des cultures ALI de cellules épithéliales bronchiques humaines ont été mises en place et le dosage des alarmines (T1/T2) a été réalisé à J28 dans les sousnageants de cultures. A l'état basal, les cellules épithéliales sont capables de sécréter les alarmines T1/T2 mais leurs taux varient en fonction des pathologies. L'IL33 est une cytokine retrouvée dans les modèles murins de BPCO comme jouant un rôle critique dans le développement des traits physiopathologiques de la BPCO et qu'un anticorps anti-IL33 permettait de les réverser. Nos données montrent que certains patients sécrètent cette cytokine et il serait intéressant de savoir si leur sécrétion est liée à la présence d'un polymorphisme génétique connu. Le TSLP, lui, est connu pour jouer un rôle dans l'asthme mais dans nos données, on retrouve aussi cette sécrétion chez les patients BPCO ce qui est une donnée nouvelle qui serait à approfondir d'autant plus que l'anticorps anti-TSLP fonctionne dans l'asthme, quelque soit l'éosinophilie, en réduisant notamment le nombre d'exacerbations. Pour l'IL25, elle est connue pour jouer un rôle clé dans l'homéostasie notamment en régulant certaines autres cytokines dont l'IL33. Mais comme décrit dans la littérature, cette cytokine est retrouvée dérégulée dans certaines maladies chroniques des voies aériennes. Ceci est validé par les données obtenues dans notre étude notamment dans la BPCO où la quantité d'IL25 est

diminuée par rapport aux témoins. Restaurer le taux d'IL25 dans la BPCO permettrait peut-être de ramener à un état de base les sécrétions des autres cytokines et peut être diminuer les effets néfastes dans le poumon.

Les essais cliniques en cours sur les alarmines IL33 et TSLP permettront d'éclaircir le rôle potentiel de ces cytokines dans les pathologies chroniques des voies aériennes. Par contre, une faiblesse de cette étude est de ne pas avoir réalisé de stimulation de l'épithélium bronchique par le tabac ou des expositions bactériennes et/ou virales qui permettraient de modéliser les phénomènes d'exacerbations. Ceci doit être envisagé pour permettre de voir si les profils cytokiniques obtenus sont bien corrélés à leur profil de base ou s'ils changent en fonction de la stimulation. Ceci permettrait aussi de mieux regrouper les patients avec des potentiels biomarqueurs.

Toutes ces données permettent de montrer les potentiels thérapeutiques, des cellules Club, des anti-alarmines ou des drogues permettant de superviser la différenciation épithéliale, en agissant notamment sur les différents traits physiopathologiques caractéristiques des patients BPCO.

ANNEXES



Mucus Microrheology Measured on Human Bronchial Epithelium Culture

Myriam Jory¹, Karim Bellouma¹, Christophe Blanc¹, Laura Casanellas¹, Aurélie Petit², Paul Reynaud², Charlotte Vernisse², Isabelle Vachier², Arnaud Bourdin² and Gladys Massiera^{1*}

¹ L2C, Univ Montpellier, CNRS, Montpellier, France, ² PhyMedExp, INSERM U1046, CNRS UMR 9214, Department of Pneumology and Addictology, Montpellier University Hospital Arnaud de Villeneuve, Montpellier, France

We describe an original method to measure mucus microrheology on human bronchial epithelium culture using optical tweezers. We probed rheology on the whole thickness of mucus above the epithelium and showed that mucus gradually varies in rheological response, from an elastic behavior close to the epithelium to a viscous one far away. Microrheology was also performed on mucus collected on the culture, on *ex vivo* mucus collected by bronchoscopy, and on another epithelium model. Differences are discussed and are related to mucus heterogeneity, adhesiveness, and collection method.

Keywords: human bronchial epithelium (HBE), microrheology, mucus, viscoelasticity, optical tweezers (OT), mucins, rheology, biopolymer gels

OPEN ACCESS

Edited by:

Umberto D'Ortona,
UMR7340 Laboratoire de Mécanique,
Modélisation et Procédés Propres
(M2P2), France

Reviewed by:

Felix Campelo,
Instituto de Ciencias Fotónicas, Spain
Juan Guillermo Díaz Ochoa,
PERMEDIQ GmbH, Germany

*Correspondence:

Gladys Massiera
gladys.massiera@umontpellier.fr

Specialty section:

This article was submitted to
Biophysics,
a section of the journal
Frontiers in Physics

Received: 30 October 2018

Accepted: 30 January 2019

Published: 19 February 2019

Citation:

Jory M, Bellouma K, Blanc C,
Casanellas L, Petit A, Reynaud P,
Vernisse C, Vachier I, Bourdin A and
Massiera G (2019) Mucus
Microrheology Measured on Human
Bronchial Epithelium Culture.
Front. Phys. 7:19.
doi: 10.3389/fphy.2019.00019

INTRODUCTION

The mucociliary function of bronchial epithelia ensures the continuous clearance of the airways. Mucus is a visco-elastic gel trapping dust and pathogens present in the inhaled air and thus acts as a protective barrier on top of the airway tissue. Its transport is a key element to ensure an efficient clearance of the respiratory system. It relies on two main elements: cilia beating coordination and mucus rheology.

Mucus are gels made of glycoproteins fibers that form a complex and heterogeneous viscoelastic network [1]. In the past, rheological characterization of airway mucus has been restricted to sputum or mucus from dead mammals because rheology methods require large volumes of sample (mL) and because of the difficulty of collecting human bronchial mucus. Models of human bronchial epithelium (HBE) culture have been developed these last decades [2–5]. While these models have been validated by biological factors demonstrating, for various pathologies, that the phenotype is conserved, a few studies [6–8] describe the physical characteristics of these models and in particular the mucus flowing properties. Even for these cultures, the amount of mucus that can be collected varies with the pathology and is in all cases very small. Typically, when secretion level is high, up to 1 mL can be collected during the 28 days of culture, but some cultures have such a small production that no mucus can be collected at all. Rheology can be performed at a microscale with several advantages: small volumes are required (min 10 μ L), it is a measure of the local response and therefore allows to investigate the heterogeneity of the sample, and finally it corresponds to probing how mucus flows at a relevant scale, the scale of a cilium. Common passive microrheology methods are based on the fluctuation-dissipation theorem and consist in using the thermal fluctuations of beads dispersed in the mucus to infer the elastic complex modulus, whereas active methods use optical or magnetic tweezers to apply local forces and measure the consequent deformation. Microrheological studies have been reported on horse airway mucus [9, 10], marine worm mucus [11], porcine respiratory mucus [1], and even human respiratory mucus [6, 12], using either active or passive methods. This literature reports two main findings. Probe size and probe/mucus interaction have to

be considered to correctly select the probe and perform reliable microrheological measurements [1]. More importantly, the mucus is described as a highly heterogeneous multi-scale network [10, 11] and conceptual models of mucus elastic structure are proposed: a coupled two-fluid model, or an interlinked scaffolds model. The high heterogeneity of the mucus renders their measurement and interpretation difficult. In particular, the collection of mucus itself could introduce a bias as it is limited to the upper fraction of the mucus layer, potentially the less elastic part as it is the easier part to collect. Moreover, mucus is sensitive to shear stress, pH, and extremely sensitive to water loss. The consequence could be that measurements performed on collected mucus give a less elastic response than mucus present on the epithelium.

In this paper, we use an original method that allows to measure microrheology and probe its variation with the distance from the epithelium, directly on HBE culture, thus avoiding any mucus collection. We will compare microrheology measurements performed on mucus collected from human bronchial cultures, collected during bronchoscopy, and measured on another epithelium model. We will discuss differences and relate them to mucus heterogeneity, adhesiveness and collection method. Finally, we will discuss the potential of this method for future studies and its potential use as a biomarker.

METHODS

Human Bronchial Epithelial (HBE) Cultures

Bronchial biopsies from control, smoker, and COPD subjects were collected during fiberoptic bronchoscopy on a subsegmental bronchus of the *left lower lobe* at *Arnaud de Villeneuve* hospital (Montpellier, France). All donors signed a consent form after being informed about the biomedical research on airway epithelium performed thanks to their donation. The protocol was approved by the institutional ethics commission of *Sud Méditerranée III* (CHRU Montpellier-AOI 9244–NCT02354677). Primary human bronchial epithelial cells were obtained from bronchial biopsy specimens and cultured under Air Liquid Interface (ALI) conditions [13] either with culture media provided by Lonza before January 2018, with a protocol adapted from Gras et al. [5] and Gamez et al. [14]; or with culture media provided by Stemcell Technologies after January 2018, with the manufacturer protocol. Briefly, bronchial epithelial biopsies were mechanically dissociated and suspended in bronchial epithelial growth medium (BEGM, Lonza or PneumaCult-Ex Plus, Stemcell Technologies). After an expansion phase in monolayers, cells were plated on uncoated nucleopore membranes (24-mm dia., 0.4 μm pore size, Transwell Clear, Costar) in a 1:1 mixture of BEGM and Dulbecco's modified Eagle's medium (DMEM, Lonza) or with Pneumacult-Ex Plus until confluence. After confluence, the ALI phase can begin by applying media [a 1:1 mixture of BEGM and Dulbecco's modified Eagle's medium (DMEM, Lonza) or with the PneumaCult ALI maintenance (Stemcell Technologies)] only at the basal side. Cells were cultured for 28 days to obtain a polarized and differentiated cell population with a mucociliary phenotype.

Mucus Collected From HBE Culture

For cultures with BEGM media, mucus, when efficiently produced by the culture, was gently collected with a micropipette every 2 days and stored at 4°C, for a maximum of 6 months. Typically, for one culture well, we obtained around 50 μL of secreted mucus after 2 days. For the cultures with Stemcell Technologies media, mucus is strongly stuck to the epithelium. To collect it, 60 μL of culture medium [PneumaCult ALI maintenance (Stemcell Technologies)] is spread on top of the culture well for 24 h. Then the medium is gently withdrawn. We apply then repeatedly a soft flow of media using a micropipette until some mucus detaches. Mucus is then collected from the medium with a micropipette and analyzed the same day. Typically, for one culture well, after 1 week, we obtained around 20 μL of mucus.

“Ex vivo” Mucus Samples From Clinical Examination

Mucus is collected during a bronchoscopy on healthy patients by blind soft aspiration through a catheter inserted up to 6–9th airway division always done by the same practitioner. The typical amount sampled is small, around 20 μL , and stored inside a 1.5 mL tube with water saturated air for transport. Samples containing blood are discarded. The chamber for microrheology analysis is prepared <2 h after mucus collection. Microrheology is performed straightaway.

Optical Tweezers Micro-Rheology

Optical Tweezers

Our set-up is built on an inverted optical microscope LEICA DMI 3000 B supported by an air-damped anti-vibration table (Workstation Series, Melles Griot). The optical trap is generated by the focalization of a laser beam (1064 nm laser YLM 5W, from IPG Photonics) through an x100 (NA 1.4) oil immersion objective. The oscillating trap position is controlled thanks to a pair of acousto-optic deflectors (AA optoelectronic). Alternatively, for lower frequencies and higher laser intensity, the sample is moved thanks to a piezoelectric XY stage (Nano-Bio100 from MCL with a subnanometer accuracy). The trapped microsphere is imaged with a CCD camera Basler Scout-F. A multifunction Field Programmable Gate Array (FPGA) is used to control the different devices and acquire data through a LabVIEW homemade program. The bead position is obtained by image correlation analysis under LabVIEW at a sub-pixel resolution (≈ 4 nm). In our experiments, we typically impose $A_s = 1 \mu\text{m}$ or $A_s = 0.5 \mu\text{m}$ depending on the elasticity of our sample. We measure both A_b and φ for a range of frequency, f in between 0.09 and 50 Hz. All of our experiments are conducted at room temperature. Nevertheless, due to local heating of the laser, we measured that the temperature of the sample close to the trap could reach 30°C.

Principle

Microrheology was investigated using oscillating optical tweezers. Once an isolated bead is trapped with a laser, typical experiments consist in applying a small sinusoidal displacement either to the trap or to the sample. The motion of the bead

then gives information about the viscoelastic properties of the matrix at the driving frequency ω [15–17]. We consider now a displacement of the stage $x_s^* = A_s e^{j\omega t}$ (with A_s the amplitude of the stage displacement) and a fixed trap. In the linear regime, a bead of radius a follows the sinusoidal displacement with a phase shift φ , and its trajectory is given by $x_b^* = A_b e^{j\omega t} e^{-j\varphi}$ (with A_b the amplitude of the bead displacement). Following the analysis by Shundo et al. [17] and other authors, the complex shear modulus $G^* = G' + jG''$ is related to the ratio of the fluid forces acting on the bead to its displacement with respect to the fluid (taking into account a $6\pi a$ factor for a spherical bead). The fluid forces being opposed by the restoring harmonic force of the trap of stiffness k_{OT} , one gets:

$$G^* = \frac{k_{OT} x_b^*}{6\pi a (x_b^* - x_s^*)} = \frac{k_{OT} A_b e^{-j\varphi}}{6\pi a (A_b e^{-j\varphi} - A_s)}$$

and gives:

$$G' = \frac{k_{OT}}{6\pi a} \frac{A_b^2 - A_s A_b \cos \varphi}{A_b^2 + A_s^2 - 2 A_b A_s \cos \varphi}$$

$$G'' = \frac{k_{OT}}{6\pi a} \frac{A_s A_b \sin \varphi}{A_b^2 + A_s^2 - 2 A_b A_s \cos \varphi}$$

where G' and G'' are, respectively, the elastic and loss modulus.

To determine the absolute values of elastic moduli, the stiffness k_{OT} of the trap is required. We obtained k_{OT} using two different methods depending on samples. For weakly elastic mucus, the Gaussian distribution of the trapped bead position [18] is analyzed. For the most elastic samples, a strong laser intensity is required in order to trap the bead. As a consequence, the Brownian motion cannot be detected. We thus have calibrated the stiffness of the trap as a function of the power intensity in water using the drag force method [18]. In this case, we have hypothesized that the optical force is identical in mucus and in water. This hypothesis is supported by the fact that the optical index of the medium ($n \approx 1.335$) is very close to the water one, as measured using a refractometer. The laser optical path differs depending on the thickness and on the transparency of the sample, which can be affected by the presence of impurities (see **Figure S1**). We thus checked its effect on the laser trap stiffness and on its isotropy. As discussed in the Supplemental Information section, we show that the homogeneity of the laser trap is conserved through $100 \mu\text{m}$ of sample depth (**Figure S3**) but we observe a decrease of the laser stiffness around 35% (**Figure S2**), and that impurities play a minor role. We also discuss in Supplemental laser heating and temperature issues. The laser trap indeed causes a local heating of the sample ($<10^\circ\text{C}$). We thus checked that an increase in temperature of up to 7°C has little effect on the mucus viscoelasticity (**Figure S4**).

Chambers Preparation

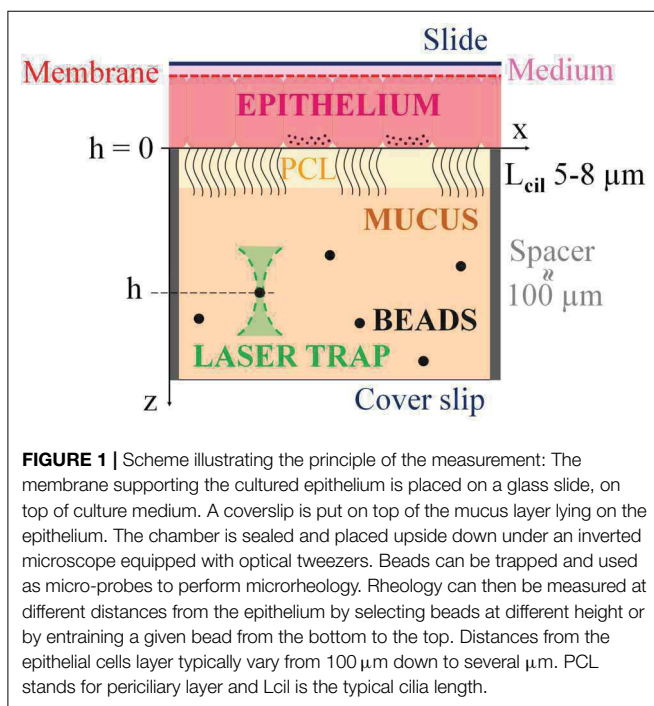
In order to work on isolated microspheres, the concentration of beads was chosen in order to have one bead per $100 \times 100 \mu\text{m}^2$ in a $100 \mu\text{m}$ thick sample.

For the mucus collected from HBE cultures, carboxylated melamine resin beads, diameter $3 \mu\text{m}$ (Fluka Analytical, Sigma-Aldrich), are dispersed in the collected supernatant mucus to a final concentration of 0.004 \%v/v . Melamine resin beads, diameter $5 \mu\text{m}$, and silica beads, diameter 1 and $4.5 \mu\text{m}$, have also been tested and gave comparable results. The sample is then sandwiched in between two pegylated glass plates separated by a mylar spacer. The thickness of the spacer (100 or $175 \mu\text{m}$) and the dimension of the chamber are chosen accordingly to the mucus volume available in order to minimize the residual air volume. To prevent evaporation, the chamber is immediately (in <2 min) sealed with a UV curable adhesive (ThorLabs NOA81). During Ultra-Violet (UV) exposure, the sample is protected by a reflector (aluminum foil). For “*in vivo*” mucus, we proceed exactly the same way.

For measurements performed on HBE cultures, $0.5 \mu\text{L}$ of the 0.4 \%v/v bead solution are firstly mixed with mucus collected from the culture wells ($\sim 50 \mu\text{L}$). The culture membrane is then cut and deposited on a $3 \mu\text{L}$ volume of culture medium on a glass slide as illustrated in **Figure 1**. Mucus containing beads is then gently spread on the epithelium and covered with a cover slip onto which a spacer was previously fixed. Three spacers have been tested: (i) silica debris of $60 \pm 10 \mu\text{m}$ distributed approximately every $500 \mu\text{m}$; (ii) adhesive circular spacers (Grace Bio-Labs, 654004), 13 mm in diameter and $120 \mu\text{m}$ in thickness together with a $4 \times 4 \text{ mm}^2$ central piece; (iii) UV curable adhesive squared pillars of $100 \times 100 \mu\text{m}^2$ and $100 \mu\text{m}$ in height, distributed every 0.5 mm and produced using microlithography. The chamber is immediately UV sealed as previously described, in <5 min after membrane cutting. The sample is left to rest 30 min before performing the experiment.

Experimental Method on HBE Cultures

Experiments are conducted no longer than 3 h, during which average of 15 experiments can be performed. We observed cell death after 1 h under the microscope with a laser on at 0.1 – 1 W. We checked that measurements performed at the same height h , at 1 and 2 h, gave overlapping results. The distance h separating the bead from the epithelium was measured using the microscope fine focus graduations ($2 \mu\text{m}$). For each measurement, a bead is selected and trapped close to the cover slip (far from the epithelium) and used to measure the rheological response at this height. The bead is then gradually dragged to different heights in the direction of the epithelium and the distance h_c to the coverslip is recorded for each rheological measurement. The distance between the coverslip and the tissue, h_t , is measured once the bead reached the cell tissue and is used to compute h , the distance between the bead and the epithelium: $h = h_t - h_c$. The distance h_t is measured for each bead at the end of the experiment since it cannot be removed from the epithelium once it contacted it. For each experiment, the bead is dragged to a given height h , and we then wait a minimum of 3 min before measurement, to allow stress relaxation (see **Figure S5**). A measurement is performed every $10 \mu\text{m}$ approximatively when possible: the number of heights per bead is limited by bead loss during the dragging or during the measurement. To evaluate the



robustness of our results and explore our samples heterogeneity, a height sweep is performed with at least three different beads, taken at different xy locations, and dragged to several heights. On average, 15 measurements are obtained by chamber. In most cases, a few heights are obtained per beads. We then use more beads to increase our statistics. When measuring microrheology close to the epithelium, cilia beating hinder proper rheology measurement. We thus need areas without beating cilia. In the case of BEGM cultures, the density of beating ciliated cells is low (<20%), and we simply worked in areas without beating. In the case of Pneumacult cultures, cilia density is high (60–80%). We locally stopped cilia beating activity by focalizing the laser on ciliated cells at 2.5W for around 5 s, on an area of a few micrometers.

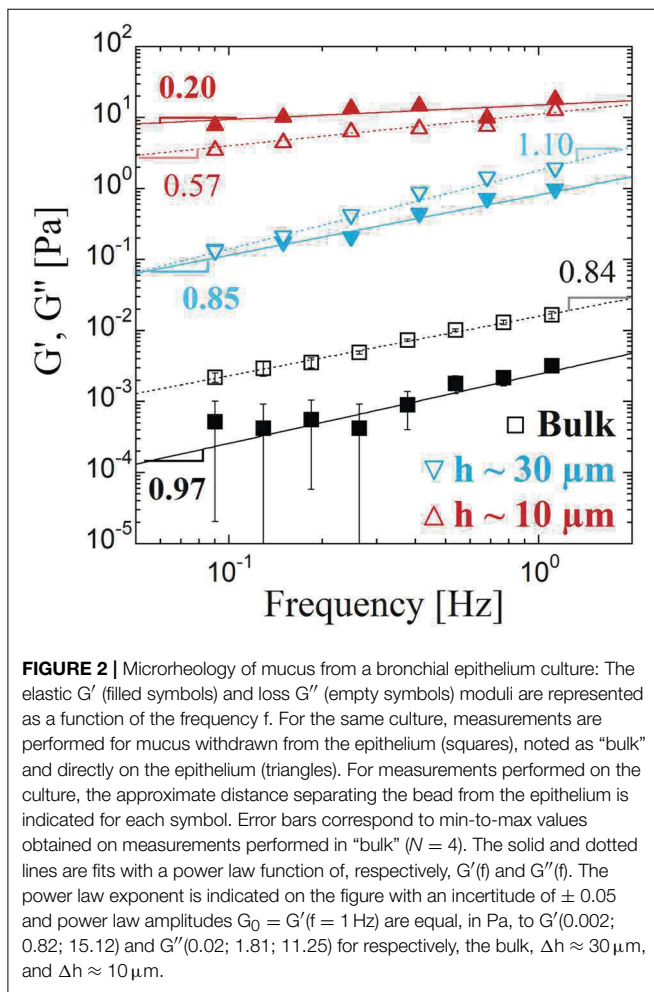
RESULTS

Mucus collection from cultured wells depends on the mucus flowing properties, which could introduce a bias in their characterization. Indeed, withdraw is easier when the mucus is poorly elastic and is in all cases limited to the mucus layer far from the epithelium to avoid damaging of the culture. To measure the microrheology response within the mucus layer lying on top of cultured HBE and probe its variation with the distance to the epithelium, we developed a new protocol and adjusted our setup. **Figure 1** illustrates the principle of the experiment: Beads are dispersed in the mucus layer as described in the methods section. An optical tweezer is used to trap a bead at a given height in the chamber. The selected bead is then used as a rheological probe: a deformation is applied by oscillating the bead and measuring the resulting force. The elastic G' and loss G'' moduli can be computed

as detailed in the method section. Rheology can be measured at different distances from the epithelium by selecting beads at different heights in the mucus layer or by entraining a given bead from the bottom to the top. Distances from the epithelial cells layer typically vary from 100 micrometers down to several micrometers.

Figure 2 compares the rheological response measured directly on the culture and on the mucus collected from the same epithelium (named “bulk” in the following). The elastic moduli $G'(f)$ and $G''(f)$ are represented on a log-log plot over a decade of frequency f , from 0.09 to 1.1 Hz, and are fitted with a power law function. In “bulk,” we find the hallmarks of a viscous fluid: G'' is 10x larger than G' , and both moduli can be fitted by a power law with exponents very close to 1. Their values correspond to a fluid ~ 10 times more viscous than water. Results obtained on the culture drastically differ in amplitude, by 2 to 3 orders of magnitude, and G' is now larger than G'' for $h < 20 \mu\text{m}$ approximatively. The response also evolves with the distance probe-epithelium. The power law exponents are much lower when the probe gets closer to the epithelium layer ($\approx 10 \mu\text{m}$): 0.2 for G' and 0.57 for G'' . Within the mucus layer, when the probe distance h from the epithelium is varied from close (a few microns) to far ($> 50 \mu\text{m}$), we observe that the mucus rheological response evolves gradually from the response of a viscoelastic to a viscous fluid, as illustrated in **Figure 3** for four cultures obtained from three different biopsies: two smokers (Patient 1 and 3) and a control (Patient 2). On **Figure 3**, each type of symbol corresponds to a measurement performed with a different bead, i.e., a different xy location on the epithelium. Due to the bead loss during dragging or measurement, measurements can only be performed for a few heights per bead (**Figure 3A**). Nevertheless, we obtain that different beads at the same height give similar results, as illustrated in **Figure 3D** with the overlap of the curves in red at $h = 14 \mu\text{m}$ (squares and diamonds) or also the curves in pink at $h = 22 \mu\text{m}$ (diamonds and triangles up). BEGM cultures thus seem homogeneous in the xy plan. The power law exponent α measured on $G'(f)$ is plotted as a function of h and increases with the distance to the epithelium, clearly showing that mucus is less elastic far from the epithelial layer (**Figure 3E**). The robustness of our results is shown by measuring microrheology on two different wells obtained from the same biopsy (Patient 3). Data are consistent (**Figures 3C,D**) and result in the same slope for α vs. h (**Figure 3F**).

To evaluate how these data obtained from a model of bronchial epithelium can be compared to the rheological response of mucus “*ex vivo*,” we performed microrheology on mucus extracted from bronchia during clinical examination. Collecting mucus inside bronchia is challenging. Nevertheless, on some occasions, tiny amounts could be obtained, enough to be probed by microrheology. All of our data are reported in **Figure 4**, for seven patients. These samples contain a large quantity of floating cells. Therefore, in our results description, we consider two distinct cases as illustrated in **Figure 4**: Case I (squares), the probe is in the vicinity of an aggregate, at least $3 \mu\text{m}$ away, and Case II (circles), the probe is far ($> 15 \mu\text{m}$) from cells, in a transparent region, as illustrated in **Figure S6**. Elastic moduli vs. frequency curves, corresponding



to 11 different measurements, cover almost 5 decades. The curves corresponding to Case I, with a probe in the vicinity of cell aggregates, have amplitudes varying from 0.4 to 30 Pa and power law exponents in between 0.01 and 0.5, G' being always greater than G'' . These are hallmarks of an elastic complex fluid. Case I curve is close to an elastic plateau at 5 Pa, while curves corresponding to probes far away from cells (Case II) are closer to what we obtain for measurements in “bulk”: a viscous response with G'' greater than G' , small moduli with power law exponents close to 1.

Figure 5 gathers all the results previously presented, highlighting two families of curves: rheology curves reflecting the viscous nature of the mucus measured in “bulk” or “*ex vivo*” for probes isolated from cell aggregate, and a second family of curves highlighting the elastic nature of the mucus for experiments performed on culture wells with a probe close to the epithelium, or when the probe is located near surfaces or cellular structures for mucus collected from HBE culture and “*ex vivo*” mucus samples, respectively.

Again with the objective of evaluating the HBE culture model from the physical perspective, we compare the mucus flow properties of two HBE cultures which differ by the culture

method and in particular the culture medium used to feed the cells as described in the method section. In the following, we will name these two models “BEGM” and “Pneumacult,” using the names of the culture media used for each method. The results that have been described so far all correspond to the “BEGM” culture model. Figure 6 gather the microrheological measurements obtained “in bulk” with $N = 4$ “Pneumacult” and $N = 10$ “BEGM” cultures (Figure 6A), and obtained on the culture with $N = 2$ and $N = 4$ for, respectively, “Pneumacult” and “BEGM” cultures (Figure 6B). The elastic moduli value and dependence on the frequency f are considerably different for the two models, and even more obviously when mucus is probed in “bulk”. “BEGM” mucus, as previously described, has the hallmarks of a viscous fluid “in bulk” and behave as an elastic fluid close to the epithelium. “Pneumacult” mucus is highly elastic with an elastic plateau at 8 Pa “in bulk”. On HBE “Pneumacult” cultures, mucus rheology (Figure 7) is characterized by power law exponents in the range 0.3–0.5 and elastic moduli values spanning two decades [$G'(f = 1 \text{ Hz}) = 0.7\text{--}70\text{Pa}$], without any correlation with the distance h to the epithelium (Figures 7B,C). The power law exponent (the degree of elasticity vs. viscosity) is a constant function of h , around 0.3–0.5 (Figure 7B), except for distances to the epithelium $< 10 \mu\text{m}$, for which α surprisingly reaches values as high as 1. Because of the high beating activity for “Pneumacult” cultures, we consider with caution results obtained for $h < 10 \mu\text{m}$, which probably corresponds to distance to cilia $< 5 \mu\text{m}$. “Pneumacult” measurements on HBE cultures do not display the continuous increase in α with the distance h to the epithelium that we obtained on “BEGM” HBE cultures. It is important though to mention here that these two culture methods result in remarkably different epithelia features. “Pneumacult” cultures have much more beating ciliated cells and a lower production of mucus with a thicker and more elastic aspect. The mucus observed on “Pneumacult” culture contains numerous cellular debris (see Figure S1D) and is highly inhomogeneous (Figure 7D), while mucus from “BEGM” culture is transparent, and floating cells are observed only on some occasions (see Figures S1A,C).

DISCUSSION

Difficulties in characterizing human airway mucus are essentially related to the small amount of high quality physiological mucus that can be collected [19–21]. To respond to the requirement of measuring rheology on small volumes of mucus, novel techniques named microrheology have been proposed [1, 10, 22]. However, the collection of mucus itself could lead to a biased picture of the *ex vivo* mucus properties as only the supernatant mucus can be collected. The less elastic, the easier it is to collect the mucus. The consequence could be that collected mucus is less elastic than the one on the epithelium. In addition the mucus as a layered structure with a gel phase on top of a periciliary watery layer [19]. To measure how microrheology vary within the mucus layer lying on top of cultured bronchial epithelium and probe its variation with the distance from the epithelium, we developed a new protocol and implemented our setup.

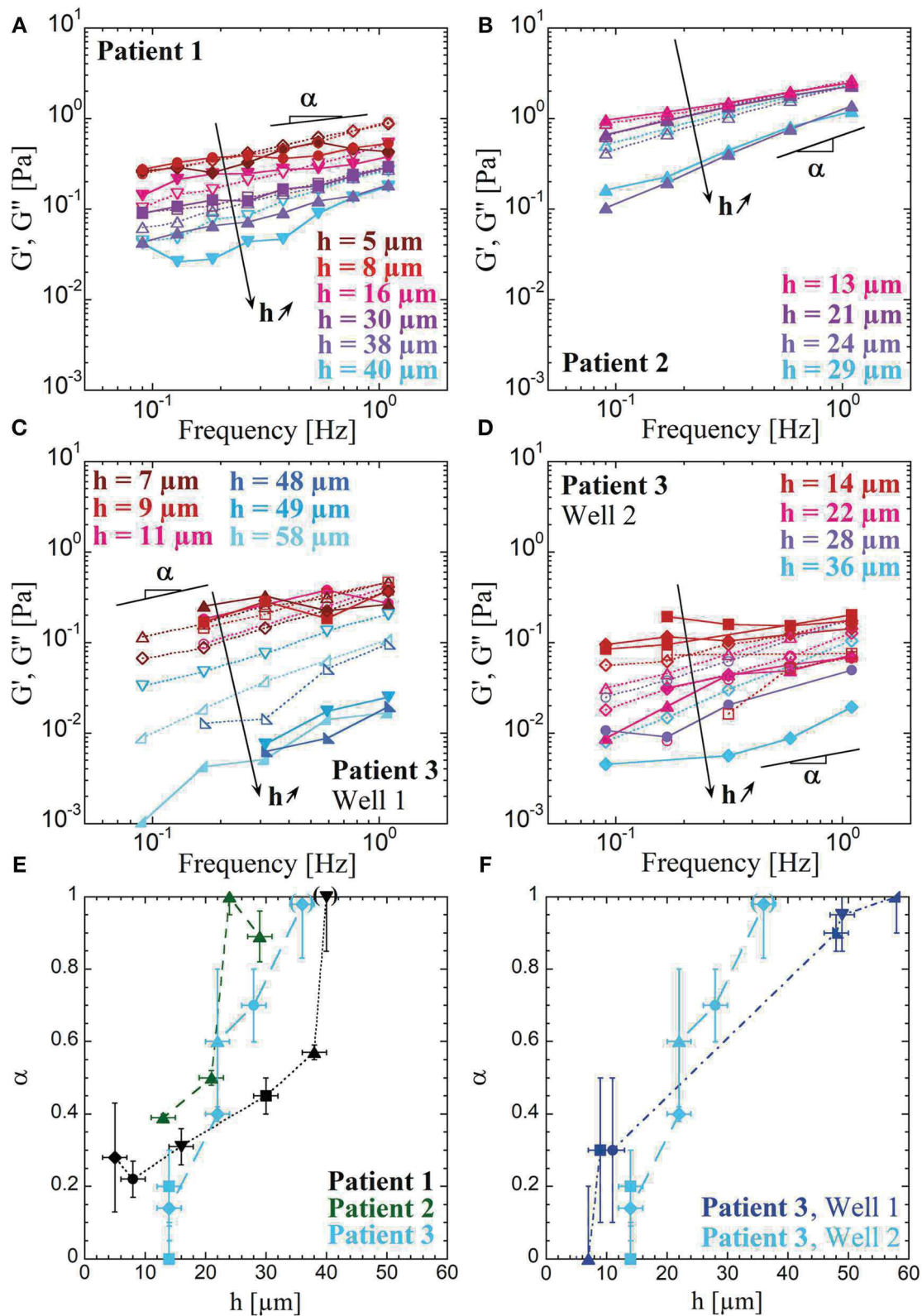
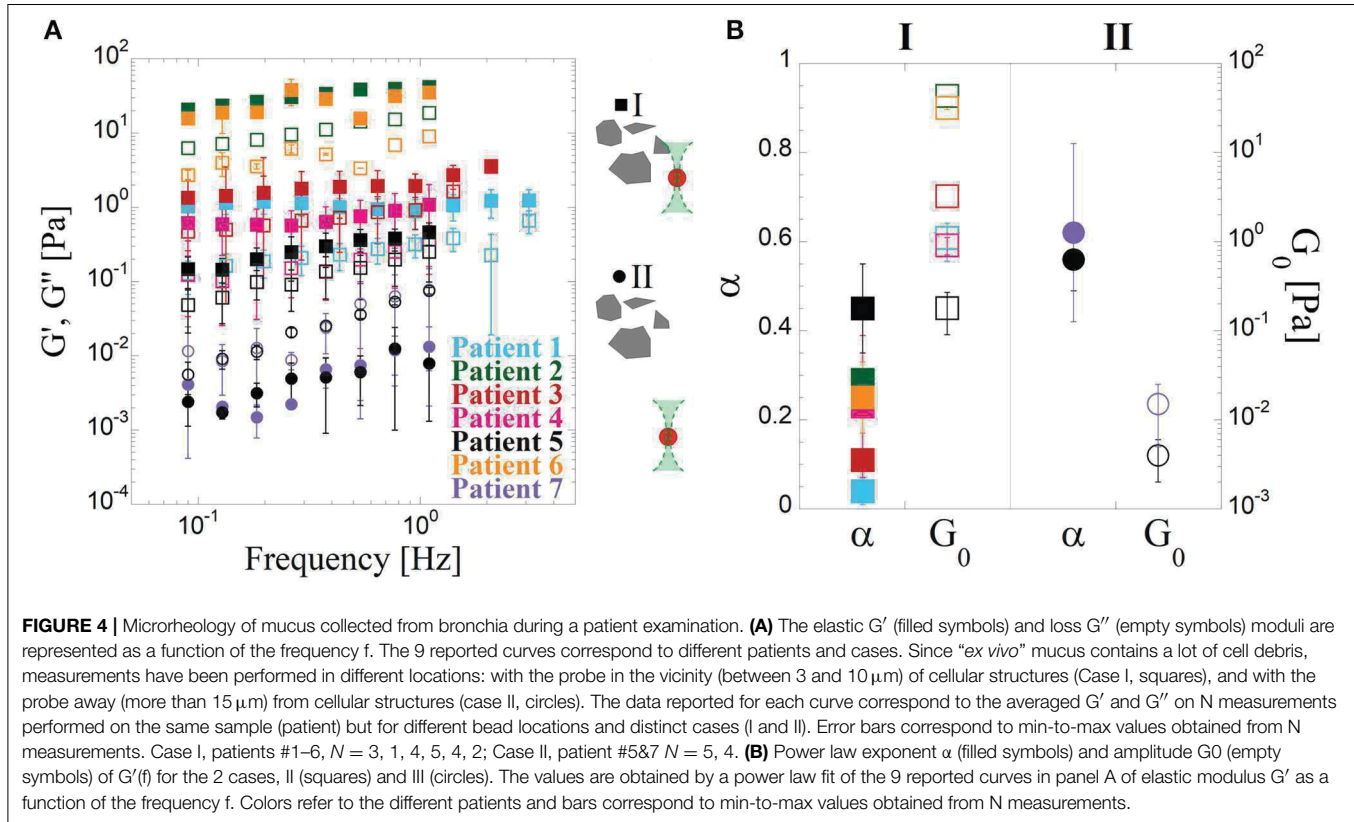


FIGURE 3 | Variation of the microrheology response with the distance to the epithelium: The elastic G' (filled symbols and solid lines) and loss G'' (empty symbols and dotted lines) moduli are represented as a function of the frequency f in panels (A–D). Measurements are performed by entraining beads from the bottom to the top. (Continued)

FIGURE 3 | Each symbol corresponds to a different bead. The four bronchial epithelia are cultured starting from biopsy of a smoker (Patient 1) for (A), a control (Patient 2) for (B) and two wells obtained from the same smoker (Patient 3) for (C,D). Power law exponents α of $G'(f)$ are represented in panels (E,F) as a function of the distance h from the epithelium cells layer, with in (E) the three patients: Patient 1 (black, dotted line), Patient 2 (dark green, short dashed line) and Patient 3 (light blue, long dashed line); and in (F) the comparison between two wells of Patient 3: well 1 (dark blue, dotted and dashed line) and well 2 (light blue, long dashed line). Each symbol corresponds to different beads and are kept identical to the corresponding data of panels (A-D). Error bars report on errors on the height h and on the determination of α by fitting $G'(f)$ by a power law. The parentheses around some points at $h > 30 \mu\text{m}$ indicate inaccurate values of α when the behavior of the corresponding curve $G'(f)$ is not a power law.



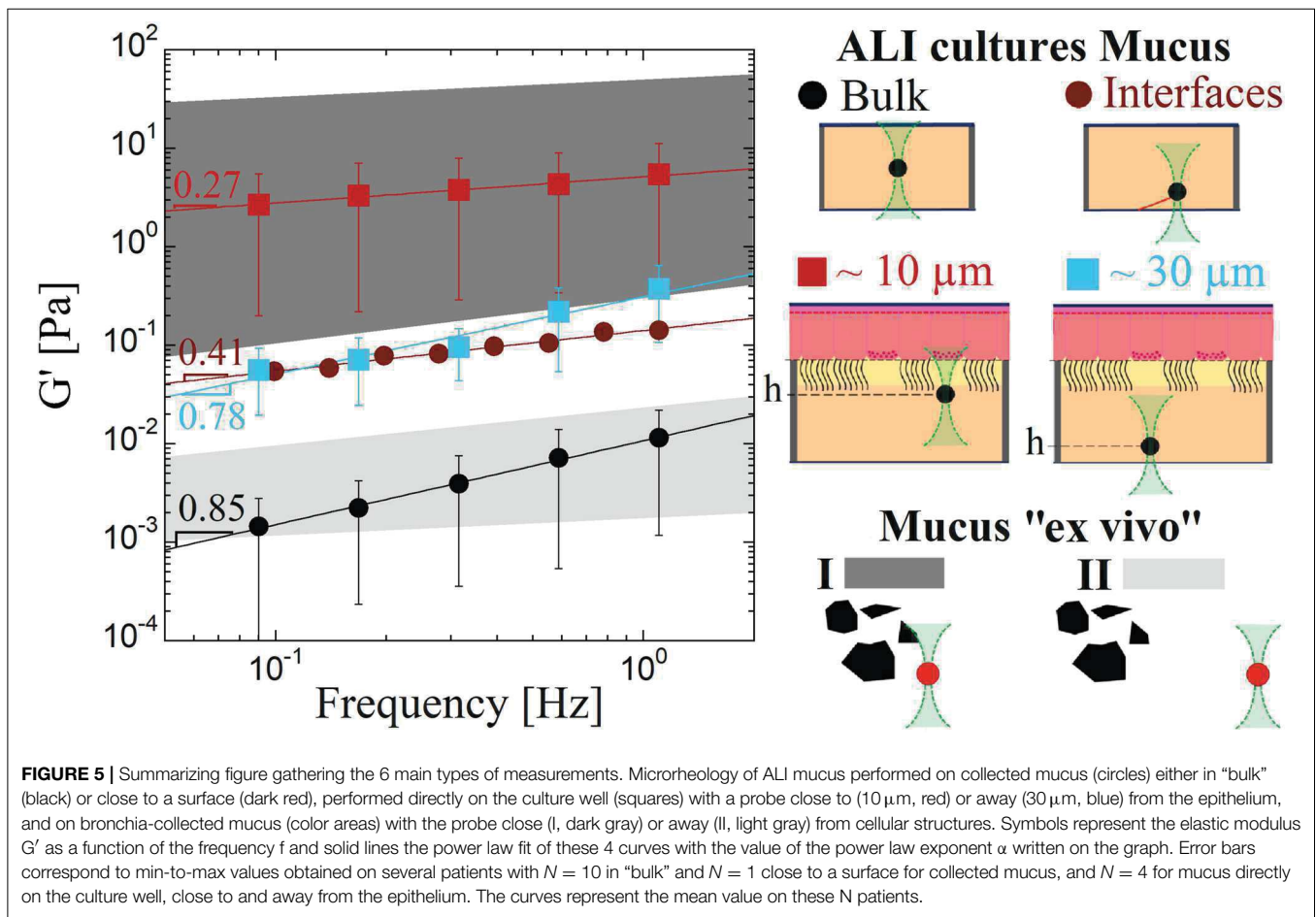
Collected Mucus and Mucus on the Epithelium Have a Different Microrheology Response

Recent papers are focused on the mucus rheology and compare the rheological response of mucus measured at the macro-scale using standard rheometers to measurements performed at a microscale [9–12, 23]. These studies have been performed on mucus of various origin: horse airway mucus [9, 10], marine worm mucus [11], porcine respiratory mucus [1], and even HBE mucus [6, 12], using either active or passive methods for microscale measurements. It is shown that probe size and probe/mucus interaction have to be considered to correctly select the probe and perform reliable microrheological measurements [1]. Furthermore, mucus appears as a highly heterogeneous multi-scale network with coupled two-fluid or interlinked scaffolds models being proposed [10, 23]. Micro and macro-rheology consequently result in different behaviors and values [10, 12, 23]. In addition to the scale at which mucus rheology is probed, we discuss here how mucus collection can

introduce a bias. We show, using mucus from the same well, that mucus measured once collected and measured directly on the epithelium have very different responses. Elastic moduli are several orders of magnitude larger on the epithelium with an elastic response rather than a viscous behavior as for the “bulk” case (Figure 2). This confirms that mucus collection is delicate and might lead to a misinterpretation of the results as only the less elastic fraction of mucus can be withdrawn from the epithelium.

Microrheology Gradually Varies Within the Mucus Layer on the Epithelium From Elastic to Viscous

More importantly, we find that the mucus rheology is not homogeneous but consistently varies from elastic to viscous when probed at increasing distances from the epithelium (Figure 3). The viscoelastic moduli G' and G'' variation with the frequency f is used to quantify and analyse the mucus viscoelastic response. We consider three main features of $G'(f)$

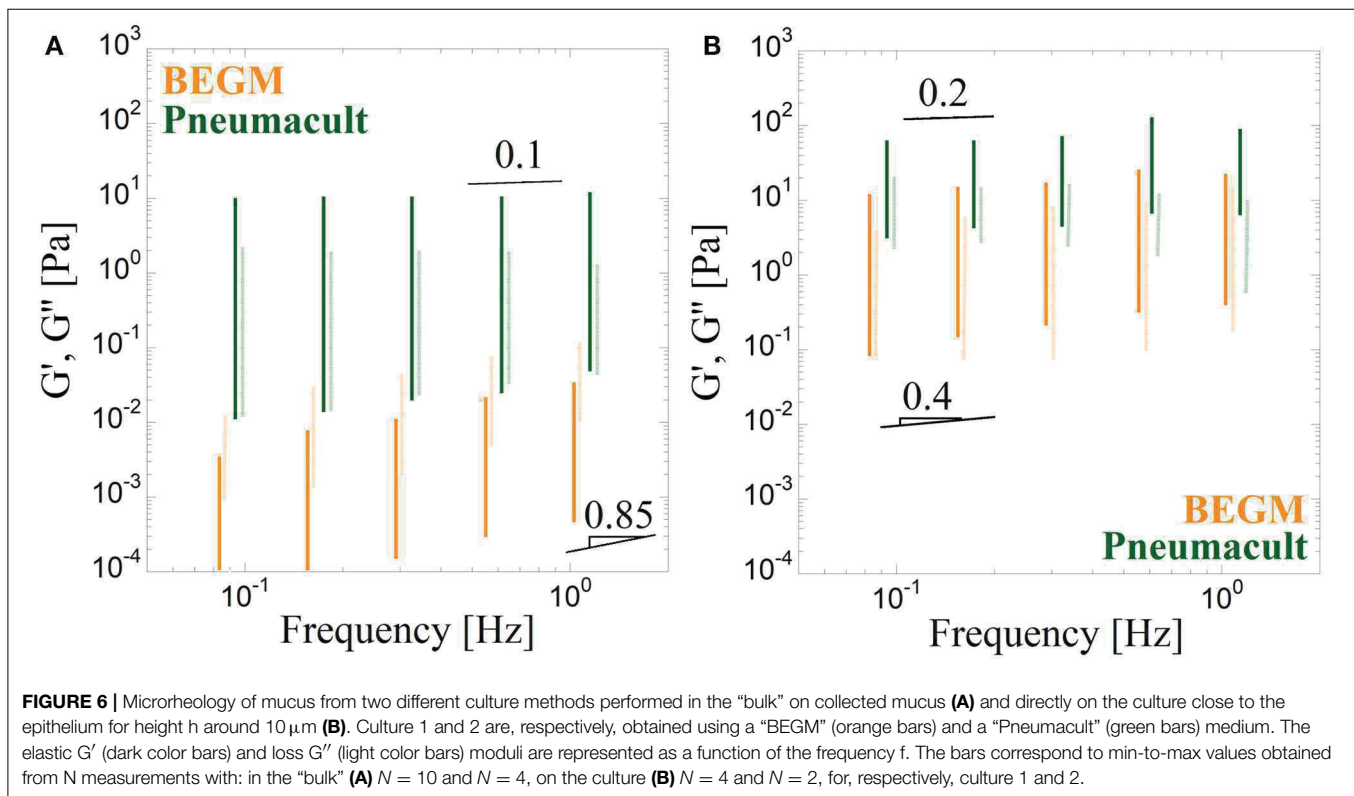


and $G''(f)$: the amplitude of the elastic moduli $G_0 = G'(f = 1 \text{ Hz})$, that give the viscoelasticity level; the ratio G'/G'' , and the power law exponent α , which both are a measure of the elastic vs. viscous character of the complex fluid. In particular, the exponent α is expected to be equal to 1 when the fluid is purely viscous and to 0 for a purely elastic solid. α increases roughly linearly with the distance h to the epithelium thus going from an elastic to a viscous behavior. The rate at which the behavior goes from elastic to viscous with the distance h is highly dependent on the culture, but the variation in α for two wells obtained from the same biopsy consistently overlaps (Figure 3F), bringing robustness to our results. This is the first demonstration of a gradient in viscoelasticity in the mucus layer of bronchial epithelium, even if the hypothesis has been present in the literature for long in particular because of its layered structure [19].

Mucus "ex vivo" Collected From Bronchia Contains a Lot of Cell Debris That Affect the Microrheology Response

All the difficulties related to collecting native mucus have restricted mucus physical and biochemical studies to sputum for which it is difficult to prevent saliva contamination. Some

techniques have been proposed to measure mucus collected during bronchofibroscopy allowing to collect mucus sample without saliva but they are extremely constrained [19]. We attempt to characterize the flowing properties of mucus collected from human bronchia by simple aspiration during a clinical examination. We obtain a very broad set of data (Figure 4) probably due to the variability of the mucus, and of its collection. Cell debris are present in large amount and contribute to the microscale rheology measurements. The rheology response, indeed, essentially depends on the probe vicinity to cellular structures. Far from any structure, elastic moduli are consistent with what we find for mucus collected from HBE: the rheology corresponds to a medium of viscosity equal to 2–20 times the water viscosity (Figure 4). Close to cellular structure, our results are rather consistent with the elastic behavior obtained on mucus collected from HBE when the probe is close to surfaces such as the glass plate. We hypothesize as discussed in another publication [19], that this elastic response occurs thanks to filaments-like structures that could form when the probe contacts any surface because of the highly adhesive nature of the mucus. Mucus is composed of mucins, proteinglycans, lipids, that interact together to form a gel network, but that also interact with cilia and other cellular structures. Flow properties of these "ex vivo" samples can be subjected to various contributions affecting rheology such



as water loss, collection method, or collection region, stress induced hypersecretion, tissue damage. We thus consider that these measurements are only indicative of what could be the bronchia mucus microrheology.

Figure 5 summarizes all of our results and show that depending on how mucus is measured, G' and G'' fall on one of two families of curves: curves corresponding to a viscous behavior with low value of the moduli or curves corresponding to an elastic behavior with lower exponent and higher moduli values. Collection of mucus seems to have a huge role on the type of behavior that is obtained as a result without being strictly related to the bronchia mucus properties. Measuring the viscoelastic moduli as a function of the frequency directly on the epithelium seems to be the most reliable way to evaluate the microrheological response of respiratory mucus.

On the Role of the Culture Method on Physical Features of the Human Bronchia Epithelium: “BEGM” and “Pneumacult”

Finally, we compared two methods of culture, essentially differing in the culture media used to feed the cells “BEGM” and “Pneumacult”. They give different results both on collected mucus and when rheology is measured on the epithelium (**Figure 6**). This is in agreement with macroscopic observation of the samples, as the mucus from “Pneumacult” culture appears as highly elastic and sticky in comparison with “BEGM” mucus. These first experiments show that the gradual variation observed on the whole mucus layer for “BEGM” culture is not found for “Pneumacult” culture (**Figure 7**). On the reverse, the elasticity

is always high and does not seem to be as dependent on the distance to the epithelium. This has to be confronted to the very high heterogeneity of this mucus and to the large number of cell debris it contains. This culture method which is the one used in our group since January 2018, provides epithelia which are singularly different in its physical characteristics, while it has been proven to represent a reliable and robust model of respiratory epithelia by means of biological markers and tissues characterization [24, 25]. Pneumacult cultures are probably more physiologically relevant since epithelia are much more active with a density of beating cells probably closer to *in vivo* tissues. Nevertheless, the mucus is produced in much lower quantity and difficult to collect. The presence of cells alters mucus rheology determination. Overall, BEGM cultures were an easier tool to investigate mucus rheology on culture and to show robustly the existence of a variation in the viscoelastic behavior with the distance to the epithelium, which was never assessed before. Pneumacult cultures because of heterogeneity do not exhibit such a clear variation and need more biological investigation to be considered as a good biological model. Further investigations on these culture are to be performed to analyze other physical characteristics such as cilia beating and mucus flow [7].

CONCLUSION

Mucus is a complex biofluid that fulfills numerous biological functions. Among its physical properties, rheology is crucial to understand how mucus flow is generated in the mucociliary system. Mucus collection to evaluate its physical properties

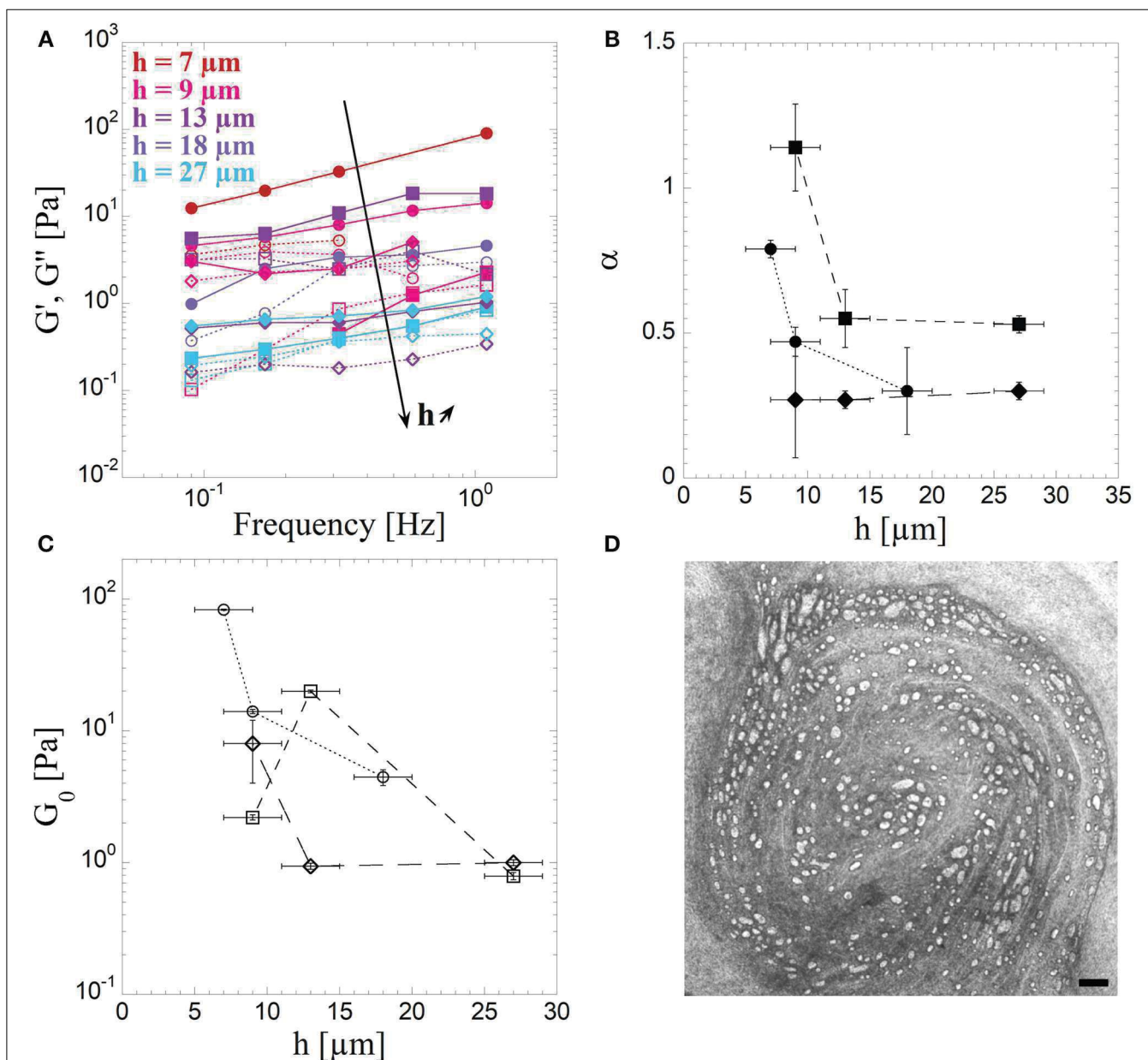


FIGURE 7 | “Pneumacult” culture characteristics: **(A)** Microrheology of mucus from bronchial epithelium culture obtained using a “Pneumacult” culture medium. The elastic G' (filled symbols and solid lines) and loss G'' (empty symbols and dotted lines) moduli are represented as a function of the frequency f . Measurements are performed by entraining 3 different beads at different spatial (xy) localizations (circles, squares, diamonds) from the bottom to the top. **(B)** The exponent α of the $G'(f)$ power law fit for the 3 xy localizations (circles, squares, diamonds) as the function of the probe distance h to epithelium. Bars represent the errors on the height h and on the determination of α by the power law fit. **(C)** Amplitude of the power law fit of the elastic modulus $G_0 = G'(f = 1\text{Hz})$ vs. probe to epithelium distance h for the 3 xy localizations (circles, squares, diamonds). Error bars represent the errors on the height h and on the determination of G_0 by the power law fit. **(D)** Picture of the culture at low magnification focalized above the mucus layer. Scale bar: 200 μm .

results in very small volumes of a selected fraction of mucus because of mucus high heterogeneity and interaction with the epithelium. Collected mucus is consequently poorly representative of native mucus rheology. We took full advantage of the human bronchial epithelia models developed thanks to air-liquid interface cultures and developed an original method to measure mucus rheology directly on the epithelium. Our

main experimental findings are that beside the heterogeneous structures formed by the mucus, which remains difficult to decipher, mucus rheological response varies, for BEGM cultures, from an elastic behavior close to the epithelium to a viscous one far away, and with up to a two-fold decrease in elastic moduli on distances to the epithelium from 10 to 50 μm . On Pneumacult cultures which are now the one available, similar experiments

need to be performed at an earlier stage, before cilia density becomes too high. Our findings could now be used at various levels to understand how this variation in elasticity with the distance to the epithelium could contribute to mucus transport when coupled to cilia beating. On a clinical point of view, it is not obvious at this stage if this method could be used for diagnosis as a clinical marker, mainly because experiments are delicate and time consuming. On a more fundamental point of view though, these experimental results could now be used in numerical models [26, 27] describing the whole epithelium, and in particular the emergence of metachronal waves and mucus transport thanks to cilia beating in a mucus with elastic properties varying with the distance to the epithelium.

AUTHOR CONTRIBUTIONS

IV, AB, and GM conceived the project. MJ, LC, IV, AB, and GM coordinated the experimental and data analysis activity. AP

and CV provided cultures. PR performed bronchoscopies. CB developed the optical tweezers and adapted it to microrheology experiments. MJ, CB, and KB performed experiments. MJ analyzed data. GM wrote the first draft of the manuscript. MJ and CB wrote sections of the manuscript. All authors contributed to manuscript revision, read, and approved the submitted version.

FUNDING

Labex Numev, FSFR AAP2015-2-053, Vaincrelamucoviscidose AP2016 RF20160501673, ANR Mucocil 13-BSV5-0015.

SUPPLEMENTARY MATERIAL

The Supplementary Material for this article can be found online at: <https://www.frontiersin.org/articles/10.3389/fphy.2019.00019/full#supplementary-material>

REFERENCES

- Lai SK, Wang YY, Wirtz D, Hanes J. Micro- and macrorheology of mucus. *Adv Drug Deliv Rev.* (2009) **61**:86–100. doi: 10.1016/j.addr.2008.09.012
- Gras D, Petit A, Charriot J, Knabe L, Alagha K, Gamez AS, et al. Epithelial ciliated beating cells essential for *ex vivo* ALI culture growth. *BMC Pulm Med.* (2017) **17**:1–7. doi: 10.1186/s12890-017-0423-5
- Leslie Fulcher M, Gabriel S, Burns KA, Yankaskas JR, Randell SH. Well-differentiated human airway epithelial cell cultures. *Hum Cell Cult Protoc.* (2005) **107**:183–206. doi: 10.1385/1-59259-861-7:183
- Liu Y, Fire AZ, Boyd S, Olshen RA. Rescue of CF airway epithelial cell function *in vitro* by a CFTR potentiator, VX-770. *Proc Natl Acad Sci USA.* (2014) **106**:18825–830. doi: 10.1016/j.pmlaen.2014.05.008
- Gras D, Bourdin A, Vachier I, De Senneville L, Bonnans C, Chanez P. An *ex vivo* model of severe asthma using reconstituted human bronchial epithelium. *J Allergy Clin Immunol.* (2012) **129**:1259–1266.e1. doi: 10.1016/j.jaci.2012.01.073
- Hill DB, Vasquez PA, Mellnik J, McKinley SA, Vose A, Mu F, et al. A biophysical basis for mucus solids concentration as a candidate biomarker for airways disease. *PLoS ONE* (2014) **9**:1–11. doi: 10.1371/journal.pone.0087681
- Khelloufi MK, Loiseau E, Jaeger M, Molinari N, Chanez P, Gras D, et al. Spatiotemporal organization of cilia drives multiscale mucus swirls in model human bronchial epithelium. *Sci Rep.* (2018) **8**:1–10. doi: 10.1038/s41598-018-20882-4
- Feriani L, Juenet M, Fowler CJ, Bruot N, Chioccioli M, Holland SM, et al. Assessing the collective dynamics of motile cilia in cultures of human airway cells by multiscale DDM. *Biophys J.* (2017) **113**:109–19. doi: 10.1016/j.bpj.2017.05.028
- Bokkasam H, Ernst M, Guenther M, Wagner C, Schaefer UF, Lehr CM. Different macro- and micro-rheological properties of native porcine respiratory and intestinal mucus. *Int J Pharm.* (2016) **510**:164–7. doi: 10.1016/j.ijpharm.2016.06.035
- Kirch J, Schneider A, Abou B, Hopf A, Schaefer UF, Schneider M, et al. Optical tweezers reveal relationship between microstructure and nanoparticle penetration of pulmonary mucus. *Proc Natl Acad Sci USA.* (2012) **109**:18355–60. doi: 10.1073/pnas.1214066109
- Weigand WJ, Messmore A, Tu J, Morales-Sanz A, Blair DL, Deheyn DD, et al. Active microrheology determines scaledependent material properties of Chaetopterus mucus. *PLoS ONE* (2017) **12**:1–19. doi: 10.1371/journal.pone.0176732
- Schuster BS, Suk JS, Woodworth GE, Hanes J. Nanoparticle diffusion in respiratory mucus from humans without lung disease. *Biomaterials* (2013) **34**:3439–46. doi: 10.1016/j.biomaterials.2013.01.064
- Jeffery P, Holgate S, Wenzel S. Methods for the assessment of endobronchial biopsies in clinical research: application to studies of pathogenesis and the effects of treatment. *Am J Respir Crit Care Med.* (2003) **168**:S1–17. doi: 10.1164/rccm.200202-150WS
- Gamez AS, Gras D, Petit A, Knabe L, Molinari N, Vachier I, et al. Supplementing defect in club cell secretory protein attenuates airway inflammation in COPD. *Chest* (2015) **147**:1467–76. doi: 10.1378/chest.14-1174
- Tassieri M, Gibson GM, Evans RML, Yao AM, Warren R, Padgett MJ, et al. Measuring storage and loss moduli using optical tweezers: Broadband microrheology. *Phys Rev E* (2010) **81**:1–5. doi: 10.1103/PhysRevE.81.026308
- Tassieri M, Del Giudice F, Robertson EJ, Jain N, Fries B, Wilson R, et al. Microrheology with optical tweezers: Measuring the relative viscosity of solutions “at a glance.” *Sci Rep.* (2015) **5**:1–6. doi: 10.1038/srep08831
- Shundo A, Hori K, Penalzoa DP, Tanaka K. Optical tweezers with fluorescence detection for temperature-dependent microrheological measurements. *Rev Sci Instrum.* (2013) **84**:14103. doi: 10.1063/1.4789429
- Neuman KC, Block SM. Optical trapping. *Rev Sci Instrum.* (2004) **75**:2787–09. doi: 10.1063/1.1785844
- Girod S, Zahm JM, Plotkowski C, Beck G, Puchelle E. Role of the physiochemical properties of mucus in the protection of the respiratory epithelium. *Eur Respir J Off J Eur Soc Clin Respir Physiol.* (1992) **5**:477–87.
- Jeanneret-Grosjean A, King M, Michoud MC, Liote H, Amyot R. Sampling technique and rheology of human. *Am Rev Respir Dis.* (1988) **137**:707–10.
- Zayas JG, Man GCW, King M. Tracheal mucus rheology in patients undergoing diagnostic bronchoscopy interrelations with smoking and cancer. *Am Rev Respir Dis.* (1989) **141**:1107–13.
- King M, Macklem PT. Rheological quantities properties of microliter of normal mucus. *J Appl Physiol Respir Exerc Physiol.* (1977) **42**:797–802.
- Gross A, Torge A, Schaefer UF, Schneider M, Lehr CM, Wagner C. A foam model highlights the differences of the macro- and microrheology of respiratory horse mucus. *J Mech Behav Biomed Mater.* (2017) **71**:216–22. doi: 10.1016/j.jmbbm.2017.03.009
- Gohy ST, Hupin C, Pilette C, Ladjemi MZ. Chronic inflammatory airway diseases: the central role of the epithelium revisited. *Clin Exp Allergy* (2016) **46**:529–42. doi: 10.1111/cea.12712

25. Gohy ST, Hupin C, Fregimilicka C, Detry BR, Bouzin C, Chevronay HG, et al. Imprinting of the COPD airway epithelium for dedifferentiation and mesenchymal transition. *Eur Respir J.* (2015) **45**:1258–72. doi: 10.1183/09031936.00135814
26. Chatelin R, Anne-Archard D, Murriss-Espin M, Thiriet M, Poncet P. Numerical and experimental investigation of mucociliary clearance breakdown in cystic fibrosis. *J Biomech.* (2017) **53**:56–63. doi: 10.1016/j.jbiomech.2016.12.026
27. Chateau S, Ortona UD, Poncet S, Favier J, David T. Transport and mixing induced by beating cilia in human airways. *Front Physiol.* (2018) **9**:161. doi: 10.3389/fphys.2018.00161

Conflict of Interest Statement: The authors declare that the research was conducted in the absence of any commercial or financial relationships that could be construed as a potential conflict of interest.

Copyright © 2019 Jory, Bellouma, Blanc, Casanellas, Petit, Reynaud, Vernisse, Vachier, Bourdin and Massiera. This is an open-access article distributed under the terms of the Creative Commons Attribution License (CC BY). The use, distribution or reproduction in other forums is permitted, provided the original author(s) and the copyright owner(s) are credited and that the original publication in this journal is cited, in accordance with accepted academic practice. No use, distribution or reproduction is permitted which does not comply with these terms.



Early View

Original article

CCSP counterbalances airway epithelial-driven neutrophilic chemotaxis

Lucie Knabe, Aurélie Petit, Charlotte Vernisse, Jérémy Charriot, Martine Pugnère, Corinne Henriquet, Souphatta Sasorith, Nicolas Molinari, Pascal Chanez, Jean-Philippe Berthet, Carey Suehs, Isabelle Vachier, Engi Ahmed, Arnaud Bourdin

Please cite this article as: Knabe L, Petit Aélie, Vernisse C, *et al.* CCSP counterbalances airway epithelial-driven neutrophilic chemotaxis. *Eur Respir J* 2019; in press (<https://doi.org/10.1183/13993003.02408-2018>).

This manuscript has recently been accepted for publication in the *European Respiratory Journal*. It is published here in its accepted form prior to copyediting and typesetting by our production team. After these production processes are complete and the authors have approved the resulting proofs, the article will move to the latest issue of the ERJ online.

CCSP counterbalances airway epithelial-driven neutrophilic chemotaxis

Lucie Knabe^{1,2}, Aurélie Petit², Charlotte Vernisse^{1,2}, Jérémy Charriot², Martine Pugnère³, Corinne Henriquet³, Souphatta Sasorith⁴, Nicolas Molinari⁵, Pascal Chanez⁶, Jean-Philippe Berthet⁷, Carey Suehs², Isabelle Vachier², Engi Ahmed², Arnaud Bourdin^{1,2}.

1. PhyMedExp, University of Montpellier, INSERM U1046, CNRS UMR 9214, France.
2. Department of Respiratory Diseases, CHU Montpellier, University of Montpellier, France.
3. IRCM, Institut de Recherche en Cancérologie de Montpellier, INSERM U1194, Université de Montpellier, Institut régional du Cancer de Montpellier, Montpellier, F-34298, France.
4. CHU de Montpellier, Laboratoire de Génétique Moléculaire, Montpellier, France; University of Montpellier, EA7402, Montpellier, France.
5. IMAG U5149, Department of Medical Information, CHU Montpellier, University of Montpellier, France.
6. C2VN - Inserm U1263 INRA 1260, AP-HM, Department of respiratory diseases, Aix Marseille University, France.
7. Department of Thoracic Surgery, CHU Montpellier, University of Montpellier, France.

Correspondence:

Professor Arnaud Bourdin
Department of Respiratory Diseases
Hôpital Arnaud de Villeneuve, CHU Montpellier
371 Av. Doyen G. Giraud
34295 MONTPELLIER Cedex 5, France
Telephone: + 33 4 67 33 61 26
Fax: +33 4 67 63 36 45
E-mail: a-bourdin@chu-montpellier.fr

Take home message

rhCCSP prevents airway neutrophilia. This might occur via a direct neutralization of IL8 in humans.

Abstract

CCSP knockout mice exhibit increased airway neutrophilia, as found in COPD. We therefore investigated whether treating COPD airway epithelia with rhCCSP could dampen exaggerated airway neutrophilia.

Control, smoker and COPD Air-Liquid Interface (ALI) cultures exposed to Cigarette Smoke Extract (CSE) were treated with and without rhCCSP. The chemotactic properties of their supernatants were assessed by Dunn chambers. Neutrophil chemotaxis along rhIL8 gradients (with/without rhCCSP) was also determined. rhCCSP-rhIL8 interactions were tested through co-immunoprecipitation, Biacore-Surface Plasmon Resonance (SPR) and *in silico* modelling. The relationship between CCSP/IL8 concentration ratios in the supernatant of induced sputum from COPD patients versus neutrophilic airway infiltration assessed in lung biopsies was assessed.

Increased neutrophilic chemotactic activity of CSE-treated ALI cultures followed IL8 concentrations and returned to normal when supplemented with rhCCSP. rhIL-8 induced chemotaxis of neutrophils was reduced by rhCCSP. rhCCSP and rhIL8 co-immunoprecipitated. SPR confirmed this *in vitro* interaction ($KD = 8\mu M$). *In silico* modelling indicated that this interaction was highly likely. CCSP/IL8 ratios in induced sputum correlated well with the level of small airway neutrophilic infiltration ($r^2=.746$, $p<.001$).

CCSP is a biologically relevant counter-balancer of neutrophil chemotactic activity. Altogether, these different approaches suggest that among the possible mechanisms involved, CCSP may directly neutralize IL8.

Keywords: Club Cell Secretory Protein (CCSP), Club Cell 10 (CC10), IL8, neutrophils, Chronic Obstructive Pulmonary Disease (COPD), Cigarette Smoke Extract (CSE), Airway epithelium.

ClinicalTrials.gov Identifier: NCT02354677, NCT01947218.

Funding: This study have been supported by grants from the Agence Nationale de Recherche (ANR) Mucocil (ANR-13BSV5-0015-02), the Programme Hospitalier de Recherche Clinique (PHRC IR) AP-HM (2013-14), and the CHRU Montpellier (AOI 9244).

Introduction

Imbalance between injury and repair universally trends with inflammatory processes. Exaggerated neutrophilic influx hallmarks most chronic airway diseases such as neutrophilic asthma, cystic fibrosis, idiopathic pulmonary fibrosis and Chronic Obstructive Pulmonary Disease (COPD)[1], a growing cause of morbidity and mortality worldwide. In addition, increased neutrophilic inflammation is characteristic of patients with severe disease [2] or with acute exacerbations [3]. Airway neutrophilia is associated with an accelerated decline in lung function [4, 5] and with the severity of peripheral airway dysfunction in COPD [6, 7].

Chemotaxis, a process whereby cells migrate according to a chemical concentration gradient, critically mediates neutrophil recruitment in tissue [8]. Neutrophils express multiple chemoattractant receptors and can be sensitive to individual gradients or combinations thereof. Several chemoattractants for neutrophils are increased in the bronchial secretions of COPD patients. The most abundant and studied are interleukin (IL)8 and leukotriene B4 [9, 10]. These chemokines bind to neutrophil CXCR1/CXCR2 and BLT1 GPCR, respectively, to amplify cell recruitment [11]. Past *in vitro* studies often employed N-Formyl-L-methionyl-L-leucyl-L-phenylalanine (fMLP) due to its highly potent chemoattractant ability, which ligates with neutrophil formyl peptide receptors (FPRs) [12]. COPD neutrophils, relative to those from healthy patients, have been demonstrated to be disoriented, migrating faster but with less accuracy [13].

Interestingly, the Club Cell Secretory Protein (CCSP, CC10 or SCGB1A1) produced by non-ciliated club cells is known to have immunoregulatory and anti-inflammatory functions [14-17], but the mechanisms of action remain largely unknown in the absence of an identified specific receptor. CCSP is defective in COPD airways [17-19]. Appropriately, Lauchon-Contreras et al. demonstrated that increased lung neutrophilia was observed in CCSP^{-/-} mice

exposed to cigarette smoke, as seen in COPD airways. Moreover, this could be rescued by exogenous CCSP supplementation [18].

The exact mechanisms by which CCSP mediates its anti-inflammatory activities, including whether or not it binds to a receptor, have not yet been determined. To date, its paracrine signalization is unknown and remains hypothetical. Of note, CCSP levels are known to be reduced in sera, sputum and bronchoalveolar lavage fluid from COPD patients. Furthermore, two studies demonstrated that serum CCSP levels predict accelerated lung function decline [20, 21].

We hypothesized that injury/repair imbalance may explain exaggerated airway neutrophilia and CCSP defects could be involved in this process in COPD patients. Our aim was to test whether rhCCSP interacts with airway neutrophilic influx in a human model of COPD, and whether this interaction was due to an effect of CCSP on the airway epithelial cells or due to an endogenous IL8 binding counter-balancer. For this purpose, Air-Liquid Interface (ALI) cultures of epithelial cells were treated with rhCCSP (exposed to Cigarette Smoke Extract (CSE) or not). The collected supernatants were used to assess neutrophilic chemotaxis. Furthermore, neutrophils were directly exposed to chemotactic agents and treated with rhCCSP. Their chemotactic parameters were also assessed. Finally, we developed an *in vitro* three-step demonstration of CCSP-IL8 direct binding, and sought possible converging evidence of the relationship between CCSP and IL8 in lung airways.

Materials and methods

Epithelial cell cultures and stimulation

Bronchial biopsies from control subjects (n = 4), smokers (n = 10), and COPD patients (n = 13) were collected during surgery. Subjects were recruited at the Arnaud de Villeneuve Hospital, Montpellier, France. The local ethics committee, *Comité de Protection des Personnes Sud-Méditerranée III*, approved the study design (approval number: 2013 11 05; NCT02354677) and all patients agreed to participate by reading and signing written informed consent forms.

Human primary bronchial epithelial cells (HBECs) were cultured under Air-Liquid Interface (ALI) conditions, adapted from Gras et al. and Gamez et al. [17, 22]. Details on this method are available in the online supplement. Cells from bronchial biopsies of 4 control subjects, 10 smokers, and 13 COPD patients were maintained in culture for 28 days to obtain a differentiated cell population with a pseudostratified mucociliary epithelium. Cells were treated for 24 hours with or without cigarette smoke extract (CSE) and with or without rhCCSP supplementation (3µg/ml), applied at the apical surface. The supernatants were collected by washing the apical surface and stored until used for neutrophil experiments and CCSP/IL8 ELISA test (Biovendor/Diaclone).

Cigarette smoke extract (CSE)

CSE was prepared as previously described [17]. Briefly, the smoke of 3 commercial cigarettes (Marlboro®) was withdrawn into a Pasteur pipette and bubbled into 30 ml of PBS. CSE was adjusted to pH 7.4 and sterilized through a 0.22µm filter. We obtained a 100% stock solution of CSE diluted to 50% for the experiments.

Isolation of peripheral blood neutrophils

Neutrophils were isolated from the whole blood of 5 healthy control subjects and 5 COPD patients (approval number: 0811738) using discontinuous Percoll gradients followed by hypotonic lysis of residual red blood cells [23]. The neutrophils (purity at 95% and viability assessed by trypan blue exclusion of dead cells, at 95%) were re-suspended in RPMI 1640 medium containing 0.15% bovine serum albumin.

Neutrophil chemotaxis assays and analyses

The chemotaxis assays were performed using Dunn chambers [24]. Details on this method are available in the online supplement. Chemotaxis was quantified using the XFMI value, which is the ratio of the distance travelled during the acquisition and the final position of the neutrophils on the x-axis in the direction of the chemoattractant gradient.

ImageJ software was used to track cells and analyse chemotaxis. All analyses were performed by a single analyst, blinded to the subject group.

Basically, three sets of assays were performed. Supernatants gathered by a brief wash at the apical side of ALI cultures of airway epithelial cells at baseline first and treated in each of the above-mentioned conditions second, were applied in the outer ring and neutrophil chemotaxis from both controls and COPD patients was assessed. Third, only pharmacological agents separately or combined were applied in the outer ring in order to delineate whether the observed results in the first set of assays could be modulated and reproduced without any epithelial interaction.

Co-immunoprecipitation

To detect whether a potential interaction exists between CCSP and IL8, co-immunoprecipitation and immunoblotting were performed using anti-Protein A Sepharose 4 Fast Flow magnetic beads (GE Healthcare). Details on this method are available in the online

supplement. All immunoblots were developed and quantified by using the Odyssey Infrared Imaging System (LICOR Biosystems) and infrared-labelled secondary antibodies.

BIACORE measurements

Real-time Surface Plasmon Resonance (SPR) analyses were performed on a Biacore T200 apparatus (GE Healthcare, Uppsala Sweden) at 25°C, in HBS-EP+ buffer (10mM HEPES, 150mM NaCl, 3 mM EDTA, 0.05% Polysorbate 20 surfactant). rhCCSP, diluted at 10µg/ml in 10mM acetate pH4, was covalently immobilized at 2400 RU on a CM5S sensor chip (GE Healthcare) using an amine coupling protocol according to the manufacturer's instructions.

Kinetic titration experiments (single-cycle kinetics) of IL8 were performed at a flow rate of 100µl/min with two-fold serial dilutions (62nM-1000nM). All curves were evaluated (T200Evaluation Software 3.0) after double-referencing subtraction using a bivalent fitting model. This experiment was repeated with a new immobilization of rhCCSP with a similar result.

3D protein modelling and protein-protein docking

A homology model of the homo sapiens (hs)CCSP homodimer has been generated according to the crystal structure of the rabbit ortholog (PDB: 2UTG), using the software Modeller [25]. The protein-protein docking server ZDOCK[26] was used with blind docking parameters to explore the putative interaction between the 3D homology model of hsCCSP and the experimental human IL8 structure (PDB: 3IL8).

Surgical lung samples and induced sputum collection

A cross-sectional cohort of 10 COPD patients undergoing surgery for peripheral nodules was recruited after patients were informed and signed an informed consent form. This study was

approved by an ethics committee (*Comité de Protection des Personnes de Nîmes*; AOI 2000, CPP 000901, DGS 2001/0075). Both CCSP and IL8 concentrations were assessed in the induced sputum of patients 3 to 5 days before they underwent lung surgery. Surgical lung samples were optimally processed to allow for quantification of Neutrophil Elastase (NE) positive cells in the submucosal area of small airways at a maximum depth of 100 µm beneath the basement membrane. Methodological details are available in the online supplement.

Statistical analysis

Details on statistical analysis are available in the online supplement.

Results

COPD airway epithelia attracted neutrophils

Dunn chemotaxis chambers were filled with ALI-epithelial supernatants. Figure 1A displays representative examples of healthy and COPD neutrophil migratory tracks induced by supernatants from ALI-reconstituted-airway-epithelia derived from healthy controls, smokers and patients with COPD. Consistent with our previous observations, fMLP was confirmed as a positive control, and PBS as a negative one ($p < 0.0001$, indicated by stars, dark columns) (Figure 1B). Although epithelial supernatants from all groups increased neutrophil chemotaxis (indicated by stars), only neutrophil chemotaxis induced by COPD supernatants was significantly higher than that induced by control supernatants ($p = 0.0012$, indicated by a hash sign (#)) (Figure 1B). Neither CCSP nor IL8 concentrations were measured in this set of assays.

Treating the airway epithelium with rhCCSP prevents neutrophil chemotaxis when exposed to CSE to an extent that fits with CSE-induced IL8 release

We further focused on whether treating CSE exposed-COPD airway epithelia with rhCCSP could reduce exaggerated neutrophil influx. As expected, smoker and COPD epithelia exposed to CSE increased neutrophil chemotaxis (Figures 2A and 2B). When smoker and COPD airway epithelia were exposed to CSE, we observed for the first time on human cells that rhCCSP prevented neutrophil chemotaxis, which returned nearly to baseline values ($p < 0.0001$ and $p = 0.0035$, respectively) (Figures 2A and 2B). IL8 and CCSP concentrations in the supernatants were assessed (Figures 2C and 2D, supplemental Figure 1). In this set of experiments, CSE tended to induce IL8 release, but without differences between smokers and COPD. Similar chemotactic measures were obtained with neutrophils from COPD patients (Supplemental Figure 2). It should be noted that XFMI was used to represent neutrophil chemotaxis in our study, except for COPD neutrophils. Since the latter are disoriented (according to the literature[13]), considering the distance travelled by the neutrophils was a

more appropriate measure for demonstrating that rhCCSP had the same effect on COPD neutrophils as on healthy neutrophils.

rhCCSP directly inhibited neutrophil chemotaxis induced by rhIL8 and by fMLP

Neutrophil migration along the fMLP gradient was reduced by rhCCSP ($p < 0.0001$ for the XFMI) but not along the rhIL8 gradient (Figure 3A). Likewise, no CXCR1/2 inhibitor effects were observed (Figure 3A). Since XFMI is the ratio of the distance travelled during acquisition and the final neutrophil positions on x-axis in the direction of the chemoattractant gradient, we analysed these parameters (i.e. the so called X endpoints and the distance travelled). Interestingly, the final position of healthy neutrophils in the presence of rhCCSP was significantly delayed in the direction of the rhIL8 gradient ($p = 0.028$) to a similar extent as found for the CXCR1/2 inhibitors (Figure 3B), but these neutrophils travelled shorter distances ($p < 0.0001$) (Figure 3C). When performed with neutrophils from COPD patients, rhIL8-induced neutrophil chemotaxis, as assessed by XFMI ($p < 0.0001$), X endpoints ($p < 0.0001$) and the distance travelled ($p < .0001$) were both inhibited by rhCCSP (Supplemental Figures 3A, 3B and 3C).

rhCCSP and rhIL8 had a direct interaction

The hypothetical direct rhCCSP-rhIL8 interaction was evaluated by co-immunoprecipitation with anti-IL8 antibodies followed by anti-CCSP antibody blotting. We found that rhCCSP co-immunoprecipitated with rhIL8 (Figures 4A and 4B). The reverse demonstration was performed (Figures 4A and 4C) and confirmed this interaction. This finding was validated by SPR analyses using single-cycle kinetics without regeneration (Figure 4D). Accordingly, we determined an equilibrium dissociation constant (KD) of 8 μ M. Three-dimensional (3D) protein modelling and protein-protein docking were performed in order to illustrate the molecules' *in silico* compatibility (Figure 4E). The docking results of ZDOCK demonstrated a set of *Homo sapiens* (hs) CCSP-hsIL8 complex structures, where the 5 top-ranked predictions

(selected based on the internal ZDOCK scoring function) adopted similar conformations. Given the known binding of IL8 to CXCR1/2 on neutrophils, we next compared both binding sites. The superimposition of the hsCCSP-hsIL8 complex model with the experimental structure of hsCXCR1(C-terminal part)/hsIL8 complex (1ILP) showed that CXCR1 and CCSP would be located in the same area.

The small airway wall infiltration by neutrophils negatively correlated with the CCSP/IL8 ratio measured in the induced sputum of COPD patients undergoing surgery.

In order to verify whether these findings are observable *in vivo*, neutrophilic infiltration of the small airway wall of COPD patients was quantified in human lung samples obtained during surgery. These results were confronted with the CCSP/IL-8 ratio assessed in the induced sputum collected before the surgery. The level of this negative correlation was as high as 0.746 (Figure 5), indicating a greater intensity of neutrophilic infiltration when the CCSP/IL8 ratio was low and vice versa.

Discussion

In this study, we found that the airway epithelium of COPD patients reconstituted using ALI kept one important feature of the disease [17] as it exerted an increased neutrophilic chemotactic activity at steady state: CSE-induced IL8 release by these epithelia obtained from either smokers and COPD was reduced by exogenous rhCCSP supplementation. The latter was true for the neutrophils of both controls and COPD patients, which is important considering the disorientation shown to affect COPD neutrophils [13]. Because rhCCSP reduced both fMLP and rhIL8-induced chemotaxis irrespective of the presence of the airway epithelium in a magnitude similar to a CXCR1/2 antagonist, we strove to find evidence that rhCCSP could bind to rhIL8. We developed *in vitro* (through two way co-immunoprecipitation and Biacore SPR method), *in-silico* and *in vivo* assays indicating convergent support for the observed correlation between CCSP/IL8 ratios in induced sputum versus levels of neutrophilic airway infiltration.

The development of COPD treatments is probably the greatest challenge for respiratory medicine for the next twenty years. The role played by airway inflammation is unclear at steady state, but neutrophilic bursts (associated with exacerbation episodes) are the established culprits of irreversible “stair-shaped” decline [27]. The role played by the only “bronchiolar-specific” epithelial cell type, the club cell, is emerging as a potential regulator of these pathogenic COPD features [16, 17, 28]. We and others were able to establish their role at the interface between structural alterations and inflammation, with possible modifications according to smoking status. In particular, serum CCSP levels are decreased in COPD and restoring their normal values decreased CSE-induced-IL8 and LPS-induced-MUC5AC [17, 29]. Indeed, though rhCCSP appears ready to be tested in humans, major knowledge gaps concerning its mechanisms of action should be filled [30].

Different approaches have been previously used to assess CCSP effects on neutrophils in animals. In an equine model, incubating neutrophils with rhCCSP significantly reduced their respiratory oxidative bursts and increased their phagocytic activity [31]. Furthermore, neutrophil counts were increased in the bronchoalveolar lavage of CCSP^{-/-} mice exposed to cigarette smoke for 6 months [18]. With our human model, we assessed neutrophil chemotaxis in Dunn Chambers using rhIL8 and fMLP as controls, and ALI epithelium supernatants. Using epithelial supernatants made sense because physiologically, chemokines are also secreted by bronchial epithelial cells in order to attract neutrophils within the bronchial airway lumen [32]. These chemotactic chambers have the advantage of not being affected by gravity (e.g. compared to Boyden chambers), which is important for this model. Sapey et al. first used this model to demonstrate that neutrophil chemotactic responses were different in COPD compared to healthy subjects [13]. Our initial results suggest that COPD airway epithelia are exerting an increased neutrophilic chemotaxis at steady state. Interestingly, CSE exposure increased this chemotactic activity both in smokers and COPD and could be prevented by treating the epithelium with rhCCSP. We failed to pinpoint the intracellular signalling pathway involved. The small quantity of proteins extracted through ALI cultures on filters did not enable western blot analysis of changes in NF- κ B p65 subunits. NF- κ B inhibition was suggested as a possible CCSP target by Lacho-Contreras, [18] whereas Tokita [29] alternatively mentioned ERK1/2. CCSP is also known as a specific PLA2 inhibitor, but this is highly controversial in the literature [18, 33]. Surprisingly, COPD airway epithelia in the present assays were not very high IL8 producers when exposed to CSE. The heterogeneity of COPD may at least partially explain this finding. In any case, the chemotactic activity measurements fit with the IL8 concentrations and supported our overall interpretation of the findings.

Pharmacologically, neutrophil chemotaxis was increased by fMLP and rhIL8, and there again rhCCSP was efficient in reducing this activity. Candidate mediators of neutrophil chemotactic activity, such as LTB₄ or GRO α , can be found in the literature [34, 35]. rhCCSP may act through those different mechanisms. It also suggests that rhCCSP interferes with neutrophilic chemotaxis not only via an epithelial effect, such as decreased IL8 signalling mimicked by CXCR1/2 antagonism, but also through FPR2 as suggested by Vasanthakumar et al [36] and probably, given the unspecific effects of CSE, through broader interactions. Because this pharmacological modulation could be obtained irrespective of the presence of the airway epithelium, we strove to evidence whether rhCCSP could directly neutralize IL8.

Over twenty years ago, a striking property was identified for CCSP: the presence of a hydrophobic pocket that binds airway pollutants [37, 38]. Indeed, our *in silico* experiments not only showed that hsCCSP directly binds hsIL8, but hsCCSP also seemed to interact with hsIL8 through the same binding site at CXCR1. As a consequence, CCSP and CXCR1 most likely compete with each other for IL8 binding (suggesting that IL8 can either bind CCSP or CXCR1, but not both at the same time). A treatment with an antagonist of CXCR2 (another IL8 receptor) led to significant improvement in FEV1 in patients with COPD, suggesting clinically important anti-inflammatory effects associated with CXCR2 antagonism [39]. Such results further support that CCSP is a credible therapeutic strategy. We hypothesized that rhCCSP could directly trap rhIL8. Co-immunoprecipitation assays were reproduced twice and bi-directionally. By SPR, an up-to-date real-time and label-free technology [40], the direct interaction of rhIL8 on immobilized rhCCSP has been measured from dose-response curves (KD =8 μ M). Whether these rhCCSP-rhIL8 complexes are biologically active or not is difficult to address. The reality of this interaction with non recombinant protein remains to be demonstrated.

In vivo, we observed a statistically significant relationship between the intensity of the neutrophilic airway inflammation in the small airway of COPD patients and the CCSP/IL8 ratio measured in the induced sputum collected just before the lung surgery. Although inconclusive and not evidencing any kind of causality, this observation is convergent with the hypothesis. Once again, we acknowledge that this convergence shouldn't be over-interpreted.

In conclusion, this study confirms that ALI reconstituted COPD airway epithelia exert an increased neutrophilic chemotactic activity and that rhCCSP is likely able to prevent airway neutrophilia in humans. We suggest that multiple mechanisms of action exist, including the possibility of direct IL8 neutralization. A therapeutic strategy that limits airway neutrophilia must simultaneously address potential infection risks. Compared to CXCR1/2 blockades that induced systemic neutropenia, rhCCSP has the potential, due to its bronchial specificity, to have a narrower compartment target and subsequently tighter regulation of neutrophilia.

Author contributions: LK collected the clinical data, performed the experiments and statistical analyses, interpreted the data and wrote the manuscript. AP, CV and JC helped perform the experiments. MP and CH performed SPR experiments and provided their expertise. SS performed 3D protein modelling and protein-protein docking analyses. NM provided statistical expertise and helped analyse the data. PC, JDV, JPB, IV and EA participated in the study design, interpreted the data, and provided critical edits of the manuscript. CS helped in correcting the language and style. JC and JPB recruited patients. AB designed the study, recruited patients, collected the clinical data, performed statistical analyses, interpreted the data, and provided critical edits of the manuscript. All authors provided critical review of the manuscript and approved its submission.

Acknowledgments: The authors are grateful to Valérie Scheuermann for her technical assistance.

The authors have no conflicting financial interests.

References

1. Kunz LIZ, Lapperre TS, Timens W, Kerstjens HAM, Schadewijk A, Vonk JM, Sont JK, Snoeck-Strob JB, Postma DS, Sterk PJ, Hiemstra PS, Hacken ten NHT, van Schadewijk A, Snoeck-Stroband JB. Airway inflammation in COPD after long-term withdrawal of inhaled corticosteroids. *The European Respiratory Journal* 2017; 49: 1600839.
2. Pilette C, Colinet B, Kiss R, André S, Kaltner H, Gabius H, Delos M, Vaerman J, Decramer M, Sibille Y. Increased galectin-3 expression and intra-epithelial neutrophils in small airways in severe COPD. *The European respiratory journal* 2007; 29: 914-22.
3. Gompertz S, O'Brien C, Bayley DL, Hill SL, Stockley RA. Changes in bronchial inflammation during acute exacerbations of chronic bronchitis. *The European respiratory journal* 2001; 17: 1112-9.
4. Stănescu D, Sanna A, Veriter C, Kostianev S, Calcagni PG, Fabbri LM, Maestrelli P. Airways obstruction, chronic expectoration, and rapid decline of FEV1 in smokers are associated with increased levels of sputum neutrophils. *Thorax* 1996; 51: 267-71.
5. Donaldson GC, Seemungal TAR, Patel IS, Bhowmik A, Wilkinson TMA, Hurst JR, Maccallum PK, Wedzicha JA. Airway and systemic inflammation and decline in lung function in patients with COPD. *Chest* 2005; 128: 1995-2004.
6. Hogg JC, Chu F, Utokaparch S, Woods R, Elliott WM, Buzatu L, Cherniack RM, Rogers RM, Sciurba FC, Coxson HO, Paré PD. The nature of small-airway obstruction in chronic obstructive pulmonary disease. *The New England journal of medicine* 2004; 350: 2645-53.
7. O'Donnell RA, Peebles C, Ward JA, Daraker A, Angco G, Broberg P, Pierrou S, Lund J, Holgate ST, Davies DE, Delany DJ, Wilson SJ, Djukanovic R. Relationship between

peripheral airway dysfunction, airway obstruction, and neutrophilic inflammation in COPD. *Thorax* 2004; 59: 837-42.

8. Adams DH, Lloyd AR. Chemokines: leucocyte recruitment and activation cytokines. *Lancet (London, England)* 1997; 349: 490-5.

9. Beeh KM, Kornmann O, Buhl R, Culpitt SV, Giembycz MA, Barnes PJ. Neutrophil chemotactic activity of sputum from patients with COPD: role of interleukin 8 and leukotriene B4. *Chest* 2003; 123: 1240-7.

10. Murdoch C, Finn A. Chemokine receptors and their role in inflammation and infectious diseases. *Blood* 2000; 95: 3032-43.

11. Mócsai A, Walzog B, Lowell CA. Intracellular signalling during neutrophil recruitment. *Cardiovascular research* 2015; 107: 373-85.

12. Selvatici R, Falzarano S, Mollica A, Spisani S. Signal transduction pathways triggered by selective formylpeptide analogues in human neutrophils. *European Journal of Pharmacology* 2006; 534: 1-11.

13. Sapey E, Stockley JA, Greenwood H, Ahmad A, Bayley D, Lord JM, Insall RH, Stockley RA. Behavioral and structural differences in migrating peripheral neutrophils from patients with chronic obstructive pulmonary disease. *American Journal of Respiratory and Critical Care Medicine* 2011; 183: 1176-86.

14. Wang S, Rosenberger CL, Bao Y, Stark JM, Harrod KS. Clara cell secretory protein modulates lung inflammatory and immune responses to respiratory syncytial virus infection. *Journal of immunology (Baltimore, Md. : 1950)* 2003; 171: 1051-60.

15. Pilon AL. Rationale for the development of recombinant human CC10 as a therapeutic for inflammatory and fibrotic disease. *Annals of the New York Academy of Sciences* 2000; 923: 280-99.
16. Knabe L, Fort A, Chanez P, Bourdin A. Club cells and CC16: another “smoking gun?” (With potential bullets against COPD). *The European respiratory journal* 2015; 45: 1519-20.
17. Gamez AS, Gras D, Petit A, Knabe L, Molinari N, Vachier I, Chanez P, Bourdin A. Supplementing defect in Club Cell Secretory Protein attenuates airway inflammation in COPD. *Chest* 2014.
18. Laucho-Contreras ME, Polverino F, Gupta K, Taylor KL, Kelly E, Pinto-Plata V, Divo M, Ashfaq N, Petersen H, Stripp B, Pilon AL, Tesfaigzi Y, Celli BR, Owen CA. Protective role for club cell secretory protein-16 (CC16) in the development of COPD. *The European respiratory journal* 2015; 45: 1544-56.
19. Pilette C, Godding V, Kiss R, Delos M, Verbeken E, Decaestecker C, de Paepe K, Vaerman JP, Decramer M, Sibille Y. Reduced epithelial expression of secretory component in small airways correlates with airflow obstruction in chronic obstructive pulmonary disease. *American Journal of Respiratory and Critical Care Medicine* 2001; 163: 185-94.
20. Guerra S, Halonen M, Vasquez MM, Spangenberg A, Stern DA, Morgan WJ, Wright AL, Lavi I, Tarès L, Carsin A, Dobaño C, Barreiro E, Zock J, Martínez-Moratalla J, Urrutia I, Sunyer J, Keidel D, Imboden M, Probst-Hensch N, Hallberg J, Melén E, Wickman M, Bousquet J, Belgrave DCM, Simpson A, Custovic A, Antó JM, Martinez FD. Relation between circulating CC16 concentrations, lung function, and development of chronic obstructive pulmonary disease across the lifespan: a prospective study. *The Lancet. Respiratory medicine* 2015; 3: 613-20.

21. Hurst JR, Vestbo J, Anzueto A, Locantore N, Müllerova H, Tal-Singer R, Miller B, Lomas DA, Agusti A, Macnee W, Calverley P, Rennard S, Wouters EFM, Wedzicha JA. Susceptibility to exacerbation in chronic obstructive pulmonary disease. *The New England journal of medicine* 2010; 363: 1128-38.
22. Gras D, Bourdin A, Vachier I, de Senneville L, Bonnans C, Chanez P. An ex vivo model of severe asthma using reconstituted human bronchial epithelium. *The Journal of allergy and clinical immunology* 2012; 129: 1259-1266.e1.
23. Roberts RL, Gallin JI. Rapid method for isolation of normal human peripheral blood eosinophils on discontinuous Percoll gradients and comparison with neutrophils. *Blood* 1985; 65: 433-40.
24. Chaubey S, Ridley AJ, Wells CM. Using the Dunn chemotaxis chamber to analyze primary cell migration in real time. *Methods in molecular biology (Clifton, N.J.)* 2011; 769: 41-51.
25. Sali A, Blundell TL. Comparative protein modelling by satisfaction of spatial restraints. *Journal of molecular biology* 1993; 234: 779-815.
26. Pierce BG, Wiehe K, Hwang H, Kim B, Vreven T, Weng Z. ZDOCK server: interactive docking prediction of protein-protein complexes and symmetric multimers. *Bioinformatics (Oxford, England)* 2014; 30: 1771-3.
27. Stockley RA. Neutrophils and the pathogenesis of COPD. *Chest* 2002; 121: 151S-155S.
28. Laicho-Contreras ME, Polverino F, Tesfaigzi Y, Celli BR, Owen CA. Club Cell Protein 16 (CC16) Augmentation: A Potential Disease-modifying Approach for Chronic Obstructive Pulmonary Disease (COPD). *Expert opinion on therapeutic targets* 2016.

29. Tokita E, Tanabe T, Asano K, Suzaki H, Rubin BK. Club cell 10-kDa protein attenuates airway mucus hypersecretion and inflammation. *The European respiratory journal* 2014; 44: 1002-10.
30. Knabe L, Varilh J, Bergougnoux A, Gamez A, Bonini J, Alex, Pommier A, Pommier R, Petit A, Molinari N, Vachier I, Taulan-Cadars M, Bourdin A. CCSP G38A polymorphism environment interactions regulate CCSP levels differentially in COPD. *American journal of physiology. Lung cellular and molecular physiology* 2016; 311: L696-L703.
31. Katavolos P, Ackerley CA, Clark ME, Bienzle D. Clara cell secretory protein increases phagocytic and decreases oxidative activity of neutrophils. *Veterinary immunology and immunopathology* 2011; 139: 1-9.
32. Hoenderdos K, Condliffe A. The neutrophil in chronic obstructive pulmonary disease. *American journal of respiratory cell and molecular biology* 2013; 48: 531-9.
33. Yoshikawa S, Miyahara T, Reynolds SD, Stripp BR, Anghelescu M, Eyal FG, Parker JC. Clara cell secretory protein and phospholipase A2 activity modulate acute ventilator-induced lung injury in mice. *Journal of applied physiology (Bethesda, Md. : 1985)* 2005; 98: 1264-71.
34. Traves SL, Culpitt SV, Russell REK, Barnes PJ, Donnelly LE. Increased levels of the chemokines GROalpha and MCP-1 in sputum samples from patients with COPD. *Thorax* 2002; 57: 590-5.
35. Corhay JL, Moermans C, Henket M, Dang DN, Duysinx B, Louis R. Increased of exhaled breath condensate neutrophil chemotaxis in acute exacerbation of COPD. *Respiratory Research* 2014: 1-11.

36. Vasanthakumar G, Manjunath R, Mukherjee AB, Warabi H, Schiffmann E. Inhibition of phagocyte chemotaxis by uteroglobin, an inhibitor of blastocyst rejection. *Biochemical pharmacology* 1988; 37: 389-94.
37. Stripp BR, Lund J, Mango GW, Doyen KC, Johnston C, Hultenby K, Nord M, Whitsett JA. Clara cell secretory protein: a determinant of PCB bioaccumulation in mammals. *The American journal of physiology* 1996; 271: L656-64.
38. Mukherjee AB, Zhang Z, Chilton BS. Uteroglobin: A Steroid-Inducible Immunomodulatory Protein That Founded the Superfamily. *Endocrine Reviews* 2007; 28: 707-725.
39. Rennard SI, Dale DC, Donohue JF, Kanniss F, Magnussen H, R E, Sutherland ER, Sutherl, Watz H, Lu S, Stryszak P, Rosenberg E, Staudinger H. CXCR2 Antagonist MK-7123. A Phase 2 Proof-of-Concept Trial for Chronic Obstructive Pulmonary Disease. *American Journal of Respiratory and Critical Care Medicine* 2015; 191: 1001-11.
40. Schneider CS, Bhargav AG, Perez JG, Wadajkar AS, Winkles JA, Woodworth GF, Kim AJ. Surface plasmon resonance as a high throughput method to evaluate specific and non-specific binding of nanotherapeutics. *Journal of controlled release: official journal of the Controlled Release Society* 2015; 219: 331-344.

Figure 1: At steady state, ALI-reconstituted COPD airway epithelia maintained in a clean environment promoted an exaggerated neutrophilic chemotaxis.

A: Representative examples of healthy neutrophil migratory tracks induced by supernatants of ALI-reconstituted airway epithelium derived from a healthy control, a smoker and a patient with COPD. The last picture represents COPD neutrophil migratory tracks induced by COPD ALI supernatant epithelial cell cultures. The large red arrow at the right side of each picture represents the chemoattractant signal (30 minutes of phase time-lapse recordings).

B: The XFMI of healthy neutrophils on fMLP- and epithelial supernatant-gradients (control subjects n=4, smoker subjects n=3, COPD patients n=5). Epithelial supernatants from all groups increased neutrophil chemotaxis. COPD supernatants attracted neutrophils ($p = 0.0012$).

Approximately 100 tracked neutrophils by condition. Data were expressed as means \pm SEM. Paired comparisons were made using Mann-Whitney tests. Significant differences compared to controls were indicated by stars. Hash signs (#) indicate significant differences between compared groups.

Figure 2: Treating the airway epithelium with exogenous CCSP prevented CSE-induced neutrophil chemotaxis.

A: The XFMI of healthy neutrophils on a gradient of smoker ALI supernatants (n=7) stimulated by CSE with or without CCSP supplementation. CSE increased neutrophil chemotaxis ($p < 0.0001$). CCSP inhibited neutrophil chemotaxis when epithelia were exposed to CSE ($p < 0.0001$).

B: The XFMI of healthy neutrophils on a gradient of COPD ALI supernatants (n=8) stimulated by CSE with or without CCSP supplementation. CSE increased neutrophil chemotaxis ($p = 0.0056$). CCSP inhibited neutrophil chemotaxis when epithelia were exposed to CSE ($p = 0.0035$).

Approximately 100 tracked neutrophils by condition. Data were expressed as means \pm SEM. Paired comparisons were made using Mann-Whitney tests indicated by hash signs (#).

C and D: CSE-induced IL8 secretion by epithelial cells from smokers (n=7) and COPD patients (n=8), with or without CCSP supplementation. CSE tended to increase IL8. CCSP supplementation had no effect on IL8 secretion.

Figure 3: Stimulated-neutrophil migration was slowed down by CCSP.

A: The XFMI of healthy neutrophils on fMLP- or IL8- gradients with or without CCSP and with or without CXCR1/2 inhibitors. CCSP inhibited the chemotaxis of neutrophils stimulated by fMLP ($p < 0.0001$), but no difference was observed for IL8-induced neutrophil chemotaxis. No effects associated with CXCR1/2 inhibitors were observed.

B: The X endpoints of healthy neutrophils on fMLP- or IL8- gradients with or without CCSP and with or without CXCR1/2 inhibitors. fMLP was confirmed as a positive control and PBS (“Control”) as a negative one ($p < 0.0001$). CCSP inhibited the movement of neutrophils in the direction of the fMLP-gradient ($p < 0.0001$), and in the direction of the IL8-gradient ($p < 0.0001$) to a similar extent as found for CXCR1/2 inhibitors.

C: The distance travelled by healthy neutrophils on fMLP or IL8- gradients with or without CCSP and with or without CXCR1/2 inhibitors. CCSP inhibited the movement of neutrophils induced by the fMLP-gradient ($p = 0.0005$) and the IL8-gradient ($p < 0.0001$).

Approximately 100 tracked neutrophils by condition. All conditions were reproduced three times. Data were expressed as means \pm SEM. Paired comparisons were made using Mann-Whitney tests. Significant differences compared to controls were indicated by stars. Hash signs (#) indicate significant differences between compared groups.

Figure 4: ***In vitro*, CCSP interacted with IL8.**

A: Western Blot of IL8 immunoprecipitation detected with CCSP antibodies. Lane 1: negative control. Lane 2: positive controls (rhIL8+rhCCSP). Lane 3: rhIL8 immunoprecipitated with CCSP detected with CCSP antibodies (red band). rhCCSP immunoprecipitated with IL8 detected with IL8 antibodies (green band).

B, C: Graphs of CCSP immunostaining intensity of the IL8 immunoprecipitation and IL8 immunostaining intensity of the CCSP immunoprecipitation. No error bars are shown because the immunoprecipitation was performed once and then (c) reproduced with the inverse relationship.

D: Single-cycle kinetics of IL8 on immobilized CCSP: two-fold serial dilutions (62nM-1000nM) are injected on immobilized CCSP at a flow rate of 100 μ l/min with a contact time of 60s and 400s of dissociation after the last injection. The dotted line represents the fitting curve using a bivalent model. K_{a1} (1/Ms) = $(2.36\pm 0.06) \times 10^{+3}$; K_{d1} (1/s) = $(1.89\pm 0.04) \times 10^{-2}$; $KD1$ (M) = 8.02×10^{-6} ; χ^2 (RU²) = 0.675.

E: Superimposition of the hsCCSP-hsIL8 complex (in red) with the experimental structure of hsCXCR1 (C-terminal part)/hsIL8 complex (PDB: 1ILP; CXCR1 in green and IL8 in blue).

Figure 5: The small airway wall infiltration by neutrophils negatively correlated with the CCSP/IL8 ratio measured in the induced sputum of COPD patients undergoing surgery. Correlation between the neutrophilic infiltration of the small airway wall of COPD patients (n=10) and CCSP/IL8 ratio in their induced sputum collected before the surgery. The level of this negative correlation was as high as 0.75, indicating a greater intensity of neutrophilic infiltration.

Figure 1

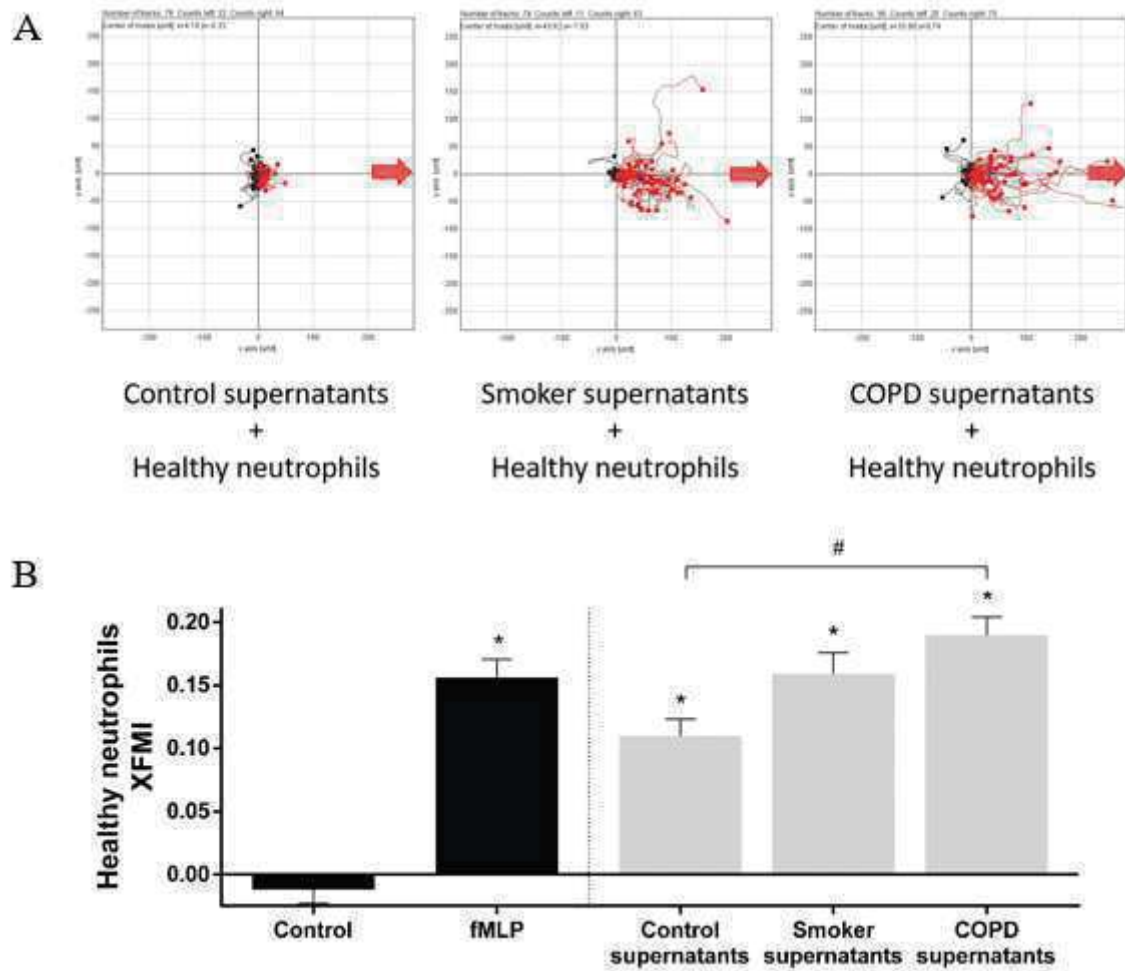
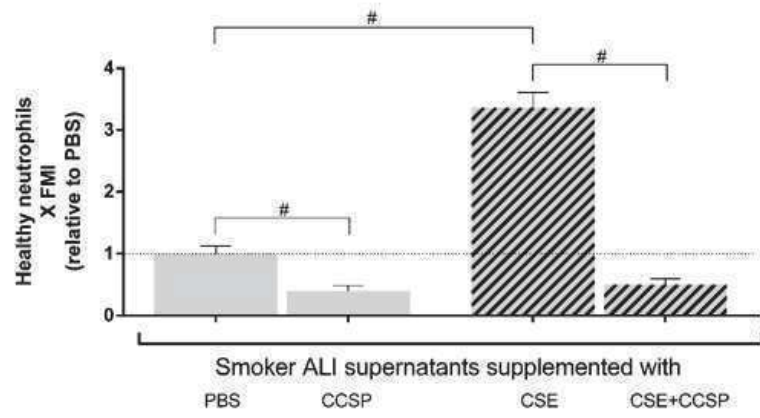
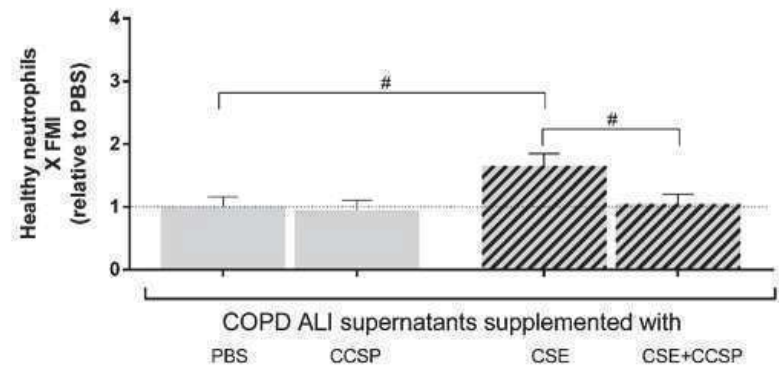


Figure 2

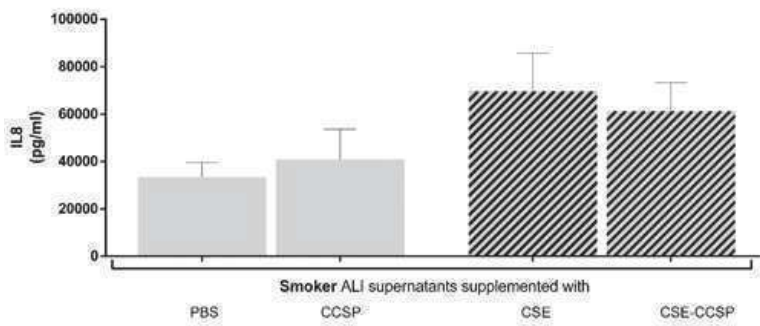
A



B



C



D

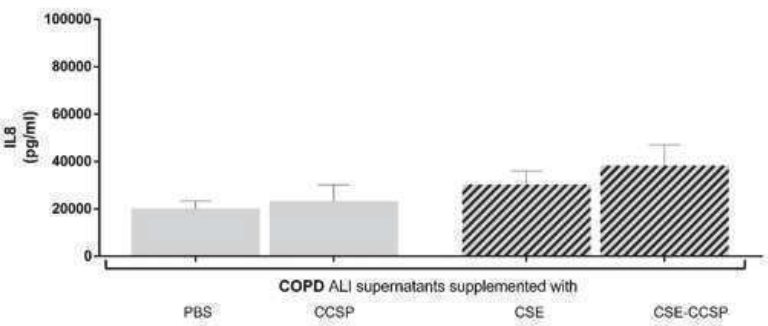
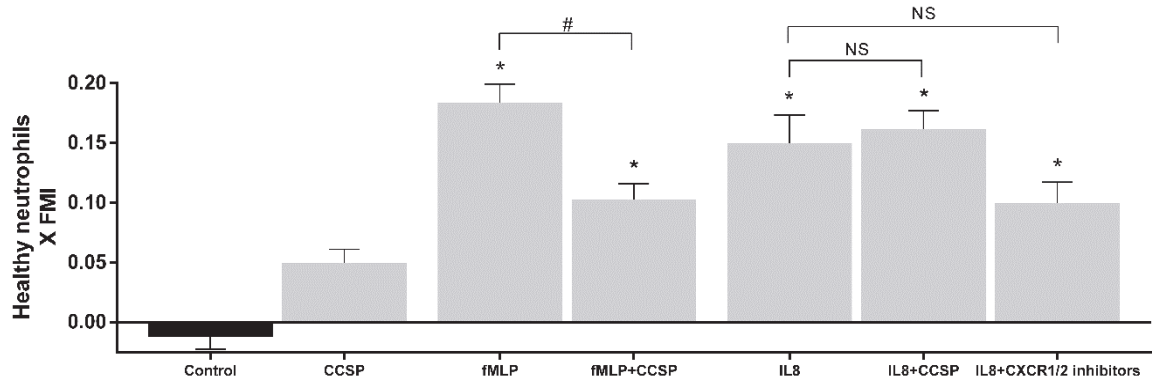
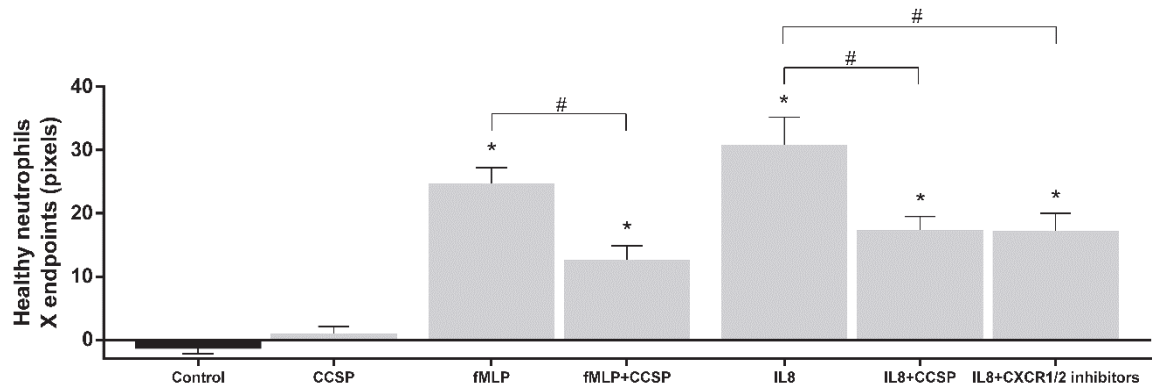


Figure 3

A



B



C

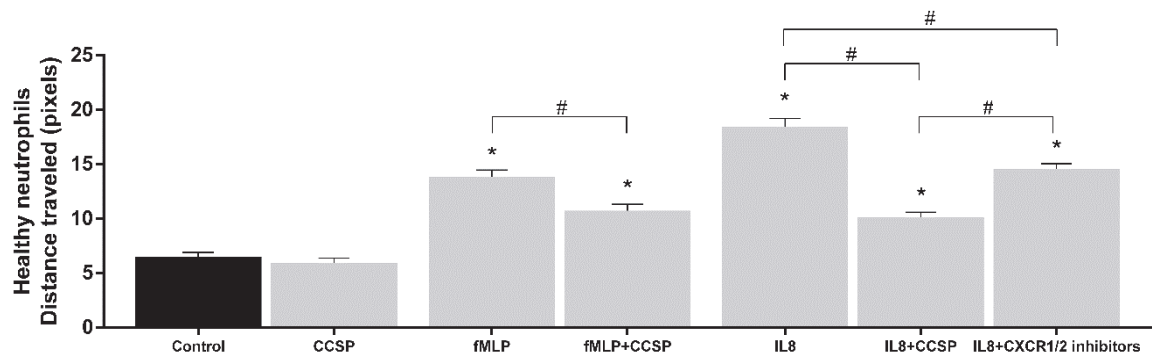


Figure 4

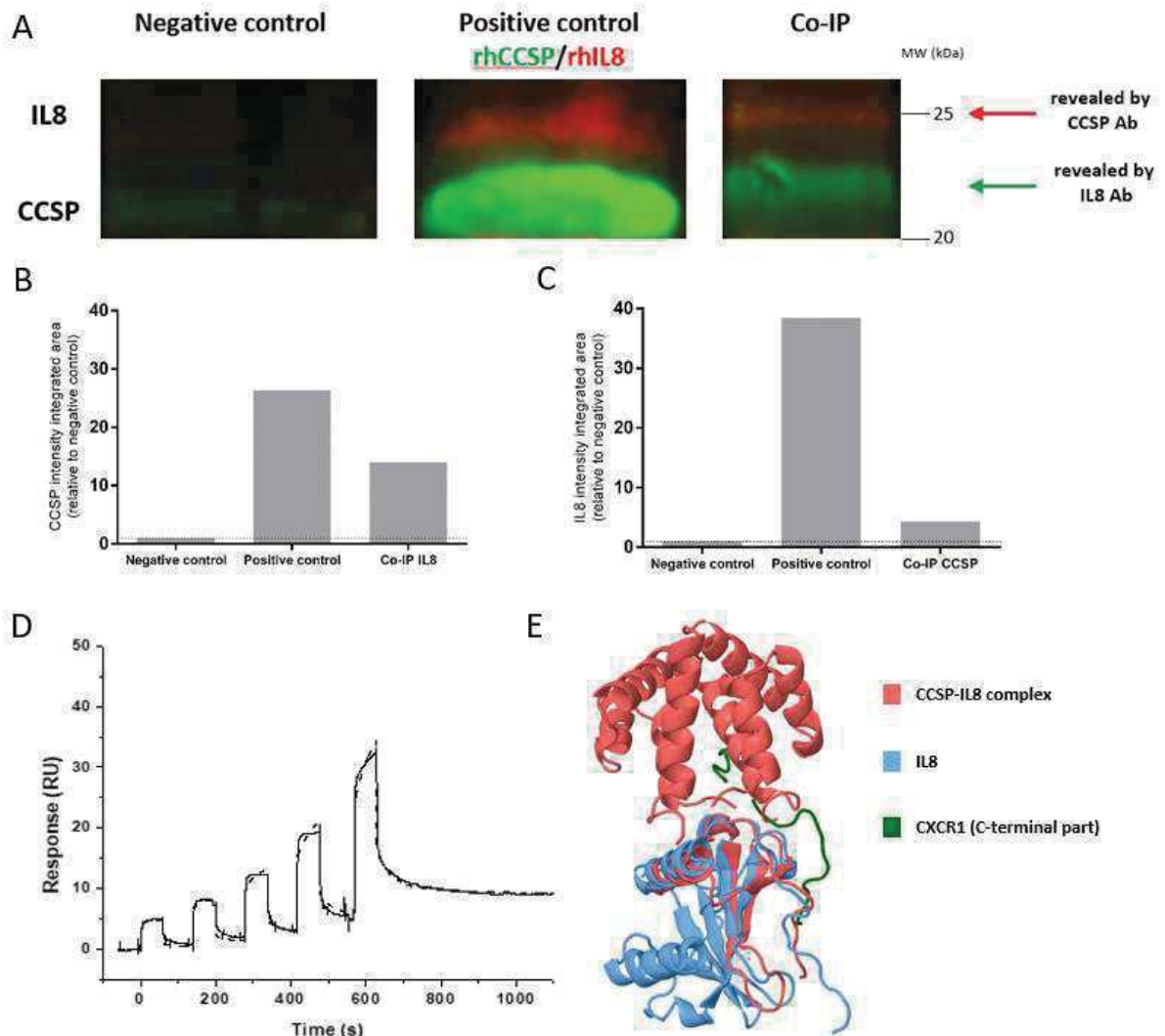
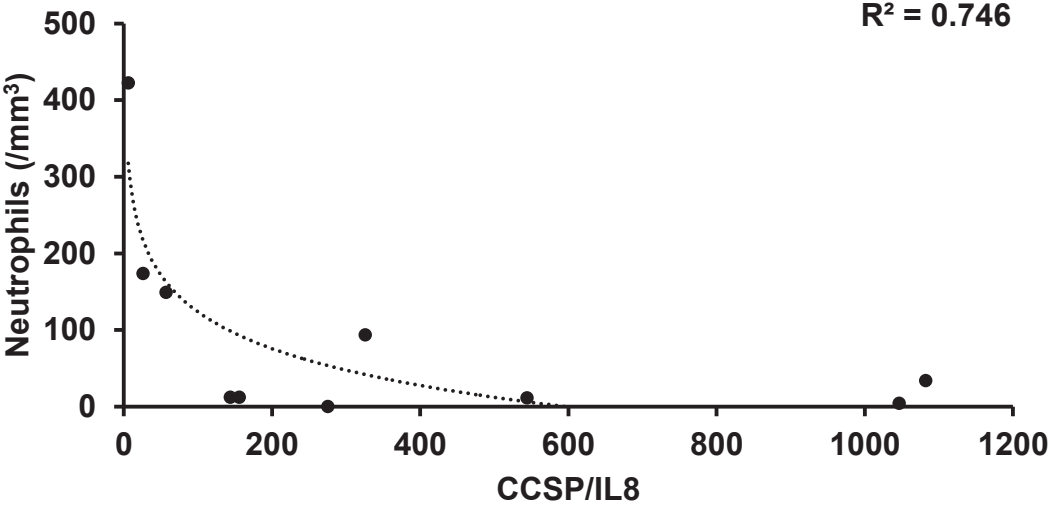


Figure 5



ONLINE SUPPLEMENT

CCSP counterbalances airway epithelial-driven neutrophilic chemotaxis

Lucie Knabe^{1,2}, Aurélie Petit², Charlotte Vernisse^{1,2}, Jérémy Charriot², Martine Pugnère³, Corinne Henriquet³, Souphatta Sasorith⁴, Nicolas Molinari⁵, Pascal Chanez⁶, Jean-Philippe Berthet⁷, Carey Suehs², Isabelle Vachier², Engi Ahmed², Arnaud Bourdin^{1,2}.

8. PhyMedExp, University of Montpellier, INSERM U1046, CNRS UMR 9214, France.
9. Department of Respiratory Diseases, CHU Montpellier, University of Montpellier, France.
10. IRCM, Institut de Recherche en Cancérologie de Montpellier, INSERM U1194, Université de Montpellier, Institut régional du Cancer de Montpellier, Montpellier, F-34298, France.
11. CHU de Montpellier, Laboratoire de Génétique Moléculaire, Montpellier, France; University of Montpellier, EA7402, Montpellier, France.
12. IMAG U5149, Department of Medical Information, CHU Montpellier, University of Montpellier, France.
13. C2VN - Inserm U1263 INRA 1260, AP-HM, Department of respiratory diseases, Aix Marseille University, France.
14. Department of Thoracic Surgery, CHU Montpellier, University of Montpellier, France.

Supplementary Methods

Chemotaxis assay and analysis

The chemotaxis assays were performed using Dunn chambers [24]. Peripheral neutrophils were placed on a coverslip and incubated for 20 min at 37°C. The coverslip was placed inverted onto the Dunn chamber. This slide comprises a bridge separating inner and outer concentric rings. The outer circle was filled with the studied solution. Subsequently, neutrophil chemotaxis along the chemoattractant gradient was observed on the bridge. Healthy neutrophil chemotaxis phenomena were studied using a negative control (PBS), a positive control (fMLP), and cell supernatants with or without previous stimulation, or with drugs alone. One part of the bridge region was filmed and snapshots were acquired at 1-min intervals during 30 min using a Zeiss inverted microscope equipped with a 20x objective. Chemotaxis was quantified using the XFMI value, which is the ratio of the distance travelled during the acquisition and the final position of the neutrophils on the x-axis in the direction of the chemoattractant gradient.

ImageJ software was used to track cells and analyse chemotaxis. All analyses were performed by a single analyst, blinded to the subject group.

Cell culture

Human primary bronchial epithelial cells (HBECs) were cultured under Air-Liquid Interface (ALI) conditions, adapted from Gras et al. and Gamez et al. [17, 22]. Bronchial epithelial cells from 4 control subjects, 10 smokers, and 13 COPD patients were mechanically dissociated and suspended in Bronchial Epithelial Growth Medium (BEGM). After seeding in multiwell plates coated with a solution of fibronectin and collagen, cells were expanded in a flask (0.75 cm²) and then plated (250,000 cells per well) on uncoated nucleopore membranes in a 1:1 mixture of BEGM and Dulbecco Modified Eagle Medium (DMEM) applied at the basal side

only to establish the ALI. Cells were maintained in culture for 28 days to obtain a differentiated cell population with a pseudostratified mucociliary epithelium. Cell cultures were maintained at 37°C under 5% CO₂. Cells were treated for 24 hours with or without cigarette smoke extract (CSE) and with or without CCSP supplementation (at the physiological concentration of 3µg/ml according to Gamez et al., Chest, 2015), applied at the apical surface. The supernatants were collected and stored until used for neutrophil experiments and CCSP/IL8 ELISA test (Biovendor/Diaclone).

Reagents and antibodies

Recombinant human (rh)CCSP and anti-CCSP antibody were purchased from Biovendor (Brno, Czech Republic). rhIL8 and fMLP were purchased from Sigma-Aldrich. Anti-IL8 antibody was purchased from Santa Cruz. Anti-CXCR1 antibody was purchased from R&D systems and CXCR2 inhibitor from Tocris.

Co-immunoprecipitation

To detect whether a potential interaction exists between CCSP and IL8, co-immunoprecipitation and immunoblotting were performed using anti-Protein A Sepharose 4 Fast Flow magnetic beads (GE Healthcare). Briefly, mouse anti-human IL8 antibodies were used to immunoprecipitate rhIL8 and rhCCSP. If rhIL8/rhCCSP bound covalently, a complex will be formed and will attach to anti-IL8 antibodies. To confirm our results, rabbit anti-human CCSP antibodies were also used to immunoprecipitate the rh proteins. The immune complexes were incubated with anti-Protein A Sepharose magnetic beads and captured on a magnetic beaded support to immobilize them. Any proteins not precipitated on the beads were washed away. Finally, the complexes were recovered, denatured and analysed by SDS-PAGE gel electrophoresis and Western blotting. The amount of rhIL8/rhCCSP that co-immunoprecipitated with anti-IL8 antibodies was determined from immunoblots developed

with anti-CCSP antibodies (1:500). Inversely, the amount of rhIL8/rhCCSP that co-immunoprecipitated with anti-CCSP antibodies was determined from immunoblots developed with anti-IL8 antibodies (1:500). Rh proteins without antibody were used as a negative control. A solution of rhCCSP/rhIL8 was used as a positive control for CCSP and IL8 expressions. All immunoblots were developed and quantified by using the Odyssey Infrared Imaging System (LICOR Biosystems) and infrared-labelled secondary antibodies.

Surgical lung samples and induced sputum collection

10 COPD patients scheduled for lung removal because of small peripheral lung lesions consented to participate in this study (AOI 2000, CPP 000901, DGS 2001/0075). All adequate samples were collected 3 to 5 days before surgery according to international guidelines and processed for analyses (Djukanovic et al., Eur Respir J Suppl, 2002). Before sputum induction, all subjects underwent spirometry before and 10 min after inhalation of 200 µg salbutamol by metered-dose inhaler. Hypertonic saline was nebulised with an ultrasonic nebuliser (DP 100 Syst'am; Paris, France). This nebuliser generates particles with a mean mass aerodynamic diameter of 4.5 µm and has an output of 2.4 mL·min⁻¹. Subjects inhaled hypertonic saline solution for 5-min periods up to 30 min, and were asked to rinse their mouth out with water before induction to avoid salivary contamination. The concentration of saline was increased, if possible, at intervals of 10 min (two nebulisations of each concentration) from 3% to 4% to 5%. Spirometry was repeated at 5-min intervals throughout the procedure and immediately after sputum induction was completed. At the end of the test, a nebulisation with bronchodilators was given.

The concentration of saline was not increased if the FEV₁ fell by 10% or more from the post-bronchodilator value. Sputum induction was discontinued if the FEV₁ declined >20% or if troublesome symptoms occurred (i.e., dyspnoea, wheezing, severe cough). Selected sputum plugs from saliva were then analysed. The volume of the induced sputum plugs was

determined and overlaid with an equal volume of 0.1% dithiothreitol (Sputalysin 10%; Behring Diagnostics Inc., Somerville, NJ, USA). The sample was then vortexed and placed in a shaking water bath at 37°C for 30 min. The homogenised sample was centrifuged (GR4.22; Jouan, St Herblain, France) at 2,000 rpm (400 × g) for 10 min. The supernatant was aspirated and frozen at -80°C for later analysis. ELISA tests were used in order to assess CCSP (Biovendor) and IL-8 (Diacclone) after adequate dilution of the samples (1:1000 and 1:2).

Lung histology

At the time of surgery, a lung slice at distance from the neoplastic lesion was provided by the surgeon. It was first inflated with a needle mounted on a syringe and then fixed by immersion in formalyn 4% then embedded in paraffin. Samples of fixed tissue were processed into paraffin blocks, cut into sections that were 4 to 5 micrometers thick, and placed on glass slides. Blocks were fully cut until exhausted in order to reach at least 6 airways per patient. Hematoxylin eosin staining was used to perform small airway morphometry analysis. Briefly, adequately orientated small airways were delineated using an image analyzer (AnalySIS 7.2 for Windows, Olympus Soft Imaging Solutions, Muenster, Germany) linked to a CCD camera (Sony DXC950P, Sony Group, Tokyo, Japan) connected to a light microscope (Olympus BHS, Olympus Optical, Tokyo, Japan).

Immunohistochemistry

Sections of pre-identified small airways were stained separately to identify polymorphonuclear neutrophils (Neutrophil Elastase NE, Dako-cytomation, dilution 1:50). Control sections were treated with mouse IgG1 isotype at the same dilution. Manual cells counts were performed within each bronchioli wall at 100 micrometers maximal depth and expressed as a number/mm² of submucosal area.

Statistical analysis

Clinical data were expressed as means \pm SEM. The effect of supernatants obtained from COPD patients, smokers and control subjects were compared using Kruskal-Wallis tests for quantitative data and Fisher tests for qualitative data. Chemotactic data were expressed as means \pm SEM. Paired comparisons were made using Mann-Whitney tests. Data were considered statistically significant at a p-value <0.05 . All graphical data and statistical analyses were generated with GraphPAD Prism software (Version 6.0).

Supplementary Tables and Figures

Table S1. Subject baseline characteristics: neutrophil donors.

	Healthy controls	COPD
N	5	5
Age, years (mean \pm SEM)	42 \pm 5.8	68 \pm 1.2
Gender [n (% male)]	1 (20)	4 (80)
Smoking history, pack years (mean \pm SEM)	0 \pm 0.0	60 \pm 13
Smoking status [n (%weaned >1 year)]	NA	5 (100)
FEV ₁ , % predicted (mean \pm SEM)	106 \pm 4.0	29.0 \pm 5.3
FEV ₁ /FVC (mean \pm SEM)	83.8 \pm 3.6	44.0 \pm 6.1
Treatments:		
ICS (n)	0	0
LABA (n)	0	5
LAMA (n)	0	5

Definition of abbreviations: FEV₁, forced expiratory volume in 1 s; FVC, forced vital capacity; ICS, inhaled corticosteroid; LABA, long acting β agonist; LAMA, long acting muscarinic agonist

Table S2. Subject baseline characteristics: ALI cultures.

	Healthy controls	Smokers	COPD	p- value
n	4	10	13	NA
Age, years (mean \pm SEM)	48 \pm 9.9	59 \pm 4.7	61 \pm 2.0	0.405
Gender [n(%male)]	2 (50)	7 (70)	8 (62)	0.774
Smoking history, pack years (mean \pm SEM)	0.75 \pm 0.7	34 \pm 5.6	46 \pm 6.6	0.005
Smoking status [n (%weaned >1 year)]	4 (100)	5 (50)	7 (54)	0.196
FEV ₁ , % predicted (mean \pm SEM)	87.8 \pm 3.7	109 \pm 5.3	50.8 \pm 7.2	< 0.0001
FEV ₁ /FVC (mean \pm SEM)	82.3 \pm 4.3	82.0 \pm 3.0	53.4 \pm 5.8	0.0015
Treatments				
ICS (n)	0	0	0	NA
LABA (n)	0	0	13	NA
LAMA (n)	0	0	13	NA

Definition of abbreviations: FEV₁, forced expiratory volume in 1 s; FVC, forced vital capacity; ICS, inhaled corticosteroid; LABA, long acting β agonist; LAMA, long acting muscarinic agonist

Figure S1

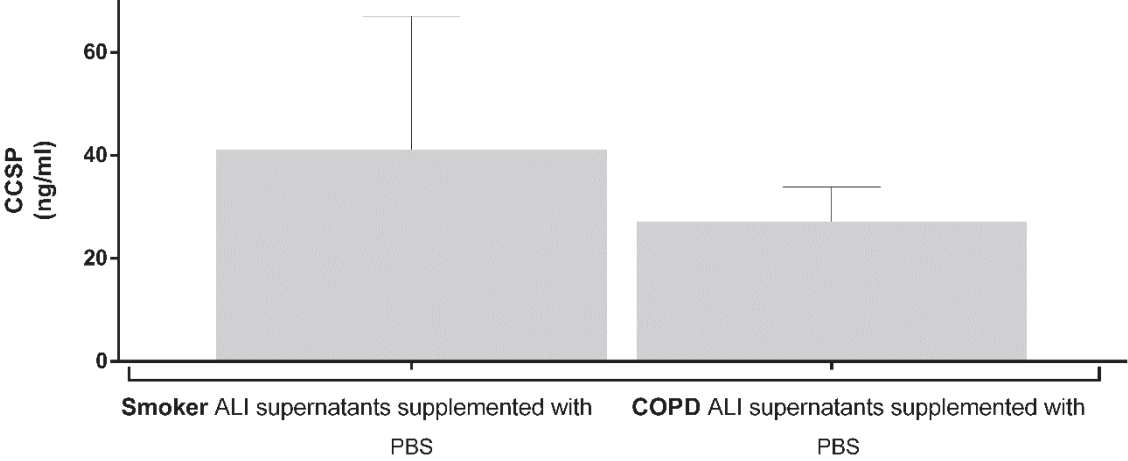


Figure S2

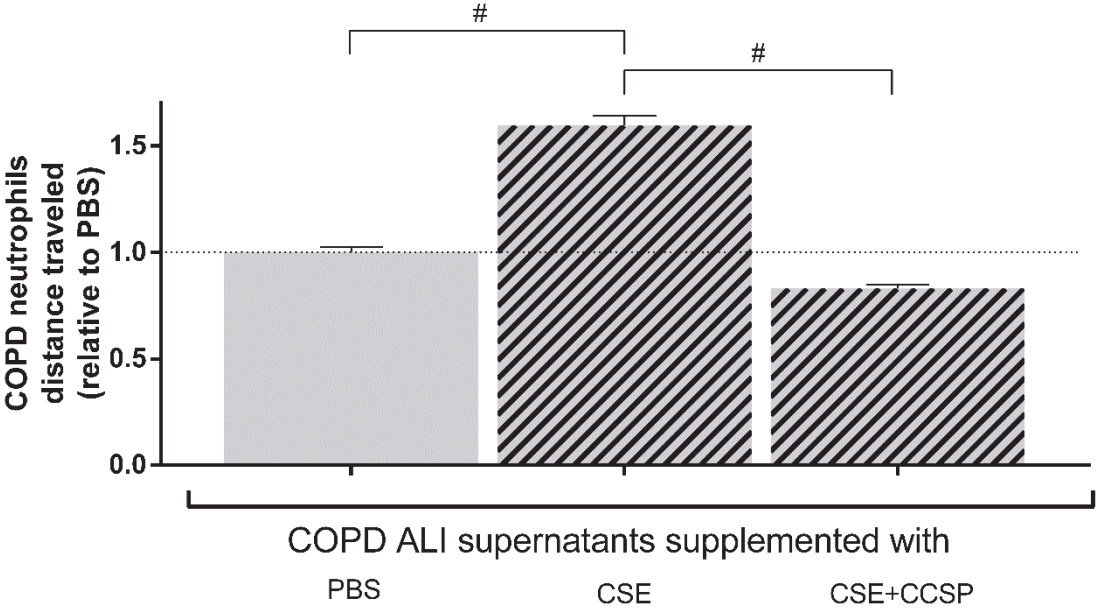
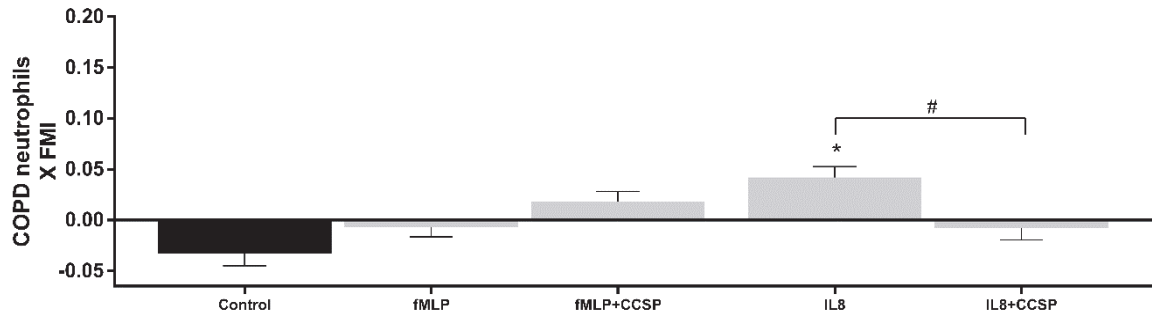
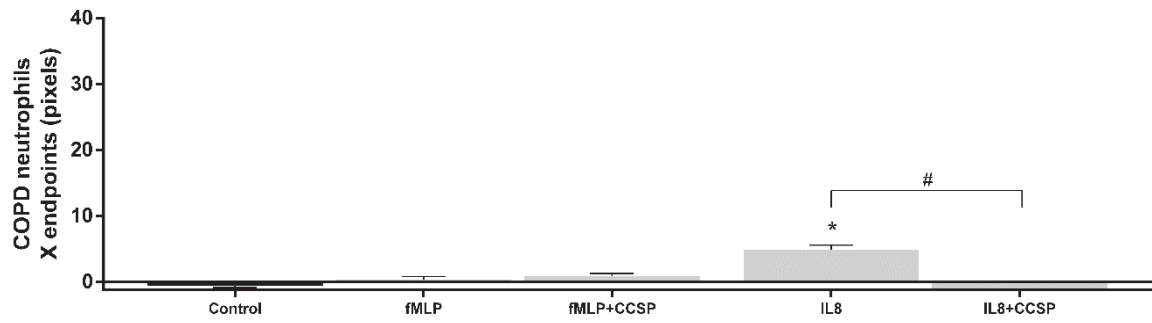


Figure S3

A



B



C

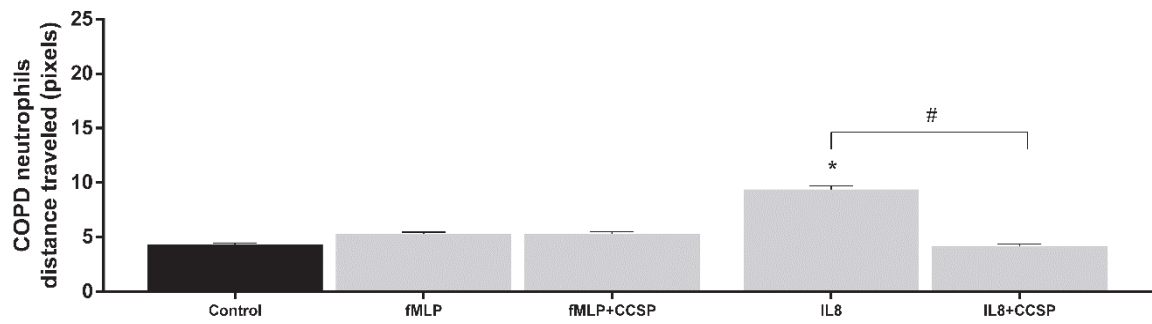


Figure S1: Baseline CCSP secretion.

CCSP secretion by epithelial cells from smokers (n=7) and COPD patients (n=8). CCSP secretion tended to be reduced in COPD cells compared to those from smokers.

Figure S2: Treating the airway epithelium with exogenous CCSP prevented CSE-induced COPD neutrophil chemotaxis.

The distance travelled by COPD neutrophils on a gradient of COPD ALI supernatants (n=8) stimulated by CSE with or without CCSP supplementation. Since the latter are disoriented, considering the distance travelled by the neutrophils was a better measure for demonstrating that CCSP had the same effect on COPD neutrophils as on healthy neutrophils. Indeed, CCSP inhibited COPD neutrophil recruitment when exposed to CSE ($p < 0.0001$).

Approximately 100 tracked neutrophils by condition. Data were expressed as means \pm SEM. Paired comparisons were made using Mann-Whitney tests indicated by hash signs (#).

Figure S3: Stimulated-COPD neutrophil migration was slowed down by CCSP.

A: The XFMI of COPD neutrophils on fMLP- or IL8- gradients with or without CCSP. CCSP inhibited the chemotaxis of neutrophils stimulated by IL8 ($p < 0.0001$).

B: The X endpoints of COPD neutrophils on fMLP- or IL8- gradients with or without CCSP. CCSP inhibited the neutrophil movement in the direction of the IL8-induced gradient ($p < 0.0001$).

C: The distance travelled by COPD neutrophils on fMLP- or IL8- gradients with or without CCSP. CCSP inhibited the neutrophil movement induced by IL8 ($p < 0.0001$).

Approximately 100 tracked neutrophils by condition. All conditions were reproduced three times. Data were expressed as means \pm SEM. Paired comparisons were made using Mann-Whitney tests. Significant differences compared to controls were indicated by stars. Hash signs (#) indicated significant differences between compared groups.




ORIGINAL ARTICLE

WILEY

Asthma and Rhinitis

Goblet cell hyperplasia as a feature of neutrophilic asthma

Khuder Alagha^{1,2} | Arnaud Bourdin^{1,3,4}  | Charlotte Vernisse^{3,4} | Céline Garulli² |
 Céline Tummino⁵ | Jérémy Charriot¹ | Isabelle Vachier¹ | Carey Suehs¹ |
 Pascal Chanez^{2,5} | Delphine Gras²

¹Département de Pneumologie et Addictologie, University of Montpellier, Montpellier, France

²Aix Marseille University, INSERM, INRA, C2VN, Marseille, France

³PhyMedExp, Hôpital Arnaud de Villeneuve, INSERM U1046, CNRS, UMR 9214, University of Montpellier, Montpellier, France

⁴CHU Montpellier, Montpellier, France

⁵Clinique des Bronches, Allergies et Sommeil, Hôpital Nord, AP-HM, Aix Marseille Université Marseille, Marseille, France

Correspondence

Delphine Gras, Laboratoire d'Immunologie, Hôpital de la Conception, C2VN - Inserm U1263 INRA 1260, Marseille, France.
 Email: Delphine.GRAS@univ-amu.fr

Funding information

PHRC inter regional and ANR and RRR and COBRA; PHRC IR AP-HM 2013-14; ANR-13-BSV5-0015-02 Mucocil; RC-Ext CHU Montpellier PROM-9244.

Summary

Background: Goblet cell hyperplasia (GCH) is a pathological finding classically reported across asthma severity levels and usually associated with smoking. Multiple biological mechanisms may contribute to excessive mucus production.

Objective: We aimed to decipher the clinical meanings and biological pathways related to GCH in non-smokers with asthma.

Methods: Cough and sputum assessment questionnaire (CASA-Q) responses at entry and 1 year later were compared to clinical and functional outcomes in 59 asthmatic patients. GCH was assessed through periodic-acid shift (PAS) staining on endobronchial biopsies obtained at entry in a subset of 32 patients.

Results: Periodic-acid shift-staining analysis revealed a double wave distribution discriminating patients with (>10% of the epithelial area) or without GCH. CASA-Q scores were mostly driven by overall asthma severity ($P < 0.0001$). CASA-Q scores remained stable at 1 year and were independently associated with BAL eosinophil content irrespective of the presence of GCH. GCH was unrelated to the presence of bronchiectasis at CT, GERD or chronic rhinosinusitis, but correlated well with neutrophilic inflammatory patterns observed upon BAL cellular analysis ($P = 0.002$ at multivariate analysis). BALF bacterial loads were unrelated to GCH or to CASA-Q.

Conclusions and Clinical Relevance: Goblet cell hyperplasia is disconnected from chronic cough and sputum when assessed by a specific questionnaire. GCH is related to neutrophilic asthma whereas symptoms are related to airway eosinophilia. The clinical counterpart of GCH is unlikely assessed by the CASA-Q.

KEYWORDS

asthma, goblet cell hyperplasia, mucus

1 | INTRODUCTION

Chronic bronchitis, defined as recurrent and prolonged cough and sputum production, is commonly associated with COPD, though its clinical significance remained controversial.¹ Interestingly, cough and chronic mucus production are non-specific symptoms also often reported by asthmatic patients. Moreover, autopsy reports

of fatal asthma cases have reported excessively narrowed airways completed by spectacular mucus casts.^{2,3} Increased goblet cells and MUC5AC airway epithelial staining in asthma have been described before and this is now clearly acknowledged as a significant component of asthma pathophysiology.⁴⁻⁶ Interestingly, these outcomes are usually not assessed during asthma care, nor in clinical trials.

New insights into the mechanisms involved in excessive mucus production and goblet cell hyperplasia suggest a predominant role for IL-13 and T2 related inflammation.^{7,8} Unfortunately, most of the IL-13 targeting mAbs failed to improve severe asthma outcomes.^{9,10} In patients with high levels of periostin as a surrogate marker of T2-driven asthma, FEV1 improvements were reported with lebrikizumab—a monoclonal antibody directed against IL13, but no data were provided in terms of prevention or changes in mucus hypersecretion.¹¹ Likewise, no data related to mucus hypersecretion were provided in both tralokinumab or dupilumab recent clinical trials reports.

Symptoms of mucus hypersecretion are mostly subjective and may reflect not only airway goblet cell hyperplasia (GCH) or bronchial gland enlargement but also other mechanisms such as post-nasal drip or GERD, which are likely to be confounding sources.¹² Endoscopists familiar with the assessment of chronic airway diseases often describe discrepancies between reported symptoms and endoscopic findings (high level of complaint but no secretion found in the airways and vice versa).¹³

These symptoms may fluctuate with the level of airway inflammation and whether it should be considered as a phenotypic characteristic remains unknown.¹⁴ Interestingly, the “Cough And Sputum Assessment Questionnaire” (CASA-Q) has been developed in COPD in order to standardize the quantification of these symptoms.¹⁵

In the present study, we investigated the relationships between the potential clinical phenotype of cough and mucus production in asthma with various clinical, pathological and biological parameters in order to assess its potential relevance for pinpointing diagnoses and management.

2 | MATERIAL AND METHODS

2.1 | Patients

In 2010-2012, we enrolled 59 patients with asthma referred to our specialized tertiary expert centre for asthma management who consented to participate in the COBRA cohort (IDRCB:2008-A00294-51).¹⁶ Thirty-two of them consented to undergo bronchoscopy examination. The present study was approved by an independent Ethics Committee (*Comité de Protection des Personnes d'Ile de France I*; reference number 09-11962) and written-informed consent was obtained for all participants at inclusion before any procedure. Active or past smoking (with a smoking history of 10 pack-years or more) was exclusion criteria. The flow chart for the present study is detailed in Figure 1.

In addition to all the demographic, clinical and physiologic parameters recorded during routine visits, CASA-Q forms were filled out by the patients before bronchoscopy during the initial visit and again at the second visit (1 year later). CT scans were also routinely performed at entry, and the presence of bronchiectasis (defined as a bronchus to vessel diameters ratio greater or equal to 1.5 and then quoted as present or absence by the expert radiologist blinded to any clinical parameters) was recorded for this specific study.

2.2 | Bronchoscopy

Briefly, a flexible bronchoscope was inserted by the nose under local anaesthesia. A BAL was performed according to routine practice in the right lower lobe by instillation and gentle suction of 50 mL of isotonic saline (twice). Endobronchial biopsies were taken in the left lower lobe as previously described.¹⁷ Two biopsies were immediately stored in formalin for subsequent paraffin-embedding. No safety issues arose during this study.

BAL samples were routinely assessed in order to measure total and differential cells counts and perform routine bacterial cultures. Bacterial cultures were considered positive only when a respiratory pathogen grew at a significant ($\geq 10^3$ cfu/mL) concentration.

2.3 | Staining procedure

Formalin-fixed, paraffin-embedded airway tissue sections (4 μ m) were used for staining. Sections were dewaxed and rehydrated. For morphology, we used Haematoxylin (TM) and Periodic-acid shift (PAS) specific staining to analyse epithelium and RBM thicknesses and mucous cell presence, respectively.

Pictures were obtained using a Nikon Eclipse NiE microscope equipped with a DS-Ri2 camera (Nikon, Tokyo, Japan). Images were captured at room temperature with NIS-Elements software (Nikon; version 4.3) at a resolution of 4908 \times 3264 pixels per manual exposure with fixed shutter time, gain amplification and illumination.

2.4 | Measurement of basal membrane, epithelial thickness and mucus production

Measurements of epithelium and basement membrane thickness were determined and were expressed as the average area/length ratio by using Wilson's method.^{18,19} In brief, a length of 1 mm of basement membrane at least was measured at $\times 40$ magnification by delineating the area and the length of the BM (corresponding more or less to 5 fields, where the orientation was estimated to be correctly perpendicular given the monolayer aspect of the surrounding

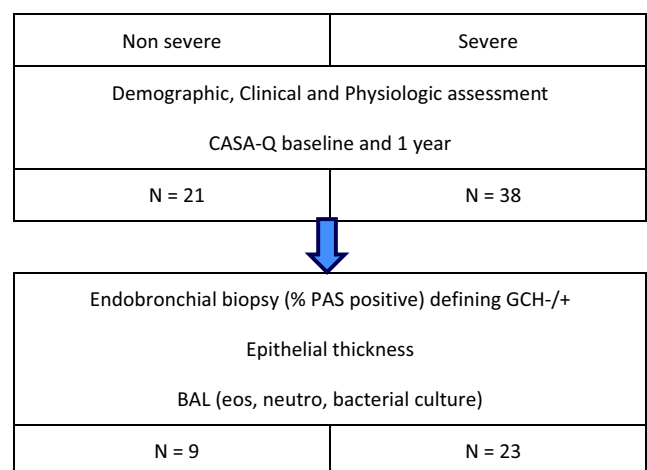


FIGURE 1 Flow chart

epithelium). PAS-staining quantification corresponded to the area of stained bronchial surface epithelium weighted by the bronchial epithelium thickness and was expressed as a percentage of staining intensity per μm using colour segmentation. All measurements were generated with an image analysis program (ImageJ; National Institutes of Health, Bethesda, Md).

2.5 | Statistical analysis

CASA-Q questionnaires were quantified according to the initial report¹⁵ (low scores denoting high levels of symptoms) and variability was assessed using paired *t* tests and linear R^2 regression

coefficients. We also tested the first domain of the CASA-Q score (dedicated to daily sputum production, whereas other domains address the burden of chronic sputum production, the level of cough and its impact).

Patients were divided by the intensity of the PAS staining as a GCH- and GCH+ group since a bimodal distribution clearly identified a clear cut-off value of 10% of the epithelial area stained by PAS.

Between-group comparisons were assessed using a Mann Whitney U test. Rho's Spearman correlation coefficients were computed when required. Data were presented as mean and standard deviation when normally distributed and as median and interquartiles otherwise.

TABLE 1 Patient characteristics

	Non-severe	Severe	P Value
N	21	38	
Age	53 (27)	51 (16)	0.52
Gender (% F)	57	65	0.71
Median BMI (interquartiles)	27 (24-31)	27 (24-29)	0.84
Disease duration (y)	33 (30)	26 (15)	0.12
Median age at onset (interquartile) (y)	36 (16-46)	27 (20-34)	0.16
Formerly smokers (%yes)	24	21	1
Smoking history (P/Y)	5.6 (2.5)	2 (1)	0.58
Exacerbations in the last 12 mos	0.5 (1)	2.9 (2)	<0.01
Bronchiectasis at CT (% yes)	43	50	0.80
GERD (% yes)	80	75	0.75
Rhinosinusitis (% yes)	86	92	0.66
Allergy (% with at least one positive skin prick test)	48	58	0.63
Positive bacterial BAL culture (%)	1 (5%)	3 (8%)	0.99
Blood eosinophils (cell/mm ³)	206 (145)	450 (590)	<0.01
Inhaled steroids (% with daily dose > 1000 μg eq beclo)	33	97	<0.01
Maintenance OCS (% yes)	0	50	<0.01
Median OCS daily dose mg/d (interquartile)	0	10 (20)	<0.01
LAMA n (% yes)	2 (9)	7 (18)	<0.01
SAMA n (% yes)	0 (0)	23 (61)	<0.01
LTRA n (% yes)	2 (9)	6 (16)	
Macrolides n (% yes)	0	3 (8)	0.61
FEV1 (% predicted value)	92 (30)	70 (25)	<0.01
FVC (% predicted value)	98 (24)	80 (22)	<0.01
VR (% predicted value)	118 (32)	141 (40)	<0.01
Reversibility (%)	5 (12)	12 (8)	<0.01
BAL Cellularity (1000 cell/mL)	107 (50.5)	153 (103)	<0.01
Eosinophils (%)	1.5 (2.25)	3.1 (4)	0.13
Neutrophils (%)	10 (14.7)	18 (19)	0.05
Lymphocytes (%)	6 (7.5)	8 (6)	0.12
Macrophages (%)	74 (15.2)	64 (27)	0.03
CASA-Q score at entry	62.2 (3.5)	33.9 (13)	<0.01
CASA-Q score at 1 y	62.8 (7)	33 (12)	<0.01

Data are presented as median with (interquartiles ranges) or percentages.

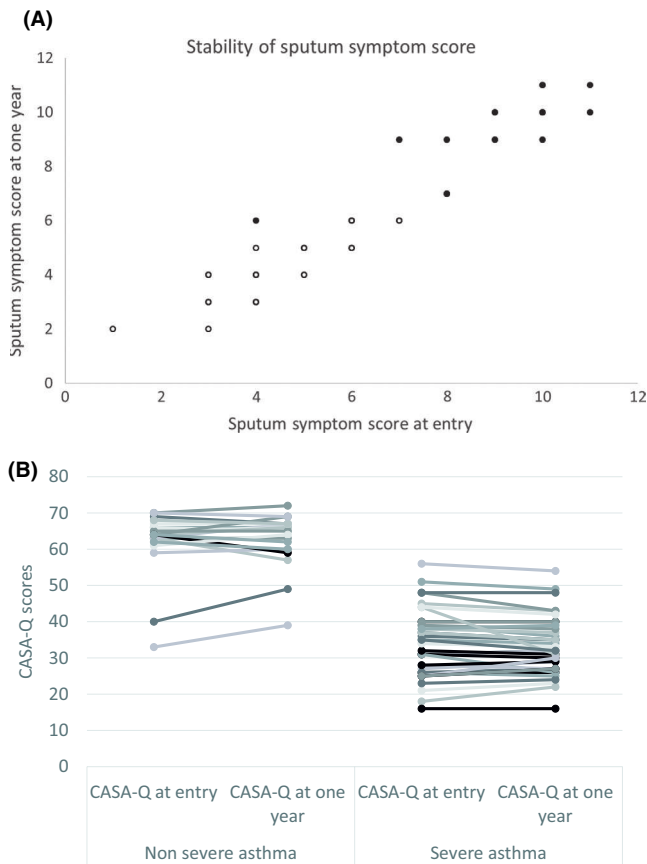


FIGURE 2 A, Linear regression between sputum symptom score at entry and at 1 y in severe (open circles) and non-severe (black circles) asthma patients. B, Stability of CASA-Q total score at entry and 1 y later among non-severe (left panel) and severe (right panel) asthma patients. (colour changes are just intending to improve clarity)

3 | RESULTS

Patient characteristics are presented in Table 1. Fifty-nine patients were enrolled and had complete follow-up at 1 year. Thirty-eight (64.5%) patients presented severe asthma as defined by the ERS/ATS task force: these patients were poorly controlled, with two exacerbations or more in the last 12 months while receiving a GINA step 4/5 treatment (half required a maintenance regimen with daily oral steroids). All others had non-severe asthma controlled with treatment below step 4 of the GINA scale (Table 1). CASA-Q values at entry and 1 year later showed high stability. Higher CASA-Q and "sputum domain" scores were recorded in severe versus non-severe asthmatics (Figures 2A,B). BAL culture was found positive for a respiratory pathogen in three severe and one non-severe asthma patients. No fungi were found.

Periodic-acid shift-staining analysis (Figure 3A) demonstrated a bimodal distribution distinguishing one group with stained areas below 10% (called GCH-) and one group with stained areas >10% (called GCH+). CASA-Q scores (both at entry and 1 year later) were not significantly different between the two groups (Figure 3B).

Patients with GCH had higher BAL neutrophil content (expressed as a percentage of total BAL leucocytes count), and thicker airway epithelia ($P < 0.001$). Absolute leucocytes counts differed between groups: BAL eosinophils 79.5 (79.9) in GCH+ vs 14.1 (17.8) in GCH- and BAL neutrophils 5.6 (3.8) vs 9.6 (12.5). Results were expressed as median and interquartile values.

Univariate and multivariate analysis were conducted to identify factors related to¹ CASA-Q at entry and 1 year later, and² GCH (Table 2). Interestingly, only BAL eosinophil content (expressed as a percentage of total BAL leucocytes count) was significantly and independently related to CASA-Q at entry, such that BAL eosinophilia was protective vis-à-vis cough and sputum symptoms. This was confirmed 1 year later, where asthma severity was found as an additional predictor. Age at onset did not affect any of these outcomes. In contrast, GCH based on PAS staining of the endobronchial biopsy was found to be independently associated with BAL neutrophilia (expressed as a percentage of total BAL leucocytes count). When patients were categorized as neutrophilic or eosinophilic according to classically reported thresholds (neutrophilic when >61% and eosinophilic when >1.9%), exact Fisher's tests failed to detect any relationship between GCH and the so-called inflammatory phenotype. Nonetheless, BAL neutrophilia significantly differed between groups ($28.0\% \pm 14.6$ vs $8.6\% \pm 6.2$, $P < 0.001$). Of note, BMI was not associated with the neutrophilic trait (26 ± 5 kg/m² in eosinophilic vs 29 ± 7 kg/m² in neutrophilic asthma patients, $P = 0.27$). Noteworthy, positive BAL bacterial culture, bronchiectasis at CT, GERD and rhinosinusitis were not significantly associated with GCH.

4 | DISCUSSION

Cough and sputum are troublesome symptoms often reported by asthmatic patients. In order to address the specificity of this phenotype, we queried chronic mucus production in lifelong non-smoking asthmatic patients. Interestingly, we found that the clinical phenotype assessed by measuring the cough and sputum questionnaire CASA-Q was very stable over 1 year, mostly associated with asthma severity. Moreover, BAL eosinophilia was found to be protective. Surprisingly, CASA-Q scores were not related to Goblet Cell Hyperplasia (GCH) assessed by the percentage of positive staining of goblet cells on endobronchial biopsies. Nor was it related to the ability of reconstituted ALI cultures to release mucin in vitro. Moreover, rhinosinusitis, GERD, bronchiectasis or the presence of bacteria in the BAL fluid were not related to this phenotype. Surprisingly, GCH was related to BAL neutrophilia.

Chronic mucus hypersecretion is classically seen as a feature of COPD and might be seen as an overlapping criterion between asthma and COPD,²⁰ whereas key studies demonstrated that GCH is a pathophysiological feature of asthma.⁴⁻⁶ Asthmatic patients often complain about these symptoms, and we found that it was associated with severe asthma. The clear discrimination between severe

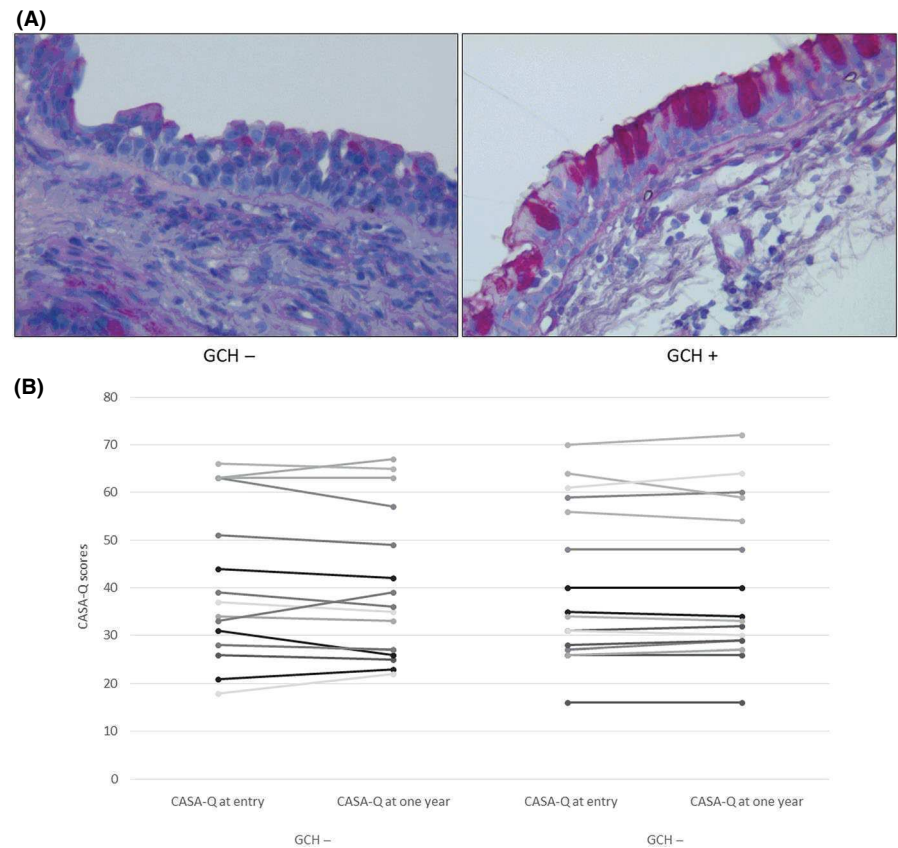


FIGURE 3 A, PAS staining in GCH+ and GCH- (representative pictures). B, Stability of CASA-Q total score at entry and 1 y later among patients without (left panel) and with (right panel) goblet cell hyperplasia (GCH). (colour changes are just intending to improve clarity)

asthma and COPD is not established according to symptoms or imaging parameters.²¹ For example, bronchiectasis is described on HRCT-scan images both in COPD and asthma.²²

Whereas T2 inflammation mostly through IL13 signalling is known to affect mucus hypersecretion in asthma, other known pathways such as EGFR appear more relevant to COPD, but here again overlap may exist.^{1,23,24} Indeed, in the SPIROMICS analysis, no relationships between T2 biomarkers and mucin concentration assessed in the induced sputum were found.

The CASA-Q questionnaire was highly stable over 1 year. This finding was expected according to clinical experience and previous reports. Indeed, patients were included and interviewed at steady state in order to limit the risk that an exacerbation could bias the responses. Although the four domains of the CASA-Q explore different items, the domain specifically related to sputum production was highly correlated to the total score, and so both analyses were found to provide exactly the same results. It seems that coughing is highly related to sputum complaints, even in asthma (at least in this population). Mucus biophysical properties including viscosity, elasticity and tenacity are likely more closely related to Patient Reported Outcomes and clearly deserves more focused studies using clinically approved rheometers.^{25,26}

Interestingly, BAL eosinophil counts expressed in percentages were unrelated with sputum production symptoms, whereas it is now considered as a surrogate T2 marker. GCH is in the predictive T2 model thought to occur especially as a consequence of excess of IL13.⁸ This is surprising given that IL-13, IL-5 and eotaxin are

released by T2 cells (both ILC2 and Th2) and are involved in the recruitment and activation of eosinophils. Previous studies^{6,27,28} have reported an association between sputum eosinophils and airway mucus in stable asthma. Charcot Leyden crystals have the potential to explain the link between T2 airway inflammation and mucus rheological properties.²⁹ Unfortunately, chronic mucus hypersecretion remained unaddressed in all recent trials that tested biologics directed towards T2 cytokines, including the anti IL-13 monoclonal antibodies lebrikizumab, tralokinumab and less specifically dupilumab. Indeed, most of the current literature associates mucus hypersecretion with viral and/or bacterial infection,^{30,31} bronchiectasis or with neutrophilic asthma.³² Noteworthy, neutrophilic asthma is frequently presented as a manifestation of asthma-COPD overlap, or associated with smoking asthma. LAMA or macrolides are potentially interfering with chronic mucus secretion, but the present study could not address this interesting issue; it clearly deserves additional studies. Macrolides were thought to interfere more with neutrophilic asthma,³³ but finally a significant reduction in the exacerbation rates were observed irrespective of the presence of T2-surrogate biomarkers.³⁴

As mentioned above, although BAL eosinophils appeared *unrelated* with high sputum symptom scores, BAL neutrophilia was associated with GCH.

Whether these are coincident findings, or inter-twined variables, or consequences of a common physiopathological pathway, remains unknown. Of note, targeting neutrophils in asthma was shown to improve certain asthma outcomes.³⁵

TABLE 2 Multivariate analyses identifying factors independently related to CASA-Q at entry and at 1 y, then to the presence of goblet cell hyperplasia (GCH) and mucin production in air-liquid interface (ALI) cultures

	Estimate	Std. Error	P-value
CASA-Q at entry			
(Intercept)	60.317	7.492	<0.001
Age (y)	0.063	0.098	0.522
Bronchiectasis	1.74	2.733	0.527
Severe vs non-severe	-30.681	3.653	<0.001
Duration of asthma	-0.017	0.102	0.871
Age at onset (y)	3.455	0.011	0.244
Exacerbations last 12 mos	0.84	1.004	0.407
GERD	-3.851	2.99	0.204
Rhinosinusitis	-1.566	4.247	0.714
Pack-years	0.2	0.169	0.242
BAL eosinophils (% leucocytes)	1.007	0.411	0.018
BAL neutrophils (% leucocytes)	-0.073	0.123	0.555
Positive bacterial BAL culture	3.98	6.617	0.550
CASA-Q at 1 y			
(Intercept)	60.24	6.196	<0.001
Age (y)	0.092	0.081	0.263
Bronchiectasis	1.056	2.261	0.643
Severe vs non-severe	-31.368	3.021	<0.001
Age at onset (y)	0.964	0.01	0.488
Duration of asthma (y)	-0.028	0.084	0.741
Exacerbations in the last 12 mos	0.716	0.831	0.393
GERD	-3.137	2.473	0.211
Rhinosinusitis	-1.676	3.513	0.635
Pack-years	0.15	0.14	0.288
BAL eosinophils (% leucocytes)	0.948	0.34	0.008
BAL neutrophils (% leucocytes)	-0.111	0.102	0.283
Positive bacterial BAL culture	5.082	5.473	0.358
Presence of GCH			
(Intercept)	-9.353	10.678	0.392
Age (y)	0.007	0.097	0.945
Bronchiectasis	0.637	2.443	0.797
Severe vs non-severe	7.855	5.267	0.152
Duration of disease (y)	-0.058	0.095	0.550
Age at onset (y)	6.022	1.022	0.322
Exacerbations in the last 12 mos	-1.572	0.83	0.073
GERD	2.291	2.823	0.427
Rhinosinusitis	0.196	3.621	0.957
Pack-years	-0.025	0.184	0.894
CASA-Q at 1 y	0.168	0.142	0.250
BAL eosinophils (% leucocytes)	0.002	0.404	0.997
BAL neutrophils (% leucocytes)	0.407	0.115	0.002
Positive bacterial BAL culture	-10.365	6.339	0.118

Airway mucus is a complex assembly of mucin, water, salts, inflammatory cells, desquamated epithelial cells, bacteria and exogenous particles, and the relative contribution of each of these components to symptoms is probably highly subject to variations among patients and diseases.

We further explored the symptoms reported by the patients and found that despite their stability, they were unrelated to any specific comorbid condition, such as GERD or rhinosinusitis.

The obvious limitation of the present report is the subjectivity of the symptoms reporting, even though a validated questionnaire was used. Other limitations include that GERD was rated according to patient declaration and CT scans were not quantitatively assessed.

Airway inflammation was presently assessed in the BAL, whereas classically asthma endotypes are determined from induced sputum samples³⁶ and it is rather unknown how the two overlap. We should also recall that patterns of airway inflammation are variable spontaneously or with corticosteroids,^{37,38} whereas the present study was based on a unique sample. Whether sputum neutrophil percentages or absolute numbers are more biologically relevant is worth a debate for the present study but also in general. It can be argued that mediator concentration in sputum would depend more on absolute rather than relative numbers³⁹ but this could not be confirmed in the present study.

The other potential explanation for our negative findings is that we could not address the bronchial gland contribution to symptoms. Finally, one may hypothesize that a little bit of each of these potential contributors may participate in sputum symptoms (ie, a little from the airway epithelium, a little from the nose and a little from the gut, for example), and in the end we believe that mucus hypersecretion should be seen as a component of all traits to be addressed in a future precision medicine strategy. Given our results, the CASA-Q is not adapted for achieving this goal.²¹

In conclusion, chronic mucus hypersecretion complaints among lifelong non-smoking (or very mild smoking) asthmatics are frequently seen in severe patients. Although very stable, this feature was unrelated to biopsy GCH phenotype. Interestingly, *in our study the neutrophilic phenotype was associated* with GCH, suggesting that this specific *phenotype* needs to be specifically targeted in clinical trials. Better understanding the mechanisms related to GCH phenotypes may offer new therapeutic avenues.

AUTHOR CONTRIBUTION

KA included patients, performed samples, assessed data, prepared and reviewed the MS. AB supervised and analysed data, participated in the study design, reviewed statistical analysis and wrote the MS. CV, CG, CT, JC and IV performed assays and reviewed the MS. PC and DG designed the study, assessed the data and reviewed the MS.

CONFLICT OF INTEREST

Pr. Chanez reports grant support and personal fees from Boehringer Ingelheim, GlaxoSmithKline, AstraZeneca, Novartis, Teva, Chiesi,

Boston Scientific and ALK, personal fees from Johnson & Johnson, Merck Sharp & Dohme, Sanofi, SNCF, Centocor and Almirall, grant support from Roche outside the submitted work. Pr. Bourdin reports personal fees, non-financial support and other support from Astra Zeneca, grant support, personal fees, non-financial support and other support from GlaxoSmithKlein, grant support, personal fees, non-financial support and other support from Boehringer Ingelheim, personal fees, non-financial support and other support from Novartis, personal fees and other support from Teva, personal fees and other support from Regeneron, personal fees, non-financial support and other support from Chiesi Pharmaceuticals, personal fees, non-financial support and other support from Actelion, other support from Gilead, and personal fees and non-financial support from Roche outside the submitted work. Mrs Vernisse, Mrs Garulli, Dr Alagha, Dr Tummino, Dr Charriot, Dr Vachier, Dr Gras report having nothing to disclose.

ORCID

Arnaud Bourdin  <https://orcid.org/0000-0002-4645-5209>

REFERENCES

1. Kesimer M, Ford AA, Ceppe A, et al. Airway mucin concentration as a marker of chronic bronchitis. *N Engl J Med*. 2017;377(10):911-922.
2. Green FHY, Williams DJ, James A, McPhee LJ, Mitchell I, Mauad T. Increased myoepithelial cells of bronchial submucosal glands in fatal asthma. *Thorax*. 2010;65(1):32-38.
3. James AL, Elliot JG, Abramson MJ, Walters EH. Time to death, airway wall inflammation and remodelling in fatal asthma. *Eur Respir J*. 2005;26(3):429-434.
4. Carroll NG, Mutavdzic S, James AL. Increased mast cells and neutrophils in submucosal mucous glands and mucus plugging in patients with asthma. *Thorax*. 2002;57(8):677-682.
5. Arthur GK, Duffy SM, Roach KM, et al. KCa3.1 K⁺ channel expression and function in human bronchial epithelial cells. *PLoS ONE*. 2015;10(12):e0145259.
6. Dunican EM, Elicker BM, Gierada DS, et al. Mucus plugs in patients with asthma linked to eosinophilia and airflow obstruction. *J Clin Invest*. 2018;128(3):997-1009.
7. Lambrecht BN, Hammad H. The airway epithelium in asthma. *Nat Med*. 2012;18(5):684-692.
8. Lambrecht BN, Hammad H. The immunology of asthma. *Nat Immunol*. 2015;16(1):45-56.
9. Hania NA, Korenblat P, Chapman KR, et al. Efficacy and safety of lebrikizumab in patients with uncontrolled asthma (LAVOLTA I and LAVOLTA II): replicate, phase 3, randomised, double-blind, placebo-controlled trials. *Lancet Respir Med*. 2016;4(10):781-796.
10. Brightling CE, Chanez P, Leigh R, et al. Efficacy and safety of tralokinumab in patients with severe uncontrolled asthma: a randomised, double-blind, placebo-controlled, phase 2b trial. *Lancet Respir Med*. 2015;3(9):692-701.
11. Corren J, Lemanske RF, Hania NA, et al. Lebrikizumab treatment in adults with asthma. *N Engl J Med*. 2011;365(12):1088-1098.
12. Fahy JV, Dickey BF. Airway mucus function and dysfunction. *N Engl J Med*. 2010;363(23):2233-2247.
13. Van Vyve T, Chanez P, Lacoste JY, Bousquet J, Michel FB, Godard P. Assessment of airway inflammation in asthmatic patients by visual endoscopic scoring systems. *Eur Respir J*. 1993;6(8):1116-1121.

14. de Marco R, Marcon A, Jarvis D, et al. Prognostic factors of asthma severity: a 9-year international prospective cohort study. *J Allergy Clin Immunol*. 2006;117(6):1249-1256.
15. Crawford B, Monz B, Hohlfeld J, et al. Development and validation of a cough and sputum assessment questionnaire. *Respir Med*. 2008;102(11):1545-1555.
16. Pretolani M, Soussan D, Poirier I, et al. Clinical and biological characteristics of the French COBRA cohort of adult subjects with asthma. *Eur Respir J*. 2017;50(2):1700019.
17. Vachier I, Chiappara G, Vignola AM, et al. Glucocorticoid receptors in bronchial epithelial cells in asthma. *Am J Respir Crit Care Med*. 1998;158(3):963-970.
18. Bourdin A, Serre I, Flamme H, et al. Can endobronchial biopsy analysis be recommended to discriminate between asthma and COPD in routine practice? *Thorax*. 2004;59(6):488-493.
19. Bourdin A, Neveu D, Vachier I, Paganin F, Godard P, Chanez P. Specificity of basement membrane thickening in severe asthma. *J Allergy Clin Immunol*. 2007;119(6):1367-1374.
20. Postma DS, Rabe KF. The asthma-COPD overlap syndrome. *N Engl J Med*. 2015;373(13):1241-1249.
21. Agusti A, Bel E, Thomas M, et al. Treatable traits: toward precision medicine of chronic airway diseases. *Eur Respir J*. 2016;47(2):410-419.
22. Gupta S, Hartley R, Khan UT, et al. Quantitative computed tomography-derived clusters: redefining airway remodeling in asthmatic patients. *J Allergy Clin Immunol*. 2014;133(3):729-738.e18.
23. Burgel P-R, Nadel JA. Epidermal growth factor receptor-mediated innate immune responses and their roles in airway diseases. *Eur Respir J*. 2008;32(4):1068-1081.
24. Woodruff PG, Wolff M, Hohlfeld JM, et al. Safety and efficacy of an inhaled epidermal growth factor receptor inhibitor (BIBW 2948 BS) in chronic obstructive pulmonary disease. *Am J Respir Crit Care Med*. 2010;181(5):438-445.
25. Daviskas E, Anderson SD, Gomes K, et al. Inhaled mannitol for the treatment of mucociliary dysfunction in patients with bronchiectasis: effect on lung function, health status and sputum. *Respirology*. 2005;10(1):46-56.
26. Ma JT, Tang C, Kang L, Voynow JA, Rubin BK. Cystic fibrosis sputum rheology correlates with both acute and longitudinal changes in lung function. *Chest*. 2018;154(2):370-377.
27. Jinnai M, Niimi A, Ueda T, et al. Induced sputum concentrations of mucin in patients with asthma and chronic cough. *Chest*. 2010;137(5):1122-1129.
28. Welsh KG, Rousseau K, Fisher G, et al. MUC5AC and a glycosylated variant of MUC5B alter mucin composition in children with acute asthma. *Chest*. 2017;152(4):771-779.
29. Zhu Z, Homer RJ, Wang Z, et al. Pulmonary expression of interleukin-13 causes inflammation, mucus hypersecretion, subepithelial fibrosis, physiologic abnormalities, and eotaxin production. *J Clin Invest*. 1999;103(6):779-788.
30. Singanayagam A, Glanville N, Bartlett N, Johnston S. Effect of fluticasone propionate on virus-induced airways inflammation and anti-viral immune responses in mice. *Lancet*. 2015;385(Suppl 1):S88.
31. Simpson JL, Phipps S, Gibson PG. Inflammatory mechanisms and treatment of obstructive airway diseases with neutrophilic bronchitis. *Pharmacol Ther*. 2009;124(1):86-95.
32. Carr TF, Zeki AA, Kraft M. Eosinophilic and non-eosinophilic asthma. *Am J Respir Crit Care Med*. 2017;197(1):22-37.
33. Brusselle GG, Vanderstichele C, Jordens P, et al. Azithromycin for prevention of exacerbations in severe asthma (AZISAST): a multicentre randomised double-blind placebo-controlled trial. *Thorax*. 2013;68(4):322-329.
34. Gibson PG, Yang IA, Upham JW, et al. Effect of azithromycin on asthma exacerbations and quality of life in adults with persistent uncontrolled asthma (AMAZES): a randomised, double-blind, placebo-controlled trial. *Lancet*. 2017;390(10095):659-668.
35. Nair P, Gaga M, Zervas E, et al. Safety and efficacy of a CXCR2 antagonist in patients with severe asthma and sputum neutrophils: a randomized, placebo-controlled clinical trial. *Clin Exp Allergy*. 2012;42(7):1097-1103.
36. Haldar P, Pavord ID. Noneosinophilic asthma: a distinct clinical and pathologic phenotype. *J Allergy Clin Immunol*. 2007;119(5):1043-1052; quiz 1053-4.
37. Cowan DC, Cowan JO, Palmay R, Williamson A, Taylor DR. Effects of steroid therapy on inflammatory cell subtypes in asthma. *Thorax*. 2010;65(5):384-390.
38. Wang F, He XY, Baines KJ, et al. Different inflammatory phenotypes in adults and children with acute asthma. *Eur Respir J*. 2011;38(3):567-574.
39. Brightling CE. Clinical applications of induced sputum. *Chest*. 2006;129(5):1344-1348.

How to cite this article: Alagha K, Bourdin A, Vernisse C, et al. Goblet cell hyperplasia as a feature of neutrophilic asthma. *Clin Exp Allergy*. 2019;49:781-788. <https://doi.org/10.1111/cea.13359>



Vitiligo Skin Is Imprinted with Resident Memory CD8 T Cells Expressing CXCR3

Katia Boniface¹, Clément Jacquemin¹, Anne-Sophie Darrigade², Benoît Dessarthe¹, Christina Martins¹, Nesrine Boukhedouni¹, Charlotte Vernisse¹, Alexis Grasseau¹, Denis Thiolat¹, Jérôme Rambert³, Fabienne Lucchese¹, Antoine Bertolotti², Khaled Ezzedine⁴, Alain Taieb^{1,2} and Julien Seneschal^{1,2}

Vitiligo is a chronic autoimmune depigmenting skin disorder that results from a loss of melanocytes. Multiple combinatorial factors have been involved in disease development, with a prominent role of the immune system, in particular T cells. After repigmentation, vitiligo frequently recurs in the same area, suggesting that vitiligo could involve the presence of resident memory T cells (T_{RM}). We sought to perform a thorough characterization of the phenotype and function of skin memory T cells in vitiligo. We show that stable and active vitiligo perilesional skin is enriched with a population of CD8 T_{RM} expressing both CD69 and CD103 compared with psoriasis and control unaffected skin. CD8 T_{RM} expressing CD103 are mainly localized in the epidermis. Expression of CXCR3 is observed on most CD8 T_{RM} in vitiligo, including the population of melanocyte-specific CD8 T cells. CD8 T_{RM} displayed increased production of IFN- γ and tumor necrosis factor- α with moderate cytotoxic activity. Our study highlights the presence of functional CD8 T_{RM} in both stable and active vitiligo, reinforcing the concept of vitiligo as an immune memory skin disease. The CD8 T_{RM} that remain in stable disease could play a role during disease flares, emphasizing the interest in targeting this cell subset in vitiligo.

Journal of Investigative Dermatology (2018) **138**, 355–364; doi:10.1016/j.jid.2017.08.038

INTRODUCTION

Vitiligo is a commonly acquired chronic skin depigmenting disorder that affects 0.5–1.0% of the general population and results from a loss of epidermal melanocytes. Several mechanisms have been implicated to explain melanocyte disappearance, including genetic predisposition, environmental triggers (such as friction), metabolic alteration, and altered inflammatory and immune responses (Boniface et al., 2017; Picardo et al., 2015).

Several studies have pointed out the involvement of T cells in vitiligo, with an altered proportion and/or function of effector and regulatory T cells (Dwivedi et al., 2013; Le Poole et al., 1996; Nigam et al., 2011). Previous reports support a direct role for cytotoxic CD8 T cells in vitiligo (van den Boorn et al., 2009; Lili et al., 2012; Wańkiewicz-Kalińska et al., 2003; Wu et al., 2013), and CD8 T cells specific for melanocyte antigens have been identified in the blood of vitiligo patients (Adams et al., 2008; Lang et al., 2001; Mandelcorn-Monson et al., 2003; Ogg et al., 1998; Palermo et al., 2001;

van den Boorn et al., 2009; Wańkiewicz-Kalińska et al., 2003). IFN- γ , tumor necrosis factor (TNF)- α , and IL-17 expression by skin T cells is increased in vitiligo patients (van den Boorn et al., 2009; van den Wijngaard et al., 2000; Wańkiewicz-Kalińska et al., 2003), and studies performed in mice have shown a major role of IFN- γ for epidermal pigmentation homeostasis and autoimmune vitiligo (Carroll et al., 1997; Gregg et al., 2010; Harris et al., 2012; Natarajan et al., 2014). In line with involvement of the IFN- γ pathway, we have previously shown a major role for IFN- α , mainly produced by plasmacytoid dendritic cells, which could induce an adaptive T-cell response characterized by the recruitment and activation of Th1 and Tc1 cells expressing CXCR3 (Bertolotti et al., 2014; Jacquemin et al., 2017). Functional studies in disease-prone mouse models further emphasize a critical role of the CXCR3/CXCL10 pathway in vivo (Gregg et al., 2010; Harris et al., 2012; Rashighi et al., 2014). Nonetheless, most studies deciphering the involvement of immune cells in vitiligo are performed on mouse models that may not adequately reflect the complexity of human disease. Studies analyzing the T-cell immune infiltrate in human vitiligo mainly rely on immunohistochemistry studies, and most studies on human samples analyzed peripheral blood cells without any comparison with other inflammatory skin disorders. Therefore, the precise T-cell subpopulations that are involved in melanocyte disappearance in vitiligo have yet to be thoroughly defined.

With the recent progress made regarding the skin immune system, and more particularly the concept of resident memory T cells (T_{RM}) (Clark, 2015; Park and Kupper, 2015), it becomes critical to analyze the phenotype of T cells locally in the skin of vitiligo patients. Two subsets of memory T cells have been described and display distinct homing capacities and effector functions: effector memory T cells (T_{EM}) and

¹INSERM U1035, Biothérapies des Maladies Génétiques, Inflammatoires et Cancers (BMGIC), Immuno-dermatology ATIP-Avenir team, University of Bordeaux, Bordeaux, France; ²Department of Dermatology and Pediatric Dermatology, National Reference Center for Rare Skin Disorders, Hôpital Saint-André, Bordeaux, France; ³AQUIDERM, University of Bordeaux, Bordeaux, France; and ⁴Department of Dermatology, AP-HP, Hôpital Henri-Mondor, Créteil, France

Correspondence: Katia Boniface, INSERM U1035, BMGIC, Immuno-Dermatology Team, Bâtiment TP zone sud, 4eme étage, 146 rue Léo Saignat, 33076 Bordeaux, France. E-mail: katia.boniface@u-bordeaux.fr

Abbreviations: CLA, cutaneous lymphocyte antigen; T_{CM} , central memory T cell; T_{EM} , effector memory T cell; TNF, tumor necrosis factor; T_{RM} , resident memory T cell

Received 6 April 2017; revised 25 August 2017; accepted 29 August 2017; accepted manuscript published online 16 September 2017; corrected proof published online 12 December 2017

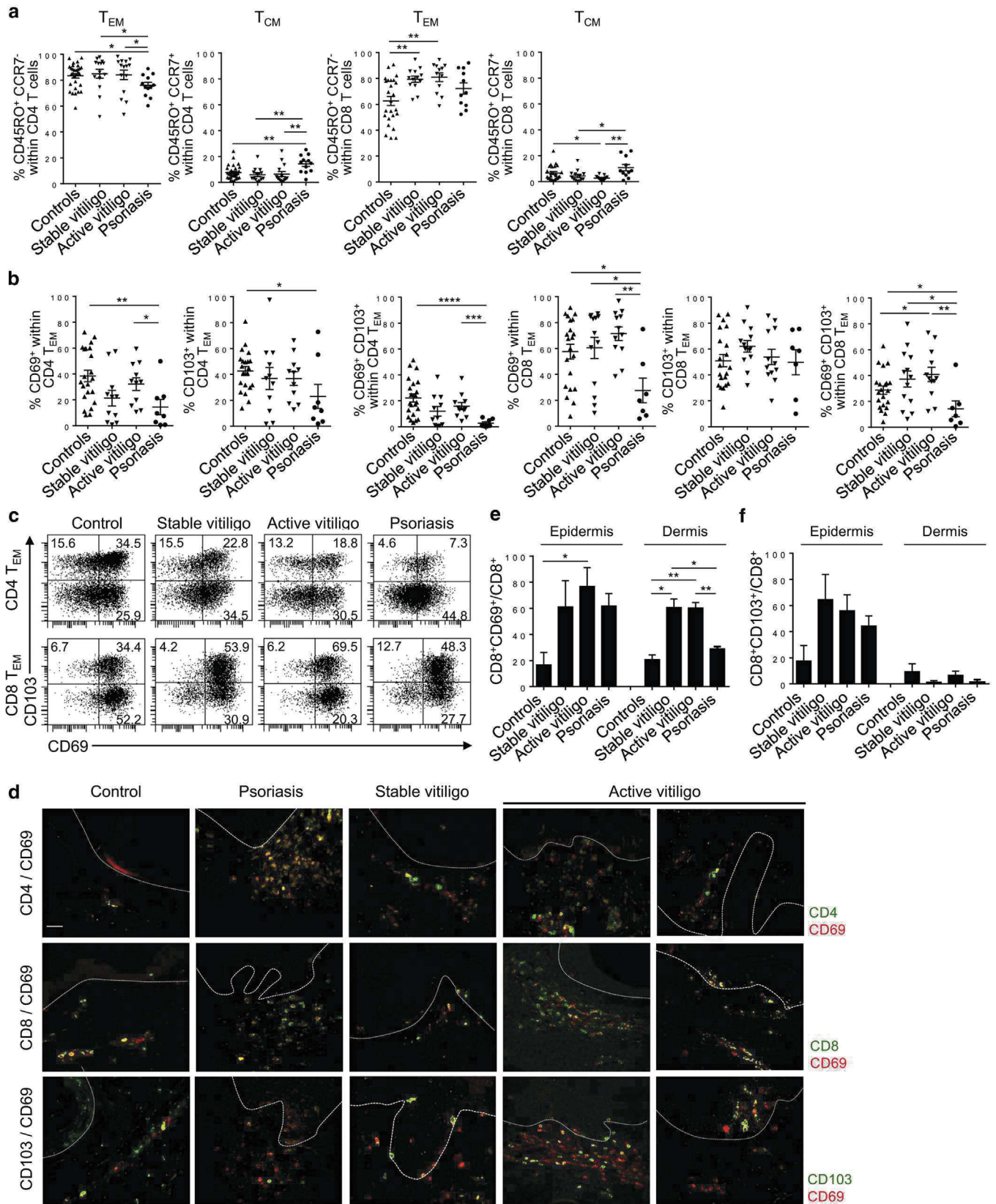


Figure 1. High frequency of resident memory CD8 T cells in the skin of vitiligo patients. (a) T cells were isolated from control unaffected skin (n = 25–30), perilesional skin of patients with stable (n = 13–14) or active vitiligo (n = 11–15), and psoriasis skin (n = 11–12). The proportion of CD4 and CD8 T_{EM} and T_{CM} expressing was determined by flow cytometry. (b, c) T cells were isolated from control unaffected skin (n = 21), perilesional skin of patients with stable (n = 11–13) or progressive vitiligo (n = 11–12), and psoriasis skin (n = 7–8). The proportion of CD4 and CD8 T_{EM} expressing CD69 and/or CD103 was determined by flow cytometry. Each symbol represents one specimen. The mean ± standard error of the mean is shown. Representative CD69 and CD103 staining is shown in panel c. (d) Immunofluorescence microscopy analysis of CD4, CD8, CD69, and CD103 expression in skin biopsy samples from

central memory T cells (T_{CM}). T_{CM} bear the chemokine receptor CCR7, allowing homing to lymphoid tissues, where they can differentiate into effector T cells upon secondary stimulation; T_{EM} lack CCR7 and express tissue homing receptors for migration to inflamed tissues, where they mediate effector functions (Sallusto et al., 1999). In addition, it is now well established that skin and other epithelial barriers are populated by different subsets of memory T cells (non-recirculating T_{RM} and recirculating memory T cells) (Clark et al., 2006a). T_{RM} have the propensity to rapidly respond to pathogen or foreign antigens that attempt to breach skin epithelium, independent of T-cell recruitment from the circulation. These skin T_{RM} do not recirculate in the systemic blood flow, have an effector memory phenotype, and are defined by expression of CD69 (a C-type lectin also known to be a T-cell activation marker) and CD103 (integrin α_E). If tissue T_{RM} have a protective role against most commonly encountered pathogens, dysregulation of T_{RM} can be very harmful in the context of inflammatory disorders, such as psoriasis (Clark, 2015) and potentially vitiligo. To date, the presence and involvement of pathogenic autoreactive skin T_{RM} cell subsets in vitiligo have yet to be characterized. Such assessment is of particular interest because vitiligo often recurs on the same anatomic sites, suggesting the presence of a local memory immune response.

This study aimed to perform a thorough analysis of the phenotype and function of circulating and skin-infiltrating T cells in vitiligo patients and to compare such infiltrate to that observed in psoriasis, the archetype of a skin inflammatory disorder. We found that vitiligo skin is enriched with CD8 T_{RM} that express CXCR3. Strikingly, a higher frequency of skin melanocyte-specific CD8 T cells was found within the CXCR3⁺ subset. Skin memory CD8 T cells produced elevated levels of the proinflammatory cytokines TNF- α and IFN- γ , and their propensity to produce cytotoxic molecules was similar to control or psoriasis skin CD8 T cells. Our results not only add to a better understanding of the specific immune memory response occurring in the skin during this autoimmune condition, they also emphasize the mechanistic concept of vitiligo as an immune memory skin disease and provide possible new therapeutic strategies to modulate these skin-resident T-cell populations.

RESULTS

Vitiligo is enriched with populations of skin CD8 T cells expressing a resident memory phenotype

We first analyzed the proportion of T_{EM}, T_{CM}, and T_{RM} in perilesional skin of vitiligo patients. As shown in Figure 1a, skin CD4 and CD8 T cells from vitiligo patients (with either stable or active disease), psoriasis, or unaffected control subjects display an effector memory phenotype (CD45RO⁺CCR7⁻), T_{CM} being less than 10% of the lymphocyte pool. The frequency of CD8 T_{EM} isolated from vitiligo perilesional skin (independent of disease activity) was significantly higher than that obtained from control unaffected skin (with an increase of

13.4% or 25.1%, respectively, in patients with stable or active vitiligo). We performed multiparametric flow cytometry analyses to assess and compare the expression of CD69 and CD103 within circulating and skin CD4⁺ and CD8⁺ T_{EM} cell subsets in patients with vitiligo and psoriasis and in unaffected control subjects. We identified two subsets of CD69⁺ T_{RM} with respect to their expression or non-expression of CD103 (Figure 1b and c). CD8 T_{RM} were more abundant than CD4 T_{RM} (Figure 1b–d). The frequency of skin CD69⁺CD103⁺ CD8 T_{RM} was significantly higher in vitiligo patients (independent of disease activity) compared with unaffected control subjects (increase of 42.2%) or psoriasis (increase of 186.7%). In contrast, few T_{RM} populations were identified in patient blood (see Supplementary Figure S1 online). To selectively study the localization of T_{RM} in vitiligo, we subsequently performed immunofluorescence studies in situ on skin samples. The number of CD8 T_{RM}, defined by the expression of CD69, was higher in the skin of vitiligo and psoriasis patients compared with control unaffected skin and tended to positively correlate with vitiligo disease activity (Figure 1d and e). Although in psoriasis skin CD8 T_{RM} cell infiltrate was predominantly found in the epidermis (Figure 1d and e), this T-cell subset was found in the dermis and epidermis in both active and stable vitiligo. Despite a more prominent CD8 T_{RM} infiltrate in patients with a progressive disease, the proportion of CD8 T cells expressing residency markers was similar between stable and active vitiligo, suggesting that stable vitiligo retains a significant number of CD8 T_{RM} (Figure 1b–f). Moreover, CD8 T cells expressing CD103 were mainly found in the epidermis, and a higher number of these cells was found in patients with vitiligo or psoriasis (Figure 1f). No statistical difference was found in the proportion of CD8 T_{RM} expressing CD103 among psoriasis, stable vitiligo, or progressive vitiligo. These observations are in line with the concept of an “immune memory skin disorder” for vitiligo.

Most CD8 T_{RM} express CXCR3 in vitiligo patient skin

The study of chemokine receptor expression and their interaction with their cognate ligands is of interest regarding the function and survival of skin T_{RM} subpopulations, as exemplified with new results from the literature suggesting that CXCR3 is important for epidermal localization of effector T cells and formation of T_{RM} (Mackay et al., 2013). This prompted us to investigate the proportion of CXCR3⁺ T cells within circulating and skin memory T-cell populations. A significant decrease in the proportion of circulating CXCR3⁺ cells within the CD4 and CD8 T_{EM} subsets was observed in patients with vitiligo (decrease of 12.7% and 22.9%, respectively) and psoriasis (decrease of 31.3% and 42.0%, respectively) compared with unaffected subjects (Figure 2a and b). Nonetheless, circulating CD8 T_{EM} from vitiligo patients maintained higher proliferative capacities compared with unaffected control subjects (Figure 2c), resulting from increased proliferation of CXCR3⁺CD8 T_{EM} rather than their negative counterpart (Figure 2d). We observed a prominent

← an unaffected control subject, patients with stable or active vitiligo, or patient with psoriasis. Images are representative of at least four independent experiments. Scale bar = 50 μ m. (e, f) Quantification of the proportion of CD8 cells coexpressing (e) CD69 or (f) CD103 over CD8 cells in unaffected control skin (n = 4), perilesional skin of patients with stable (n = 5) or active vitiligo (n = 5), and psoriasis skin (n = 4). The mean \pm standard error of the mean is shown. *P < 0.05, **P < 0.01, ***P < 0.001, ****P < 0.0001. T_{CM}, central memory T cell; T_{EM}, effector memory T cell; T_{RM}, resident memory T cell.

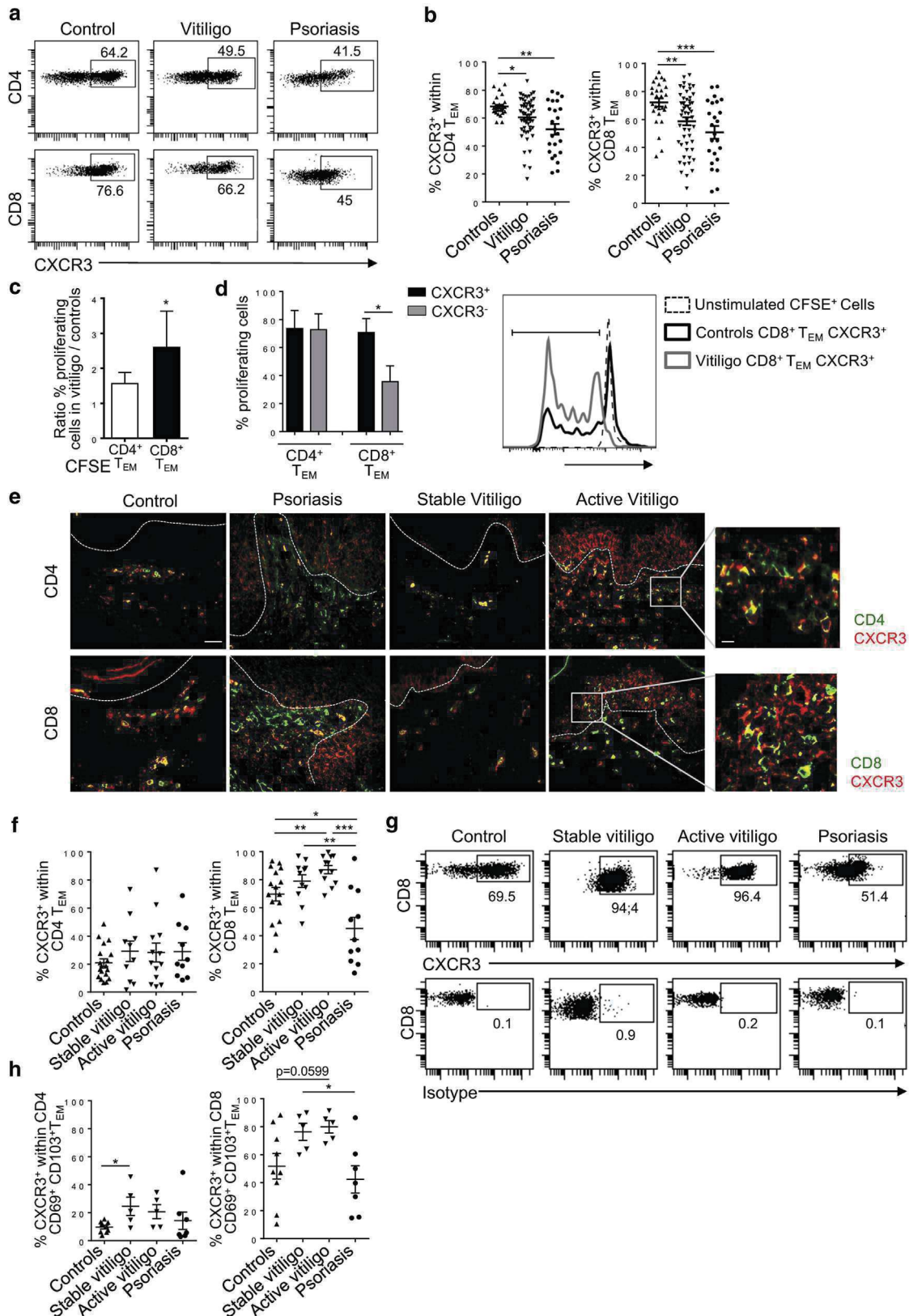


Figure 2. Prominent infiltration of skin inflammatory effector memory T cells expressing CXCR3 in vitiligo. (a, b) Flow cytometry analysis of the proportion of circulating CXCR3⁺ CD4 and CD8 T_{EM} in unaffected control subjects (n = 26), patients with vitiligo (n = 54), or patients with psoriasis (n = 24). (c, d) Proliferative capacities of CFSE-labeled CXCR3⁺ and/or CXCR3⁻ CD4 and CD8 T_{EM} were compared between unaffected control subjects (n = 6) and vitiligo patients (n = 6) after 5 days of culture. (e) Immunofluorescence microscopy analysis of CD4, CD8, and CXCR3 expression in skin biopsy samples from an unaffected control subject, psoriasis patient, and stable or progressive vitiligo patients. Images are representative of at least four independent experiments. Scale bar = 50 μm (left panel) or 10 μm (right panel). (f–h) T cells were isolated from control unaffected skin (n = 9–19), perilesional skin of patients with stable

infiltration of CD4 and CD8 T cells expressing the chemokine receptor CXCR3 in perilesional skin from patients with active disease compared with patients with stable vitiligo and unaffected control subjects (Figure 2e, and see Supplementary Figure S2a online). Compared with psoriasis skin samples, a more prominent infiltrate of CXCR3⁺ CD8 T cells was observed in active vitiligo. CXCR3⁺ CD8 T cells were mainly found in the epidermis, whereas CXCR3⁺ CD4 T-cell infiltrate was more prominent in the upper dermis. After extraction from the skin, we noticed that most CD8 T_{EM} expressed CXCR3 in patients with vitiligo, and such expression was significantly higher than in psoriasis (Figure 2f and g). The relative frequency of T_{RM} subsets (CD69⁺ and/or CD103⁺) expressing CXCR3 was higher in vitiligo perilesional skin compared with control or psoriasis skin samples (Figure 2h, and see Supplementary Figure 2b). Expression of residency or skin homing markers (cutaneous lymphocyte antigen [CLA] and CCR4) was similar within the CXCR3⁺ or CXCR3⁻ T_{EM} subsets (see Supplementary Figure S3a and b online).

Melanocyte-specific CD8 T_{EM} from perilesional skin of patients with active vitiligo display increased expression of CXCR3

We next analyzed by flow cytometry the presence of HLA-A2–restricted melanocyte-specific CD8 T_{EM} lymphocytes in vitiligo patients. CD8 T_{EM} specific for diverse melanocyte antigens (gp100, MART-1, tyrosinase) were identified in perilesional skin of vitiligo patients with either stable or active disease (Figure 3), in agreement with a previous report (van den Boorn et al., 2009). The frequency of gp100 or MART-1 skin-specific CD8 T_{EM} was significantly higher within the CXCR3⁺ subset in patients with active disease (Figure 3). A similar observation was made in perilesional skin of patients with stable disease, although this did not reach statistical significance. The proportion of melanocyte-specific CXCR3⁺ CD8 T_{EM} in perilesional skin tended to be higher in patients with active disease compared with patients with stable disease. In addition, exploration of the T-cell receptor repertoire diversity showed that CD8 T_{EM} from stable and active vitiligo patients skin displayed distinct T-cell receptor repertoire patterns (see Supplementary Figure S4 online). Stable vitiligo skin contained CD8 T-cell subsets with a skewed Vβ repertoire, suggesting the presence of oligoclonal CD8 T cells that could be important during disease flares. Compared with skin from patients with stable vitiligo, skin from patients with active disease seems to be infiltrated with CD8 T cells with a more diverse repertoire, because we did not find an enrichment of specific clones, suggesting that during the progression of the disease, both melanocyte-specific and non-melanocyte-specific T cells infiltrate the skin.

CD8 T_{EM} from vitiligo perilesional skin exhibit a skewed inflammatory cytokine profile with moderate cytotoxic activity

We further studied the cytokine secretion profile and cytotoxic activity of T cells extracted from the skin of vitiligo

patients by flow cytometry. Both skin CD4 and CD8 T cells from patients with active disease produced significantly higher levels of the type-1 related cytokine IFN-γ than those from patients with stable disease or control skin (Figure 4a and b). TNF-α, known to be secreted by most T-cell subsets, was produced by most CD4 and CD8 T cells. Most IFN-γ–secreting cells were also TNF-α producers. Such an increase in IFN-γ– and TNF-α–producing T cells in vitiligo patients was not observed in the blood (see Supplementary Figure S5 online). In contrast, the proportion of IL-17–producing T cells from vitiligo skin remained comparable to that in control subjects and was significantly lower than in psoriasis patients (Figure 4b). Unexpectedly, the relative frequency of granzyme B-producing CD8 T_{EM} in vitiligo perilesional skin of patients with either stable or active disease was similar to unaffected control subjects or psoriasis patients (Figure 4c and d). This result prompted us to analyze granzyme B expression by CD8 T_{EM} isolated from cutaneous lupus erythematosus, a chronic inflammatory skin disorder associated with major infiltration of cytotoxic CD8 T cells (Wenzel and Tüting, 2008). As expected, granzyme B levels were significantly increased in CD8 T_{EM} isolated from cutaneous lupus erythematosus compared with CD8 T_{EM} isolated from vitiligo, supporting our finding that CD8 T_{EM} in vitiligo skin display moderate cytotoxic activity. Together, these data reinforce the concept that IFN-γ and TNF-α are the major cytokines involved in vitiligo pathogenesis.

DISCUSSION

Vitiligo is a stigmatizing skin condition characterized by the development of white macules due to melanocyte disappearance. Vitiligo can be stable for a long period but will flare unexpectedly from poorly understood triggers, except possibly for stress or friction (Nicolaidou et al., 2007; Sitek et al., 2007). Vitiligo lesions usually recur at the same sites as those previously affected, suggesting that vitiligo could be considered as an immune memory skin disorder. In line with this concept, our study showed that skin from vitiligo patients contains significant infiltrate characterized by a combination of CD103⁻ and CD103⁺CD69⁺ CD8 T_{RM}. Very recently, CD49a was reported to define a subset of resident memory T cells in inflammatory dermatoses, including vitiligo and psoriasis (Cheuk et al., 2017). A high proportion of CD8 T_{RM} persist in the perilesional skin of patients with stable disease compared with control normal human skin, and these cells are mostly found in the epidermis where melanocytes are located. These data suggest that these remaining CD8 T_{RM} could be an important mediator for disease flares, or alternatively, for blocking the renewal of epidermal melanocytes or their entry from the follicular reservoir of melanocyte precursors, both important mechanisms for repigmentation (Gan et al., 2017). In addition, few studies so far evaluated long-term follow-up in patients treated with UV lights (Nicolaidou et al., 2007; Sitek et al., 2007). Almost 50% of

◀ (n = 5–11) or active vitiligo (n = 5–13), and lesional psoriasis skin (n = 7–11). Proportion of CXCR3-expressing cells (f, g) within skin CD4 and CD8 T_{EM} or (h) within CD103⁺CD69⁺ skin T_{RM} was determined by flow cytometry. Each symbol represents one specimen. The mean ± standard error of the mean is shown. Representative CXCR3 staining is shown in panels a and g. *P < 0.05, **P < 0.01, ***P < 0.001. CFSE, carboxyfluorescein diacetate succinimidyl ester; T_{EM}, effector memory T cell.

recurrent flares were situated at the same location within 1 year after treatment termination, reinforcing our hypothesis that T_{RM} in the skin of vitiligo patients are likely involved in disease flares.

Research in both mice and humans has now better defined the phenotype and function of T_{RM} in the context of infections or, more recently, in the understanding of chronic inflammatory skin disorders such as mycosis fungoides or psoriasis (Park and Kupper, 2015). As suggested, when activated, T_{RM} could proliferate locally in the skin as a first line of defense before the recruitment of nonspecific T cells from the blood, increasing the skin T-cell infiltrate (Clark, 2015). It has now been shown in mouse models of skin infection that these T_{RM} can persist long after clearance of the pathogens (Jiang et al., 2012). In human skin diseases, there is also evidence to suggest that T_{RM} can remain for a long period of time in the skin (Clark, 2015). For example, recurrence of new psoriasis lesions in the same location as lesions previously treated and resolved suggest involvement of T_{RM} in this pathology. Indeed, analysis of cells extracted from resolved psoriatic lesions showed the presence of remaining CD8 T cells expressing cytokines that are important for disease development (Clark, 2011; Suárez-Fariñas et al., 2011). Therefore, the high proportion of CD8 T_{RM} in both active and stable vitiligo supports the concept of vitiligo as an immune memory skin disease. However, in contrast to vitiligo, our study shows that psoriasis lesional skin is characterized by a significant proportion of re-circulating memory cells. This is consistent with the fact that these re-circulating memory T cells could be important for the development of systemic symptoms associated with psoriasis such as psoriatic arthritis.

Our work highlights the critical role of CXCR3-expressing T cells locally in human vitiligo skin. We previously showed an increase in CXCR3 expression in perilesional skin of patients with a progressive vitiligo (Bertolotti et al., 2014). In this study, we further show that most skin-infiltrating CD8 T_{RM} in vitiligo bear expression of CXCR3 and are poised for secretion of both IFN- γ and TNF- α . These results are in line with functional studies previously performed in mice that support a critical role of the CXCR3/IFN- γ pathway in depigmentation in vivo (Gregg et al., 2010; Harris et al., 2012; Rashighi et al., 2014). Moreover, we and others have reported an increased expression of CXCR3 ligands: CXCL9 or CXCL10 in vitiligo patients (Bertolotti et al., 2014; Rashighi et al., 2014; Wang et al., 2016), and these chemokines could serve as clinical biomarkers of vitiligo disease activity (Strassner et al., 2017; Wang et al., 2016). Therefore, targeting this pathway naturally appears an attractive strategy for treating depigmenting disorders like vitiligo. Vitiligo-prone mouse models support the role of cytotoxic CD8 T cells during disease development (Harris et al., 2012; You et al., 2013). This contrasts with our observation that in human vitiligo perilesional skin, CD8 T cells have only moderate cytotoxic activity, suggesting that available mouse models might not completely reflect the complexity of human disease. To support our finding, previous reports showed that depigmentation in mice depends on IFN- γ , whereas cytotoxic mediators like perforin or granzyme are dispensable (Gregg et al., 2010; Harris et al., 2012; Webb et al., 2015). Previous studies have also reported expression of cytotoxic

markers by vitiligo T cells (van den Boorn et al., 2009; van den Wijngaard et al., 2000). However, the comparison with other inflammatory skin diseases was lacking, especially with chronic inflammatory skin disorders associated with elevated cytotoxic response and cell apoptosis, such as lupus. Although we did observe expression of cytotoxic markers on freshly isolated CD8 T_{EM} from vitiligo skin, these levels remained comparable to those observed in CD8 T_{EM} isolated from control or psoriasis skin and are significantly lower than those observed in CD8 T_{EM} extracted from lupus skin. Melanocyte-specific T cells have been previously characterized in vitiligo patient blood, yet only a few studies observed these cell subsets in perilesional vitiligo skin (Dwivedi et al., 2013; van den Boorn et al., 2009;). Our study confirmed the presence of melanocyte-specific T cells in vitiligo skin and showed that these cells are characterized by the expression of CXCR3. Arakawa et al. (2015) recently highlighted the presence of melanocyte-specific CD8 T cells in psoriasis. However, although authors could detect granules containing granzyme B in melanocyte-specific T cells, they could not detect signs of cell death in melanocytes. In line with this observation, it was previously shown that lytic granules constitute an important effector mechanism of CD8 T cells, but their directed release does not necessarily induce apoptosis of target cells (Knickelbein et al., 2008). Altogether, our data suggest that cytotoxicity is not the only mechanism involved in melanocyte disappearance in vitiligo and highlight that IFN- γ and TNF- α produced by skin CXCR3⁺ T cells could play a more important role, as suggested in the literature (Englaro et al., 1999; Wang et al., 2011; Yang et al., 2015). However, such hypotheses have to be further investigated in human disease. Hence, an integrated understanding of the crosstalk between CXCR3-expressing T_{RM} and the epidermis, that is, melanocytes and keratinocytes, by studying human vitiligo skin directly seems critical to precisely determining how these cells are involved in the process leading to melanocyte loss.

If IL-17-producing T cells are clearly critical in skin inflammatory disorders like psoriasis, their role in vitiligo is still unclear. Several studies suggested an increase of T helper type 17 cells in the blood of vitiligo patients, together with an increase in IL-17 levels in vitiligo skin (Singh et al., 2016). However, the link between IL-17 expression and melanocyte loss has yet to be fully understood. We show that T cells from vitiligo perilesional skin do not produce elevated levels of IL-17 compared with psoriasis skin T cells, supporting our finding that IFN- γ and TNF- α are the primary cytokines involved in melanocyte loss.

Commonly used therapies for vitiligo mainly consist of topical corticosteroids, topical calcineurin inhibitors, and/or UV light (Whitton et al., 2015). These skin-targeted therapies can repress activation/proliferation of T_{RM}. Similarly, a recent study showed that maintenance therapy of adult vitiligo with tacrolimus ointment is effective in preventing the depigmentation of vitiligo patches that have previously been successfully repigmented (Cavalié et al., 2015). These skin-directed therapies may nonspecifically dampen the local activation of T_{RM}. Discovering strategies that specifically target T_{RM} could be an important step toward improving the management of vitiligo in the future. Indeed, a recent study

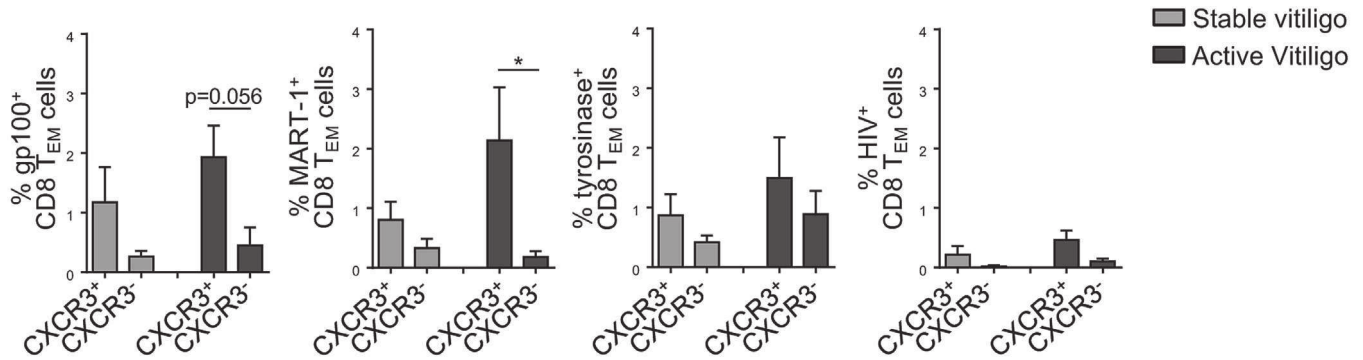


Figure 3. Increased expression of CXCR3 on melanocyte-specific CD8 T_{EM} in vitiligo skin. The relative frequency of HLA-A2 restricted melanocyte-specific CD8 T_{EM} within CXCR3⁺ and CXCR3⁻ subsets was evaluated by flow cytometry in the skin of patients with stable (n = 5) or active vitiligo (n = 5) using HLA-A2 pentamer loaded with the melanocyte peptides gp100, MART-1, or tyrosinase. The mean ± standard error of the mean is shown. *P < 0.05. T_{EM}, effector memory T cell.

showed that the survival and function of T_{RM} is dependent on the uptake of exogenous lipids and their oxidative metabolism (Pan et al., 2017), suggesting that the modulation of this pathway could be an interesting strategy to decrease the population of T_{RM}.

MATERIALS AND METHODS

Blood and skin sample collection

Blood and skin biopsy samples from patients with vitiligo, psoriasis, or lupus were obtained from the department of dermatology of Bordeaux Hospital. All patients included in this study did not receive treatments/immunosuppressive therapies during the last 6 months. Vitiligo patient characteristics are shown in Table 1. Patients were classified according to the Vitiligo European Task Force scoring system (Taïeb and Picardo, 2007) and by using Wood's lamp examinations, as previously reported (Benzekri et al., 2013; Sosa et al., 2015). Patients with a total spreading score greater than 3 according to the Vitiligo European Task Force scoring system and/or the presence of hypomelanotic lesions with poorly defined borders or confetti-like lesions were considered *active*, and those with a total spreading score less than 1 or the absence of new lesions over the past 12 months were considered *stable*. Control unaffected skin was obtained as discarded human tissue from cutaneous plastic surgery (Bordeaux Hospital). Blood from unaffected subjects was obtained from volunteers who were free of autoimmune or inflammatory disorders. All studies involving human tissues were approved by the local institutional ethics committee and the Commission Nationale de l'Informatique et des Libertés (no.1545937). All patients gave their written informed consent.

T-cell isolation

Peripheral blood mononuclear cells from unaffected donors and patients were isolated by density gradient centrifugation through Ficoll (density 1077; Eurobio, Les Ulis, France). Skin T cells were isolated from 3-week explant cultures maintained with IL-2 and IL-15 (R&D Systems, Minneapolis, MN) as described in the literature (Clark et al. 2006a, 2006b). For some experiments, tissue samples were extensively minced, and freshly isolated T cells were obtained by filtering skin through a 40-µm cell strainer.

Flow cytometry

When using peripheral blood mononuclear cells, we performed FcR blocking (Miltenyi Biotec, Cambridge, MA) before staining to increase the specificity of labeled Abs. For analysis of cell surface proteins, cells were stained with the appropriate

fluorochrome-labeled Abs (see Supplementary Table S1 online). For intracellular staining, cells were surface-stained, fixed, permeabilized, and stained with appropriately labeled Abs (see Supplementary Table S1) following the manufacturer's instructions (Cytotfix/Cytoperm Plus kit, BD Biosciences, Billerica, MA). When assessing cytokine secretion, cells were first stimulated for 4 hours with 50 ng/ml phorbol 12-myristate 13-acetate, 500 ng/ml ionomycin (Sigma Aldrich, Dorset, UK), and monensin (GolgiStop, BD Biosciences). Irrelevant isotype negative controls were used to define positive gate. For T-cell receptor Vβ analysis, cells were stained following manufacturer's instructions using the IOTest Beta Mark TCR Vbeta Repertoire Kit (Beckman Coulter, Brea, CA). Data were acquired on a Canto II cytometer and analyzed with DIVA (BD Biosciences) or FlowJo software (Tree Star, Ashland, OR).

Detection of melanocyte-specific T cells

Patients were screened for their HLA-A2 status (clone BB7.2, Biolegend, San Diego, CA) as previously described (Contin-Bordes et al., 2011). To assess the frequency of melanocyte-antigen specific T cells, phycoerythrin-conjugated HLA-A0201 restricted pentamers loaded with MART-1(26-35) (ELAGIGILTV), tyrosinase (369-377) (YMDGTMSQV), or gp100 (154-162) (KTWGQYWQV) (Prolimmune, Oxford, UK) were made by Prolimmune using Pro5 MHC Class I pentamer technology. Skin T cells were first stained with 10 µl of either phycoerythrin-labeled MART-1 pentamers, tyrosinase pentamers, or gp100 pentamers for 10 minutes at room temperature, according to the manufacturer's recommendations. Cells were subsequently stained with appropriate Abs (anti-CD3, anti-CD4, anti-CD8, anti-CD45RO, anti-CCR7, and anti-CXCR3). The frequency of melanocyte-specific T_{EM} with respect to expression of CXCR3 was determined by flow cytometry.

Cell sorting

CD3⁺ T cells were enriched from whole blood using RosetteSep Human T Cell Enrichment Cocktail kit (StemCell, Vancouver, Canada). CXCR3⁺CD4⁺ and CXCR3⁺CD8⁺ effector memory T cells were isolated by cell sorting using anti-CD8, -CD4, -CXCR3, -CD45RA, and -CCR7 Abs. Cell sorting was done with a FACS Aria instrument (BD Biosciences).

Proliferation assay

Cell-sorted T_{EM} subpopulations were labeled with 5 µmol/L carboxyfluoresceine diacetate succinimidyl ester (i.e., CFSE) (Biolegend) for 10 minutes at 37 °C. The CFSE reaction was stopped by adding

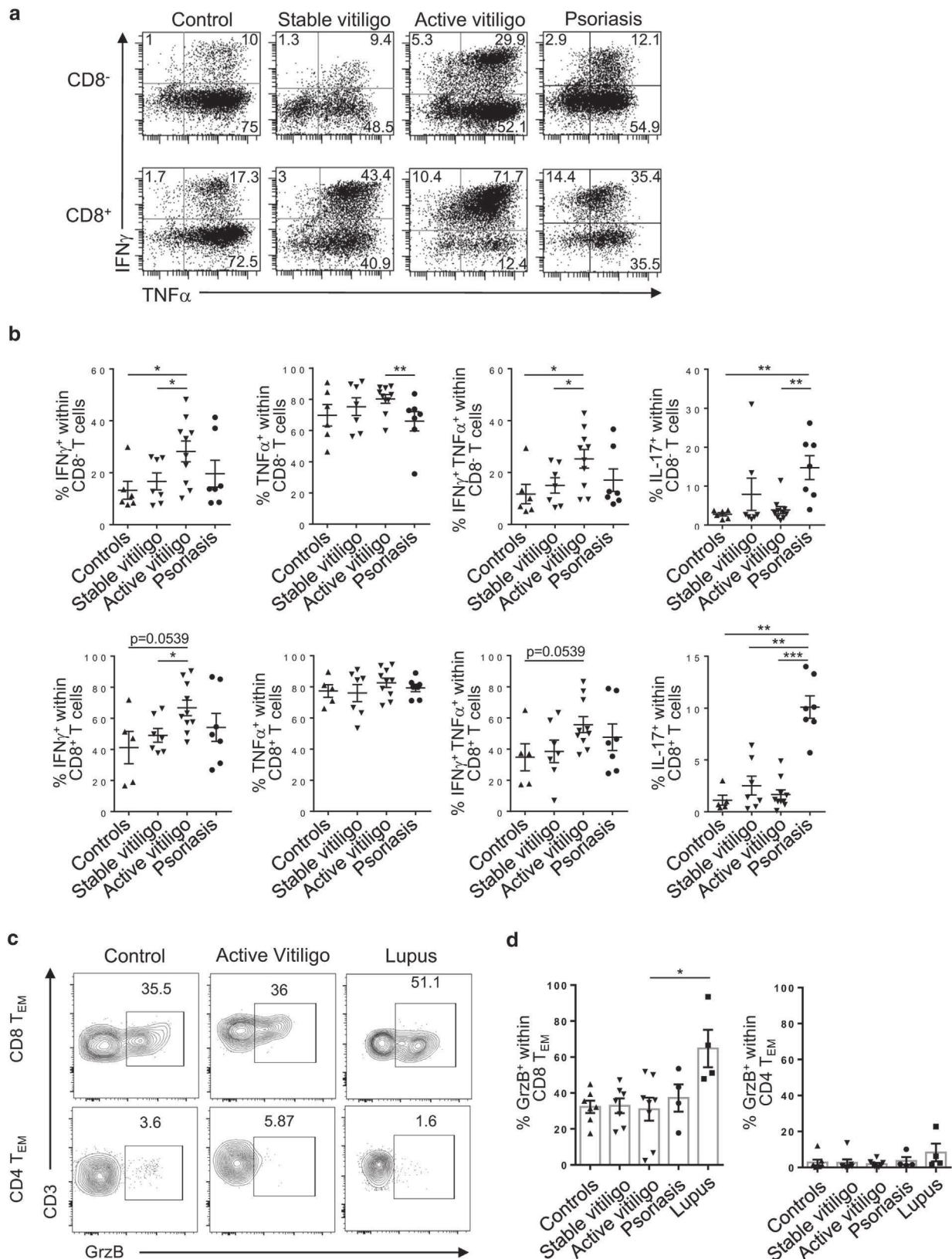


Figure 4. Skewed inflammatory cytokine secretion profiles and moderate cytotoxic activity of skin T cells from vitiligo patients. (a, b) Analysis of IFN- γ , TNF- α , IFN- γ /TNF- α , or IL-17-producing, skin-infiltrating T cells by flow cytometry in control subjects (n = 5–6), patients with stable (n = 7) or active vitiligo (n = 10), or psoriasis patients (n = 7). Representative cytokine staining is shown in panel a. (c, d) Expression of granzyme B was assessed on freshly isolated T cells from the skin of unaffected control subjects (n = 7) and patients with stable (n = 7) or active vitiligo (n = 8), psoriasis (n = 4), or lupus (n = 4). Representative granzyme B staining is shown in panel c. Each symbol represents one specimen. The mean \pm standard error of the mean is shown. * $P < 0.05$, ** $P < 0.01$, *** $P < 0.001$. T_{EM}, effector memory T cell; TNF, tumor necrosis factor.

Table 1. Clinical characteristics of vitiligo patients

Characteristic	Stable (n = 51)	Progressive (n = 42)
Sex		
Male	22	13
Female	29	29
Age (mean ± SD)	46.8 ± 15.6	48.40 ± 16.4
Age of onset of vitiligo years (mean ± SD)	34.7 ± 16.2	35.2 ± 19.5
Disease duration years (mean ± SD)	11.55 ± 12.3	13.1 ± 12.57
Type of vitiligo (%)		
Acrofacial	25	19
Generalized	67	67
Universal	2	2
Mixed	6	12
Personal history of autoimmune disease (%)		
Yes, autoimmune thyroiditis	20.0	28.5
Yes, other chronic inflammatory diseases (including atopic disease, psoriasis, type 1 diabetes, alopecia areata)	29.0	33.3
Koebner phenomenon (%)		
Type I	19.6	38.0
Type IIa	51.0	57.0
Type IIb	15.6	21.4
Unknown	13.8	0.0
Affected body surface area (mean ± SD)	15.3 ± 16.8	22.8 ± 18.7
Associated halo nevus		
Yes	5	1
No	46	41

Abbreviation: SD, standard deviation.

fetal calf serum for 5 minutes, and cells were washed twice with Iscove's modified Dulbecco's medium, 20% fetal calf serum. Thirty thousand CFSE-labeled cells were cultured in round-bottom, 96-well plates in the presence of beads coated with anti-CD3/CD28/CD2 Abs (2 beads:10 cells, Miltenyi Biotec) for 5 days at 37°C. Cell proliferation was assessed by evaluating CFSE dilution by flow cytometry.

Immunofluorescence studies

The 3-µm sections were prepared from formalin-fixed, paraffin-embedded skin biopsy samples. Sections were deparaffinized and subjected to a heat-induced epitope retrieval step. Slides were rinsed in cool running water and washed in Tris-buffered saline (pH 7.4) before incubation with relevant primary Abs. Primary and secondary Abs are listed in [Supplementary Table S2](#) (online). After subsequent washing, the sections were mounted with Prolong Gold antifade reagent with DAPI (Thermo Fisher Scientific, Cambridge, MA) and covered with a coverslip. Appropriate isotype-matched controls were included. Cells were counted per three high-power fields with an original magnification ×400, and the mean number was calculated.

Statistical analyses

All data were expressed as mean ± standard error of the mean. Comparisons between groups were performed using nonparametric Mann-Whitney *U* test or Wilcoxon match paired *t* tests. Statistical analyses were performed using GraphPad Prism software (San Diego, CA).

CONFLICT OF INTEREST

The authors state no conflict of interest.

ACKNOWLEDGMENTS

This study was funded by the ATIP-AVENIR and the ANR JCJC grants. We thank Cristina Tato for critical revision of the manuscript.

SUPPLEMENTARY MATERIAL

Supplementary material is linked to the online version of the paper at www.jidonline.org, and at <https://doi.org/10.1016/j.jid.2017.08.038>.

REFERENCES

- Adams S, Lowes MA, O'Neill DW, Schachterle S, Romero P, Bhardwaj N. Lack of functionally active Melan-A(26-35)-specific T cells in the blood of HLA-A2+ vitiligo patients. *J Invest Dermatol* 2008;128:1977–80.
- Arakawa A, Siewert K, Stöhr J, Besgen P, Kim S-M, Rühl G, et al. Melanocyte antigen triggers autoimmunity in human psoriasis. *J Exp Med* 2015;212:2203–12.
- Bertolotti A, Boniface K, Vergier B, Mossalayi D, Taieb A, Ezzedine K, et al. Type I interferon signature in the initiation of the immune response in vitiligo. *Pigment Cell Melanoma Res* 2014;27:398–407.
- Benzekri L, Ezzedine K, Gauthier Y. Vitiligo Potential Repigmentation Index: a simple clinical score that might predict the ability of vitiligo lesions to repigment under therapy. *Br J Dermatol* 2013;168:1143–6.
- Boniface K, Seneschal J, Picardo M, Taieb A. Vitiligo: focus on clinical aspects, immunopathogenesis and therapy [e-pub ahead of print] *Clin Rev Allergy Immunol* 2017; <https://doi.org/10.1007/s12016-017-8622-7> (accessed October 13, 2017).
- Carroll JM, Crompton T, Seery JP, Watt FM. Transgenic mice expressing IFN-gamma in the epidermis have eczema, hair hypopigmentation, and hair loss. *J Invest Dermatol* 1997;108:412–22.
- Cavalié M, Ezzedine K, Fontas E, Montaudie H, Castela E, Bahadoran P, et al. Maintenance therapy of adult vitiligo with 0.1% tacrolimus ointment: a randomized, double blind, placebo-controlled study. *J Invest Dermatol* 2015;135:970–4.
- Cheuk S, Schlums H, Gallais Sérézal I, Martini E, Chiang SC, Marquardt N, et al. CD49a Expression defines tissue-resident CD8(+) T cells poised for cytotoxic function in human skin. *Immunity* 2017;46:287–300.
- Clark RA. Gone but not forgotten: lesional memory in psoriatic skin. *J Invest Dermatol* 2011;131:283–5.
- Clark RA. Resident memory T cells in human health and disease. *Sci Transl Med* 2015;7(269):269rv1.
- Clark RA, Chong B, Mirchandani N, Brinster NK, Yamanaka K-I, Dowgiert RK, et al. The vast majority of CLA+ T cells are resident in normal skin. *J Immunol* 2006a;176:4431–9.
- Clark RA, Chong BF, Mirchandani N, Yamanaka K-I, Murphy GF, Dowgiert RK, et al. A novel method for the isolation of skin resident T cells from normal and diseased human skin. *J Invest Dermatol* 2006b;126:1059–70.
- Contin-Bordes C, Lazaro E, Richez C, Jacquemin C, Caubet O, Douchet I, et al. Expansion of myelin autoreactive CD8+ T lymphocytes in patients with neuropsychiatric systemic lupus erythematosus. *Ann Rheum Dis* 2011;70:868–71.
- Dwivedi M, Laddha NC, Arora P, Marfatia YS, Begum R. Decreased regulatory T-cells and CD4(+) /CD8(+) ratio correlate with disease onset and progression in patients with generalized vitiligo. *Pigment Cell Melanoma Res* 2013;26:586–91.
- Englano W, Bahadoran P, Bertolotto C, Buscà R, Dérillard B, Livolsi A, et al. Tumor necrosis factor alpha-mediated inhibition of melanogenesis is dependent on nuclear factor kappa B activation. *Oncogene* 1999;18:1553–9.
- Gan EY, Eleftheriadou V, Esmat S, Hamzavi I, Passeron T, Böhm M, et al. Repigmentation in vitiligo: position paper of the Vitiligo Global Issues Consensus Conference. *Pigment Cell Melanoma Res* 2017;30:28–40.
- Gregg RK, Nichols L, Chen Y, Lu B, Engelhard VH. Mechanisms of spatial and temporal development of autoimmune vitiligo in tyrosinase-specific TCR transgenic mice. *J Immunol* 2010;184:1909–17.
- Harris JE, Harris TH, Weninger W, Wherry EJ, Hunter CA, Turka LA. A mouse model of vitiligo with focused epidermal depigmentation requires IFN-γ for autoreactive CD8+ T-cell accumulation in the skin. *J Invest Dermatol* 2012;132:1869–76.

- Jacquemin C, Rambert J, Guillet S, Thiolat D, Boukhedouni N, Doutre M-S, et al. HSP70 potentiates interferon-alpha production by plasmacytoid dendritic cells: relevance for cutaneous lupus and vitiligo pathogenesis [e-pub ahead of print] *Br J Dermatol* 2017;177:1367–75.
- Jiang X, Clark RA, Liu L, Wagers AJ, Fuhlbrigge RC, Kupper TS. Skin infection generates non-migratory memory CD8⁺ T(RM) cells providing global skin immunity. *Nature* 2012;483(7388):227–31.
- Knickelbein JE, Khanna KM, Yee MB, Baty CJ, Kinchington PR, Hendricks RL. Noncytotoxic lytic granule-mediated CD8⁺ T cell inhibition of HSV-1 reactivation from neuronal latency. *Science* 2008;322(5899):268–71.
- Lang KS, Caroli CC, Muhm A, Wernet D, Moris A, Schittek B, et al. HLA-A2 restricted, melanocyte-specific CD8(+) T lymphocytes detected in vitiligo patients are related to disease activity and are predominantly directed against MelanA/MART1. *J Invest Dermatol* 2001;116:891–7.
- Le Poole IC, van den Wijngaard RM, Westerhof W, Das PK. Presence of T cells and macrophages in inflammatory vitiligo skin parallels melanocyte disappearance. *Am J Pathol* 1996;148:1219–28.
- Lili Y, Yi W, Ji Y, Yue S, Weimin S, Ming L. Global activation of CD8⁺ cytotoxic T lymphocytes correlates with an impairment in regulatory T cells in patients with generalized vitiligo. *PLoS One* 2012;7(5):e37513.
- Mackay LK, Rahimpour A, Ma JZ, Collins N, Stock AT, Hafon M-L, et al. The developmental pathway for CD103(+)CD8⁺ tissue-resident memory T cells of skin. *Nat Immunol* 2013;14:1294–301.
- Mandelcorn-Monson RL, Shear NH, Yau E, Sambhara S, Barber BH, Spaner D, et al. Cytotoxic T lymphocyte reactivity to gp100, MelanA/MART-1, and tyrosinase, in HLA-A2-positive vitiligo patients. *J Invest Dermatol* 2003;121:550–6.
- Natarajan VT, Ganju P, Singh A, Vijayan V, Kirty K, Yadav S, et al. IFN- γ signaling maintains skin pigmentation homeostasis through regulation of melanosome maturation. *Proc Natl Acad Sci USA* 2014;111:2301–6.
- Nicolaidou E, Antoniou C, Stratigos AJ, Stefanaki C, Katsambas AD. Efficacy, predictors of response, and long-term follow-up in patients with vitiligo treated with narrowband UVB phototherapy. *J Am Acad Dermatol* 2007;56:274–8.
- Nigam PK, Patra PK, Khodiar PK, Gual J. A study of blood CD3⁺, CD4⁺, and CD8⁺ T cell levels and CD4⁺:CD8⁺ ratio in vitiligo patients. *Indian J Dermatol Venereol Leprol* 2011;77:111.
- Ogg GS, Rod Dunbar P, Romero P, Chen JL, Cerundolo V. High frequency of skin-homing melanocyte-specific cytotoxic T lymphocytes in autoimmune vitiligo. *J Exp Med* 1998;188:1203–8.
- Palermo B, Campanelli R, Garbelli S, Mantovani S, Lantelme E, Brazzelli V, et al. Specific cytotoxic T lymphocyte responses against Melan-A/MART1, tyrosinase and gp100 in vitiligo by the use of major histocompatibility complex/peptide tetramers: the role of cellular immunity in the etiopathogenesis of vitiligo. *J Invest Dermatol* 2001;117:326–32.
- Pan Y, Tian T, Park CO, Lofftus SY, Mei S, Liu X, et al. Survival of tissue-resident memory T cells requires exogenous lipid uptake and metabolism. *Nature* 2017;543(7644):252–6.
- Park CO, Kupper TS. The emerging role of resident memory T cells in protective immunity and inflammatory disease. *Nat Med* 2015;21:688–97.
- Picardo M, Dell'Anna ML, Ezzedine K, Hamzavi I, Harris JE, Parsad D, et al. Vitiligo. *Nat Rev Dis Primers* 2015;1:15011.
- Rashighi M, Agarwal P, Richmond JM, Harris TH, Dresser K, Su M-W, et al. CXCL10 is critical for the progression and maintenance of depigmentation in a mouse model of vitiligo. *Sci Transl Med* 2014;6(223):223ra23.
- Sallusto F, Lenig D, Förster R, Lipp M, Lanzavecchia A. Two subsets of memory T lymphocytes with distinct homing potentials and effector functions. *Nature* 1999;401(6754):708–12.
- Singh RK, Lee KM, Vujkovic-Cvijin I, Ucmak D, Farahnik B, Abrouk M, et al. The role of IL-17 in vitiligo: A review. *Autoimmun Rev* 2016;15:397–404.
- Sitek JC, Loeb M, Ronnevig JR. Narrowband UVB therapy for vitiligo: does the repigmentation last? *J Eur Acad Dermatol Venereol* 2007;21:891–6.
- Sosa JJ, Currimbhoy SD, Ukoha U, Sirignano S, O'Leary R, Vandergriff T, et al. Confetti-like depigmentation: A potential sign of rapidly progressing vitiligo. *J Am Acad Dermatol* 2015;73:272–5.
- Strassner JP, Rashighi M, Ahmed Refat M, Richmond JM, Harris JE. Suction blistering the lesional skin of vitiligo patients reveals useful biomarkers of disease activity. *J Am Acad Dermatol* 2017;76:847–55.
- Suárez-Fariñas M, Fuentes-Duculan J, Lowes MA, Krueger JG. Resolved psoriasis lesions retain expression of a subset of disease-related genes. *J Invest Dermatol* 2011;131:391–400.
- Taïeb A, Picardo M. The definition and assessment of vitiligo: a consensus report of the Vitiligo European Task Force. *Pigment Cell Res* 2007;20:27–35.
- van den Boorn JG, Konijnenberg D, DelleMijn TAM, van der Veen JPW, Bos JD, Melief CJM, et al. Autoimmune destruction of skin melanocytes by perilesional T cells from vitiligo patients. *J Invest Dermatol* 2009;129:2220–32.
- van den Wijngaard R, Wankowicz-Kalinska A, Le Poole C, Tigges B, Westerhof W, Das P. Local immune response in skin of generalized vitiligo patients. Destruction of melanocytes is associated with the prominent presence of CLA⁺ T cells at the perilesional site. *Lab Invest* 2000;80:1299–309.
- Wang CQF, Cruz-Inigo AE, Fuentes-Duculan J, Moussai D, Gulati N, Sullivan-Whalen M, et al. Th17 cells and activated dendritic cells are increased in vitiligo lesions. *PLoS One* 2011;6(4):e18907.
- Wang XX, Wang QQ, Wu JQ, Jiang M, Chen L, Zhang CF, et al. Increased expression of CXCR3 and its ligands in patients with vitiligo and CXCL10 as a potential clinical marker for vitiligo. *Br J Dermatol* 2016;174:1318–26.
- Wańkowicz-Kalińska A, van den Wijngaard RMJG, Tigges BJ, Westerhof W, Ogg GS, Cerundolo V, et al. Immunopolarization of CD4⁺ and CD8⁺ T cells to Type-1-like is associated with melanocyte loss in human vitiligo. *Lab Invest* 2003;83:683–95.
- Webb KC, Tung R, Winterfield LS, Gottlieb AB, Eby JM, Henning SW, et al. Tumour necrosis factor- α inhibition can stabilize disease in progressive vitiligo. *Br J Dermatol* 2015;173:641–50.
- Wenzel J, Tüting T. An IFN-associated cytotoxic cellular immune response against viral, self-, or tumor antigens is a common pathogenetic feature in “interface dermatitis”. *J Invest Dermatol* 2008;128:2392–402.
- Whitton ME, Pinart M, Batchelor J, Leonardi-Bee J, González U, Jiyad Z, et al. Interventions for vitiligo. *Cochrane Database Syst Rev* 2015;316:1708–9.
- Wu J, Zhou M, Wan Y, Xu A. CD8⁺ T cells from vitiligo perilesional margins induce autologous melanocyte apoptosis. *Mol Med Rep* 2013;7:237–41.
- Yang L, Wei Y, Sun Y, Shi W, Yang J, Zhu L, et al. Interferon-gamma inhibits melanogenesis and induces apoptosis in melanocytes: a pivotal role of CD8⁺ cytotoxic T lymphocytes in vitiligo. *Acta Derm Venereol* 2015;95:664–70.
- You S, Cho Y-H, Byun J-S, Shin E-C. Melanocyte-specific CD8⁺ T cells are associated with epidermal depigmentation in a novel mouse model of vitiligo. *Clin Exp Immunol* 2013;174:38–44.

REFERENCES

1. GOLD-2019-POCKET-GUIDE-DRAFT-v1.7-14Nov2018-WMS.pdf.
2. Roche, N. *et al.* [The gap between the high impact and low awareness of COPD in the population]. *Rev Mal Respir* **26**, 521–529 (2009).
3. Mathers, C. D. & Loncar, D. Projections of global mortality and burden of disease from 2002 to 2030. *PLoS Med.* **3**, e442 (2006).
4. Briscoe, W. A. & Nash, E. S. THE SLOW SPACE IN CHRONIC OBSTRUCTIVE PULMONARY DISEASES. *Ann. N. Y. Acad. Sci.* **121**, 706–722 (1965).
5. Kim, V. & Criner, G. J. Chronic Bronchitis and Chronic Obstructive Pulmonary Disease. *Am J Respir Crit Care Med* **187**, 228–237 (2013).
6. Pauwels, R. A. *et al.* Global strategy for the diagnosis, management, and prevention of chronic obstructive pulmonary disease. NHLBI/WHO Global Initiative for Chronic Obstructive Lung Disease (GOLD) Workshop summary. *Am. J. Respir. Crit. Care Med.* **163**, 1256–1276 (2001).
7. Baraldo, S., Turato, G. & Saetta, M. Pathophysiology of the small airways in chronic obstructive pulmonary disease. *Respiration* **84**, 89–97 (2012).
8. Yadava, K., Bollyky, P. & Lawson, M. A. The formation and function of tertiary lymphoid follicles in chronic pulmonary inflammation. *Immunology* **149**, 262–269 (2016).
9. Barnes, P. J. *et al.* Chronic obstructive pulmonary disease. *Nature Reviews Disease Primers* **1**, 1–21 (2015).
10. Barnes, P. J. Inflammatory mechanisms in patients with chronic obstructive pulmonary disease. *J. Allergy Clin. Immunol.* **138**, 16–27 (2016).
11. Doiron, D. *et al.* Air pollution, lung function and COPD: results from the population-based UK Biobank study. *Eur. Respir. J.* **54**, (2019).
12. Jiang, X.-Q., Mei, X.-D. & Feng, D. Air pollution and chronic airway diseases: what should people know and do? *J Thorac Dis* **8**, E31-40 (2016).

13. Gauderman, W. J. *et al.* Association of improved air quality with lung development in children. *N. Engl. J. Med.* **372**, 905–913 (2015).
14. Salvi, S. S. & Barnes, P. J. Chronic obstructive pulmonary disease in non-smokers. *Lancet* **374**, 733–743 (2009).
15. Cigarette smoking and health. American Thoracic Society. *Am. J. Respir. Crit. Care Med.* **153**, 861–865 (1996).
16. Cuvelier, A. Le déficit en alpha-1 antitrypsine. *Rev Mal Respir* **12** (2020).
17. Hunninghake, G. M. *et al.* MMP12, lung function, and COPD in high-risk populations. *N. Engl. J. Med.* **361**, 2599–2608 (2009).
18. Ding, Z. *et al.* Association between glutathione S-transferase gene M1 and T1 polymorphisms and chronic obstructive pulmonary disease risk: A meta-analysis. *Clin. Genet.* **95**, 53–62 (2019).
19. Stanley, S. E. *et al.* Telomerase mutations in smokers with severe emphysema. *J Clin Invest* **125**, 563–570 (2015).
20. Shukla, R. K., Kant, S., Bhattacharya, S. & Mittal, B. Association of Cytokine Gene Polymorphisms in Patients with Chronic Obstructive Pulmonary Disease. *Oman Med J* **27**, 285–290 (2012).
21. Carraro, S., Scheltema, N., Bont, L. & Baraldi, E. Early-life origins of chronic respiratory diseases: understanding and promoting healthy ageing. *European Respiratory Journal* **44**, 1682–1696 (2014).
22. Barker, D. J. *et al.* Relation of birth weight and childhood respiratory infection to adult lung function and death from chronic obstructive airways disease. *BMJ* **303**, 671–675 (1991).
23. Todisco, T. *et al.* Mild prematurity and respiratory functions. *Eur. J. Pediatr.* **152**, 55–58 (1993).

24. Lange, P. *et al.* Lung-Function Trajectories Leading to Chronic Obstructive Pulmonary Disease. *N. Engl. J. Med.* **373**, 111–122 (2015).
25. Fletcher, C. & Peto, R. The natural history of chronic airflow obstruction. *Br Med J* **1**, 1645–1648 (1977).
26. Yousuf, A. & Brightling, C. E. Biologic Drugs: A New Target Therapy in COPD? *COPD: Journal of Chronic Obstructive Pulmonary Disease* **0**, 1–9 (2018).
27. Barnes, P. J. New anti-inflammatory targets for chronic obstructive pulmonary disease. *Nat Rev Drug Discov* **12**, 543–559 (2013).
28. Mirza, S. & Benzo, R. COPD Phenotypes - implications for care. *Mayo Clin Proc* **92**, 1104–1112 (2017).
29. Candela, M., Costorella, R., Stassaldi, A., Maestrini, V. & Curradi, G. Treatment of COPD: the simplicity is a resolved complexity. *Multidisciplinary Respiratory Medicine* **14**, 18 (2019).
30. Narendra, D. K. & Hanania, N. A. Targeting IL-5 in COPD. *Int J Chron Obstruct Pulmon Dis* **14**, 1045–1051 (2019).
31. Brightling, C. E., Saha, S. & Hollins, F. Interleukin-13: prospects for new treatments. *Clin Exp Allergy* **40**, 42–49 (2010).
32. Gauvreau, G. M., White, L. & Davis, B. E. Anti-alarmin approaches entering clinical trials. *Curr Opin Pulm Med* (2019) doi:10.1097/MCP.0000000000000615.
33. Barnes, P. J. The cytokine network in asthma and chronic obstructive pulmonary disease. *J. Clin. Invest.* **118**, 3546–3556 (2008).
34. Effros, R. M. Anatomy, development, and physiology of the lungs. *GI Motility online* (2006) doi:10.1038/gimo73.

35. Kiyokawa, H. & Morimoto, M. Notch signaling in the mammalian respiratory system, specifically the trachea and lungs, in development, homeostasis, regeneration, and disease. *Development, Growth & Differentiation* **n/a**.
36. Pongracz, J. E. & Stockley, R. A. Wnt signalling in lung development and diseases. *Respir Res* **7**, 15 (2006).
37. Rock, J. R. *et al.* Notch-dependent differentiation of adult airway basal stem cells. *Cell Stem Cell* **8**, 639–648 (2011).
38. Hajj, R. *et al.* Basal cells of the human adult airway surface epithelium retain transit-amplifying cell properties. *Stem Cells* **25**, 139–148 (2007).
39. Kajstura, J. *et al.* Evidence for Human Lung Stem Cells. *New England Journal of Medicine* **364**, 1795–1806 (2011).
40. Shebani, E., Shahana, S., Janson, C., Roomans, G. M. & BHR group. Attachment of columnar airway epithelial cells in asthma. *Tissue Cell* **37**, 145–152 (2005).
41. Watson, J. H. & Brinkman, G. L. ELECTRON MICROSCOPY OF THE EPITHELIAL CELLS OF NORMAL AND BRONCHITIC HUMAN BRONCHUS. *Am. Rev. Respir. Dis.* **90**, 851–866 (1964).
42. Yaghi, A. & Dolovich, M. B. Airway Epithelial Cell Cilia and Obstructive Lung Disease. *Cells* **5**, (2016).
43. Barnes, P. J. Cellular and molecular mechanisms of asthma and COPD. *Clin. Sci.* **131**, 1541–1558 (2017).
44. Rock, J. R. *et al.* Basal cells as stem cells of the mouse trachea and human airway epithelium. *Proc. Natl. Acad. Sci. U.S.A.* **106**, 12771–12775 (2009).
45. Rawlins, E. L. *et al.* The role of Scgb1a1+ Clara cells in the long-term maintenance and repair of lung airway, but not alveolar, epithelium. *Cell Stem Cell* **4**, 525–534 (2009).

46. Breeze, R. G. & Wheeldon, E. B. The cells of the pulmonary airways. *Am. Rev. Respir. Dis.* **116**, 705–777 (1977).
47. Rogers, D. F. Mucus hypersecretion in chronic obstructive pulmonary disease. *Novartis Found. Symp.* **234**, 65–77; discussion 77–83 (2001).
48. Ramos, F. L., Krahnke, J. S. & Kim, V. Clinical issues of mucus accumulation in COPD. *Int J Chron Obstruct Pulmon Dis* **9**, 139–150 (2014).
49. Gosney, J. R., Sissons, M. C. & Allibone, R. O. Neuroendocrine cell populations in normal human lungs: a quantitative study. *Thorax* **43**, 878–882 (1988).
50. Linnoila, R. I. Functional facets of the pulmonary neuroendocrine system. *Lab. Invest.* **86**, 425–444 (2006).
51. Stevens, T. P., McBride, J. T., Peake, J. L., Pinkerton, K. E. & Stripp, B. R. Cell proliferation contributes to PNEC hyperplasia after acute airway injury. *Am. J. Physiol.* **272**, L486–493 (1997).
52. Randell, S. H. Airway epithelial stem cells and the pathophysiology of chronic obstructive pulmonary disease. *Proc Am Thorac Soc* **3**, 718–725 (2006).
53. Ichinose, M. Differences of inflammatory mechanisms in asthma and COPD. *Allergol Int* **58**, 307–313 (2009).
54. Chung, K. F. Cytokines in chronic obstructive pulmonary disease. *European Respiratory Journal* **18**, 50s–59s (2001).
55. Wang, G. *et al.* Genes associated with MUC5AC expression in small airway epithelium of human smokers and non-smokers. *BMC Med Genomics* **5**, 21 (2012).
56. Knabe, L. *et al.* CCSP counterbalances airway epithelial-driven neutrophilic chemotaxis. *European Respiratory Journal* **54**, (2019).
57. Lafkas, D. *et al.* Therapeutic antibodies reveal Notch control of transdifferentiation in the adult lung. *Nature* **528**, 127–131 (2015).

58. Gras, D., Chanez, P., Vachier, I., Petit, A. & Bourdin, A. Bronchial epithelium as a target for innovative treatments in asthma. *Pharmacol. Ther.* **140**, 290–305 (2013).
59. Phillips, J. e. *et al.* Anti-Jagged1 Antibody AMG 430 Reduces Airway Mucus in Mouse Models of Obstructive Pulmonary Disease. in *B63. ANIMAL MODELS OF COPD* A3839–A3839 (American Thoracic Society, 2019). doi:10.1164/ajrccm-conference.2019.199.1_MeetingAbstracts.A3839.
60. Kopan, R. & Ilagan, M. X. G. The canonical Notch signaling pathway: unfolding the activation mechanism. *Cell* **137**, 216–233 (2009).
61. Eenjes, E. *et al.* A novel method for expansion and differentiation of mouse tracheal epithelial cells in culture. *Sci Rep* **8**, 7349 (2018).
62. Wang, R. N. *et al.* Bone Morphogenetic Protein (BMP) signaling in development and human diseases. *Genes Dis* **1**, 87–105 (2014).
63. Rokicki, W., Rokicki, M., Wojtacha, J. & Dźeljić, A. The role and importance of club cells (Clara cells) in the pathogenesis of some respiratory diseases. *Kardiochir Torakochirurgia Pol* **13**, 26–30 (2016).
64. Rackley, C. R. & Stripp, B. R. Building and maintaining the epithelium of the lung. *J. Clin. Invest.* **122**, 2724–2730 (2012).
65. Reynolds, S. D. *et al.* Conditional stabilization of beta-catenin expands the pool of lung stem cells. *Stem Cells* **26**, 1337–1346 (2008).
66. Morimoto, M. *et al.* Canonical Notch signaling in the developing lung is required for determination of arterial smooth muscle cells and selection of Clara versus ciliated cell fate. *J. Cell. Sci.* **123**, 213–224 (2010).
67. Laucho-Contreras, M. E. *et al.* Club Cell Protein 16 (CC16) Augmentation: A Potential Disease-modifying Approach for Chronic Obstructive Pulmonary Disease (COPD). *Expert Opin Ther Targets* **20**, 869–883 (2016).

68. Gamez, A. S. *et al.* Supplementing defect in club cell secretory protein attenuates airway inflammation in COPD. *Chest* **147**, 1467–1476 (2015).
69. Pilette, C. *et al.* Reduced epithelial expression of secretory component in small airways correlates with airflow obstruction in chronic obstructive pulmonary disease. *Am. J. Respir. Crit. Care Med.* **163**, 185–194 (2001).
70. Shijubo, N. *et al.* Serum and BAL Clara cell 10 kDa protein (CC10) levels and CC10-positive bronchiolar cells are decreased in smokers. *Eur. Respir. J.* **10**, 1108–1114 (1997).
71. Buro-Auriemma, L. J. *et al.* Cigarette smoking induces small airway epithelial epigenetic changes with corresponding modulation of gene expression. *Hum. Mol. Genet.* **22**, 4726–4738 (2013).
72. Braido, F. *et al.* Clara cell 16 protein in COPD sputum: a marker of small airways damage? *Respir Med* **101**, 2119–2124 (2007).
73. Vestbo, J. *et al.* Changes in forced expiratory volume in 1 second over time in COPD. *N. Engl. J. Med.* **365**, 1184–1192 (2011).
74. Boers, J. E., Ambergen, A. W. & Thunnissen, F. B. Number and proliferation of clara cells in normal human airway epithelium. *Am. J. Respir. Crit. Care Med.* **159**, 1585–1591 (1999).
75. Perl, A.-K. T., Riethmacher, D. & Whitsett, J. A. Conditional depletion of airway progenitor cells induces peribronchiolar fibrosis. *Am. J. Respir. Crit. Care Med.* **183**, 511–521 (2011).
76. West, J. A. A. *et al.* Induction of Tolerance to Naphthalene in Clara Cells Is Dependent on a Stable Phenotypic Adaptation Favoring Maintenance of the Glutathione Pool. *The American Journal of Pathology* **160**, 1115–1127 (2002).

77. Namburo, P. T. *et al.* The human CYP2F gene subfamily: identification of a cDNA encoding a new cytochrome P450, cDNA-directed expression, and chromosome mapping. *Biochemistry* **29**, 5491–5499 (1990).
78. Singh, G. & Katyal, S. L. Clara Cells and Clara Cell 10 kD Protein (CC10). *Am J Respir Cell Mol Biol* **17**, 141–143 (1997).
79. Weller, B. L. *et al.* Site- and cell-specific alteration of lung copper/zinc and manganese superoxide dismutases by chronic ozone exposure. *Am. J. Respir. Cell Mol. Biol.* **17**, 552–560 (1997).
80. Cruzan, G., Bus, J., Banton, M., Gingell, R. & Carlson, G. Mouse specific lung tumors from CYP2F2-mediated cytotoxic metabolism: an endpoint/toxic response where data from multiple chemicals converge to support a mode of action. *Regul. Toxicol. Pharmacol.* **55**, 205–218 (2009).
81. Singh, G. & Katyal, S. L. Clara cell proteins. *Ann. N. Y. Acad. Sci.* **923**, 43–58 (2000).
82. Broeckert, F., Clippe, A., Knoop, B., Hermans, C. & Bernard, A. Clara cell secretory protein (CC16): features as a peripheral lung biomarker. *Ann. N. Y. Acad. Sci.* **923**, 68–77 (2000).
83. Singh, G. *et al.* Identification, cellular localization, isolation, and characterization of human Clara cell-specific 10 KD protein. *J. Histochem. Cytochem.* **36**, 73–80 (1988).
84. Zuo, W.-L. *et al.* Ontogeny and Biology of Human Small Airway Epithelial Club Cells. *Am. J. Respir. Crit. Care Med.* **198**, 1375–1388 (2018).
85. Krishnan, R. S. & Daniel, J. C. ‘Blastokinin’: inducer and regulator of blastocyst development in the rabbit uterus. *Science* **158**, 490–492 (1967).
86. Beier, H. M. Uteroglobin: a hormone-sensitive endometrial protein involved in blastocyst development. *Biochim. Biophys. Acta* **160**, 289–291 (1968).

87. Buehner, M. & Beato, M. Crystallization and preliminary crystallographic data of rabbit uteroglobin. *J. Mol. Biol.* **120**, 337–341 (1978).
88. Pattabiraman, N. *et al.* Crystal structure analysis of recombinant human uteroglobin and molecular modeling of ligand binding. *Ann. N. Y. Acad. Sci.* **923**, 113–127 (2000).
89. Callebaut, I. *et al.* The uteroglobin fold. *Ann. N. Y. Acad. Sci.* **923**, 90–112 (2000).
90. Beato, M. Binding of steroids to uteroglobin. *J. Steroid Biochem.* **7**, 327–334 (1976).
91. Gillner, M. *et al.* The binding of methylsulfonyl-polychloro-biphenyls to uteroglobin. *J. Steroid Biochem.* **31**, 27–33 (1988).
92. Hermans, C. & Bernard, A. Lung epithelium-specific proteins: characteristics and potential applications as markers. *Am. J. Respir. Crit. Care Med.* **159**, 646–678 (1999).
93. Hermans, C., Aly, O., Nyberg, B. I., Peterson, C. & Bernard, A. Determinants of Clara cell protein (CC16) concentration in serum: a reassessment with two different immunoassays. *Clin. Chim. Acta* **272**, 101–110 (1998).
94. Singh, D., Edwards, L., Tal-Singer, R. & Rennard, S. Sputum neutrophils as a biomarker in COPD: findings from the ECLIPSE study. *Respir. Res.* **11**, 77 (2010).
95. Stripp, B. R. *et al.* Clara cell secretory protein deficiency alters clara cell secretory apparatus and the protein composition of airway lining fluid. *Am. J. Respir. Cell Mol. Biol.* **27**, 170–178 (2002).
96. Wang, S.-Z., Rosenberger, C. L., Bao, Y.-X., Stark, J. M. & Harrod, K. S. Clara cell secretory protein modulates lung inflammatory and immune responses to respiratory syncytial virus infection. *J. Immunol.* **171**, 1051–1060 (2003).
97. Hayashida, S., Harrod, K. S. & Whitsett, J. A. Regulation and function of CCSP during pulmonary *Pseudomonas aeruginosa* infection in vivo. *Am. J. Physiol. Lung Cell Mol. Physiol.* **279**, L452-459 (2000).

98. Laucho-Contreras, M. E. *et al.* Protective role for club cell secretory protein-16 (CC16) in the development of COPD. *Eur. Respir. J.* **45**, 1544–1556 (2015).
99. Treutlein, B. *et al.* Reconstructing lineage hierarchies of the distal lung epithelium using single-cell RNA-seq. *Nature* **509**, 371–375 (2014).
100. Zuo, W.-L. *et al.* Ontogeny and Biology of Human Small Airway Epithelial Club Cells. *Am J Respir Crit Care Med* **198**, 1375–1388 (2018).
101. McCauley, K. B. *et al.* Single-Cell Transcriptomic Profiling of Pluripotent Stem Cell-Derived SCGB3A2+ Airway Epithelium. *Stem Cell Reports* **10**, 1579–1595 (2018).
102. Vasanthakumar, G., Manjunath, R., Mukherjee, A. B., Warabi, H. & Schiffmann, E. Inhibition of phagocyte chemotaxis by uteroglobin, an inhibitor of blastocyst rejection. *Biochem. Pharmacol.* **37**, 389–394 (1988).
103. Katavolos, P., Ackerley, C. A., Clark, M. E. & Bienzle, D. Clara cell secretory protein increases phagocytic and decreases oxidative activity of neutrophils. *Vet. Immunol. Immunopathol.* **139**, 1–9 (2011).
104. Wang, Y., Xu, J., Meng, Y., Adcock, I. M. & Yao, X. Role of inflammatory cells in airway remodeling in COPD. *Int J Chron Obstruct Pulmon Dis* **13**, 3341–3348 (2018).
105. Zou, Y. *et al.* Serum IL-1 β and IL-17 levels in patients with COPD: associations with clinical parameters. *Int J Chron Obstruct Pulmon Dis* **12**, 1247–1254 (2017).
106. Barnes, P. J. Targeting cytokines to treat asthma and chronic obstructive pulmonary disease. *Nat. Rev. Immunol.* **18**, 454–466 (2018).
107. Hogg, J. C. *et al.* The nature of small-airway obstruction in chronic obstructive pulmonary disease. *N. Engl. J. Med.* **350**, 2645–2653 (2004).
108. Chiappori, A. *et al.* CD4(+)CD25(high)CD127(-) regulatory T-cells in COPD: smoke and drugs effect. *World Allergy Organ J* **9**, 5 (2016).

109. Repine, J. E., Bast, A. & Lankhorst, I. Oxidative stress in chronic obstructive pulmonary disease. Oxidative Stress Study Group. *Am. J. Respir. Crit. Care Med.* **156**, 341–357 (1997).
110. Garudadri, S. & Woodruff, P. G. Targeting Chronic Obstructive Pulmonary Disease Phenotypes, Endotypes, and Biomarkers. *Ann Am Thorac Soc* **15**, S234–S238 (2018).
111. Jasper, A. E., McIver, W. J., Sapey, E. & Walton, G. M. Understanding the role of neutrophils in chronic inflammatory airway disease. *F1000Res* **8**, (2019).
112. George, L. & Brightling, C. E. Eosinophilic airway inflammation: role in asthma and chronic obstructive pulmonary disease. *Therapeutic Advances in Chronic Disease* **7**, 34–51 (2016).
113. Yun, J. H. *et al.* Blood eosinophil count thresholds and exacerbations in patients with chronic obstructive pulmonary disease. *J. Allergy Clin. Immunol.* **141**, 2037-2047.e10 (2018).
114. Roan, F., Obata-Ninomiya, K. & Ziegler, S. F. Epithelial cell-derived cytokines: more than just signaling the alarm. *J. Clin. Invest.* **129**, 1441–1451 (2019).
115. Borger, J. G., Lau, M. & Hibbs, M. L. The Influence of Innate Lymphoid Cells and Unconventional T Cells in Chronic Inflammatory Lung Disease. *Front. Immunol.* **10**, (2019).
116. Cayrol, C. & Girard, J.-P. Interleukin-33 (IL-33): A nuclear cytokine from the IL-1 family. *Immunological Reviews* **281**, 154–168 (2018).
117. Drake, L. Y. & Kita, H. IL-33: biological properties, functions, and roles in airway disease. *Immunol. Rev.* **278**, 173–184 (2017).
118. Cayrol, C. & Girard, J.-P. IL-33: an alarmin cytokine with crucial roles in innate immunity, inflammation and allergy. *Curr. Opin. Immunol.* **31**, 31–37 (2014).

119. Liew, F. Y., Girard, J.-P. & Turnquist, H. R. Interleukin-33 in health and disease. *Nat. Rev. Immunol.* **16**, 676–689 (2016).
120. Kouzaki, H., Iijima, K., Kobayashi, T., O’Grady, S. M. & Kita, H. THE DANGER SIGNAL, EXTRACELLULAR ATP, IS A SENSOR FOR AN AIRBORNE ALLERGEN AND TRIGGERS IL-33 RELEASE AND INNATE TH2-TYPE RESPONSES. *J Immunol* **186**, 4375–4387 (2011).
121. Byers, D. E. *et al.* Long-term IL-33–producing epithelial progenitor cells in chronic obstructive lung disease. *J Clin Invest* **123**, 3967–3982 (2013).
122. Scott, I. C. *et al.* Interleukin-33 is activated by allergen- and necrosis-associated proteolytic activities to regulate its alarmin activity during epithelial damage. *Sci Rep* **8**, (2018).
123. Lefrançois, E. & Cayrol, C. Mechanisms of IL-33 processing and secretion: differences and similarities between IL-1 family members. *Eur. Cytokine Netw.* **23**, 120–127 (2012).
124. Lingel, A. *et al.* The structure of interleukin-33 and its interaction with the ST2 and IL-1RAcP receptors – insight into the arrangement of heterotrimeric interleukin-1 signaling complexes. *Structure* **17**, 1398–1410 (2009).
125. Molofsky, A. B., Savage, A. K. & Locksley, R. M. Interleukin-33 in Tissue Homeostasis, Injury, and Inflammation. *Immunity* **42**, 1005–1019 (2015).
126. Cohen, E. S. *et al.* Oxidation of the alarmin IL-33 regulates ST2-dependent inflammation. *Nature Communications* **6**, 8327 (2015).
127. Kakkar, R. & Lee, R. T. The IL-33/ST2 pathway: therapeutic target and novel biomarker. *Nat Rev Drug Discov* **7**, 827–840 (2008).
128. Pascual-Figal, D. A. & Januzzi, J. L. The Biology of ST2: The International ST2 Consensus Panel. *American Journal of Cardiology* **115**, 3B-7B (2015).
129. Griesenauer, B. & Paczesny, S. The ST2/IL-33 Axis in Immune Cells during Inflammatory Diseases. *Front Immunol* **8**, 475 (2017).

130. Hodzic, Z., Schill, E. M., Bolock, A. M. & Good, M. IL-33 and the intestine: The good, the bad, and the inflammatory. *Cytokine* **100**, 1–10 (2017).
131. Gabryelska, A., Kuna, P., Antczak, A., Białasiewicz, P. & Panek, M. IL-33 Mediated Inflammation in Chronic Respiratory Diseases-Understanding the Role of the Member of IL-1 Superfamily. *Front Immunol* **10**, 692 (2019).
132. Zhao, J. & Zhao, Y. Interleukin-33 and its Receptor in Pulmonary Inflammatory Diseases. *Crit Rev Immunol* **35**, 451–461 (2015).
133. Tworek, D. *et al.* The association between airway eosinophilic inflammation and IL-33 in stable non-atopic COPD. *Respir. Res.* **19**, 108 (2018).
134. He, H., Wang, H., Pei, F. & Jiang, M. MiR-543 Regulates the Development of Chronic Obstructive Pulmonary Disease by Targeting Interleukin-33. *Clin. Lab.* **64**, 1199–1205 (2018).
135. Chen, W.-Y., Tsai, T.-H., Yang, J.-L. & Li, L.-C. Therapeutic Strategies for Targeting IL-33/ST2 Signalling for the Treatment of Inflammatory Diseases. *CPB* **49**, 349–358 (2018).
136. Varricchi, G. *et al.* Thymic Stromal Lymphopoietin Isoforms, Inflammatory Disorders, and Cancer. *Front Immunol* **9**, 1595 (2018).
137. Caramori, G., Adcock, I. M., Di Stefano, A. & Chung, K. F. Cytokine inhibition in the treatment of COPD. *Int J Chron Obstruct Pulmon Dis* **9**, 397–412 (2014).
138. Calvén, J. *et al.* Viral stimuli trigger exaggerated thymic stromal lymphopoietin expression by chronic obstructive pulmonary disease epithelium: role of endosomal TLR3 and cytosolic RIG-I-like helicases. *J Innate Immun* **4**, 86–99 (2012).
139. Corren, J. *et al.* Tezepelumab in Adults with Uncontrolled Asthma. *N. Engl. J. Med.* **377**, 936–946 (2017).
140. Ziegler, S. F. *et al.* The biology of thymic stromal lymphopoietin (TSLP). *Adv Pharmacol* **66**, 129–155 (2013).

141. Roseti, S. *et al.* Late Breaking Abstract - Efficacy and safety of tezepelumab in adults with severe asthma: A randomized phase 2 study. *European Respiratory Journal* **50**, (2017).
142. Hallstrand, T. S. *et al.* Airway epithelial regulation of pulmonary immune homeostasis and inflammation. *Clin. Immunol.* **151**, 1–15 (2014).
143. Becerra-Díaz, M., Wills-Karp, M. & Heller, N. M. New perspectives on the regulation of type II inflammation in asthma. *F1000Res* **6**, (2017).
144. Garth, J., Barnes, J. W. & Krick, S. Targeting Cytokines as Evolving Treatment Strategies in Chronic Inflammatory Airway Diseases. *Int J Mol Sci* **19**, (2018).
145. Matloubi, M. *et al.* The Impact of Interleukin (IL)-33 Gene Polymorphisms and Environmental Factors on Risk of Asthma in the Iranian Population. *Lung* (2019)
doi:10.1007/s00408-019-00301-9.
146. Bønnelykke, K. *et al.* A genome-wide association study identifies CDHR3 as a susceptibility locus for early childhood asthma with severe exacerbations. *Nat. Genet.* **46**, 51–55 (2014).

Résumé : « Cellules Club et Susceptibilité respiratoire environnementale »

La BPCO (BronchoPneumopathie Chronique Obstructive) est une maladie chronique des voies aériennes où prédominent modifications structurelles et inflammation. Le but de ce travail a été d'étudier différents axes caractéristiques de cette pathologie comme l'hyperplasie des cellules à mucus, le déficit en cellules Club et la dérégulation des alarmines pour trouver de nouvelles cibles thérapeutiques.

Tout d'abord, nous avons réalisé la carte d'identité des cellules Club issues de cultures en interface air-liquide (ALI) de cellules épithéliales bronchiques humaines par deux méthodes (Single cell-RNAseq et puces à ADN). Les résultats obtenus en Single cell-RNA seq montrent que la totalité des cellules épithéliales expriment l'ARNm CCSP. Pour pallier à ce problème, nous avons triées les cellules selon l'expression de leur protéine spécifique SCGB1A1. Les puces à ADN ont identifié trois populations exprimant la protéine CCSP (fluorescence et granulosité différentes). Ces différentes populations ont une expression d'ARNm de type ciliée ou de type classique « Club ». Ceci permet de montrer la plasticité de ces cellules et leur potentiel pour rétablir un épithélium différencié. Ensuite, nous avons montré que les voies de signalisation BMP et Notch sont déterminantes pour le devenir des cellules épithéliales des voies aériennes. Par conséquent, il est possible de maîtriser la différenciation des cellules provenant de cultures ALI NHBE et HBEC en cellules ciliées, caliciformes, Club ou basales. Un inhibiteur de Notch, le DapT, permettait de rétablir le déséquilibre caractéristique de la BPCO en favorisant le phénotype cilié, mis en évidence aussi bien en immunofluorescence qu'en single cell RNAseq. A partir des données obtenues, il est possible d'envisager de superviser le phénotype des cellules épithéliales des voies aériennes. Pour finir, nous avons étudié différents profils de sécrétions d'alarmines dans les cultures ALI de cellules épithéliales bronchiques humaines à l'état basal. TSLP et IL33 apparaissaient augmentées dans la BPCO, tandis que l'IL25 était diminuée comparé aux sujets sains et aux asthmatiques. Ces patterns d'expression étaient associés de manière hétérogène aux marqueurs cliniques de l'inflammation de type 2.

Il n'y a donc pas une mais des cellules Club, aux morphologies, profils transcriptomiques et fonctions différentes, engagées vers des voies de différenciation distinctes. Le relatif maintien d'un profil cytokinique de type T2 d'un épithélium cultivé en ALI en relation avec les données cliniques valide ce modèle.

Summary: "Club cells and environmental respiratory susceptibility"

COPD (Chronic Obstructive Pulmonary Disease) is characterized primarily by parenchymal structural changes and inflammation. The aim of this work was to study different characteristics of this pathology such as mucus cell hyperplasia, Club cell deficits and alarmin deregulation in order to find new therapeutic targets.

First, we used two transcriptomic methods (Single cell-RNAseq and DNA chips) on air-liquid interface (ALI) cultures of human bronchial epithelial cells to produce a Club cell "identity card". Single cell-RNA seq results demonstrated that all epithelial cells express mRNA for Club cell secretory protein (CCSP), the biomarker classically used for identifying Club cells. To overcome this ubiquity problem, we sorted the cells according their relative level of SCGB1A1 (the gene encoding CCSP) protein expression. DNA chips identified three CCSP-expressing cell populations differing by fluorescence level and/or scatter. These different populations expressed not only classic "Club" mRNA transcripts, but also markers associated with ciliated cells, highlighting their plasticity and potential to restore a differentiated epithelium. We then demonstrated that the BMP and Notch signaling pathways determine the fate of airway epithelial cells, consequently enabling differentiation of cells from ALI NHBE and HBEC cultures into ciliated, goblet, Club or basal cells. A Notch inhibitor, DapT, restored the characteristic imbalance of COPD by promoting the ciliated phenotype, (demonstrated both by immunofluorescence and via single cell RNAseq). It is therefore now possible to control the phenotype of the airway epithelial cells in culture. Finally, we studied different alarmin secretion profiles in ALI cultures of HBECs at basal state. TSLP and IL33 appeared to be increased in COPD, while IL25 was decreased compared to healthy subjects and asthmatics. These expression patterns were heterogeneously associated with clinical markers of type 2 inflammation.

In conclusion, there is not a single Club cell, but multiple types of Club cells with different morphologies, transcriptomic profiles and functions that are committed to different differentiation pathways. The relative maintenance of a T2 cytokine profile of the epithelial cells cultivated in ALI in accordance with clinical data strongly supports the validity of the model.